THE FUNCTIONAL SIGNIFICANCE OF THE DUFFY NEGATIVE POLYMORPHISM

By

IGOR NICOLÁS NOVITZKY BASSO

A thesis submitted to
The University of Birmingham
For the degree of

DOCTOR OF PHILOSOPHY

School of Cancer Sciences
College of Medical and Dental Sciences
The University of Birmingham

August 2014

ABSTRACT

The human Duffy "negative" phenotype is a result of the common polymorphism of the *DARC* (Duffy antigen receptor for chemokines) gene abolishing its transcription in erythroid haematopoietic lineage only, designated *FYB(ES)*. This polymorphism is highly prevalent in individuals of African ancestry and is associated with "benign ethnic" neutropenia. I investigated the impact of DARC expression in the bone marrow (BM) on haematopoiesis using DARC-deficient (DD) mice and newly developed humanised transgenic DARC models expressing the *FYB(ES)* and *FYB* human genes.

Firstly, I developed murine irradiation chimeras with differential DARC expression on either the endothelium or erythroid cells or both, and showed that the absence of erythroid DARC but continued DARC endothelial expression was associated with reduced peripheral blood neutrophil counts. To study underlying mechanisms, I developed two transgenic (TG) murine strains expressing DARC as encoded by *FYB(ES)* or *FYB*. FYB(ES)TG mice showed reduced peripheral neutrophil counts and expansion of myelopoiesis in the BM, and reduced lymphopoiesis and erythropoiesis, compared to FYBTG mice. FYB(ES)TG and also DD mice had reduced granulocyte-macrophage progenitor (GMP) cells and lineage negative, $cKit^+$, $Sca1^+$ (LSK) cells, and proliferation and apoptosis of these cells were reduced. Microarray analysis of differentially expressed genes showed increased myeloid gene expression in GMP and LSK cells. Mixed irradiation chimeras showed that DDBM (DARC deficient BM) retained these changes, suggesting an intrinsic cell effect. In wild-type BM DARC is expressed in erythroid cells only but not in other BM cells, including progenitors and

LSK cells. Analysis of BM and serum showed a significant increase in G-CSF and eotaxin. Immunofluorescent analysis of myeloid cells in frozen femur sections revealed increased myeloid cell clustering in DD and FYB(ES)TG mice. These data suggest that neutrophils are preferentially retained in the DDBM, possibly as a result of loss of optimal chemokine gradients created by erythroblast DARC which may favour neutrophil egress and thereby leading to peripheral neutropenia.

The impact of carrying FYB(ES) polymorphism on the overall survival following AML treatment was also studied in a large UK cohort but revealed no statistically significant effect. However, individuals of African ancestry had improved survival as compared to Caucasians.

ACKNOWLEDGEMENTS

I wish thank my supervisors Prof Paul Moss and Prof Antal Rot for the opportunity to undertake this work, and for providing the academic support and direction when it was needed. I would like to thank Dr Guy Pratt for his generous support of my work from the beginning.

I am grateful to our collaborators, Prof A K Burnett, Dr Aude Thiriot and Prof Ulrich von Andrian for their contributions to this project. In addition I am indebted to my group members to my group members, Dr Maria Ulvmar, Miss Beth Lucas, Miss Poonam Kelay and Dr Elin Hub for their contributions to my work. In addition I would like to thank intercalating medical students Hrushikesh Vyas, Laura Archer and Li Chan for their efforts and diligence.

I wish to recognise those who have helped me with advice and troubleshooting during my project, and who have taught me new techniques. These individuals include, in no particular order, Dr Neil Smith, Mr Nageeb Ali, Dr Frances Spring, Dr Matt Harrison, Dr Johan Duchene, Dr Mark Pearson, Dr Sylvie Freeman, Dr Naeem Khan, Dr Ewan Ross, Miss Charlotte Cook, Dr Saeeda Bobat, Mrs Hema Chahalal, Mr Mahmood Khan, Dr Andrea White, Dr Souad Messahel, Mr Ian Ricketts, Dr Giacomo Volpe, Dr Pierre Cauchy, Dr Mary Clarke, Dr Paloma Garcia, Dr Christopher Weston, Dr Yotis Senis, Dr Annette Pachnio, Dr Jo Croudace and Dr Charlotte Inman.

I am grateful to the Wellcome Trust for funding my work and permitting me the opportunity to undertake it.

I would like to thank my family, Marcina and Mikhail, who have supported and encouraged me throughout this challenging period, and my parents Julia and Nicolás, who gave me the opportunity to receive a higher education and were a source of inspiration throughout my studies.

AUTHOR'S NOTE

The work described in this thesis was carried out in the School of Immunity and Infection and the School of Cancer Sciences, at The University of Birmingham between September 2009 and August 2014 and was funded by the Wellcome Trust. This thesis has not been submitted in part or in totality to any other university.

I, Igor Nicolás Novitzky Basso, was responsible for all of the work described in this thesis with the following exceptions:

1. Preliminary development and cloning of the FYB(ES) transgene by Dr Maria Ulvmar
2. Micro-injections of purified transgenes into fertilised oocytes by Dr Andrea Bacon
3. RNA extraction from FACS sorted cells, and performing the microarray labelling and scanning by Mr Stephen Kissane
4. Scanned microarray images were analysed and data was extracted and normalised by Dr Wen Bin Li
5. Cryosectioning of mouse femurs by Dr Cesar Nombela Arrieta

CONTENTS

LIST OF ILLUSTRATIONS

LIST OF TABLES

LIST OF ABBREVIATIONS

ACKR	Atypical Chemokine Receptor
AML	Acute Myeloid Leukaemia
APC	Antigen Presenting Cell
BFL	Benign Familial Leukopenia
BMP	Bone Morphogenic Protein
bp	Base Pairs
BPI	Bactericidal/Permeability-Increasing Protein
C/EBP	CCAAT-Enhancer-Binding Proteins
CAR	CXCL12 Abundant Reticular Cells
cDNA	Complementary DNA
CFU-E	Colony Forming Unit-Erythroid
CFU-G	Colony Forming Unit-Granulocyte
CFU-GEMM	Colony Forming Unit-Granulocyte-Erythroid-Monocyte-Macrophage
CFU-GM	Colony Forming Unit-Granulocyte-Monocyte
CFU-M	Colony Forming Unit-Monocyte
CLP	Common Lymphoid Progenitors
CMP	Common Myeloid Progenitors
CPM	Counts Per Minute
CSF	Colony-Stimulating Factor
DARC	Duffy Antigen Receptor For Chemokines
DCs	Dendritic Cells
ddH2O	Double-Distilled Water
DNA	Deoxyribonucleic Acid
EPO	Erythropoietin
ETS	E26 Transformation-Specific Family Of Transcription
FACS	Fluorescence-Activated Cell Sorting
FcγR	Fc-Gamma Receptors
FCS	Fetal Calf Serum, Heat Inactivated

FL	Flt3 Ligand
Flt3	Fms-Related Tyrosine Kinase 3
fMLP	N-Formyl-Methionyl-Leucyl-Phenylalanine
G-CSF	Granulocyte Colony Stimulating Factor
G-CSFR	G-CSF Receptor
GM-CSF	Granulocyte-Macrophage Colony Stimulating Factor
GMLP	Granulocytic/Monocytic/Lymphocytic Progenitor
GPCR	G Protein-Coupled Receptor
Hb	Haemoglobin
HDFN	Haemolytic Disease of the Foetus or Newborn
HGH	Human Growth Hormone
HIV	Human Immunodeficiency Virus
hMGSA	Human Melanoma Growth Stimulating Activity, Alpha;
HSC	Haematopoietic Stem Cells
HSPC	Haematopoietic Stem and Progenitor Cells
IAT	Indirect Anti-Globulin Test
ICAM-1	Intercellular Adhesion Molecule-1
KO	Knock-out
LFA-1	Lymphocyte Function-Associated Antigen-1
LT-HSC	Long-Term Stem Cell
MADCAM-1	Mucosal Vascular Addressin Cell-Adhesion Molecule-1
M-CSF	Macrophage Colony-Stimulating Factor
MHC	Major Histocompatibility Complex
min	Minutes
MMP	Matrix Metallopeptidase
MMP-9	Matrix Metallopeptidase-9
MPO	Myeloperoxidase
MPP	Multipotent Progenitors
MSC	Mesenchymal Stromal Cells
mTOR	Mammalian Target Of Rapamycin
NETs	Neutrophil Extracellular Traps

NK	Natural Killer
NLR	NOD-Like Receptors
OB	Osteoblasts
OPN	Osteopontin
PAMP	Pathogen Associated Molecular Pattern
PCR	Polymerase Chain Reaction
PMN	Polymorphonuclear Neutrophils
PRR	Pattern Recognition Receptor
rh	Recombinant Human
rm	Recombinant Murine
RNA	Ribonucleic Acid
RT	Reverse Transcription
S	Seconds
SD	Standard Deviation
SCF	Stem Cell Factor
ST-HSC	Short-Term Stem Cells
TCR	T-Cell Receptor
TG	Transgenic
TGF-β	Transforming Growth Factor B
TLR	Toll-Like Receptors
TNF-α	Tumour Necrosis Factor Alpha
TPO	Thrombopoeitin
VCAM-1	Vascular Cell Adhesion Molecule-1
VLA-4	Very Late Antigen-4
WHIM syndrome	Warts, Hypergammaglobulinemia, Immunodeficiency and Myelokathexis syndrome
WT	Wild-type

Chapter 1

Introduction

1.1 The role of the immune system

1.1.1 Introduction

The immune system has developed in order to protect the individual organism from external pathogens. Primary mechanisms of defence include both chemical and physical barriers. Once breached, both specialised cells and effector molecules are activated in order to limit tissue damage, eliminate infecting pathogens and subsequently achieve tissue repair.

The immune system is divided in two main components, the innate and the adaptive arms. Innate immunity is a non- or broadly-specific response to counter a wide range of pathogens, characterised by a typically immediate response, with the purpose of limiting peripheral tissue infiltration by a broad range of organisms. The skin and the epithelia of the gut and pulmonary systems provide an initial barrier to pathogen entry. Once this is breached, cells of the innate immune response limit further tissue infiltration. The key cellular players of the innate immune system are granulocytes (neutrophils, eosinophils, and basophils), monocytes and macrophages, these share in common the ability to phagocytose pathogens, and mast cells.

Conversely, adaptive immunity is exquisitely specific for individual pathogens, and can provide immune 'memory' leading to a quicker and stronger response on re-exposure.

Antigen presenting cells (APC) such as dendritic cells (DCs) link innate and adaptive immunity while lymphocytes are central to the effector responses of the adaptive immune system (Janeway, 2001). The majority of the leukocyte subsets orchestrating the immune response are derived from bone marrow precursors whose origin is the haematopoietic stem cell. However, some specific tissue macrophages develop in the yolk sac independently of the haematopoietic stem cell (Schulz *et al.*, 2012).

1.1.2 The innate immune system

Innate immune cells respond to infiltrating microorganisms through the recognition of highly conserved molecular structures known as Pathogen Associated Molecular Patterns (PAMPs), facilitated by Pattern Recognition Receptors (PRR) such as Toll-like receptors (TLR) and NOD-like receptors (NLR) (Janeway and Medzhitov, 2002). Interaction between TLR and PAMP induces NFκB signalling and subsequent secretion of pro-inflammatory and co-stimulatory molecules. PRR such as retinoic acid inducible protein 1 and melanoma differentiation associated protein-5 are involved in responses against viruses whereas other bacterial molecules are recognised by the NLR family. Secreted PRR such as mannose-binding lectin, bind via sugar groups, phospholipids, nucleic acids and various proteins to a broad range of micro-organisms, including bacteria, protozoa and fungi. Opsonins, which may be antibodies or proteins involved in the complement cascade, coat the surface of the pathogens to enhance

internalisation. Subsequent triggering of the complement cascade results in the recruitment of phagocytes to sites of infection, and direct killing of micro-organisms. 'Danger signals' provided by endogenous molecules which are associated with tissue damage or stress, such as high mobility group box 1, heat shock proteins and hyaluronic acid, can also help induce an immune response (Tsan, 2011).

An acute inflammatory response is characterised by the infiltration of leukocytes in which neutrophils dominate. Neutrophils are the most abundant leukocyte in human blood and in common with other cells of the innate immune system play a major role in the primary defence against invading pathogens by utilising several mechanisms: (i) phagocytosis and killing of microorganisms, (ii) the release from cytoplasmic granules of pre-formed soluble anti-microbial products such as defensins, myeloperoxidase, elastase, proteinase-3 and cathepsin G and properdin, and (iii) release of neutrophil extracellular traps (NETs), structures that comprise of de-condensed chromatin and antimicrobial proteins which prevent spreading of microorganisms extracellularly (Brinkmann *et al.*, 2004).

Present in less abundance than neutrophils, eosinophils and basophils also contain granules incorporating enzymes and toxic proteins which are released on activation. These two cell groups are thought to be primarily important in the defence against parasites too large to be ingested by neutrophils or macrophages, and participate in allergic inflammatory responses. Effector function by eosinophils is firstly by the release of toxic cytoplasmic granule proteins and free oxygen radicals, and secondly by the production of prostaglandins, leukotrienes and cytokines which activate epithelial cells and recruit other leukocytes, amplifying the immune response. By the

release of major basic protein, eosinophils induce the degranulation of mast cells and basophils. Basophils contain IgE bound on the cell surface, and upon activation by antigen binding to IgE or by cytokines, histamine is released from basophilic granules, leading to immediate allergic reactions.

Following the arrival of neutrophils, monocytes migrate into the tissue from the blood across the vascular endothelium. Some monocytes differentiate into tissue macrophages. Macrophages are polarised functionally in response to cytokines to mount specific functional actions. The two main macrophage classes are termed M1 (classically activated macrophages) if induced by IFN-γ, TNF-α and LPS; and M2 (alternatively activated) if induced by IL-4 or IL-10 (Martinez *et al.*, 2008). Macrophages phagocytose pathogens, and produce cytokines which activate endothelial cells of local blood vessels leading to leukocyte transmigration into the inflamed tissue. In addition, macrophages produce lipid mediators of inflammation such as prostaglandins, leukotrienes and platelet-activating factor.

Mast cells differentiate in peripheral tissues and play an important role in orchestrating allergic responses. Mast cells are located near surfaces exposed to allergens and pathogens, including connective tissues surrounding blood vessels and mucosal tissues. This cell type is involved in the immune response to parasitic worms, and upon activation releases large cytoplasmic granules containing histamine, heparin, serine esterases and proteases which lead to local vasodilation and increased vascular permeability.

1.1.3 The adaptive immune response

The adaptive immune response is activated by production of inflammatory cytokines during the innate immune response. Contrary to innate immunity, the adaptive immune response is characterised by specificity and memory. After the initial encounter with an invading pathogen, the adaptive immune response begins after 5-7 days post-infection. Subsequent exposure to the antigen requires only 24-48 hours for an effective response to occur. The major cell subsets of the adaptive immune response are (i) B and T lymphocytes, (ii) the natural killer (NK) cells, initially considered to be innate immune cells but recently shown to contribute to adaptive immune responses (Vivier *et al.*, 2011), and (iii) the antigen presenting cells (APCs), primarily DCs but also macrophages and B cells, are able to capture, process and present antigens. DCs become activated once they encounter a pathogen and migrate via the lymphatics to the lymph nodes and antigen presentation occur. If the antigen is of viral origin, it is presented to naïve $CD8^+$ lymphocytes within the major complex histocompatibility complex, class I. Thereafter the $CD8^+$ lymphocytes are activated and differentiated to cytotoxic cells or to memory $CD8^+$ cells (Dempsey *et al.*, 2003, Radtke *et al.*, 2013)). APCs presenting an antigen in combination with MHC class II molecules, activate $CD4^+$ cells to secrete cytokines such interleukin 2 (IL-2) that trigger the proliferation of other $CD4^+$ and $CD8^+$ T cells. T cells become activated upon binding of specific antigen presented by APCs within the MHC to the T-cell receptor (TCR). In addition to the interaction of the T-cell TCR and an antigen embedded in the MHC on the APC membrane, a second co-stimulatory signal is provided to the T-cell through the interaction of its CD28 with B7 molecules of the

APCs (Sharpe and Freeman, 2002). Activated $CD4^+$ cells release IL-4, leading to B cell antigen class switching.

B and T cells are derived from common progenitor cells in foetal liver and in adult life from the bone marrow. B cells originate and develop in the bone marrow (Hirose *et al.*, 2002). In contrast, T cell precursors migrate from the bone marrow to the thymus where they mature and undergo a selection for functional TCRs and a deletion of self-reactive clones (Kyewski and Klein, 2006). T-cells then migrate to the lymph nodes and other secondary lymphoid organs where they undertake immune surveillance (Masopust and Schenkel, 2013). B cells are responsible for the humoral response, undergoing clonal expansion following the ligation of an antigen presented on a professional APC. These then differentiate into plasma cells which subsequently secrete large amounts of immunoglobulins specific to that antigen. T cells are important for efficient humoral responses, as co-stimulatory factors (such as IL-2, IL-4 and IL-5) derived from antigen stimulated T-cells are essential for B-cell maturation (Meffre *et al.*, 2000).

Five isotypes of immunoglobulins are produced by plasma cells: the IgA, IgD, IgE, IgG and IgM. Each isotype performs a different function; IgA is present in secretions (e.g. mucus) and in epithelia, IgM is the first to be secreted in the primary immune response via activation of the complement system, IgE is involved in mast cell degranulation and allergic and anti-parasite responses, IgG is the major isotype in the blood involved in the opsonisation of pathogens. IgD however is not well understood, and is present mainly in the intravascular pool. B-cells perform class switching when

activated and secrete different isoforms of the antibody specialised to the different phases of the immune response (Rosenthal and Tan, 2011).

1.2 Haematopoiesis

1.2.1 Haematopoietic stem cells

Haematopoiesis is organised in a hierarchy of cell types that differ in their capacity for self-renewal, proliferation and differentiation. The top of the hierarchy is represented by haematopoietic stem cells (HSC), which generate mature cells committed along specific lineages of the blood, bone marrow, spleen and thymus (Orkin, 2000).

Since the existence of a HSC was demonstrated by Till and McCulloch in 1961, this cell type has undergone extensive investigation to understand how it differentiates into mature blood cells and also retains the essential capacity to reproduce, termed self-renewal. Through this process, one or both daughter cells retain the exact developmental potential of the parent stem cell and ensure the maintenance of a lifelong pool of stem cells, named symmetrical division. Conversely, asymmetric division results in the generation of two distinct daughter cells, one with an identical parental form, and another with more differentiated characteristics. Alterations in this balance provide the ability to support a rapid response to haematological stress and return to homeostasis.

Self-renewal is tightly regulated, since sustained commitment of stem cells without replacement would lead to depletion of the stem cell pool; alternatively self-renewal is a primary feature of leukaemia. Self-renewal is regulated and modulated at the so-called stem cell niche by altering the decision of stem cells to enter symmetric or

asymmetric division (Till and McCulloch, 1961, Becker *et al.*, 1963, Siminovitch *et al.*, 1963) .

During physiological conditions the HSC and many progenitors are quiescent in the G0 phase of the cell cycle (Cheshier *et al.*, 1999). Haematological stressors such as infection or haemorrhage induce the quiescent HSCs to enter the cell cycle and complete asymmetrical division, thereby generating committed progenitors in response to demand for a specific lineage. Upon restoration of normal physiological conditions, the stem cell pool returns to its normal turnover rate, with HSCs undergoing asymmetrical division in order to maintain blood homeostasis. Should the number of HSC in the bone marrow stem cell pool exceed an intrinsic limit, excess HSC enter into an apoptotic sequence (Opferman, 2007).

The complex process of haematopoiesis occurs in different sites during vertebrate development according to the differing demands of the developing organism. Initially haematopoiesis takes place in the primitive yolk sac, before transferring to the foetal liver. Finally the bone marrow and spleen become the major sites of haematopoiesis in late foetal development, with the bone marrow being the exclusive site for haematopoiesis in humans under physiological conditions, whereas in the mouse the spleen remains a minor compartment for erythropoiesis (Durand and Dzierzak, 2005).

Both endothelial and haematopoietic cells develop from the yolk sac, and may share a common parental cell. Haematopoietic stem and progenitor cells (HSPC) do not resemble endothelial cells in morphological appearance, however they have several

transcription factors and surface markers in common, including stem cell ligand, GATA-2, CD34, C-kit, Flt-3 ligand, Sca-1, VEGFR-1 and -2 (Zhu and Emerson, 2002).

1.2.2 Haematopoietic differentiation

HSC lose self-renewal potential during differentiation towards the multipotent progenitor (MPP). These MPP cells lack self-renewal capacity (Adolfsson *et al.*, 2001) but are able to undergo multilineage differentiation, giving rise to the common myeloid progenitors (CMP) (Akashi *et al.*, 2000) and the common lymphoid progenitors (CLP) (Serwold *et al.*, 2009, Kondo *et al.*, 1997). CLPs further differentiate, giving rise to B and T lymphocytes and NK cells. CMPs instead differentiate into the major components of the myeloid compartment: megakaryocytes/platelets, erythrocytes, monocytes/macrophages basophils and mast cells, eosinophils and neutrophils. DC can arise from both CMP (Traver *et al.*, 2000) and CLP (Manz *et al.*, 2001) in response to specific stimuli, or alternatively can bypass both these progenitor stages (del Hoyo *et al.*, 2002). Under physiological conditions, haematopoietic stem cells are required to give rise to approximately 1 million cells per second (Ogawa, 1993), and rapidly undergo an increase in activity in response to haematopoietic stress, particularly when a specific mature blood component requires replenishment. Upon restoration of physiological conditions, stem cells will then return to their steady states.

1.2.3 Phenotypic characterisation of HSC and committed progenitors

The bone marrow stem cell compartment consists of a heterogeneous population of rare cells that can be organised into three subpopulations depending on the ability to re-form the haematopoietic system of lethally irradiated mice. The most undifferentiated fraction of the HSC is the long-term stem cell (LT-HSC), which has the greatest capacity for self-renewal as evidenced by the ability to repopulate the haematopoietic system of lethally irradiated mice for more than six months. LT-HSC can be subsequently be re-isolated and serially transplanted into secondary irradiated recipients (Morrison and Weissman, 1994). LT-HSC generate their immediate progeny, the short-term stem cells (ST-HSC), which are capable of multilineage commitment but have reduced self-renewal potential, as they are able to repopulate irradiated mice for only 6-8 weeks and cannot be serially transplanted (Christensen and Weissman, 2001). The third sub-population of the bone marrow stem cell compartment consists of the multipotent progenitors (MPP) (Adolfsson *et al.*, 2001). This group of cells has no reconstitution potential and gives rise to the CMP and the CLP, which are lineage-restricted.

Despite their presence at a very low level in the bone marrow, the HSC can be isolated based on immunophenotypic characteristics. HSCs are lineage negative (Lin^-) as they do not express mature haematopoietic markers such as those of granulocytes, monocytes and macrophages (CD11b and Gr-1), erythrocytes (Ter119), B cells (B220), T cells (CD3, CD5) and natural killer cells (CD8a). Lin^- cells are further

characterised in the murine bone marrow by their expression of the stem cell antigen Sca-1 (Ly6A/E) and of the tyrosine kinase receptor cKit (CD117). The HSC population described as Lin^- $Sca1^+$ $cKit^+$, termed 'LSK', entails the LT-HSC, ST-HSC and MPP. These populations were originally discriminated based on the differential expression of the adhesion molecule CD34 and the tyrosine kinase receptor Flt3. The staining for Flt3 allowed for the separation of the self-renewing HSC ($Flt3^{low}$) from the non-self-renewing $Flt3^{high}$ MPP (Christensen and Weissman, 2001). While these initial reports indicated that MPP have similar differentiation potentials as HSC, more recent evidence has suggested MPP may have reduced erythrocyte and megakaryocyte potential (Adolfsson *et al.*, 2005). The expression of the Flt3 receptor may therefore function to direct MPP toward lymphoid development, and is then down-regulated on myeloid commitment. While it is clear that MPP are able to generate erythrocytes and megakaryocytes upon transplantation (Forsberg *et al.*, 2006), the level of functional heterogeneity and lineage bias within the MPP is unclear (Lai and Kondo, 2006). Further data suggest that a step-wise progression is not necessary as it appears that HSC may skip the MPP stage (Takano *et al.*, 2004) at times of haematopoietic stress.

Following the MPP stage in the differentiation pathway, the common myeloid progenitors (CMP) were found to give rise *in vitro* to erythrocytes, platelets and granulocytes. After the CMP stage, progenitors restricted to megakaryocyte/erythroid lineages (MEP: Lin^- $Sca1^-$ $cKit^+$ $CD34^-$ $CD16/CD32^-$) or granulocyte/myelomonocytic lineages (GMP: Lin^- $Sca1^-$ $cKit^+$ $CD34^+$ $CD16/CD32^+$) develop. The MEP are thought to give rise to two unipotent progenitors, either erythroid progenitors or megakaryocytic progenitors (Akashi *et al.*, 2000).

In addition to the generally accepted 'classical' model of progenitor maturation described above, an alternative pathway is thought to exist (see **Figure 1.1)**. With the reduction in MEP potential, a granulocytic/monocytic/lymphocytic progenitor (GMLP) (Adolfsson *et al.*, 2005) develops within the MPP sub-population of LSK. Those expressing the highest levels of Flt3 are termed lymphoid-primed multipotent progenitors (LMPP), with the Lin^{-} $Sca1^{+}$ $cKit^{+}$ $CD62L^{+}$ $VCAM^{-}$ $Flt3^{Hi}$ immunophenotype. These LMPP may then form CLP (Lin^{-} $Sca1^{low}$ $cKit^{low}$ $IL7RA^{Hi}$ $Flt3^{Hi}$). The subpopulation with granulocytic-monocytic potential, the GM-primed MPP (GMPP) characterised by the Lin^{-} $Sca1^{+}$ $cKit^{+}$ $CD62L^{+}$ $VCAM^{+}$ $Flt3^{lo}$ immunophenotype may differentiate into GMP (Lai *et al.*, 2005). Evidence exists for the ability of lineage commitment switches at this stage to occur from LMPP to GMP, potentially as a rapid mechanism for coping with haematopoietic stressors. Furthermore T-lineage development has been described from the CMP population, further underpinning the concept that haematopoietic development is both fluid and dynamically able to respond to acute changes in requirements for mature cells (Chi *et al.*, 2011). Work in myeloid leukaemia has suggested that the LMPP sub-population and consequently more mature GMP of LMPP derivation may account for the abnormal progenitors detected in up to 80% of primary acute myeloid leukaemia (Goardon *et al.*, 2011, Mead *et al.*, 2013).

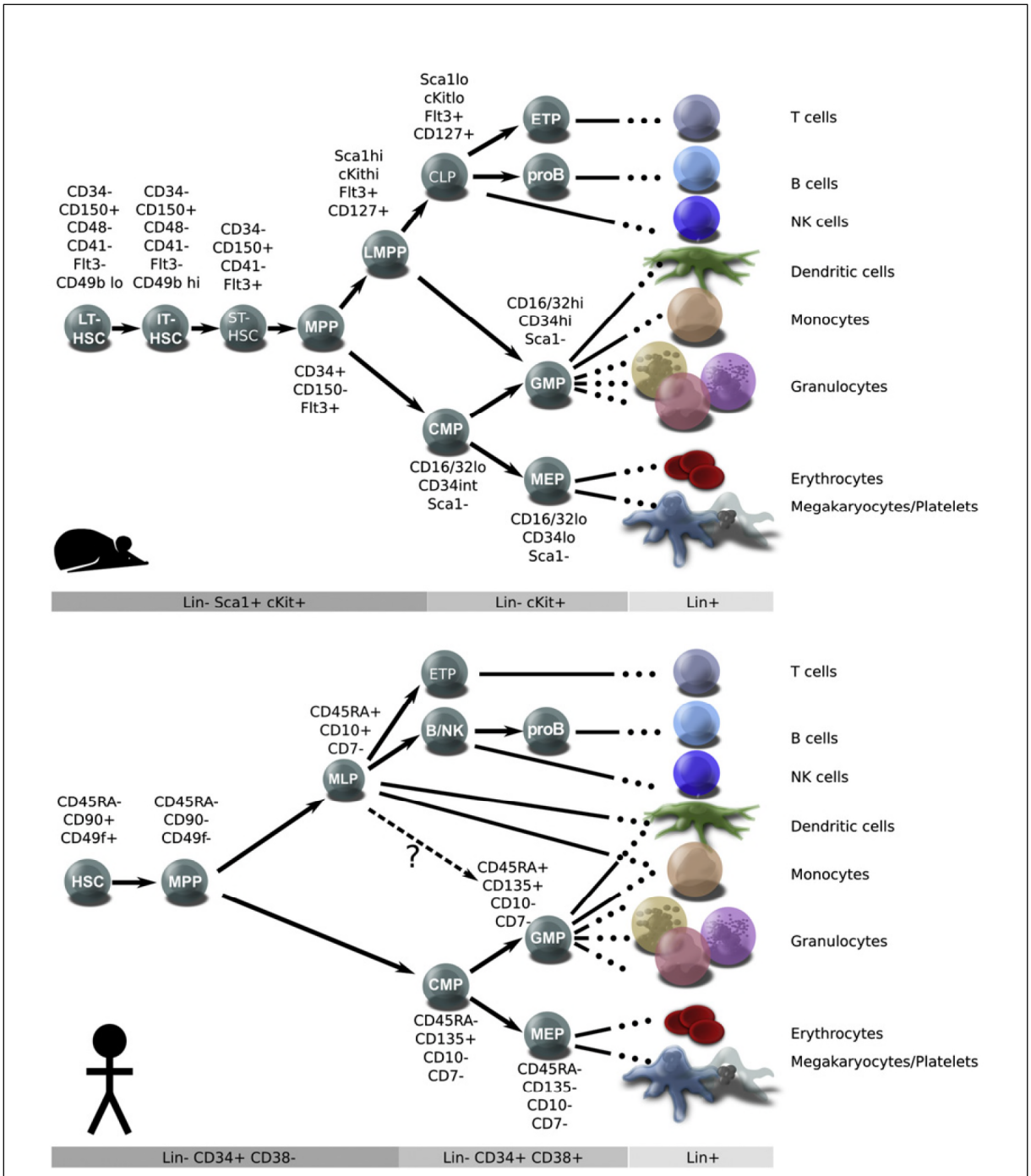

Figure 1.1 Diagram representing haematopoietic stem and progenitor cell differentiation in murine and human haematopoiesis with phenotypic description. From Doulatov *et al.*, 2012

1.2.4 Localisation of haematopoietic stem and progenitor cells: the haematopoietic stem cell niche

HSC are located in trabecular cavities predominantly within long and flat bones, although the precise topological localisation remains controversial. HSC have been identified adjacent to the endosteum immediately proximate to osteoblasts (OB), and near the sinusoidal endothelium, suggesting the existence of two niches within the bone marrow: the endosteal niche and the perivascular niche, respectively. (Ehninger and Trumpp, 2011). Recent work has shown that HSCs occupy primarily the perivascular niche and early lymphoid progenitors preferentially occupy the endosteal niche (Ding and Morrison, 2013).

HSC are found in intimate association with stromal cells, namely OB, mesenchymal stromal cells (MSC) and CXCL12 abundant reticular cells (CAR cells), and these cells are critical to maintenance, self-renewal and quiescence of HSC. Depletion of OB leads to HSC mobilisation (Mendez-Ferrer *et al.*, 2010). Vascular cell adhesion molecule 1 (VCAM-1) and stem cell factor (SCF) are amongst several cell surface proteins expressed by OB, in addition to secreted factors such as thrombopoietin (TPO), angiopoietin-1 (Ang-1), CXCL12 and osteopontin (OPN), keeping HSC quiescent and metabolically inactive.

Most nestin^{+} MSC are localised near blood vessels, and fewer numbers are near the endosteum. These cells are associated with HSC and adrenergic nerve fibres. (Mendez-Ferrer *et al.*, 2010). MSC express high levels of SCF, Ang-1, IL7, VCAM-1 and OPN, all HSC maintenance factors, in comparison to other stromal cells (Ehninger

and Trumpp, 2011). Depletion of MSC leads to loss of bone marrow HSC, whereas parathyroid hormone leads to increased numbers of MSC and directs them to osteoblastic differentiation (Mendez-Ferrer *et al.*, 2010). CAR cells resemble MSC in that they are mesenchymal progenitor cells, but are more abundant. CAR cells support B-cell progenitors, and function to retain haematopoietic progenitors in the bone marrow via high expression of CXCL12 (Greenbaum *et al.*, 2013). Loss of both of these cell types interferes with HSC maintenance (Ehninger and Trumpp, 2011).

1.2.5 Key regulators of haematopoiesis

HSC are controlled by cellular extrinsic and intrinsic factors, such as secreted cyto- and chemokines, and the interaction with bone marrow stromal cells. Signalling pathways, transcription factors and cell cycle regulators are all necessary for HSC maintenance.

1.2.5.1 Haematopoietic cytokines and factors

Several factors are important in maintenance of HSC, or are able to expand HSC, including Flt3-ligand, SCF, TPO and interleukin 3 (IL-3) (Zhu and Emerson, 2002). SCF is the ligand for cKit, the tyrosine receptor expressed on all HSC, and has been shown to prevent HSC apoptosis. TPO primarily regulates megakaryocytic and consequently platelet development, but this cytokine and its receptor Mpl have critical effects on HSC. Mpl is expressed in all HSC and TPO enhances the survival of HSC, in addition to promoting expansion of HSC (Zhang and Lodish, 2008). IL-3 promotes proliferation and differentiation of HSC although it reduces their repopulation ability (Nitsche *et al.*, 2003).

Angiopoietin interacts with its receptor Tie2 on HSC to maintain their long term re-populating ability and *in vivo* enhance their quiescence and bone adhesion (Arai *et al.*, 2004).

1.2.5.2 Signalling pathways

Notch signalling pathways originally described in embryonic development are crucial for the maintenance of HSC, and in cell fate decisions. Constitutive activation of notch signalling enhances HSC self-renewal; however, deletion of notch ligands does not affect HSC maintenance underlining the complexity in HSC biology and implying that other ligands may have a role here (Mancini *et al.*, 2005).

Wnt signalling pathway is a key regulator in several stem cell types, however deletion of Wnt family members (β or γ catenin) has no effect on HSC maintenance. Inhibition of Wnt signalling in OB leads to loss of HSC quiescence and reduced engraftment upon transplantation (Fleming *et al.*, 2008), suggesting an indirect role for Wnt signalling on HSC through the osteoblastic stem cell niche.

Transforming growth factor β (TGF-β) and bone morphogenic proteins (BMP) regulate several processes both in embryogenesis and in adult HSC. TGF-β1 inhibits expansion of HSC *in vitro* and induces cell cycle arrest, although TGF-β1 receptor deficient mice demonstrate no HSC-related deficiencies (Scandura *et al.*, 2004). BMP4 deficient bone marrow has a micro-environment defect which leads to reduced HSC and diminishes repopulating by wild-type HSC in a BMP4-deficient environment (Goldman *et al.*, 2009).

Taken together, these multiple signalling pathways are critical regulators of HSC, and there is likely significant redundancy among them, with potential for cross-talk in the regulation of HSC maintenance and of the stem cell niche environment.

1.2.5.3 Transcriptional regulation of haematopoiesis

Haematopoietic development from the HSC through to mature cells is critically dependent on regulation of gene expression. Transcription factors influence HSC and progenitor lineage commitment depends on both the recognition of specific DNA elements and the recruitment of co-activators or co-repressors to target gene promoter and enhancer regions. Specific proteins mediating chromatin changes may recruit transcription factors leading to either gene activation or silencing. Diverse transcription factors are critical regulators of haematopoietic development and through specific interactions establish the lineage and stage specific patterns of gene expression, ultimately defining cellular identity (Laiosa *et al.*, 2006). It is clear that positive and antagonistic roles exist for major transcription factors, permitting efficient determination of lineage choices. Examples include GATA-1 and PU.1 promoting MEP or myeloid development by opposing effects (Orkin and Zon, 2008). For the purposes of this thesis, transcription factors regulating myelopoiesis and subsequent granulopoiesis will be examined in further detail in that section.

Transcription factors may be divided between those required for HSC development and homeostasis, and those directing differentiation towards a particular lineage. However, this distinction may be arbitrary since factors affecting HSC may also be expressed later in differentiation, and others considered to have lineage-restricted

roles (e.g. C/EBPα), are active in HSC. Both the chronological and appropriate lineage restricted inactivation of transcription factors may be required for the resultant observed phenotype within individual lineages.

Haematopoietic stem cells

In the HSC compartment, several transcription factors are active in maintaining HSC homeostasis. These include Runx1, SCL, Lmo-2, MLL, Tel, BMI-1, GFI-1 and GATA-2 (Orkin and Zon, 2008).

Multipotent progenitors

The correct scheduling of transcription factor expression is essential for normal HSPC differentiation. Within the LSK population, there are phenotypically distinct populations with skewed lineage potential. Transcription factors such as GATA-1 and PU.1 direct HSC to either erythroid or myeloid differentiation (Arinobu et al., 2007). Ikaros and PU.1 are necessary for the development of myeloid and lymphoid progenitors, and direct further differentiation in a lymphoid direction, with disruption of either transcription factor leading to B cell differentiation. Ikaros promotes lymphoid differentiation by activating Flt3 expression, and repressing the GM-CSF gene. As described in more detail later, PU.1 loss leads to profound inhibition of B cell and myelomonocytic production (Laiosa *et al.*, 2006).

Lymphoid Lineage

PU.1, Ikaros, EBF, E2A and Pax5 are all critical transcription factors in B cell development. Progenitors are committed to a B cell fate by Pax5, whereas E2A and

EBP activate genes appropriate for this lineage. In T cell development GATA-3 and Notch-1 are essential at the earliest developmental stage. Notch signalling serves a more focused role committing progenitors by inhibiting factors which lead to other lineage fates. On the other hand, GATA-3 promotes T cell development only in the context of Notch signalling (Laiosa *et al.*, 2006).

Erythroid and megakaryocytic lineage

The direction of haematopoiesis towards the production of erythroid cells depends on the integration of numerous transcription factors. SCL, c-Myb, LMO2 and GATA-2 are important broad-spectrum factors, whereas in erythropoiesis GATA-1, FOG, EKLF, PU.1, Stat5 and Herf1 are required for the formation of normal mature erythrocytes (Perry and Soreq, 2002). In earlier precursors PU.1 directs haematopoiesis towards a myeloid fate. GATA-2 is critical for early haematopoiesis and GATA-2 down-regulation is necessary for the initiation of differentiation. GATA-2 is expressed in erythroid and megakaryocytic progenitors but is down regulated as GATA-1 replaces it at the B gene locus to induce haemoglobin gene expression. Both GATA-1 and GATA-2 deficient embryos succumb to a lethal anaemia. GATA-1 is also required in megakaryocytic maturation, and GATA-1 interacts with FOG-1 during erythroid differentiation and, is also essential for megakaryopoiesis (Laiosa *et al.*, 2006). There is also evidence for an interaction between the pro-lymphoid transcription factor Ikaros, regulating the signalling of Notch and GATA-1 to inhibit megakaryopoiesis. (Malinge *et al.*, 2013)

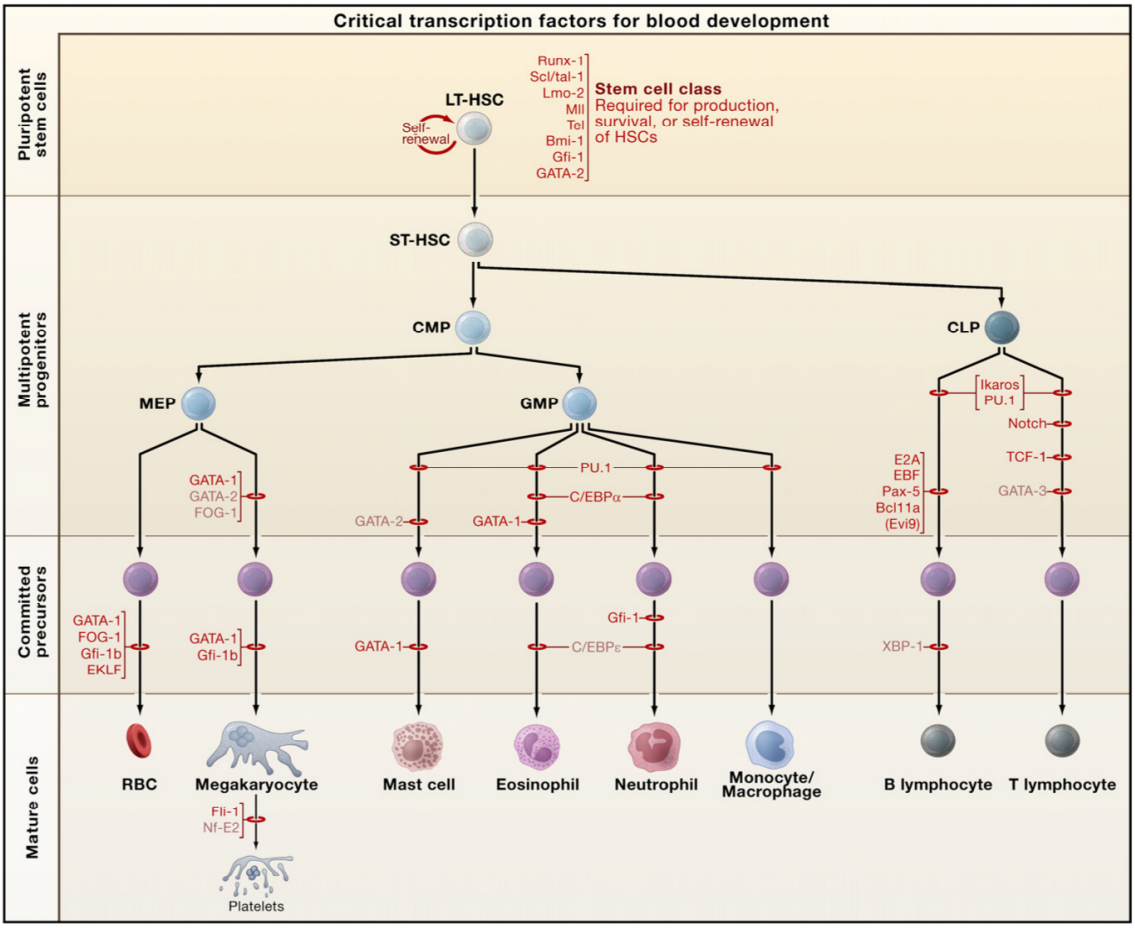

Figure 1.2 Diagram representing important transcription factors in haematopoietic development. Red bars represent stages at which development is blocked in the absence of the relevant transcription factor. From Orkin and Zon, 2008.

Granulopoiesis

Important transcription factors in granulopoiesis will be examined in detail in section "1.2.7.1 Transcription factors regulating granulopoiesis"

1.2.5.4 Other regulators of haematopoiesis

Flt3 and FLt3 ligand

Flt3 or FMS-like tyrosine kinase 3 (CD135) is a membrane-bound tyrosine kinase receptor expressed in HSPC, where it has an important role in development, and in the immune system. Ligation of Flt3 leads to phosphorylation of Stat3 and Stat5 associated with JAK pathway, and mTOR (mammalian target of rapamycin) pathway activation. Flt3 ligand (FL) is part of the family of cytokines which includes SCF and M-CSF (Stirewalt and Radich, 2003). FL mRNA is expressed in most haematopoietic and non-haematopoietic tissues, although the FL protein is detectable only in T lymphocytes and stromal fibroblasts in the bone marrow. FL is able to induce proliferation in the stem cell compartment not on its own but in synergy with haematopoietic growth factors and cytokines, such as IL3, SCF, granulocyte colony stimulating factor (G-CSF) and granulocyte macrophage colony stimulating factor (GM-CSF). FL is highly expressed in progenitors with lymphoid and myeloid potential, and to a lesser extent in B cells and DC precursors (Gilliland and Griffin, 2002). Flt3 deficient mice develop apparently normal haematopoiesis yet exhibit deficiencies in primitive B lymphoid progenitors (Mackarehtschian *et al.*, 1995). Flt3 deficient stem cells fail to contribute to both B cells and myeloid cells upon transplantation, and targeted disruption of FL results in significant reductions in the number of B cell progenitors, DC and NK cells.

Key differences between human and murine Flt3 are the absence of Flt3 expression in murine CMP and GMP, yet Flt3 is required for the promotion of these same populations in human haematopoiesis (Kikushige *et al.*, 2008).

1.2.5.5 Haematopoietic stem and progenitor cell mobilisation

HSPC are retained within their own niche as described above by a number of mechanisms regulating their localisation and quiescence. HSPC can leave the bone marrow to be detected in the peripheral blood, as well other organs such as heart and brain, serving to aid in the repair of damaged tissues, and be a part of host immunity (Massberg *et al.*, 2007). HSPC leave the bone marrow in several conditions of stress, such as exercise, inflammation, bleeding and the administration of cytotoxic agents (To *et al.*, 1984, Kroepfl *et al.*, 2012, Cline *et al.*, 1977). A number of mechanisms have been shown to mobilise HSPC, and are discussed below.

G-CSF induced HSPC mobilisation

The G-CSF receptor (G-CSFR, see in section 1.2.7.2, subsection "G-CSF induced neutrophil mobilisation") is present on HSPC and ligation of this receptor by the cytokine G-CSF, and subsequent receptor signalling is associated with mobilisation of HSPC. As discussed in the section on granulopoiesis, the G-CSFR is expressed also on neutrophils, monocytes, myeloid progenitors and other cells. G-CSF is produced in the context of inflammation and infection, when emergency granulopoiesis is required, and at lower levels in steady-state in the homeostatic maintenance of neutrophil levels in the peripheral blood (see in section 1.2.7.2, subsection "Regulation of G-CSF levels"). G-CSF induces HSPC mobilisation via a number of mechanisms, in part by

effects on a number of other factors which serve to maintain HSPC in their niche and regulate their quiescence. HSPC mobilisation by repetitive G-CSF stimulation over days leads to accelerated myelopoiesis and increases in HSPC motility and egress into the circulation (Greenbaum and Link, 2011). Evidence suggests that an intermediary is required for mobilisation of HSPC by G-CSF, since mixed chimeric mice reconstituted with both wild-type and G-CSFR deficient bone marrow mobilised HSPCs from both types of cells equally well in response to G-CSF (Liu *et al.*, 2000), yet G-CSFR deficient mice failed to mobilise in response to this cytokine. G-CSFR expression by HSPC is therefore not necessary for their mobilisation by G-CSF, implying that such mobilisation occurs indirectly by various mechanism, as discussed further below The mediator of HSPC mobilisation by G-CSF has not been defined, although it has been shown that monocyte-lineage cells may be involved (Christopher *et al.*, 2011).

The CXCR4 and CXCL12 axis

CXCL12 is produced in bone marrow by stromal cells (Ponomaryov *et al.*, 2000) including OB and endothelial cells, and it is the sole ligand for CXCR4, as well as a ligand for the atypical chemokine receptor CXCR7. As described above, CXCL12 has important roles in HSPC homing, retention, survival and quiescence. CXCL12 is expressed constitutively at high levels in the bone marrow and within the stem cell niche, and is a potent chemoattractant for HSPC (Wright *et al.*, 2002). It can activate matrix metallopeptidases (MMP) and is short-lived in the blood owing to degradation

by proteases such as CD26, dipeptidyl peptidase -4 (DPPIV) (Christopherson *et al.*, 2003).

CXCL12 ligation of CXCR4 leading to downstream signalling is critical for maintenance of HSPC homeostasis. CXCR4 and CXCL12 knockout (KO) mice die at the time of birth with a hypocellular bone marrow (Eash *et al.*, 2009) and conditional knock-out of CXCR4 or CXCL12 in the adult murine bone marrow leads to a hypocellular bone marrow, increased numbers of HSC in cell cycle and increased HSPC in the peripheral blood (Sugiyama *et al.,* 2006). The CXCR4 antagonist AMD3100 (Plerixafor) will induce mobilisation of HSPC within hours in mice and humans alone or in combination with G-CSF (Broxmeyer *et al.*, 2005b) and is used for this purpose for the mobilisation of stem cell donors. Furthermore, plasma CXCL12 elevation induces mobilisation of haematopoietic precursors and mature cells, possibly by attracting HSPC to the blood and inducing other indirect mechanisms of mobilisation (Hattori *et al.*, 2001), and suggesting that CXCL12 in the blood has opposing effects to that of CXCL12 secreted locally in the stem cell niche.

G-CSF induced HSPC mobilisation is associated with reduction in bone marrow CXCL12 after a transient upregulation (Petit *et al.*, 2002). Furthermore blocking CXCR4 or CXCL12 reduces or abolishes G-CSF-induced mobilisation. OB are a source of CXCL12, and G-CSF treatment leads to marked decrease in expression of this chemokine by OB (Semerad *et al.*, 2005), and suppresses their number and function (Christopher and Link, 2008). In addition, G-CSF treatment of mice leads to a reduction in bone marrow macrophages and is associated with reduced CXCL12 expression in nestin+ MSC within the stem cell niche (Christopher *et al.*, 2011),

contributing to the reduction in retention signalling via CXCR4 and leading to HSPC mobilisation (Christopher *et al.,* 2011).

The VCAM-1 and VLA-4 axis and other adhesion molecules

HSPC express VLA-4 (very late antigen-4)/$\alpha_4\beta_1$ integrin and this tethers them to VCAM-1 expressed on sinusoidal endothelial cells, stromal reticular cells and fibronectin (Jacobsen *et al.*, 1996). This axis contributes to the regulation of HSPC trafficking between the bone marrow and peripheral sites (Papayannopoulou *et al.*, 1995). Blocking of either VCAM-1 or VLA-4 with antibodies leads to HSPC mobilisation, and a molecule inhibitor of VLA-4 has shown potent mobilisation in mice (Ramirez *et al.*, 2009). Under physiological conditions, G-CSF induced MMP-8 release cleaves VCAM-1 and leads to HSPC mobilisation (Steinl *et al.*, 2013).

CD44 is an adhesion molecule expressed on HSPC and interacts with the extra-cellular matrix, binding to hyaluronan. Loss of this adhesion is an important mechanism for HSPC release from the bone marrow (Vermeulen *et al.*, 1998), and its expression is essential for re-engraftment of HSPC in the bone marrow. Neutrophil proteases induced by G-CSF cause CD44 shedding and extra-cellular matrix degradation, leading to HSPC mobilisation. Conversely bone marrow endothelial expression of CXCL12 leads to upregulation of CD44 for retention of HSPC within the bone marrow (Avigdor *et al.*, 2004).

Other mediators of HSPC mobilisation

The cKit receptor together with SCF play another important role in regulating HSPC, with crucial roles in maintaining HSC quiescence (Thoren *et al.*, 2008). Although controversies exist, G-CSF is thought to lead to HSPC mobilisation by inducing proteases which cleave cKit and SCF (Levesque *et al.*, 2003b, Heissig *et al.*, 2002). Administration of kit ligand by stimulating cKit signalling will induce significant HSPC mobilisation (Molineux *et al.*, 1991), and in contrast cKit-deficient mice have reduced mobilisation of HSPC in response to G-CSF (Papayannopoulou *et al.*, 1998).

FL, which is also required for the regulation of early haematopoiesis, can induce HSPC mobilisation upon administration alone or with G-CSF (Papayannopoulou *et al.*, 1997).

In addition to effects on neutrophils, CXCL2 can rapidly mobilise HSPC which have improved engraftment characteristics on re-transplantation, by inducing MMP (Pelus and Fukuda, 2006, Fukuda *et al.*, 2007). Several other chemokines can induce mobilisation in minutes, and mobilisation with chemokines and G-CSF is synergistic (see section 1.7 Chemokines and chemokine receptors in haematopoiesis).

Under physiological conditions, circulating HSPC are released in a circadian rhythm, in opposite manner to the expression of CXCL12 regulated by genes responding to noradrenaline secretion by the sympathetic nervous system via nerves in the bone marrow (Mendez-Ferrer *et al.*, 2008). It has been shown that one mechanism by which chemotherapy leads to impaired HSPC mobilisation is by injury to sympathetic nerves in the bone marrow (Lucas *et al.*, 2013).

A mechanism for the release of HSPC in the context of tissue injury or fibrinolysis has been shown for plasminogen activation in haematopoiesis. Upon activation by tPA of plasminogen (tissue-type plasminogen activator) to plasmin, this enzyme increases steady-state egress of HSPC from bone marrow, and enhances the mobilisation response to G-CSF as shown in mice, by inducing MMP-9 activity which downregulates CXCL12 in the bone marrow and modulates CXCR4 expression on HSPC (Tjwa *et al.*, 2008, Gong *et al.*, 2011). A membrane plasminogen activator receptor (MuPAR) is expressed by HSPC and is involved in cell-cycle regulation, preventing abnormal HSPC proliferation. This may be a further mechanism of HSPC egress, whereby plasmin may cleave MuPAR during mobilisation (Tjwa *et al.*, 2009).

Other mechanisms for mobilisation such as lipid rafts have been shown to contribute to HSPC mobilisation by modulating CXCL12-CXCR4 signalling (Wysoczynski *et al.*, 2005), and enhancing extra-cellular matrix degradation by MMP (Shirvaikar *et al.*, 2010). Bioactive lipid molecules such as sphingosine-1-phosphate receptor 1 (S1P1) have been shown to be important mediators of HSPC mobilisation. Receptors for S1P1 are present on HSPC, and these interact with CXCL12-CXCR4 signalling. S1P1 deficient mice or those treated with S1P1 inhibitors show a reduced capacity to mobilise HSPC in response to AMD3100 or G-CSF. S1P1 induces the secretion of CXCL12 by nestin+ MSC into the blood leading to HSPC egress (Golan *et al.*, 2012). Inducers of S1P1 production include the sympathetic nervous system (Mendez-Ferrer *et al.*, 2008)

Various elements of the innate immune system modulate the responsiveness of HSPC to a CXCL12 gradient and are involved in the regulation of HSPC release from the bone marrow, such as cationic antimicrobial peptides (Karapetyan *et al.*, 2013), prostaglandin E_2 (Hoggatt *et al.*, 2009) and the complement system (Ratajczak *et al.*, 2004).

Proteases

Neutrophils themselves have been implicated in HSPC mobilisation as they are a major source of neutrophil elastase, cathepsin G and matrix metallopeptidase-9 (MMP-9), all implicated in mobilisation of haematopoietic precursors (Borregaard and Cowland, 1997). These proteases may degrade and inactivate several proteins required for retaining HSC and progenitor cells in the bone marrow, such as VCAM-1, CXCL12, CXCR4 and cKit (Winkler and Levesque, 2006). The implication of this is unclear since mice lacking neutrophil MMP-9, neutrophil elastase or cathepsin G mobilise HSPC normally (Levesque *et al.*, 2004), although more recently other investigators have shown that MMP-8 from neutrophils performs an essential role in HSPC mobilisation by cleaving CXCL12 (Steinl *et al.*, 2013).

1.2.6 Erythropoiesis

The generation of mature erythrocytes is an important and therefore tightly controlled process since the number of these cells should remain constant (approximately 45% of blood volume) to ensure adequate tissue oxygenation. The average lifespan of an erythrocyte in mice is 60 days (Walker *et al.*, 1984) and human 120 days (Greer and

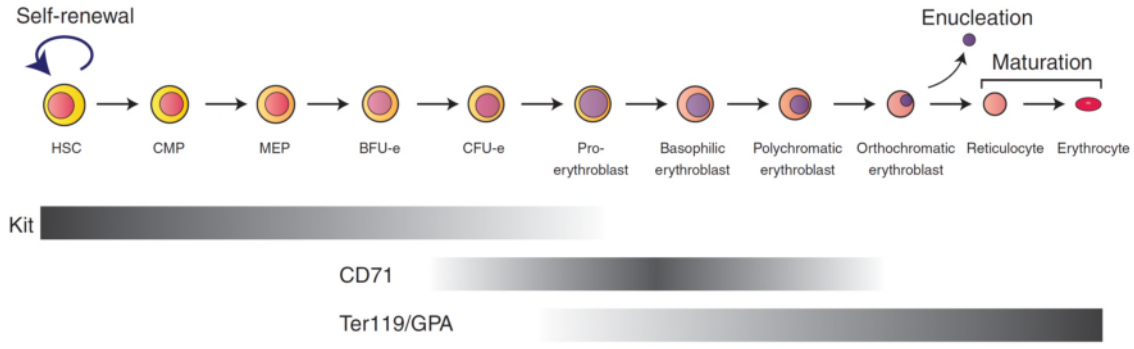

Figure 1.3 Schematic diagram representing erythroid differentiation from HSC (left) sequentially to mature erythrocyte (right), with significant expression of surface markers represented in the bars below. From Dzierzak and Philipsen, 2013

Wintrobe, 2004), requiring 2.4 x 10^6 cells to be produced every second in an average human to support this turnover (Bessis, 1973).

Following the differentiation of HSC into CMP and subsequently MEP, the Burst-Forming Unit-Erythroid (BFU-E) is the most primitive erythroid-restricted progenitor, identifiable exclusively by functional assays (see **Figure 1.3**). In the presence of erythropoietin, FL, IL-3, GM-CSF, TPO and SCF, this cell can give rise to colonies containing over 500 haemoglobinised erythroblasts after 5-7 days of methylcellulose supported culture (mouse) or 10-14 days (human). The BFU-E further differentiates into the Colony Forming Unit-Erythroid (CFU-E), composed of more mature erythroid progenitors with close similarity to the pro-erythroblast. In the presence of low concentrations of EPO, CFU-Es give rise to small colonies, containing 8 to 64 haemoglobinised erythroblasts after 2-4 days of culture (mouse) or 5-8 days (human) (Dzierzak and Philipsen, 2013). The earliest morphologically identifiable erythroid progenitor is the proerythroblast, derived from the CFU-E. This is a large cell characterised by a substantial nucleus with visible nucleoli surrounded by a basophilic

cytoplasm. Basophilic erythroblasts are slightly smaller cells, harbouring a nucleus with a granular appearance, as nuclear condensation begins, and the basophilic aspect of the cytoplasm is due to the presence of large numbers of ribosomes. Haemoglobin can be detectable for the first time at the next polychromatophilic erythroblast stage. These cells and their nuclei are smaller. Full haemoglobinisation occurs at the subsequent orthochromatic erythroblast stage. These cells are the smallest nucleated erythrocyte precursors and their nuclei undergo pycnotic degeneration with chromatin condensation and nuclear shrinkage. Subsequently the nucleus is extruded from what is now a reticulocyte, which is larger than mature erythrocytes and has an irregular form with a stippled appearance due to presence of scanty remaining cytoplasmic organelles. Terminal differentiation from proerythroblast to reticulocyte occurs in 48 to 72 hours, and reticulocyte maturation occurs for a further 48 hours until the remaining organelles are eliminated and the cell develops the discoid shape of the mature erythrocyte (Dzierzak and Philipsen, 2013).

Terminal erythroid differentiation occurs in the erythroid or erythroblastic island, an anatomic unit which provides an exclusive environment for maturing erythroid precursors (Manwani and Bieker, 2008). This consists of a central macrophage surrounded by erythroid precursors at different stages of maturation (**Figure 1.4**). More immature precursors are located at the centre, moving away distally as they mature and maintaining close contact with cytoplasmic extensions of the macrophage until the occurrence of erythroid enucleation. A function of the macrophage is phagocytosis of the ejected nucleus, but this is unlikely to be the only function. It is known that the presence of the macrophage is not essential for the amplification or

maturation of the erythroblasts in different culture systems but these are not representative of the *in vivo* environment. It is likely that the macrophage affects the local concentration of growth factors and nutrients, considering both the proximity of the erythroblasts and the presence of gap junction-like structures between the macrophages and erythroblasts.

Adhesion molecules help to maintain the proximity of the maturing erythroblast to the macrophage. A molecule named erythroblast-macrophage protein is expressed on both the macrophage and the erythroblast and its expression is necessary for normal erythoid development (Soni *et al.*, 2006). The role of other adhesion molecules is less clear. It is known that the immature erythroid cells to the reticulocyte stage express VLA-4, whereas the macrophages express the counterpart VCAM-1. In addition, ICAM4 (LW blood group) and CD51 (α_v integrin) are also expressed by erythroblast and macrophage respectively, and recent work supports a critical role for ICAM4 in erythoid island development (Lee *et al.*, 2006a).

a

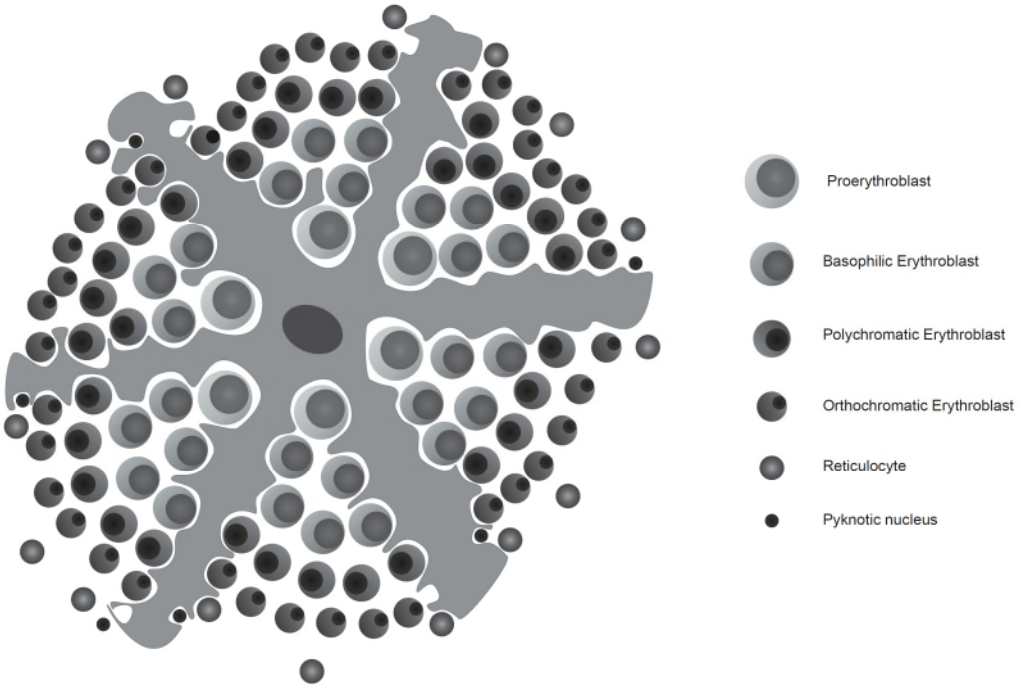

b

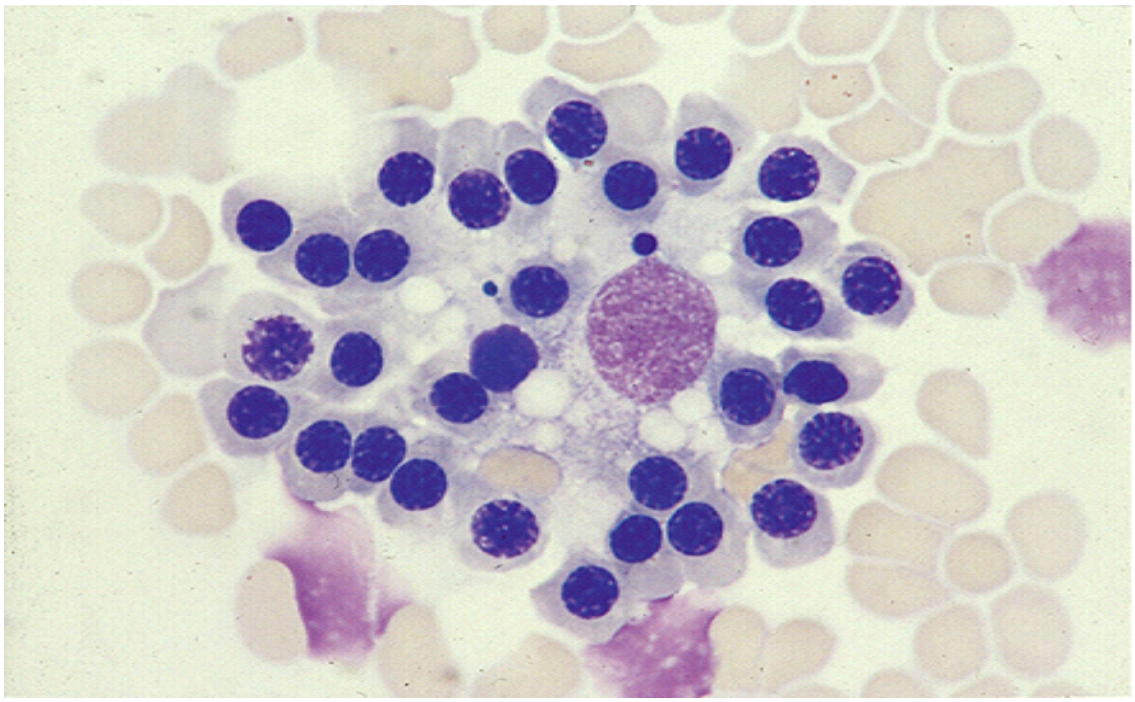

Figure 1.4 The erythroblastic island (a) Schematic diagram (Dzierzak and Philipsen, 2013) (b) Photograph (Bain, 1999)

1.2.7 Myelo- and granulopoiesis

Neutrophils and monocytes/macrophages all derive from a common progenitor and the production of neutrophils is extensive in steady state with 1-2x10^{11} cells being produced per 24 hours in a normal adult human. Differentiation of myeloid cells occurs over 10-14 days, and is followed by the release of mature myeloid cells into the peripheral blood. Myelopoiesis occurs from the GMP, as evidenced by cell-sorted and plated GMP in semi-solid medium which give rise to three distinct colony forming unit types; CFU-G (granulocyte), CFU-M (monocyte) and CFU-GM (granulocyte-monocyte), (Akashi *et al.*, 2000). Histological staining of bone marrow cells has identified several intermediate states of myeloid differentiation, where the promyelocyte is the most undifferentiated progenitor, which sequentially differentiates into either basophilic, neutrophil or eosinophilic myelocytes, and then metamyelocytes which mature into their terminally differentiated counter parts, basophils, neutrophils and eosinophils respectively (Bain *et al.*, 2010). Cytokines required for coordinated myeloid maturation are G-CSF, GM-CSF, M-CSF and IL3 (Liu *et al.*, 1996, Ward *et al.*, 2000). These cytokines maintain survival and stimulate proliferation, leading to maturation and functional activation of the target cells and subsequently influencing the activity of transcription factors important for myeloid lineage commitment.

The mature blood neutrophils, also called polymorphonuclear neutrophils (PMN), contain several granules types which form over the sequential differentiation steps. The earliest appearing granules are formed at the promyelocyte stage and are named

azurophilic or primary, followed subsequently by the specific/secondary and gelatinase/tertiary granules. Finally secretory vesicles develop, which importantly have a membrane with high expression of receptors which include CD11b, CD14 and FcγRII (CD32) (Borregaard and Cowland, 1997). Primary granules exclusively contain the protein myeloperoxidase (MPO), and are further divided into subgroups dependent not only on size, shape and protein content, but also their appearance during myelopoiesis. Alpha-defensins form together with MPO in azurophilic granules, but also proteins such as bactericidal/permeability-increasing protein (BPI) and neutrophil elastase, proteinase 3, azurocidin and cathepsin G. Secondary and tertiary granules do not contain MPO, and can be divided into subgroups according to lactoferrin and gelatinase content. The expression of these MPO-negative granules occurs as a continuum in myelocytes, metamyelocytes, and PMN, and in addition to lactoferrin and gelatinase, these granules contain HCAP-18, lipocalin, lysozyme and collagenase. (Borregaard and Cowland, 1997)

1.2.7.1 Transcription factors regulating granulopoiesis

PU.1

The PU.1 transcription factor is a member of the ETS (E26 transformation-specific) family of transcription factors and is crucial in the specification of haematopoietic lineages. It is required for the development of early MPP and plays a further critical role in the differentiation of monocytes/macrophages in later stages (DeKoter *et al.*, 1998). PU.1 expression is high in B-cells and myelomonocytic cells, with lower expression in HSCs and CMPs. The loss of PU.1 leads to late embryonic or early

neonatal death due to the lack of B-cells and myelomonocytic development (McKercher *et al.*, 1996). In addition, the HSC formed in PU.1 conditionally deficient mice have a reduced repopulation potential (Iwasaki *et al.*, 2005). Loss of C/EBPα expression however has the opposite effect by enhancing the repopulation potential (Zhang *et al.*, 2004).

C/EBP family

The C/EBP family of transcription factors includes C/EBPα, -β, -γ, -δ and -ε, which are similar in their C-terminal leucine-zipper domains and DNA-binding domains, but differ in the N-terminal transactivation domains (Ramji and Foka, 2002, Lekstrom-Himes and Xanthopoulos, 1998). The C/EBP proteins are able to form homodimers with themselves or heterodimers with all the other proteins of this family owing to the high degree of conservation of the leucine zipper domain (Williams *et al.*, 1991).

The precise mechanisms of further differentiation from committed MPP into either neutrophils or the monocytic lineage are not completely understood. It is thought that the continued expression of PU.1 leads differentiation of myeloid cells into the monocytic lineage. Conversely, C/EBPα can inhibit the function of PU.1 and upregulation of C/EBPα results in the induction of granulocytic development and inhibition of monocytic development (Reddy *et al.*, 2002). C/EBPα and PU.1 interact to regulate genes encoding myeloid-specific growth factor receptors G-CSF-receptor *(CSF3)*, M-CSF-receptor and GM-CSF-receptor (Hohaus *et al.*, 1995, Smith *et al.*, 1996). Differentiation into monocytic lineage depends on the expression of the M-CSF receptor and this will only occur if the cells respond to this specific growth factor

(Anderson *et al.*, 1999). PU.1 deficient cells can commit into the granulocytic and monocytic lineages, but cannot fully support maturation along these lineages. Mice deficient in C/EBPα lack mature PMN as myeloid cells fail to differentiate past the myeloblast stage, but show no monocytic deficiencies (Zhang *et al.*, 1997). As opposed to PU.1 deficiency, loss of C/EBPα downregulates G-CSFR mRNA expression but mRNA of GM-CSF and M-CSF receptors are not affected (Iwama *et al.*, 1998). Furthermore it appears to block the transition from CMP to GMP, leading to a profound loss of granulocytic potential and accumulation of myeloblasts (Zhang *et al.*, 2004) Therefore C/EBPα effects in myeloid differentiation include the activation of genes which encode for the G-CSFR (Hohaus *et al.*, 1995, Smith *et al.*, 1996), myeloperoxidase (Wang *et al.*, 2001) and the inhibition of proliferation (Theilgaard-Monch *et al.*, 2005) by interacting with the E2F cell cycle regulator. During terminal neutrophil differentiation, the expression of C/EBPα is progressively reduced from the myeloblast stage, whereas C/EBPε expression is maximal at the myelocyte stage.

C/EBPε is up-regulated by C/EBPα and G-CSF through the CSF3 signalling pathway (Nakajima and Ihle, 2001). Mice with a targeted disruption of C/EBPε fail to produce mature neutrophils and to express the late-appearing secondary and tertiary granule proteins (Yamanaka *et al.*, 1997). Other transcription factors such as PU.1, C/EBPβ, C/EBPδ and C/EBPγ increase continuously through differentiation to the metamyelocyte stage (**Figure 1.5**). Mice deficient in C/EBPβ or C/EBPδ demonstrated no haematopoietic defects in relation to terminal granulopoiesis. However there is an essential role for C/EBPβ in emergency granulopoiesis, but C/EBPα or C/EBPε were

not induced under the conditions of cytokine treatment or fungal infection (Hirai *et al.*, 2006).

Hence, C/EBPα is essential for the commitment of HSCs toward promyelocytes, whereas C/EBPϵ, which acts downstream of C/EBPα, regulates the transition from promyelocytes to mature neutrophils.

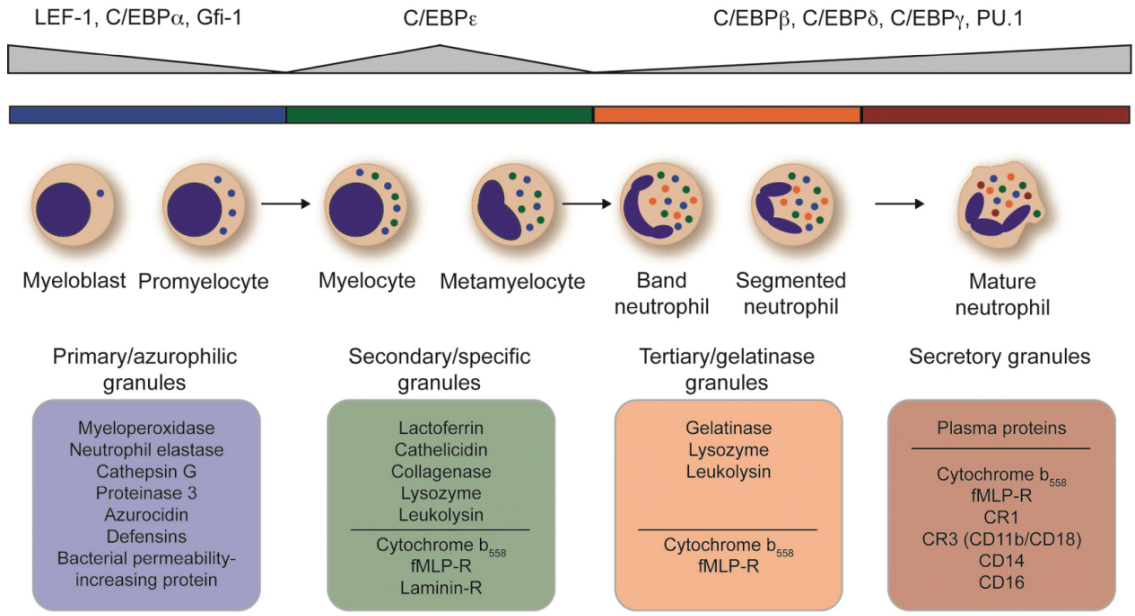

Figure 1.5 Representative diagram illustrating terminal granulopoiesis, which is characterised by the sequential formation of granules and maturation with segmentation of the nucleus. Transcription factors indicated above the figure are critical for the regulation of granule protein maturation and appearance of granule proteins. From Fiedler and Brunner, 2012.

GATA-2

As stated above, GATA-2 is essential for early haematopoiesis: it is critical for production of mature erythrocytes at the embryonic stage, it is important at later stages of myeloid and lymphoid development, and has a central function in maintaining the proliferation and survival of developing HSC (Tsai *et al.*, 1994) . Mice

haploinsufficient for GATA-2 have low numbers of HSC associated with increased apoptosis and a reduced level of granulocyte progenitors (specifically reduced GMP) with poor performance of mature neutrophil forms in functional assays and no effect on other progenitors (CMP, CLP) (Rodrigues *et al.*, 2008).

GFI1

GFI1 is part of a network of intrinsic factors that control HSC fate, and regulates the quiescence of HSC (Hock *et al.*, 2004). In GFI1 deficient mice, there is a lack of mature neutrophils, and the myeloid cells produced harbour only primary granules and demonstrate increased monocytic gene expression. It appears that GFI1 silences monocytic genes and directs myelopoiesis toward granulocytic maturation (Hock *et al.*, 2003). In humans, rare inherited mutations of GFI1 are the cause of some forms of severe congenital neutropaenia (Person *et al.*, 2003).

In this compartment, GFI1 and PU.1 inhibit each other's function by competing for DNA binding in promoters of target genes (Spooner *et al.*, 2009). However, GFI1 also inhibits PU.1 by direct repression of the PU.1 gene and by counteracting PU.1 function through a protein–protein interaction (Dahl *et al.*, 2007). PU.1 promotes monocytic differentiation, whereas GFI1 enhances granulocytic differentiation.

1.2.7.2 Neutrophil mobilisation and clearance

Neutrophil circulation and clearance

Ex-vivo labelling and re-infusion of neutrophils to measure their clearance have suggested that the circulating lifespan of murine and human neutrophils is approximately 8 hours (Dancey *et al.*, 1976). However more recent work confirms such short lifespan for murine neutrophils but suggest a longer lifespan of over 5 days for human neutrophils (Pillay *et al.*, 2010). It is likely that *ex-vivo* manipulation of neutrophils in early studies accelerated their clearance from the blood. Only a small part of total neutrophils is present in the circulation, and a substantial proportion (c. 20%) is marginating in the vessels of the lungs, present mainly within the capillaries (Semerad *et al.*, 2002, Doerschuk *et al.*, 1994). Beta agonists such as epinephrine (adrenaline) can lead to rapid demargination of neutrophils and their return to the circulation (Bierman *et al.*, 1952)

Neutrophil clearance occurs via macrophage phagocytosis in several locations, primarily the spleen, the bone marrow and the liver in roughly equal proportions (Suratt *et al.*, 2001). Depending on the method of stimulation, neutrophils may preferentially home to a specific organ, e.g. in a model of thioglycollate induced peritonitis, peritoneal exudate neutrophils re-infused into untreated recipient mice homed to the liver, whereas those harvested from bone marrow of the thioglycollate treated mice, home to the bone marrow of untreated recipients (Suratt *et al.*, 2001).

Aging of neutrophils correlates with cell surface expression of CXCR4, with increased expression resulting in greater response to CXCL12, thus directing aged neutrophils to

the bone marrow for clearance (Martin *et al.*, 2003). Blocking antibodies to CXCR4 impede this process, but this is a non-critical mechanism as CXCR4 deficient neutrophils show comparable clearance to those expressing CXCR4 (Eash *et al.*, 2009).

Neutrophil release

Neutrophils develop from precursors in bone marrow sinusoids and as they mature, accumulate away from the bone marrow trabeculae. The bone marrow is a large reservoir of mature cells, and a wide range of mediators is capable of triggering release. These include chemokines (CXCL1, CXCL2, CXCL5, CXCL8, CXCL6, CXCL12), cytokines (G-CSF, IL-6, GM-CSF, SCF) (Seymour *et al.*, 1997, Liu *et al.*, 1997, Lapidot and Petit, 2002, Hattori *et al.*, 2001), bacterial products, (N-formyl-methionyl-leucyl-phenylalanine, fMLP), complement fragments such as C5a (Jagels *et al.*, 1995) and Flt3 ligand (Molineux *et al.*, 1997).

To enter the blood, neutrophils migrate through the diaphragmatic fenestrae of endothelial cells lining the sinusoids, wherein abluminal and luminal endothelial cell membranes are fused (Burdon *et al.*, 2008).

The CXCR4 and CXCL12 axis

CXCL12 and its receptor CXCR4 are important regulators of neutrophil release from the bone marrow. HSPC express CXCR4 at high levels, whereas neutrophils express low amounts of CXCR4 on the cell surface, with higher intracellular levels of this receptor. CXCR4 is required for the retention of myeloid precursors within the bone

marrow, as evidenced by the premature release of granulocytic precursors in mice lacking haematopoietic CXCR4 (Ma *et al.*, 1999).

In addition, mice with myeloid only CXCR4 or CXCL12 deletions exhibit constitutive neutrophilia and impaired mobilisation from the bone marrow (Eash *et al.*, 2009). CXCL12 expression is significantly decreased following G-CSF treatment (Levesque *et al.*, 2003a). G-CSF induces a transient increase in CXCR4 expression subsequently leading to its downregulation, which correlates with HSPC mobilisation (Semerad *et al.*, 2002). CXCL12 is degraded by elastase from neutrophils (Petit *et al.*, 2002), but production of CXCL12 may also be reduced due to suppression by G-CSF of bone marrow OB, the primary bone marrow source of CXCL12 (Semerad *et al.*, 2005, Katayama *et al.*, 2006). This suggests that CXCL12 is a retention factor for bone marrow neutrophils, supported by work demonstrating that following the administration of the CXCR4-antagonist AMD3100 (Plerixafor) there is a rapid increase in circulating neutrophils due to the egress of neutrophils from the bone marrow (Martin *et al.*, 2003).

More recent work suggests different roles for CXCR4 and G-CSF in neutrophil mobilisation. G-CSF increases neutrophil mobilisation within the bone marrow, leading to their localisation near vessels for entry into the circulation (Devi *et al.*, 2013), whereas CXCR4 antagonism reduces neutrophil bone marrow retention (Eash *et al.*, 2010), with G-CSF contributing to the reduction in CXCR4 signalling by its effects on OB and CXCL12 production. The combination of these and other signals leads to neutrophil egress from the bone marrow.

A gain-of-function mutation in CXCR4 leading to constitutive signalling of CXCR4 has been described to be the cause of WHIM syndrome (Warts, Hypo-gammaglobulinemia, Immunodeficiency and Myelokathexis). WHIM is characterised by bone marrow accumulation of neutrophils associated with peripheral neutropaenia and an inability to effectively mobilise neutrophils, leading to recurrent infections and virally induced warts (Hernandez *et al.*, 2003).

The clinical importance of the CXCR4-CXCL12 axis is demonstrated by the widespread use of the CXCR4 antagonist Plerixafor (AMD3100) to mobilise HSC and progenitor cells (Broxmeyer *et al.*, 2007). Plerixafor is also clinically effective in the treatment of WHIM syndrome (McDermott *et al.*, 2011)

G-CSF induced neutrophil mobilisation

G-CSF is the principle cytokine controlling granulopoiesis. The effects of G-CSF are mediated via the G-CSFR and mice lacking either G-CSF or G-CSFR have profound neutropaenia (Lieschke *et al.*, 1994, Liu *et al.*, 1996). Some patients with severe congenital neutropaenia have also molecular defects in G-CSF pathway as underlining causes (Dong *et al.*, 1994). G-CSFR is expressed primarily in neutrophils and their precursors but also monocytes, platelets, haematopoietic progenitor cells, NK cells and endothelial cells. The expression of G-CSF-R in several cells is induced by the transcription factor C/EBPα (Barreda *et al.*, 2004). G-CSFR is a tyrosine kinase type receptor, with signal transduction involving the JAK-STAT pathway (Barreda *et al.*, 2004). Following binding to G-CSFR, G-CSF is removed from the circulation and bone

marrow by internalisation in granulocytes and is subsequently degraded, permitting a negative feedback mechanism by effector cells. (Sarkar and Lauffenburger, 2003).

Ligation of G-CSF to neutrophil G-CSFR leads to a rapid increase in their motility within the bone marrow, leading to their emigration through blood vessels (Kohler *et al.*, 2011). G-CSF also contributes to neutrophil mobilisation by disrupting CXCR4/CXCL12 mediated bone marrow retention signals (Wengner *et al.*, 2008, Semerad *et al.*, 2002). In addition to inducing bone marrow neutrophil release, G-CSF leads to increased neutrophil phagocytic and migratory activity (Platzer *et al.*, 1985). G-CSF induced neutrophil mobilisation occurs rapidly but chronic treatment of mice with G-CSF stimulates not only mobilisation but also leads to prolonged increases in granulopoiesis (Welte *et al.*, 1987).

G-CSF leads to neutrophil mobilisation via indirect mechanisms. G-CSF is also produced by osteocytes allowing these cells to regulate myelopoiesis independently of OB in response to G protein-coupled receptor signalling pathways that act through the heterotrimeric G protein Gsα, through yet-to-be-determined mediators (Fulzele *et al.*, 2013).

Inhibition of G-CSFR occurs through SOCS3 and Stat3 activation, which are activated by G-CSFR signalling; deficiency of either leads to neutrophilia and increases in mature neutrophils in the bone marrow (Barreda *et al.*, 2004).

G-CSF is a well-established treatment for individuals with various forms of acquired or congenital neutropaenias (Lieschke and Burgess, 1992).

CXCR1-2 and ELR+ CXCL chemokines

Classical chemokine receptors CXCR1 and 2 and CCR1 are present on neutrophil cell membranes, as well as the atypical chemokine receptor D6 (ACKR2) (Fan *et al.*, 2007, Cacalano *et al.*, 1994, Bachelerie *et al.*, 2014). CXCL1-3 and CXCL5-8, cumulatively called ELR+ chemokines due to the conserved ELR, glutamic acid-leucine-arginine, motif in their N-termini, are ligands for CXCR2 and CXCR1. Mice deficient in CXCR2 have severe defects in neutrophil emigration to sites of inflammation (Cacalano *et al.*, 1994), and in normal mice exogenous administration of ELR+ chemokines leads to neutrophil mobilisation (Burdon *et al.*, 2008), which is independent of G-CSF (Semerad *et al.*, 2002). CXCR2 ligands CXCL1 and CXCL2 are constitutively expressed in bone marrow endothelial cells, and the expression of CXCL2 is upregulated by G-CSF. G-CSF and ELR+ chemokines can work synergistically in order to enhance the mobilisation of neutrophils (Wengner *et al.*, 2008). CXCR4 and CXCR2 play opposite regulatory roles as the ELR+/CXCR2 pathway antagonises CXCR4 in the release of neutrophils from the bone marrow (Eash *et al.*, 2010). The precise mechanism for this is unclear. However more recent work has shown that the administration of G-CSF leads to a CXCL1 spike in blood, which is released by bone marrow megakaryocytes. A similar CXCL1 spike is detected on thrombopoietin administration, and G-CSF increases systemic levels of thrombopoietin. Thus, G-CSF may act in part indirectly via megakaryocyte production of CXCL1, which, in turn, leads to neutrophil mobilisation (Kohler *et al.*, 2011). In particular, the localisation of megakaryocytes and OB close to bone marrow vasculature, may allow for the rapid production of CXCR2 ligands and highlights a role for these cells as gatekeepers in emergency neutrophil mobilisation.

The G-CSF target leading to thrombopoietin release remains unclear. Nevertheless this is consistent with previous data that G-CSFR on neutrophils is dispensable for their mobilisation from bone marrow (Semerad *et al.*, 2002).

Adhesion molecules

Selectin and integrins expressed on neutrophils and the vascular endothelium are critical for the emigration of neutrophils from the circulation into tissues. Loss of selectins leads to neutrophilia, and integrin deficient mice exhibit an increase in neutrophil blood numbers and their reduction in the tissues (Stark *et al.*, 2005, Robinson *et al.*, 1999, Frenette *et al.*, 1996). The neutrophilia which develops appears to be due to elevated G-CSF levels, produced as a result of reduced neutrophil phagocytosis by macrophages consequent from the reduction in neutrophil migration into tissues (Stark *et al.*, 2005). This mechanism is described in detail below.

Regulation of G-CSF levels

Neutrophils exert their effect in host defence through the release of reactive oxygen species, phagocytosis, degranulation and the release of nuclear material as NETs (Brinkmann *et al.,* 2004). Apoptotic neutrophils are cleared through phagocytosis by macrophages. Recent work suggests that blood granulocyte levels are controlled by a feedback system from the periphery 'sensing' neutrophil numbers as they are cleared by macrophages. IL-23 is produced in macrophages and its production is inhibited by neutrophil phagocytosis. IL-23 is an inducer of IL-17 production by $CD4^+$ T-cells, and IL-17 production stimulates G-CSF release. IL-23 production is reduced by neutrophil phagocytosis, and IL-17 deficient mice show decreased neutrophil counts.

Furthermore, neutrophil adhesion molecule deficient mice (lacking either CD18, LFA-1, Core2-glucosaminyltransferase or E-selectin and P-selectin) have elevated IL-17 levels and neutrophilia, with resolution upon IL-17 blockade (Stark *et al.*, 2005). Thus G-CSF production depends on peripheral clearance of neutrophils by macrophages and a feedback to bone marrow production via IL-23 and IL-17. The baseline function of macrophages is to produce IL-23 with down-stream effects, and this is negatively regulated on neutrophil phagocytosis. (Stark *et al.*, 2005, Forlow *et al.*, 2001). More recent work has further supported the role of this axis and suggested a critical role for commensal bacteria in its regulation (Deshmukh *et al.*, 2014).

1.3 The vascular endothelium

Inflammation is a fundamental mechanism essential for containing pathogens and the repair of tissue after injury, and consists of a series of vascular and cellular reactions. These lead to the removal of damaged tissue and culminate in the completion of tissue repair. The acute inflammatory process is characterised by the classical signs of swelling, redness, pain heat and loss of function. It consists of a cascade of events which include the increased permeability of the small vessels, the adherence of circulating cells to the blood vessel near the site of injury, the migration of several immune cell types, controlled cell death and removal of tissue debris, and the growth of new vessels and tissues. The recruitment and migration of blood leukocytes from the vasculature to the site of injury is a fundamental event in the process of inflammation, leading to tissue dysfunction and damage (Janeway, 2001).

The vascular endothelium is lined by a single layer of cells in direct contact with blood, and acts a barrier regulating the transfer of leukocytes, metabolites and gas. The barrier function is affected by the type of junctions between endothelial cells, and the underlying extracellular matrix and basement membrane secreted by these cells as a point of attachment. Depending on localisation there are variations in the phenotype of endothelial cells, underlying the requirements of the tissues. For example, within the spleen, sinusoid capillaries lack tight junctions and a basement membrane, allowing the slow movement of blood for erythrocyte and other cell “examination” by macrophages. Endothelial cells in post-capillary venules are most significantly involved in the tissue migration of leukocytes during inflammation. These respond to

inflammatory cytokines and express chemo-attractants and adhesion molecules (Janeway, 2001).

Independent of any inflammatory activation of the vasculature, normal blood flow leads to the direction of leukocytes towards the blood vessel wall, termed margination, allowing leukocytes to be in close contact with post-capillary venular endothelial cells. Inflammation leads to the release of inflammatory mediators which induce the high expression of adhesion molecules on the endothelium. Of these, selectins are an important group, comprising E (endothelial)-selectin and P (platelet)-selectin expressed by endothelial cells, and L(leukocyte)-selectin expressed by leukocytes (Ley *et al.*, 2007). Selectin ligands are glycoproteins and glycolipids with sialyl Lewis X motifs contained in the structure with bonds formed between selectins being calcium dependent. The bonds formed are short lived yet strong, and a continuous process of bond formation and breakage leads to a slowing and rolling of cells along the vascular wall (Zarbock *et al.*, 2011, Kansas, 1996).

L-selectin is expressed on leukocyte microvilli and is cleaved soon after leukocyte activation. It is important for leukocyte recruitment in post capillary venules and homing to the lymph node. L-selectin counter-ligands are P-selectin glycoprotein ligand-1, CD34 and glycosylated cell adhesion molecule-1 (Ley *et al.*, 2007, Zarbock *et al.*, 2011).

P-selectin is contained both in platelets and endothelial cell Weibel-Palade bodies, translocating to the membrane following stimulation with histamine, oxygen radicals or thrombin (Kansas, 1996). This molecule is important in early inflammation,

interacting with P-selectin glycoprotein ligand 1, facilitating tethering of leukocytes. Neutrophils may adhere to P-selectin on endothelial cells and activated platelets in situation of high shear stress (Kansas, 1996, Ley, 2003).

E-selectin is expressed on endothelial cells following exposure to IL-1, TNF-α and bacterial lipopolysaccharide, and ligands comprise P-selectin glycoprotein ligand 1, CD44 and E-selectin ligand-1 (Ley *et al.*, 2007, Kansas, 1996).

In addition to selectins, some integrins are also important for rolling. Leukocytes roll on immobilised mucosal vascular addressin cell-adhesion molecule-1 (MADCAM-1) and VCAM-1 via the leukocyte VLA-4. Monocytes and lymphocytes typically engage in VLA-4-dependent rolling (Ley *et al.*, 2007).

Intercellular adhesion molecule-1 (ICAM-1) is a β_2-integrin, which in conjunction with E-selectin engenders a conformation of intermediate affinity of lymphocyte function-associated antigen-1 (LFA-1; also known as $\alpha_1\beta_2$-integrin), leading to transient binding to its ligand ICAM-1. LFA-1 can alter its conformation to increase ligand bind affinity under high shear stress (Ley *et al.*, 2007).

The induction of inflammation leads to increase of endothelial E-selectin and ICAM-1, and the slowing down of leukocyte rolling, which requires LFA-1 on lymphocytes or Mac1 (CD11b/CD18 or $\alpha_4\beta_2$-integrin) on myeloid cells as counter-ligands (Ley *et al.*, 2007).

The arrest of leukocytes on the endothelium is initiated by chemoattractants such as chemokines and is mediated via activation of leukocyte integrins, their conformational

changes and subsequent binding to ICAM-1 and VCAM-1 on endothelial cells (Ley *et al.*, 2007). These molecules may be produced by endothelial cells, released by activated platelets or delivered by circulating erythrocytes and microvesicles. Chemokines are the most effective physiological triggers of integrin-mediated leukocyte adhesion, rapidly increasing both integrin affinity and valency for individual cells, and their ligation of cognate GPCRs leads through intracellular pathways to activation of integrins in less than a second (Ley *et al.*, 2007).

1.4 Chemokines

Chemokines (chemotactic cytokines or chemoattractant cytokines) are a superfamily of 7-12kDa glycoproteins. These are present in a monomeric form, and are also able to oligomerise, forming dimers or multimers. Chemokines have essential roles in various functions including angiogenesis, organogenesis and haematopoiesis. In addition there are roles in both homeostasis and disease, particularly relating to leukocyte maturation, trafficking and tissue repair. Almost 50 human chemokines have been described, grouped into four families, CXC, CC, CX3C and XC (see **Figure 1.6**), centred on the relative arrangement of cysteine residues which form disulphide bonds. In the CXC family, an amino acid residue is present between the first two cysteines, whereas in the CC family the two cysteine residues are next to each other. Similarly, in the CX3C family, represented by one molecule only, fractalkine, there are 3 amino acids between the first two cysteines, and in the XC chemokines the first and third cysteine residues are absent, possessing only one disulphide bond. All vertebrates have varying numbers of chemokine genes, with the two major human chemokine gene clusters located on chromosome 4q (CXC) and 17q (CC).

Chemokines may also be classified according to their function and expression. Following from this, inflammatory chemokines are up-regulated during inflammation, with important roles in recruitment of leukocytes to sites of inflammation. Conversely homeostatic chemokines are more typically expressed constitutively and are involved in homing under physiological conditions. The third group of chemokines have both inflammatory and homeostatic functions (Blanchet *et al.*, 2012).

Chemokine	Other Names (Human)	Category	Gene Symbol		Other Names (Mouse)	Receptor	
			Human	Mouse[a]		Agonistic	Antagonistic
CXC Subfamily							
CXCL1	GROα, MGSA	I, ELR	*CXCL1*	*Cxcl3*[b]	Gm1960	CXCR2	
CXCL2	GROβ	I, ELR	*CXCL2*	*Cxcl2*	MIP-2	CXCR2	
CXCL3	GROγ	I, ELR	*CXCL3*	*Cxcl1*[b]	KC	CXCR2	
CXCL4	PF4	Pt, non-ELR	*PF4*	–		CXCR3-B	
CXCL4L1	PF4V1	Pt, non-ELR	*PF4V1*	*Pf4*[b]		CXCR3-B	
CXCL5	ENA78	I, ELR	*CXCL5*	–		CXCR2	
CXCL6	GCP2	I, ELR	*CXCL6*	*Cxcl5*[b]	LIX	CXCR1, CXCR2	
CXCL7	NAP-2	Pt, I, ELR	*PPBP*	*Ppbp*		CXCR1, CXCR2	
CXCL8	IL-8	I, ELR	*IL-8*	–		CXCR1, CXCR2	
CXCL9	MIG	I, non-ELR	*CXCL9*	*Cxcl9*		CXCR3	CCR3
CXCL10	IP-10	I, non-ELR	*CXCL10*	*Cxcl10*		CXCR3	CCR3
CXCL11	I-TAC	I, non-ELR	*CXCL11*	*Cxcl11*		CXCR3, CXCR7	CCR3, CCR5
CXCL12	SDF-1	H, non-ELR	*CXCL12*	*Cxcl12*		CXCR4, CXCR7	
CXCL13	BLC, BCA-1	H, non-ELR	*CXCL13*	*Cxcl13*		CXCR5, CXCR3	
CXCL14	BRAK	H, non-ELR	*CXCL14*	*Cxcl14*		unknown	
–	–	U, non-ELR	–	*Cxcl15*	Lungkine, Weche	unknown	
CXCL16	SR-PSOX	I	*CXCL16*	*Cxcl16*		CXCR6	
CXCL17	DMC	U	*CXCL17*	*Cxcl17*		unknown	
CC Subfamily							
CCL1	I-309	I	*CCL1*	*Ccl1*	TCA-3	CCR8	
CCL2	MCP-1	I	*CCL2*	*Ccl2*	JE	CCR2	
CCL3	MIP-1α, LD78α	I	*CCL3*	*Ccl3*		CCR1, CCR5	
CCL3L1	LD78β	I	*CCL3L1*	–		CCR1, CCR3, CCR5	
CCL3L3	LD78β	I	*CCL3L3*	–			
CCL4	MIP-1β	I	*CCL4*	*Ccl4*		CCR5	
CCL4L1	AT744.2	I	*CCL4L1*	–			
CCL4L2	–	I	*CCL4L2*	–			
CCL5	RANTES	I, Pt	*CCL5*		Ccl5	CCR1, CCR3, CCR5	
CCL7	MCP-3	I	*CCL7*	*Ccl7*	MARC	CCR1, CCR2, CCR3	CCR5
CCL8	MCP-2	I	*CCL8*	–		CCR1, CCR2, CCR5	
–	–	I		*Ccl8*[b]		CCR8 (mouse)	
CCL11	Eotaxin	D	*CCL11*	*Ccl11*		CCR3, CCR5	CXCR3, CCR2
–	–	I	–	*Ccl12*	MCP-5		
CCL13	MCP-4	I	*CCL13*	–		CCR2, CCR3	
CCL14	HCC-1	P	*CCL14*	–		CCR1, CCR3, CCR5	
CCL15	HCC-2, Leukotactin-1	P	*CCL15*	*Ccl9*[b]	CCF18, MIP-1γ	CCR1, CCR3	
CCL16	LEC, HCC-4	U	*CCL16*	–		CCR1, CCR2, CCR5, CCR8, H4	
CCL17	TARC	D	*CCL17*	*Ccl17*	ABCD-2	CCR4	
CCL18	PARC, DC-CK1	H	*CCL18*	–		PITPNM3	CCR3
CCL19	MIP-3β, ELC	H	*CCL19*	*Ccl19*		CCR7	
CCL20	MIP-3α, LARC	D	*CCL20*	*Ccl20*		CCR6	
CCL21	SLC, 6Ckine	H	*CCL21*	*Ccl21a*		CCR7	CXCR3 (mouse)
–	–	H	–	*Ccl21b*		CCR7	
–	–	H	–	*Ccl21c*		CCR7	
CCL22	MDC	D	*CCL22*	*Ccl22*	ABCD-1	CCR4	

(Continued next page)

Chemokine	Other Names (Human)	Category	Gene Symbol Human	Gene Symbol Mouse[a]	Other Names (Mouse)	Receptor Agonistic	Receptor Antagonistic
CCL23	MPIF-1	P	*CCL23*	*Ccl6*[b]	C10	CCR1, FPRL-1	
CCL24	Eotaxin-2, MPIF-2	H	*CCL24*	*Ccl24*		CCR3	
CCL25	TECK	H	*CCL25*	*Ccl25*		CCR9	
CCL26	Eotaxin-3	I	*CCL26*	(*Ccl26*)		CCR3, CX3CR1	CCR1, CCR2, CCR5
CCL27	CTACK, ILC	H	*CCL27*	*Ccl27a*		CCR10	
-	-	H	-	*Ccl27b*			
CCL28	MEC	H	*CCL28*	*Ccl28*		CCR10, CCR3	
XC Subfamily							
XCL1	Lymphotactin, ATAC, SCM-1α	D	*XCL1*	*Xcl1*	lymphotactin	XCR1	
XCL2	SCM-1β	D	*XCL2*	–		XCR1	
CX3C Subfamily							
CX3CL1	Fractalkine	D	*CX3CL1*	*Cx3cl1*	fractalkine, neurotactin	CX3CR1	

Figure 1.6 Chemokines and respective chemokine receptors.
Abbreviations: I, inflammatory chemokines; H, homeostatic chemokines; D, dual chemokines; P, plasma or platelet chemokines that are activated by cleavage; Pt, platelet chemokines; U, unknown. H4, histamine receptor type 4; PITPNM3, phosphatidylinositole transfer protein membrane associated 3; FPRL-1, formyl peptide receptor like-1.
[a]Genes in parentheses are not expressed.
[b]Mouse gene whose human counterpart was reassigned after syntenic analysis.
Adapted from Zlotnik and Yoshie, 2012

1.5 Chemokine receptors

Chemokines exert their effects by binding to cognate receptors present on the cell surface, and are grouped into the four families based on the chemokine that they bind. All the classical chemokine receptors are 7 transmembrane domain G-protein-coupled receptors, which couple the receptor to the G-protein subunit. Eighteen human chemokine receptors are described, having first appeared in the earliest vertebrates. Approximately half of the described human chemokine receptors are located on chromosome 13 (Blanchet *et al.*, 2012). In addition to the classical receptors, several alternative chemokine receptors, termed atypical chemokine receptors (ACKR), bind numerous chemokines without signal transduction via G-proteins. ACKRs comprise the Duffy antigen receptor for chemokines (DARC, ACKR1), D6 (CCBP2, ACKR2), CXCR7 (ACKR3), CCRL1 (CCX-CKR, ACKR4) and CCRL2 (tentatively ACKR5) (Nibbs and Graham, 2013), see **Figure 1.7**.

The chemokine receptors of inflammatory chemokines tend to have large numbers of chemokine ligands, with some ligands shared by multiple receptors. It was suggested that significant promiscuity in the interaction between chemokines and their receptors meant redundancy of their function and permits robustness within the system allowing leukocyte recruitment to occur despite the loss of function of one particular chemokine (Mantovani, 1999). Investigators have however shown that neutralisation of a particular chemokine may rapidly suppress chronic inflammation, suggesting that different ligands binding the same GPCR induce different biological activities. On the other hand, a single ligand binding to its receptor may lead to different signalling

cascades, although the mechanisms of this action are still under investigation (Zohar *et al.*, 2014). The implication is that there is no redundancy of chemokines, in that unique recognition of each chemokine by the system of receptors, with differential affinity and nature of responses after ligation of the same receptor by different chemokines, leads to opposite outcomes.

Human Gene Symbol	Other Names	Category	Mouse Gene Symbol	Ligands	
				Agonistic	Antagonistic
CXCR Subfamily					
CXCR1	IL-8RA	I	*Cxcr1*	CXCL6, CXCL7, CXCL8, acPGP	
CXCR2	IL-8RB	I	*Cxcr2*	CXCL1, CXCL2, CXCL3, CXCL5, CXCL6, CXCL7, CXCL8, acPGP, MIF	
CXCR3	GPR9	I	*Cxcr3*	CXCL4 (CXCR3-B), CXCL9, CXCL10, CXCL11, CXCL13, CCL21 (mouse)	CCL11
CXCR4	LESTER, Fusin	H	*Cxcr4*	CXCL12, MIF, ubiquitin	
CXCR5	BLR1	H	*Cxcr5*	CXCL13	
CXCR6	STRL33, BONZO	H	*Cxcr6*	CXCL16	
CCR Subfamily					
CCR1	CC-CKR-1	I	*Ccr1*	CCL3, CCL3L1, CCL5, CCL7, CCL8, CCL13, CCL14, CCL15, CCL16, CCL23	CCL26
CCR2	CC-CKR-2	I	*Ccr2*	CCL2, CCL7, CCL8, CCL13, CCL16, β-defensin 2,3	CCL11, CCL26
CCR3	CC-CKR-3	I	*Ccr3*	CCL3L1, CCL5, CCL7, CCL11, CCL13, CCL14, CCL15, CCL24, CCL26, CCL28	CXCL9, CXCL10, CXCL11, CCL18
CCR4	CC-CKR-4	D	*Ccr4*	CCL17, CCL22	
CCR5	CC-CKR-5	I	*Ccr5*	CCL3, CCL3L1, CCL4, CCL4L1, CCL5, CCL8, CCL11, CCL16	CCL7, CXCL11, CCL26
CCR6	STRL22, GPR29	I	*Ccr6*	CCL20, β-defensin-2	
CCR7	EBI1, BLR2	H	*Ccr7*	CCL19, CCL21	
CCR8	TER1, GPR-CY6	H	*Ccr8*	CCL1, CCL8 (mouse)	
CCR9	GPR-9-6	H	*Ccr9*	CCL25	
CCR10	GPR2	H	*Ccr10*	CCL27, CCL28	
XCR Subfamily					
XCR1	GPR-5	D	*Xcr1*	XCL1, XCL2	
CX3CR Subfamily					
CX3CR1	V28, GPR13	D	*Cx3cr1*	CX3CL1, CCL26 (human)	
Atypical (Nonchemotactic, Recycling or Scavenger Receptors)					
CXCR7	RDC1, GPR159		*Cxcr7*	CXCL11, CXCL12	
CCBP2	D6		*Ccbp2*	CCL2, CCL3, CCL3L1, CCL4, CCL4L1, CCL5, CCL7, CCL8, CCL11, CCL12, CCL13, CCL14, CCL17, CCL22, CCL23, CCL24	
CCRL1	CCX-CKR		*Ccrl1*	CCL19, CCL21, CCL25, CXCL13	
CCRL2	HCR, CRAM		*Ccrl2*	CCL19, chemerin	
DARC	Duffy		*Darc*	CXCL1, CXCL2, CXCL3, CXCL7, CXCL8, CCL2, CCL5, CCL11, CCL13, CCL14, CCL17	

Figure 1.7 Chemokine receptors and their known ligands.
Abbreviations: acPGP, N-acetyl Pro-Gly-Pro; MIF, macrophage migration inhibitory factor
From Zlotnik and Yoshie, 2012

1.6 Chemokines in leukocyte trafficking

Leukocyte migration is a central component in immune responses and inflammatory conditions. Chemokines lead to intravascular adhesion of leukocytes to endothelial cells, and direct interstitial leukocyte migration as well as assisting location of leukocytes in healthy and inflamed tissues. The diversity of chemokines, their tissue location, patterns of expression and the timing of appearance allows exquisite fine tuning of cellular immune responses (Luster *et al.*, 2005). The switch from leukocyte rolling to firm adhesion and activation is initiated by inflammatory chemokines such as CXCL1, leading to an increase in integrin affinity. Other chemokines such as CCL2 promote transmigration of leukocytes (Blanchet *et al.*, 2012).

Chemokines are produced by a wide variety of cells, from mesenchymal stem cells, circulating leukocytes and platelets, to endothelial cells. Cognate ligand chemokines bind chemokine receptors expressed on leukocytes to induce activation. Pro-inflammatory chemokines circulate in plasma or are limited only to inflamed tissue. In order to support transendothelial migration inflammatory chemokines are transported in a luminal direction across endothelial cells by DARC (Pruenster *et al.*, 2009). A further mechanism recently proposed that lymphocytes can cross inflamed endothelium through uptake of chemokines stored in intraendothelial vesicles and released within synapses formed between endothelial cells and lymphocytes, without the presence of surface-bound chemokines or chemokine gradients (Shulman *et al.*, 2012). In addition, most chemokines can bind extracellular matrix components, including glycosaminoglycans (GAGs), being immobilised and presented to

leukocytes. This avoids chemokines being swept away under flow conditions from the cell surface. This co-immobilization with adhesion molecules will promote leukocyte activation, adhesion, and migration.

1.7 Chemokines and chemokine receptors in haematopoiesis

Chemokines and their receptors have critical roles in the maintenance of normal haematopoiesis, and in the mobilisation of leukocytes during periods of acute need. As discussed above, the CXCL12/CXCR4 axis has an indispensable role in retaining HSCs in the stem cell niche, and in maintaining their quiescence. The ELR+chemokines/CXCR2 axis in contrast is required for acute leukocyte mobilisation from the bone marrow reserve, as detailed above. Given the clinical importance in mobilisation of haematopoietic progenitors for transplantation, this aspect of chemokine biology in haematopoiesis has received considerable attention in the literature.

A number of mechanisms for regulating availability of CXCL12 have been described. The primary receptor for CXCL12, CXCR4, is highly expressed on the HSCs. It has been known for some time that the atypical chemokine receptor CXCR7 binds CXCL12 and degrades it, acting as a sink for CXCL12 (Luker *et al.*, 2010). Despite evidence that CXCR7 is expressed on endothelial cells, and has roles in embryonic development, the function of CXCR7 in the bone marrow has not been explored until recently. Initial studies in CXCR7 deficient mice have shown a crucial role for this receptor in B cell, endothelial and cardiac development but these mice have no obvious haematopoietic phenotype (Sierro *et al.*, 2007). CXCR7 is present in low levels on the cell surface of monocytes and lymphocytes (Balabanian *et al.*, 2005, Sanchez-Martin *et al.*, 2011). In HSCs it is abundant intracellularly (Hartmann *et al.*, 2008), but only recently has its presence on bone marrow $CD34^+$ HSCs cell surface

been confirmed (Torossian *et al.*, 2014). CXCR7 binds CXCL12, and together with CXCR4, promotes the effects of CXCL12. This occurs via β-arrestin which is considered to function as a scaffold protein for modulating signal transduction. Both CXCR4 and CXCR7 activation were necessary for β-arrestin to phosphorylate Akt, leading to activation of the PI3k/Akt pathway (Torossian *et al.*, 2014).

Several chemokine receptors are used by pathogens to infect haematopoietic cells. CXCR4 is utilised by HIV-1 to infect HSC and it is suggested that this would provide a source of long-term reservoir of latent virus (Carter *et al.*, 2011).

Roles for several chemokines leading to HSC mobilisation have been described. The first chemokine studied in respect of HSC mobilisation was human CCL3 (MIP-1α), which stimulated the mobilisation of HSCs in mice, but subsequent clinical trials showed modest mobilisation with a genetically engineered variant of human CCL3 (Lord *et al.*, 1995, Broxmeyer *et al.*, 1998). CXCL8 can induce stem cell mobilisation in mice and rhesus monkeys in hours by activating MMP-9 and LFA-1, although the role of MMP-9 as stated above may be redundant since CXCL8 induces mobilisation in MMP-9 deficient mice (Laterveer *et al.*, 1995, Robinson *et al.*, 2003). An additional feature of mobilisation by chemokines is that the mobilisation effect is greater when combined with G-CSF, compared to mobilisation with either chemokine or G-CSF alone (Broxmeyer *et al.*, 1999a).

Chemokines also have roles apart from retaining or mobilising HSCs and leukocytes. One of the first described roles for chemokines in haematopoiesis related to suppression of myelopoiesis by CCL3, a ligand for CCR1 and CCR5, manifest as

reduced myeloid proliferation both in vitro (Graham *et al.*, 1990) and following injection of recombinant murine CCL3 into normal mice (Maze *et al.*, 1992). CCL3 also gives protection to primitive cells from chemotherapeutic agents (Lord, 1995). An example of malignant cells harnessing this effect has been shown in a murine model of chronic myeloid leukaemia where high CCL3 levels produced by leukaemic cells help to maintain and promote leukaemic cell growth in the bone marrow while mobilising normal HSC from the bone marrow (Baba *et al.*, 2013).

Several other chemokines have been shown in vitro and in vivo to have suppressive effects on bone marrow myeloid cells (see **Table 1.1**)

It is not clear why such a large number of chemokines should have this suppressive effect, although it has been suggested that this may reflect the different cell origins of these chemokines, and the need to control cell proliferation in the different sites of action (Youn *et al.*, 2000). CXCL12 has been shown to protect HSC from the effects of these chemokines, but not against other haematopoietic suppressing cytokines such as TNF-α, IFN-γ, TGF-β or lactoferrin (Broxmeyer *et al.*, 2005a). In addition to the mobilising effects of ELR+chemokines/CXCR2 axis, other researchers have confirmed the proliferation suppressing effects of CXCL8 and CXCL1 (Sanchez *et al.*, 1998). In contrast, in addition to myelo-suppressive effects, CCL2 binding to CCR2 promotes the survival of myeloid progenitor cells (Reid *et al.*, 1999).

More recent work has shown that some of the chemokines listed in **Table 1.1** have functions which might not be discerned by in vitro co-culture of bone marrow with chemokines or their injection into mice. For example, rather than having no effect on

haematopoiesis, CCL5 has been shown to be more highly expressed in the aged murine bone marrow, and forced over-expression of CCL5 leads to pro-myeloid HSC differentiation possibly through increased mTOR signalling in LSK cells (Ergen *et al.*, 2012).

Suppressive effects on myelopoiesis		No effect
CCL1	CCL20	CCL4
CCL2	CCL21	CCL5
CCL3	CCL23	CCL7
CCL6	CCL24	CCL8
CCL9	CCL25	CCL17
CCL10	CXCL2	CCL22
CCL11	CXCL4	CXCL1
CCL12	CXCL5	CXCL3
CCL13	CXCL6	CXCL7
CCL15	CXCL8	CXCL12
CCL16	CXCL9	CX3CL1
CCL18	CXCL10	
CCL19	XCL1	

Table 1.1 Documented chemokine effects on myelopoiesis, in vitro or in vivo.
Adapted from (Broxmeyer and Kim, 1999, Broxmeyer *et al.*, 1999b)

Utilising CCL3 as an example chemokine, it is clear that chemokines have diverse actions leading to inhibition or promotion of proliferation of different subpopulations of myeloid progenitor cells, inhibition of stem cells and mobilisation of stem cells. It binds to both CCR1 and CCR5, but it remains unclear which of these receptors mediates the different CCL3 responses (de Wynter *et al.*, 2001), particularly since both receptors are present in $CD34^{+}$ bone marrow derived cells (de Wynter *et al.*, 1998).

1.8 The atypical chemokine receptors (ACKR)

The ACKR have recently been assigned a new nomenclature numbering them in the sequence of their discovery: the Duffy Antigen Receptor for Chemokines (DARC), ACKR1; D6, ACKR2; CXCR7, ACKR3; and CCRL1, also known as CCR11 and CCX-CKR, ACKR4 (Bachelerie *et al.*, 2014); however, because a large part of the thesis was written and figures produced before the introduction of the new nomenclature, within this text and in the figures the old previous naming convention will be used.

Whilst DARC binds up to 20 CXC and CC chemokines, D6 is also promiscuous, binding at least 12 CC human chemokines. The affinity of chemokines for DARC or D6 vary, and both receptors modulate the availability of inflammatory chemokines and thus affect leukocyte trafficking. CCRL1 binds the homeostatic CCL19, CCL21 and CCL25, and CCRL2 binds chimerin, although affinity for other ligands remains controversial. CXCR7 binds CXCL11 and CXCL12, the latter with higher affinity. CXCL12 has a higher affinity for CXCR7 than for CXCR4, its sole signalling receptor.

A common aspect across ACKRs is their serpentine structure with seven transmembrane domains, akin to that of classical chemokine receptors, but absence of critical sequence determinants, the DRYLAIV motif, required for coupling to G-proteins and downstream calcium-fluxed based signalling (Nibbs and Graham, 2013). Three members of the ACKR family (D6, CCRL1 and CXCR7) will be examined briefly, and in a separate section, DARC will be reviewed in greater detail.

1.8.1 D6 (ACKR2)

D6 is expressed in leukocytes such as B cells, of the spleen and those residing in body cavities. It has also been shown to be expressed on some DCs, monocytes, T cells and neutrophils. In addition, D6 is expressed on lymphatic endothelial cells lining the lymphatics of the skin, gut, lungs and lymph nodes. Interestingly, the highest expression in human is within the placental trophoblasts, in contact with maternal blood. Hepatocytes express this receptor, and it is upregulated in skin keratinocytes in psoriasis.

D6 constitutively traffics from the intracellular stores to the cell surface, where it captures chemokines, internalises them to target the chemokine cargo for lysosomal degradation, after which D6 is returned to the surface of the cell.

Overall the main function of D6 is clearing inflammatory CC chemokines as for example from lymphatic endothelial cell surfaces during inflammation, suppressing the interaction of these cells with immature DCs which have been recruited and are expressing inflammatory CC chemokine receptors (Nibbs and Graham, 2013).

1.8.2 CXCR7 (ACKR3)

CXCR7 is activated by its ligands CXCL11 and CXCL12 and induces β-arrestin mediated intracellular signalling in the absence of G-protein-mediated Ca^{2+} associated signalling (Zabel *et al.*, 2009). Moreover CXCR7 regulates the localisation and signalling of CXCR4, and a scavenging function for CXCR7 akin to that of D6 has been put forward (Naumann *et al.*, 2010). CXCR7 expression is present on vascular

endothelial cells in the brain, tumours, during inflammation and in embryonic life (Sierro *et al.*, 2007, Goguet-Surmenian *et al.*, 2013). Lymphatic endothelial cells may express CXCR7 in the tonsils or kidneys in acute allograft rejection (Neusser *et al.*, 2010).

CXCR7 has been detected in the inflamed synovia of rheumatoid arthritis patients, and in murine arthritis models. CXCR7-antagonist treated animals with experimental arthritis developed less neovascularisation, implying a role for this ACKR in angiogenesis. Within the CNS CXCR7 enhances the movement of leukocytes into the brain parenchyma (Nibbs and Graham, 2013).

1.8.3 CCRL1 (ACKR4)

CCRL1 internalises its ligands CCL19, CCL21 and CCL25, a process leading to their lysosomal degradation. It is expressed on lymphatic endothelial cells but is restricted to those lining the ceiling of the subcapsular sinus of resting lymph nodes (Ulvmar *et al.*, 2014). Furthermore CCRL1 is expressed by cortical thymic epithelial cells and keratinocytes (Nibbs and Graham, 2013). CCRL1 within the skin controls the distribution of its ligands and hence aids DC migration, while in the lymph node it modulates the distribution of its ligands to pattern functional chemokine gradients to preserve receptor responsiveness to chemokine signals for peak CCR7-directed migration into the lymph node (Ulvmar *et al.*, 2014). Its role in the thymus appears to be that of controlling lymphocyte maturation and selection process, as CCRL1-deficient mice spontaneously develop autoimmunity (Nibbs and Graham, 2013).

1.9 The Duffy Antigen Receptor for Chemokines (ACKR1)

The content of this section has been reviewed in part by the author previously in Novitzky-Basso and Rot, 2012, and others (Ulvmar *et al.*, 2011, Pruenster and Rot, 2006).

1.9.1 The Duffy blood group

The Duffy antigen / receptor for chemokines (DARC) was first described as a blood group determinant in 1950 (Cutbush and Mollison, 1950, Cutbush *et al.*, 1950) in the investigation of a multiply transfused eponymous haemophiliac (Mr Duffy) who had developed a delayed haemolytic transfusion reaction due to a previously unknown antibody, termed anti-Fy^a, detectable only by the indirect anti-globulin test (IAT). In the following year, an antibody to the second antithetical antigen of the new blood group, Fy^b, was found in a multigravida having presumably been exposed to foetal Fy^b erythrocytes (Ikin *et al.*, 1951). None of her children had shown any features of haemolytic disease of the foetus or new-born (HDFN). In due course, three phenotypes were described: Fy(a+b–), Fy(a–b+) and Fy(a+b+), sometimes referred to as 'Duffy-positive', arising from combinations of the antithetical co-dominant *FYA* and *FYB* genes which have frequencies of 0.425 and 0.557 (Klein and Anstee, 2005). In several human populations neither Fy^a nor Fy^b antigens are expressed, with the phenotypic designation Fy(a–b–) (or 'Duffy-negative'). This results from a polymorphic form of the *FYB* gene, termed *FYB(ES)*, or "erythroid silent", present in up to 99% of West Africans and the majority of African Americans (68%) (Mourant *et al.*, 1976).

1.9.2 The DARC gene and gene expression

The Duffy gene, termed *DARC*, is located on chromosome 1, position 1922 and segregates with *Un* locus, and was the first gene in humans allocated to an autosome (Donahue RP, 1968). Initial sequencing of the corresponding cDNA revealed a glycoprotein of 338 amino acids (Chaudhuri *et al.*, 1993) and was considered to be encoded by a single exon (Chaudhuri *et al.*, 1993, Chaudhuri *et al.*, 1995, Iwamoto *et al.*, 1995, Tournamille *et al.*, 1995); subsequently it became clear that in all examined tissues the principal transcript of the Fy gene represented two exons interleaved with a 479 base pair intron, and that the protein consisted of 336 amino acids (Iwamoto *et al.*, 1996). The first exon encodes a methionine codon initiating translation, and the seven N-terminal amino acids, giving the sequence MGNCLHRAEL for the major transcript (Iwamoto *et al.*, 1996). The minor transcript encodes MASSGYVLQAEL which is two amino acids longer (Chaudhuri *et al.*, 1993), as the sequence which encodes the 9 N-terminal amino acids is in fact part of the intron of the major transcript (Iwamoto *et al.*, 1996). As there is more than one transcript, in this thesis, nucleotides and amino acids will be numbered from the methionine residue of the first transcript where translation is initiated, unless otherwise stated (as in Chapter 8, 'Duffy blood group system', in Daniels, 2002).

Following the first exon of the *DARC* gene, there is a consensus splice donor sequence, the intron and subsequently the second exon containing the majority of the open reading frame (Iwamoto *et al.*, 1996). The two principle alleles *FYA* and *FYB* differ in one base substitution (125 G to A) in codon 42 in the NH_2 extracellular domain,

encoding glycine in Fy^a and aspartic acid in Fy^b (Chaudhuri *et al.*, 1995, Iwamoto *et al.*, 1995), while the *FYB(ES)* allele has a single T to C substitution at nucleotide *-67*, 33bp upstream from the erythroid transcription starting point and 46bp upstream from the start of the major transcript translation codon, within the erythroid GATA-1 promoter region of the *FYB* allele, terminating transcription in erythroid cells only (Tournamille *et al.*, 1995). This mutation (SNP *rs2814778*) will henceforth be termed T-*46*C as it is used frequently in the literature (Tournamille *et al.*, 1995). The major erythroid transcription starting point was identified at 33 base pairs upstream from the first ATG. In RNA from kidney and lung tissue, the transcription is initiated 82 base pairs upstream from the ATG (Iwamoto *et al.*, 1996). This may explain in part the different transcription patterns seen in erythroid tissues compared with other tissues, possibly allowing differential regulation in response to inflammation. Confirming this, RNA blot analysis detects 1267bp mRNA in the bone marrow of Duffy-positive but not Fy(a–b–) individuals (Chaudhuri *et al.*, 1995). The same size mRNA is identified in most extra-erythroid tissues (Chaudhuri *et al.*, 1993, Neote *et al.*, 1994); however in brain, a prominent 7.5kb and minor 1.35kb mRNA were detected (Chaudhuri *et al.*, 1993). In the cerebellum the 7.5kb transcript is highly expressed, whereas the 1.35kb transcript was prominent in the spinal cord; in other parts of the brain both transcripts are poorly expressed (Le Van Kim *et al.*, 1997). However, the DARC glycoprotein expressed in the cerebellum is identical to forms in other tissues encoded by the 1.35kb transcript. Here it is likely a different promoter leads to a larger transcript in the 5' untranslated sequence although the final protein is the same (Le Van Kim *et al.*, 1997). Finally, tissue localisation and degree of extra-

erythroid DARC expression is similar across *FYA*, *FYB* and *FYB(ES)* genotypes (Chaudhuri *et al.*, 1995, Chaudhuri *et al.*, 1997). *FYB(ES)* Fy(a–b–) individuals still express DARC at non-erythroid sites, particularly on post-capillary venules of all tissues, and other sites such as Purkinje cells, and renal and alveolar epithelium (Peiper *et al.*, 1995, Horuk *et al.*, 1997, Chaudhuri *et al.*, 1997). The importance of this site-specific loss of DARC expression was demonstrated when Miller and colleagues revealed in 1976 that volunteers with Fy(a–b–) phenotype exposed to the bites of *Plasmodium vivax*-infected mosquitoes did not develop malaria (Miller *et al.*, 1976), in contrast to their Duffy positive counterparts, thus confirming the long standing clinical observation that African populations appeared resistant to this form of malaria, noted particularly during the treatment of neurosyphilis by therapeutic *P. vivax* inoculation (Boyd and Stratman-Thomas, 1933, O'Leary, 1927). Further work showed that this parasite requires DARC for entry into the erythrocytes (Horuk *et al.*, 1993a, Miller *et al.*, 1975), leading to the hypothesis that the Fy(a–b–) phenotype evolved as a result of selective pressure to protect its carriers from vivax but not falciparum malaria (see **Figure 1.8**).

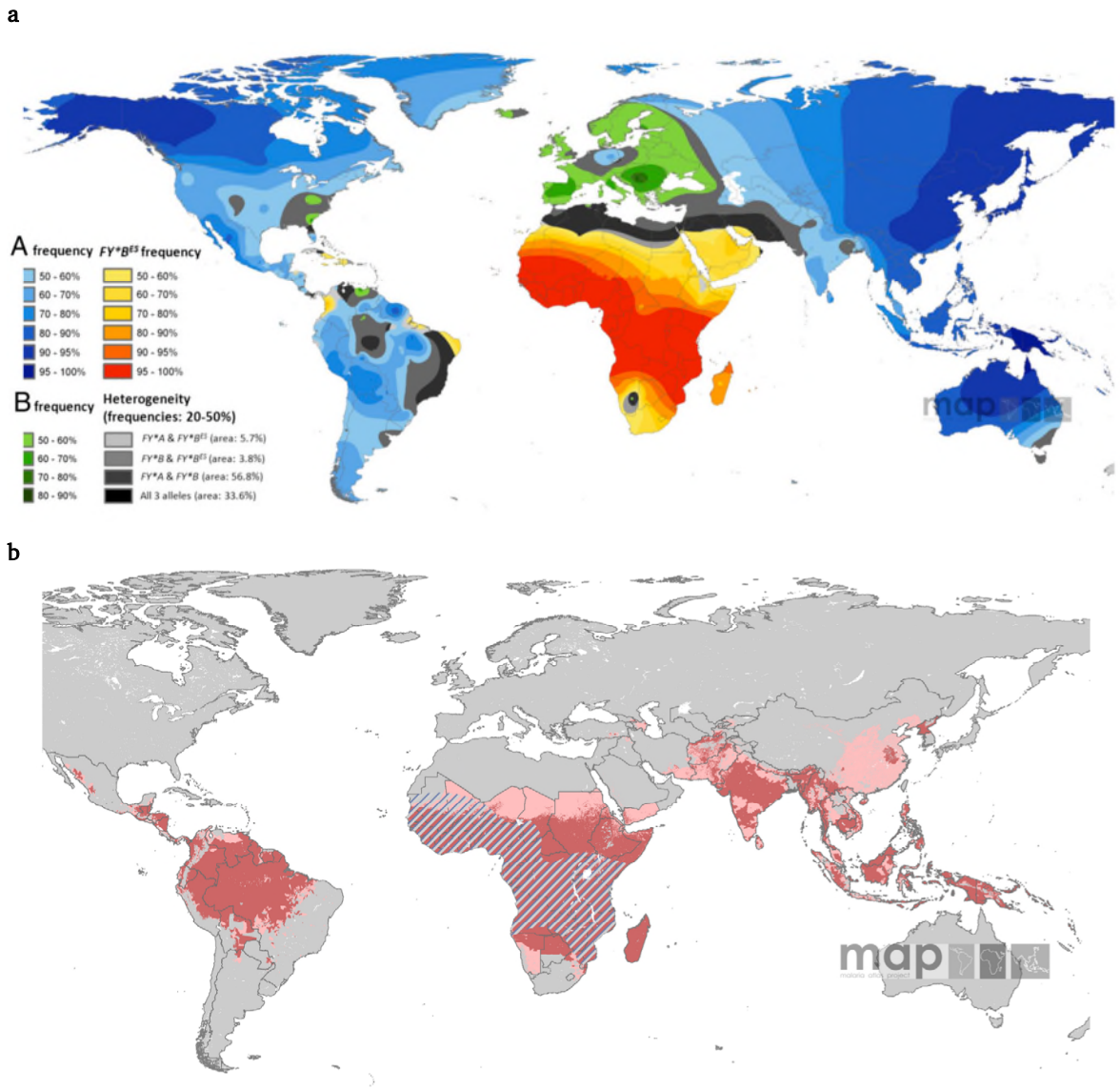

Figure 1.8 Global DARC allele and malaria distribution. a) Global frequencies of DARC alleles. Areas a single allele is dominant are represented by a colour gradient (blue, *FYA*, green, *FYB*, red/yellow, *FYB(ES)*). Areas in which no allele predominates, and 2 or more alleles each have frequencies >20% are in grey-scale. From King *et al.*, 2011.
b) The global distribution of *P. vivax* malaria transmission in 2009. Risk areas: pale pink, low risk; dark pink/red, high risk; and hatched area, predicted Duffy negativity >90%. From Guerra *et al.*, 2010.

Recent geostatistical modelling maps demonstrating Fy(a–b–) populations (Howes *et al.*, 2011) where the prevalence of this phenotype approaches 1 in West Africa, have approximate overlap with areas of expected but absent *P. vivax* infection (Guerra *et al.*, 2010). However it appears that this resistance is not complete, as some Fy(a–b–)

populations in Madagascar (Menard *et al.*, 2010), both carry parasites asymptomatically and experience symptomatic vivax malaria. Researchers in the Brazilian state of Pará found that *P. vivax* resistance between Duffy-positive and –negative individuals was not different, although the power to detect this was low owing to only 4.3% individuals harbouring *FYB(ES)*. Other researchers have noted similar findings, (Ryan *et al.*, 2006, Cavasini *et al.*, 2007b), while a larger PCR-based study examining 9 African countries with over 2500 samples reported only one positive individual, who was also Duffy-positive (Culleton *et al.*, 2008). However *P. vivax* remains transmissible in these areas given the reports of European individuals contracting *P. vivax* malaria on returning from travel in these areas (Phillips-Howard *et al.*, 1990, Mendis *et al.*, 2001). Therefore the study in Madagascar is of particular interest since greater lengths were taken to validate PCR-positivity of *P. vivax* also by microscopy. Indeed, the first observation confirming Duffy-independent *P. vivax* blood infection and development was reported in this study. In addition, analysis of the *DARC* gene DNA sequence confirmed that the Duffy-negative allele isolated in Madagascar was identical to the *FYB(ES)* allele present in West African subjects. Finally, other Duffy-negative people in Ethiopia (Woldearegai *et al.*, 2013) Mauritania (Wurtz *et al.*, 2011), Equatorial Guinea and Gabon (Mendes *et al.*, 2011) have been found to be *P. vivax* positive by PCR analysis.

Remarkably an *FYA* polymorphism with the T-*46*C change, identical to that in *FYB(ES)*, has been observed in Papua New Guinea, in an area endemic for *P. vivax*. This mutation leads to reduced Fy^a expression and consequent resistance to vivax

malaria infection (Zimmerman *et al.*, 1999, Shimizu *et al.*, 2000, Kasehagen *et al.*, 2007).

The susceptibility of individuals to *P. vivax* based on common DARC genotypes has been examined more recently. When compared to the *FYA/FYB* genotype, individuals with the *FYA/FYB(ES)* and *FYA/FYA* genotypes have 80% and 29% reduced risk of clinical disease due to vivax malaria, respectively. In keeping with the stronger affinity between the FyB variant of DARC and *P. vivax* Duffy binding protein, subjects with the *FYB/FYB(ES)* and *FYB/FYB* genotypes had a 220–270% increased risk of clinically apparent vivax malaria when compared to *FYA/FYB* and *FYB/FYB* (King *et al.*, 2011), and no association between *DARC* genotype and susceptibility for *P. falciparum* was detected. Supporting these data, Cavasini *et al.*, 2007a noted the *FYA/FYB(ES)* genotype was found to be less frequent among patients with *P. vivax* than among 330 healthy blood donors. It appears that like the *FYB(ES)* allele, *FYA* has increased in frequency in *P. vivax* endemic regions (leading to very high frequency in some populations) possibly selected by the higher resistance against *P. vivax* malaria (King *et al.*, 2011).

Other genes described altering Fy expression include a C*265*T mutation in *FYB* leading to the *FYX* allele and resulting in the "Fy^b weak" phenotype, with a 90% reduction in the expression of Fy protein on erythrocytes (Tournamille *et al.*, 1998), and associated with a gene frequency of approximately 2.5% in Caucasians (Olsson *et al.*, 1998). The G*298*A mutation leading to the Ala100Thr polymorphism has been noted to have a relatively high allelic frequency of 16.5% amongst Caucasian donors,

although it does not affect antigenic expression. This was not detected amongst any samples from black South Africans (Olsson *et al.*, 1998).

As indicated above, Fy^a and Fy^b antigen frequencies amongst human populations vary. In the Far East, Fy^a is approximately 90% prevalent, whereas Fy^b prevalence is less than 10% (Lewis *et al.*, 1957, Shimizu *et al.*, 2000). In contrast Fy^b is more common in Europeans than Fy^a (Chown *et al.*, 1965, Lewis *et al.*, 1972). Due to racial admixture, after the Fy(a–b–) phenotype, Fy^b is also expressed in African, African American and African European populations although clearly much less frequently than among Europeans.

1.9.3 The nature of Fy antigens and DARC structure

DARC is modelled as a hepta-spanning transmembrane glycoprotein (Neote *et al.*, 1994) consisting of 336 amino acids with a total molecular weight of 35733 (Chaudhuri *et al.*, 1993) (See **Figure 1.9**). DARC was originally predicted to have 9 trans-membrane domains (Chaudhuri *et al.*, 1993), but it became clear that like other chemokine receptors there are seven α-helices as transmembrane domains (Neote *et al.*, 1994). An amino-terminal extracellular domain of 65 amino acids harbours 3 potential *N*-glycosylation sites at residues 16, 27 and 33 (Czerwinski *et al.*, 2007), as well as epitopes Fy^a, Fy^b and Fy6 (Tournamille *et al.*, 2003). Fy^a and Fy^b epitopes are destroyed by enzyme treatment with papain but not trypsin (Morton, 1962, Klein and Anstee, 2005), and Fy^a is inactivated by neuramidase (Hadley *et al.*, 1986). Fy antigens appear to elute from red cells during their storage (Williams *et al.*, 1981),

possibly consistent with observations detecting red cell microparticles with Fy expression in blood (Oreskovic *et al.*, 1992, Xiong *et al.*, 2010). The number of Fy^a antigens is approximately 13300 per Fy(a+b–) erythrocyte, whilst on each Fy(a+b+) erythrocyte there are an estimated 6900 Fy^a antigens (Masouredis *et al.*, 1980). Reticulocytes have up to 49% higher Fy antigen expression compared with mature red cells (Woolley *et al.*, 2000). Fy(a–b–) cells lack complete expression of both Fy^a and Fy^b, as well as of Fy3 and Fy6, having initially been defined by sera of sensitised Fy(a-b-) humans and a mouse monoclonal antibody (Nichols *et al.*, 1987), respectively. Proteolytic enzyme treatment of red cells enhances the reactivity of Fy3, whereas Fy6, like Fy^a and Fy^b, is susceptible to degradation by this process (Klein and Anstee, 2005).

The Fy6 antigen is present within the region of residues Q19 and W26, where the *P. vivax* Duffy binding protein (cystein-rich region II) has been demonstrated to bind; hence anti-Fy6 antibodies have been shown to inhibit the invasion of human erythrocytes by *P. vivax* (Tournamille *et al.*, 2005).

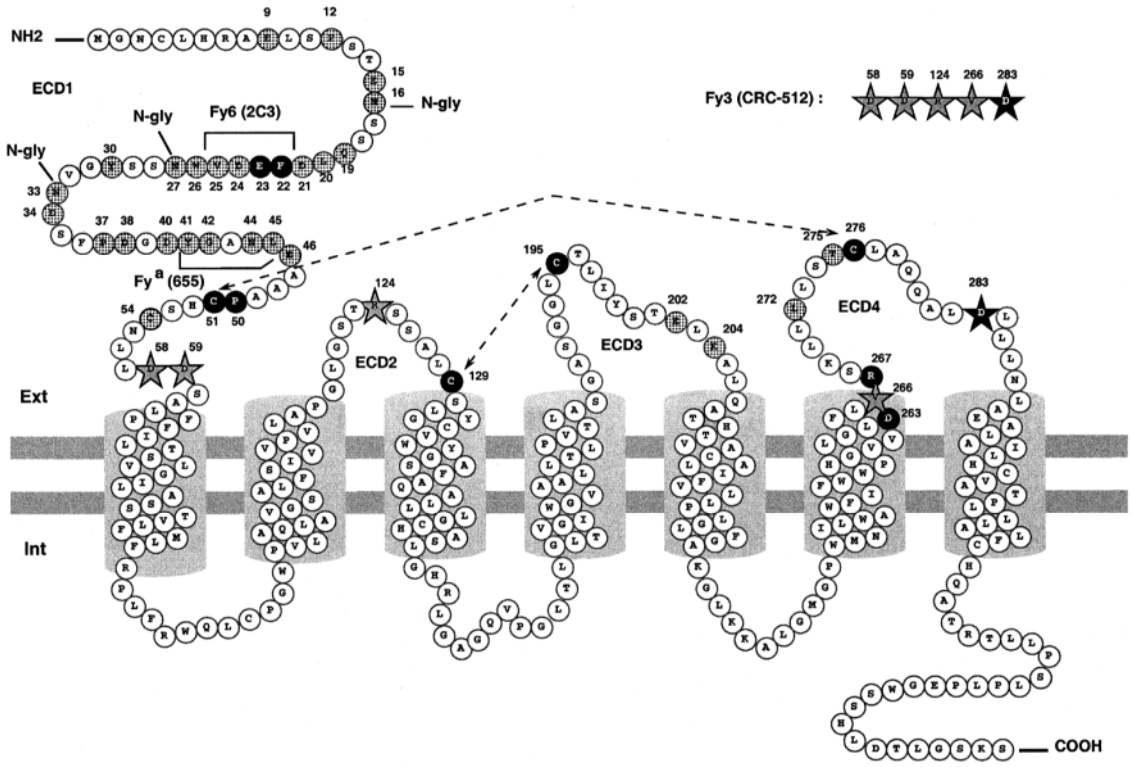

Figure 1.9 Schematic representation of DARC showing the amino acid (aa) residues that are crucial for anti-Fy antibody and chemokine binding. Function of aa residues contained in the extracellular domains: black, critical for CXCL8 binding; grey, not involved in CXCL8 binding. AA residues required for Fy^a and Fy6 epitopes, and recognised by the 655 and 2c3 monoclonal antibodies respectively, depicted. Stars emphasise the aa residues participating in the Fy3 epitope recognised by the CRC-512 anti-Fy3 antibody. Suggested disulphide bridges are indicated by broken arrows. Adapted from Tournamille *et al.*, 2003

1.9.4 Clinically significant antibodies of the Duffy blood group system

Most anti-Fy^a and anti-Fy^b are predominantly IgG_1 (Hardman and Beck, 1981, Szymanski *et al.*, 1982), and in about half of those cases studied both antibodies were able to activate complement. Anti-Fy^a is very rarely naturally occurring, and typically follows transfusion and much less commonly after pregnancy. Anti-Fy^a is often only detected by indirect antiglobulin testing (IAT) with agglutinating activity developing following antigenic stimulation, similar to anti-D and anti-K. Fy^a has been shown to be significantly more immunogenic in Fy(a–b+) subjects than in those Fy(a–b–). Four and eleven patients were Fy(a–b–) in two series of 25 and 130 patients with anti-Fy^a , respectively (Kosanke, 1983, Vengelen-Tyler, 1983). Fy(a+b–) red cells suspended in saline will be agglutinated by anti-Fy^a, and may react with these cells more strongly than Fy(a+b+) cells (Race *et al.*, 1953). Anti-Fy^b is 20 times less frequent than anti-Fy^a, and is typically identified with other allo-antibodies. Both antibodies have been shown to cause both immediate and delayed haemolytic transfusion reactions (Klein and Anstee, 2005).

Anti-Fy3 reacts with all human red cells apart from Fy(a–b–) cells, and was initially described in a Caucasian female transfused following her second delivery, then pregnant with her third child (Albrey *et al.*, 1971), with subsequent mild HDFN. The newly detected antibody reacted with Fy(a+b–), Fy(a–b+) and Fy(a+b+) cells but not Fy(a–b–) cells, and could not be separated into Fy^a or Fy^b specificities. Surprisingly despite the overwhelmingly higher frequency of Fy(a–b–) in persons of African origin,

relatively few examples of this antibody are reported in the literature (Oberdorfer *et al.*, 1974, Oakes *et al.*, 1978). This is likely to be due to ongoing expression of Fy^b on non-erythroid tissues in these individuals. Nevertheless, as some individuals do develop antibodies, anti-Fy3 may develop as a result of a different genetic cause for the Fy(a–b–) phenotype, or alternatively as a result of post-translational differences between erythrocyte Fy and endothelial Fy protein. (Notably anti-Fy3 taken from African persons reacted weakly with cord cell samples (Oakes *et al.*, 1978, Kosinski KS, 1984), whereas anti-Fy3 from those of other ethnic origins reacted clearly with red cells from adults and neonates (Buchanan *et al.*, 1976)

Anti-Fy4 reacts with Fy(a–b–) cells, some Fy(a+b–) or Fy(a–b+) but no Fy(a+b+) erythrocytes. Owing to inconsistent results between laboratories, there is even doubt as to its existence (Behzad *et al.*, 1973), particularly as it is singularly described in the literature.

Anti-Fy5 was reported in an a black child of Fy(a–b–) phenotype with leukaemia (Colledge *et al.*, 1973), and this antibody reacts with most red cells except Fy(a–b–) Rh_{null} phenotype or those carrying variant forms of the Rh ‘e’ antigen. Anti-Fy5 appears to arise as a result of an interaction between Fy and Rh blood groups, and has been reported to cause delayed haemolytic transfusion reactions in patients with sickle cell disease, who usually develop this antibody along with other Rh group or Fy antibodies (Chan-Shu, 1980).

Anti-Fy6 is a monoclonal mouse anti-human antibody and has been used to block malarial invasion of erythrocytes, as well as demonstrate the presence of DARC on

erythroid and other tissues (Nichols *et al.*, 1987), and block chemokine binding (Horuk *et al.*, 1993a). Human antibodies recognising Fy6 epitope have not been reported to date.

1.9.4.1 Clinical aspects of anti-Duffy antibodies

Duffy antibodies are not a common cause of haemolytic transfusion reactions, but there is considerable experience in Fy(a–b–) multiply transfused patients, usually in the setting of sickle cell disease and the presence of multiple allo-antibodies. In this context, implicated Fy system antibodies are usually anti-Fy^a (Le Pennec *et al.*, 1987) or occasionally anti-Fy3, and particularly this latter antibody can lead to significant difficulties in the provision of numerous units of suitable blood, given the under-representation of donors of African origin in many Western donor populations. It has been noted that anti-Fy3 develops after anti-Fy^a in persons having received multiple red cell transfusions for sickle cell disease (Vengelen-Tyler, 1985).

HDFN can be caused by Fy antibodies. The prevalence of anti-Fy^a during pregnancy is up to 5.4 percent (Goodrick *et al.*, 1997), while Fy^b antibodies are far less common and have been found to cause only mild HDFN. A case series revealed that only 2 of 18 neonates required exchange transfusion for low haemoglobin due to anti-Fy^a related HDFN, with no cases requiring intra-uterine transfusion or early delivery (Hughes *et al.*, 2007), although another noted that 2 intra-uterine transfusions were required for severe anaemia out of 68 pregnancies in which anti-Fy^a was detected (Goodrick *et al.*, 1997). Hence anti-Fy^a can lead to severe HDFN in a small number of cases, and correspondingly alloimmunised pregnancies should be monitored closely.

1.9.5 The Duffy antigen, as a receptor for chemokines

The Duffy blood group antigen was recognised as a chemokine receptor during the investigation of a promiscuous chemokine binding protein on erythrocytes (Darbonne *et al.*, 1991, Neote *et al.*, 1993, Horuk *et al.*, 1994), and this lead to its designation as the Duffy antigen / receptor for chemokines. As already mentioned, Fy(a–b–) individuals with the *FYB(ES)* genotype continue to express endothelial DARC (Peiper *et al.*, 1995), and this tissue localisation of DARC has been investigated further, particularly in its role pertaining to chemokine homeostasis. DARC binds at least 20 human inflammatory chemokines of the CC and CXC families with varying affinity (Darbonne *et al.*, 1991, Neote *et al.*, 1993, Horuk *et al.*, 1994, Gardner *et al.*, 2004, Szabo *et al.*, 1995) (See Table 1.2 from most recent study).

Strong binding		Weak binding		No binding	
Chemokine	K_i (nM)	Chemokine	K_i (nM)	Chemokine	K_i (μM)
CCL5 (RANTES)	5.6	CCL8 (MCP-2)	151.0	CXCL12 (SDF-1α)	>1
CCL7 (MCP-3)	6.6	CXCL9 (MIG)	162.0	CCL3 (MIP-1α)	>1
CXCL11 (I-TAC)	12.7	CCL18 (PARC)	206.2	CCL4 (MIP-1β)	>1
CXCL8 (IL-8)	21.3	CCL16 (HCC-4)	257.7	CCL19 (ELC)	>1
CXCL5 (ENA-78)	28.8	CXCL13 (BLC)	304.5	CCL20 (LARC)	>1
CCL13 (MCP-4)	32.8	CCL1 (I-309)	309.3	CCL21 (SLC)	>1
CCL2 (MCP-1)	34.9	CXCL10 (IP-10)	622.4	CCL22 (MDC)	>1
CCL17 (TARC)	58.0			CCL23 (MPIF-1)	>1
CXCL6 (GCP-2)	66.7			CCL25 (TECK)	>1
CCL11 (Eotaxin)	67.3			CCL27 (CTACK)	>1
CCL14 (HCC-1)	91.8			XCL1 (Lymphotactin)	>1
				CX3CL1 (Fractalkine)	>1

Table 1.2 Chemokine binding to the human Duffy antigen.

Chemokines were divided into three categories based on K_i values: those showing strong binding (K_i < 100 nM), weak binding (K_i = 100 nM–1 μM), and no binding (K_i > 1 μM). The chemokines are named according to the new nomenclature with the former nomenclature in parentheses. Results shown are geometric means of three separate determinations. CXCL4 is not included, but is suggested to be a weak DARC ligand (Szabo *et al.*, 1995). From Gardner *et al.*, 2004.

The structure of DARC is very similar to other chemokine receptors, but in notable contrast, DARC does not have the aspartyl-arginyl-tyrosine (DRY-) motif found in the second intracellular loop of all other chemokine receptors which couples them to G proteins and is required for GPCR signalling and triggering of intracellular calcium flux (Neote *et al.*, 1994). The extracellular N-terminal domain of DARC carrying the blood group determinant and *P. vivax* binding regions forms, in combination with the

fourth extracellular domain via a disulphide bond, a “pocket” with promiscuous chemokine binding properties (Tournamille *et al.*, 1997, Tournamille *et al.*, 2003). DARC cDNA has significant similarities with rabbit and human CXCL8 receptors, which also bind inflammatory chemokines with high affinity (Chaudhuri *et al.*, 1993). Given the absence of any detectable cell signalling following cognate chemokine binding to DARC in the form of measurable calcium flux (Neote *et al.*, 1994) alterations in GTPase activity (Horuk *et al.*, 1993b) or gene transcription (Lee *et al.*, 2003b), this receptor was postulated to act as a chemokine decoy. However, *in vitro* models have demonstrated that following chemokine binding, DARC is redistributed from the basolateral membrane via an intracellular vesicular compartment onto the apical membrane and was associated in particular with microvilli (Pruenster *et al.*, 2009). Only cognate chemokines are transported and minimal degradation of chemokines occurs. Supporting these findings, it has been shown that monocyte and neutrophil migration toward cognate chemokine was enhanced across an endothelial monolayer expressing DARC (Lee *et al.*, 2003b, Pruenster *et al.*, 2009). This was confirmed *in vivo* by intradermal and intraperitoneal injection of CXCL1 into transgenic mice which over-expressed DARC on the endothelium, revealing significantly greater neutrophil recruitment in the mice overexpressing DARC, compared with wild-type animals (Pruenster *et al.*, 2009). The likely biological role of DARC appears therefore to be internalisation and transport of chemokines across endothelial cells, and enhancement of leukocyte recruitment.

Although internalisation of chemokines by DARC does not lead to their degradation, DARC may still remove chemokines from extracellular environments, and thus e.g.

negatively influence angiogenesis induced by pro-inflammatory chemokines. This was demonstrated using mice over expressing endothelial DARC which had reduced angiogenic responses to CXCL2 (Du *et al.*, 2002). In the context of tumour related vascularisation, reduced angiogenesis and decreased melanoma tumour growth was observed in mice overexpressing endothelial DARC (Horton *et al.*, 2007), but tumours contained greater numbers of infiltrating leukocytes in comparison to control mice, which supports a role for endothelial DARC in promoting leukocyte migration. The angiogenesis attenuating effect has been confirmed using implanted DARC transfected breast cancer lines, with DARC expression also leading to reduction of tumorigenesis and metastasis.

DARC-expressing non-small cell lung cancer tumours transplanted into SCID mice had increased necrosis and reduced cellularity in contrast to DARC deficient control tumours (Addison *et al.*, 2004). DARC deficient mice used in a transgenic model of prostate cancer developed tumours with increased vessel density, greater intratumour angiogenic chemokine levels and augmented tumour growth (Shen *et al.*, 2006). CD82, a tetraspanin, was identified as a prostate cancer metastasis suppressor gene, and in the investigation of its function, it was demonstrated that attachment by metastatic cancer cells to the vascular endothelium occurred through direct interaction with DARC, consequently resulting in growth arrest of cancer cells and the induction of senescence. Furthermore, DARC KO mice were shown to have increased prostate cancer metastasis in comparison with controls (Bandyopadhyay *et al.*, 2006). Clinical data also support the negative regulatory role of DARC in tumour progression. Patients with breast cancers with high DARC expression have had better survival than

those with DARC-negative tumours, with additional negative correlation between DARC expression and lymph node metastasis (Wang *et al.*, 2006). It appears therefore that DARC has direct and indirect effects on tumour development and metastatic spread, at least in part by removing angiogenic chemokines from the extracellular environment.

A further functional facet of DARC activity may reflect its ability to affect the signalling by classical chemokine receptors expressed in *cis* geometry with DARC. DARC was shown to heterodimerise with CCR5 leading to reduced calcium flux and chemotaxis in respond to the CCR5-cognate chemokines (Chakera *et al.*, 2008). Internalisation of CCR5 ligand binding however was unaffected by DARC.

1.9.5.1 The role of DARC in chemokine homeostasis

Erythroid DARC was originally described as a "sink" for chemokines (Darbonne *et al.*, 1991) and this function was further supported when DARC was shown to reduce excessive increases in blood-borne inflammatory chemokines, dampening the subsequent activation of leukocytes (Dawson *et al.*, 2000). It is thought that erythrocyte DARC may serve in the preservation of leukocyte sensitivity to ELR+ chemokines by shielding blood leukocytes from overstimulation of their receptors and associated desensitisation. However, evidence suggests that previous exposure to chemokines may lead to leukocyte priming for enhanced chemokine induced migration (Brandt *et al.*, 1998) or other effects induced by different chemokines (Green *et al.*, 1996, Hauser *et al.*, 1999). These two opposing potential outcomes may help explain conflicting observations in DARC deficient mice exposed to inflammatory

stimuli (Dawson *et al.*, 2000, Luo *et al.*, 2000, Mei *et al.,* Vielhauer *et al.*, 2009, Reutershan *et al.*, 2009, Zarbock *et al.*, 2010), which will be discussed henceforth. An initial study (Dawson *et al.*, 2000) administered LPS to mice, and a marked increase in neutrophil infiltrate in the lungs and livers of DARC KO animals was described. Contemporaneous to this, another group (Luo *et al.*, 2000) using a similar methodology described decreased lung and peritoneal neutrophil recruitment in DARC KO animals. However in a subsequent retraction of this paper the authors stated that their own re-analysis of data apparently produced findings consistent with increases in LPS-induced neutrophil infiltrate in organs of DARC KO mice. Using different methodology, Lee and colleagues (Lee *et al.*, 2003a), instilled human CXCL8 into pulmonary airspace of DARC KO mice and observed significantly less leukocyte infiltrate in the broncho-alveolar lavage. This latter group subsequently undertook studies which more closely examined the differential roles of DARC on erythrocytes and endothelium using bone marrow chimeric mice (Lee *et al.*, 2006b). It was demonstrated that following intra-tracheal LPS instillation, mice lacking erythrocyte DARC showed significantly fewer airspace neutrophils. The lack of endothelial or lung parenchymal DARC was associated with higher chemokine concentrations in the airspaces compared with experiments where DARC was absent on erythrocytes. The authors suggest that DARC in different sites alters the availability of chemokines produced during inflammation and that the overall effect of DARC is to reduce chemokine concentrations in the airspace, lung tissue and to increase plasma chemokine concentrations. However, another group published conflicting findings describing diametrically opposite outcomes. Reutershan *et al.*, 2009, studied

neutrophil recruitment following a higher dose LPS inhalation in a DARC KO model of acute lung injury, and showed increased neutrophil migration into the alveolar space in DARC KO animals, along with elevated CXCL1, 2 and 3. In chimeric animals, the absence of haematopoietic DARC appeared to be the most significant factor in determining leukocyte trafficking.

The likely reason for the different results may be due to the degree of injury: more severe LPS induced injury is likely to be associated with increased microvascular permeability and reductions in inflammatory chemokines. It is suggested that the role for erythroid DARC as a sink becomes more significant (Reutershan *et al.*, 2009), by limiting excessive leukocyte infiltration into tissues and thereby opposing the pro-inflammatory properties of endothelial DARC. Of note RBC-bound chemokine concentrations during severe systemic inflammation amounted to 30% of plasma chemokine concentration suggesting a limited sink effect of erythrocyte DARC during severe inflammation (Reutershan *et al.*, 2009). This result would need verification as others have noted several hundred fold increases in chemokines from erythrocyte lysates following endotoxin challenges in humans (Mayr *et al.*, 2008).

Further investigation into the role of DARC in acute lung inflammation revealed that DARC deficiency in mice results in down-regulation of CXCR2 on neutrophils because of high levels of circulating chemokines during severe inflammation (Zarbock *et al.*). DARC was essential for chemokine mediated leukocyte recruitment, in that DARC KO animals were protected from acid induced lung injury and experienced preserved oxygenation, lack of neutrophil recruitment and lower BAL fluid protein levels. This was suggested to occur as a result of impaired leukocyte arrest on endothelial cells

and a block on pulmonary neutrophil recruitment during severe lung injury. Using a system of adoptive transfer of neutrophils, the latter effect was shown to be dependent on neutrophils and independent of endothelial cells and erythrocytes, suggesting that the role of DARC is in the maintenance of homeostasis between receptors and cognate ligands. In addition further protection was conferred by reduced neutrophil-platelet aggregates, which are instrumental for further neutrophil recruitment and acute lung injury. CXCR2 blockade reversed this, and also reversed a platelet related bleeding defect also observed in this study.

Renal models of inflammation have shown that DARC deficient mice are protected from ischaemic and LPS induced acute renal injury. Furthermore, chemokine presentation on renal endothelial cells was absent, and renal neutrophil recruitment was impaired, in the context of lower inflammatory chemokine levels during systemic inflammation (Zarbock *et al.*, 2007). In contrast however, Vielhauer and colleagues (Vielhauer *et al.*, 2009) used two models of prolonged renal inflammation (tubule-intestitial and glomerulonephritic) in DARC deficient mice, demonstrating effective leukocyte infiltration of kidneys, which was even enhanced in the early phases. However this accelerated recruitment of leukocytes did not result in worse or altered renal injury at later time points. Macrophage and T lymphocytes were recruited equally well in DARC KO and wild-type mice, suggesting that DARC does not influence disease progression.

Both human and murine studies suggest that DARC can sustain inflammatory chemokines levels on erythrocytes and in plasma (Jilma-Stohlawetz *et al.*, 2001, Fukuma *et al.*, 2003), but the purpose of this is not clear. When investigated on DARC

KO mice, basal plasma CCL2 (MCP-1) levels were noted to be one third lower in the knock-out animals. When eotaxin (CCL11) or hMGSA (CXCL1) were administered intravenously, levels of these chemokines fell more rapidly in the plasma of the DARC KO animals (Fukuma *et al.*, 2003). In humans, healthy volunteers phenotyped Fy(a–b–) were noted to have significantly lower CCL2 levels than other Fy phenotypes (Jilma-Stohlawetz *et al.*, 2001). Using a human endotoxaemia model of inflammation, this group (Mayr *et al.*, 2008) subsequently administered endotoxin to Fy positive or negative subjects, and noted higher peak levels of plasma CCL2 in Fy-positive subjects. CCL2 and CXCL1 levels but not CXCL8 or CCL4 (MIP1-β) were higher in erythrocyte lysates in Fy positive individuals at baseline, and CCL-2 and CXCL8 but not CCL4 increased significantly in Fy-positive subjects following endotoxin. Given that CXCL8 (Wong *et al.*, 2008) and CCL2 (Bozza *et al.*, 2007) levels have been shown to be predictive of survival and correlate with sepsis severity, it might be tempting to speculate that the loss of DARC expression may lead to loss of a buffering or sink activity as possibly provided by DARC. However it has been recently suggested that chemokines with different DARC binding affinities can affect the levels of other chemokines bound either on erythrocyte DARC or present freely in the plasma, affecting resultant leukocyte responses (Mei *et al.*, 2010) by inducing changes in the sensitivity of relevant receptors. These findings are also in concordance with the conclusions by Zarbock *et al.*, 2010. In addition heparin and activated coagulation factors elute chemokines off erythrocyte DARC (Schnabel *et al.*, 2010). Thus the methods used to take blood or using serum or plasma introduce additional variables

which further obscure our understanding of the role of erythrocyte DARC in chemokine homeostasis.

Recently, differences in plasma and serum chemokine levels were reported in persons with DARC variants Fy^a or Fy^b (Schnabel *et al.*, 2010), and although the mechanism for this is not yet apparent, a further genome-wide study supported this finding in Hispanic children (Voruganti *et al.*, 2012). Further work revealed Fy(a–b+) RBCs possess reduced surface DARC expression compared to Fy(a+b–) RBCs. It is already known there are fewer antigenic sites on Fy(a–b+) cells; however, surface DARC binding affinity for chemokines was not appreciably different between the two phenotypes (Xiong *et al.*, 2010). The impact of differential chemokine levels between Fy serotypes on human disease therefore requires further investigation.

As discussed above, DARC, expressed on venular endothelial cells, (Peiper *et al.*, 1995, Chaudhuri *et al.*, 1997, Kashiwazaki *et al.*, 2003), functions as a transcytosis receptor transporting chemokines from the baso-lateral to the apical side only (Pruenster *et al.*, 2009). Thus, DARC expression is important for chemokine-induced leukocyte migration. DARC is expressed and upregulated in veins, and appears in vessels usually devoid of it, in the context of inflammation, infection and transplant rejection (Geleff *et al.,* Bruhl *et al.*, 2005, Gardner *et al.*, 2006, Lee *et al.*, 2003a, Liu *et al.*, 1999, Patterson *et al.*, 2002, Segerer *et al.*, 2000). It is not clear whether DARC over-expression is a consequence of the development of these lesions or a pre-requisite. A further potential function for DARC may be one of elimination of chemokines from tissues by transcytosis across venular endothelial cells, although it is probably more likely to occur in most tissues by chemokines diffusing between

endothelial cells, or alternatively via lymphatics. Although lymphatic vessels do not express DARC, a small segment, termed the podoplanin-dull precollectors, have been shown to express DARC. This suggests that chemokine mediated cell trafficking may occur in this section of the lymphatic vasculature (Wick *et al.*, 2008).

1.9.6 DARC and human disease

1.9.6.1 Ethnic neutropaenia

The consequences of loss of erythrocyte DARC expression, as observed in populations homozygous for *FYB(ES)*, is little understood. Recently genome wide association studies have linked benign ethnic neutropaenia to persons with this genotype. The first report aimed to study the entire genome for a locus that would account for the difference in white blood counts between North American populations of African and European ancestry. Admixture mapping was used to analyse data from 6005 African Americans and demonstrate that the only causal variant was the *FYB(ES)* genotype ($P = 3.8 \times 10^{-5}$), termed the rs2814778 T allele. Importantly they also verified that these results were not as a result of linkage disequilibrium by undertaking analysis of shotgun sequencing data (Reich *et al.*, 2009, Nalls *et al.*, 2008). This study was extended to include 16388 self-identified African American individuals (Reiner *et al.*, 2011), confirming the *FYB(ES)* association ($P<10^{-236}$ for neutrophils), and introducing three further lesser associations, *CXCL2* gene (rs9131 T allele) and *CDK6* (rs445 T allele) and *PSMD3-CSF3* (rs4065321 T allele). CDK6 or cyclin-dependent kinase 6, and *PSMD3* are cell cycle regulators expressed in HSPC (Meyerson and Harlow, 1994, Bailly and Reed, 1999). Finally, the associations for *DARC* and *PSMD3-CSF3* have also

been described in another genome wide association study with 13923 individuals of African ancestry (Crosslin *et al.*, 2012).

Leukopaenia was been observed in persons of African ancestry for several decades, having been first recognised in 1941 (Forbes *et al.*, 1941) and was subsequently confirmed by later studies (Sadowitz and Oski, 1983, Broun *et al.*, 1966, Rippey, 1967). It is generally considered that the neutropaenia seen in certain ethnic groups such as those of African ancestry (Rana *et al.*, 1985), certain Middle Eastern groups (Denic *et al.*, 2009) including Yemeni Jews (Shoenfeld *et al.*, 1988) is not associated with any implications for sepsis risk (Shoenfeld *et al.*, 1985), giving rise to the term 'benign ethnic neutropaenia.' It has been suggested that benign ethnic neutropaenia should be defined as a neutrophil count of less than 1.5×10^9 / L in subjects who are otherwise well (Hsieh *et al.*, 2007, Haddy *et al.*, 1999), and is found in up to 5% of African Americans compared with 0.8% of Caucasian Americans. On average, African American subjects have a 20% lower neutrophil count (rising to 38% lower in individuals homozygous for *FYB(ES)*) (Reich *et al.*, 2009). Researchers noted a neutrophil count lower than 0.5×10^9 /L in two completely well Kuwaiti Arab brothers (Denic *et al.*, 2009), with no other explanation for the neutropaenia. In terms of underlying mechanisms for this condition, a theory for 'pseudoneutropaenia' (Karayalcin *et al.*, 1972), which suggested that neutrophils were being retained in the marginal pool, was considered the most likely explanation for the phenomenon. Initial studies determined no difference in the myeloid or other haematopoietic progenitor composition of the bone marrow of neutropaenic subjects (Mintz and Sachs, 1973). However, studies have shown a lower peak neutrophil count after infection and

exercise (Phillips *et al.*, 2000, Pastorek *et al.*, 1996) and suggested a reduced capacity for granulopoiesis in persons with benign ethnic neutropaenia, as the peak neutrophil count following glucocorticoid stimulation remains lower than in controls (Mason *et al.*, 1979, Shoenfeld *et al.*, 1982). One proposed mechanism was a defect in release of neutrophils from the bone marrow storage pool (Shoenfeld *et al.*, 1982, Mintz and Sachs, 1973). Of note, the reduced neutrophil increment on glucocorticoid administration was seen in all members of an ethnic group, not merely those with a lower neutrophil count (Mason *et al.*, 1979, Shoenfeld *et al.*, 1982). More recently it has been shown that bone marrow colony forming units for granulocytes are reduced in benign ethnic neutropaenia, suggesting that capacity for neutrophil production is lower but qualitative difference could not be detected (Rezvani *et al.*, 2001). Other authors have described higher levels of CXCL8 and G-CSF, 50 and 70% respectively, in volunteers of African origin as well as a reduced oxidative burst capacity in stimulated neutrophils from volunteers of African descent (Mayr *et al.*, 2007). In addition to CXCL8, high levels of G-CSF have also been recently described as predictive of survival from acute lung injury as well as a relationship with severe sepsis (Suratt *et al.*, 2009). The exact implications of this are not clear. Although it has been noted for some time that persons of African origin appear to fare worse in analyses of health outcomes compared with many other populations, it has been ascribed to be due to a complex mix of socio-economic factors (Barnato *et al.*, 2008). The inference of biological factors however is intriguing. A study demonstrating substantial anti-microbial effects by neutrophils against tuberculosis infection, also noted that the likelihood of acquiring this disease appeared to correlate inversely with

neutrophil counts (Martineau *et al.*, 2007). Study subjects of African origin tended to have lower neutrophil counts and the highest incidence of tuberculosis infection, compared with other groups (including South Asians) in the South London cohort. Unfortunately it is only recently that the strong link between *FYB(ES)* genotype and benign ethnic neutropaenia has been uncovered, and therefore it is not possible to classify participants in these studies in any way other than exhibiting neutropaenia and being from a particular ethnic group. Other genetic polymorphisms may play a role in modifying or contributing to the observations.

The interplay between the three factors of neutropaenia, loss of erythrocyte DARC expression and malaria has not previously been studied in detail. Notably, it has been reported that higher neutrophil counts are associated with a higher malarial parasite load, and correlate with the severity of disease and the risk for cerebral malaria (Ladhani *et al.*, 2002). This latter factor was corroborated in a mouse model where neutrophil depletion was shown to prevent cerebral malaria (Chen *et al.*, 2000). However this finding has yet to be confirmed in human studies. The association of reduced malaria severity with lower neutrophil counts nevertheless represents a possible second mechanism whereby the *FYB(ES)* gene protects from malaria, and that this would not be restricted to *plasmodium vivax* malaria.

1.9.6.2 Malaria susceptibility

DARC may have hither-to unexplored effects on erythrocyte invasion by *Plasmodium* species other than *vivax*. Platelet Factor 4 (CXCL4) and DARC have been described as being required for the platelet related killing of *plasmodium falciparum* with CXCL4

endocytosed by erythrocyte DARC and subsequently involved in directly killing this plasmodium intracellularly (McMorran *et al.*, 2012). However, this mechanism remains contentious (Nibbs and Graham, 2013) especially the fact that CXCL4 is a DARC ligand. The earliest study of DARC as the erythroid chemokine receptor indicates that CXCL4 weakly binds to erythrocyte DARC but not at all to DARC expressed on K562 cells (Chaudhuri *et al.*, 1994). Subsequently, Szabo *et al.*, 1995, demonstrated in chemokine binding-competition assays that CXCL4 was able to displace 0.5nM CCL5 at 200nM only, considered to be non-specific by the authors, but could not displace CXCL2 (MIP-2α/Gro-β) at all. The critical role of DARC in the process of intracellular killing *P. falciparum* was established by its reduction with anti-Fy6 antibody, or within DARC-deficient erythrocytes. Although only implied but not demonstrated directly, the most contentious mechanistic aspect of the study by McMorran *et al* is that DARC on plasmodium infected cells internalises CXCL4, a hitherto undescribed role for erythrocyte DARC. The implication of this work would be that the loss of DARC, presumably evolutionarily selected to protect against *P. vivax,* puts the individual at a disadvantage when faced with *P. falciparum*, a more deadly pathogen. However other researchers could not show an association between DARC genotype and risk for *P. falciparum* (King *et al.*, 2011, Kasehagen *et al.*, 2007, Woldearegai *et al.*, 2013).

1.9.6.3 Human Immunodeficiency Virus

DARC has been implicated in modifying the epidemiology and course of another serious infectious disorder, the human immunodeficiency virus (HIV), with significant

geographical overlap in the prevalence of both HIV and the *FYB(ES)* gene. Initial reports indicated that erythrocyte DARC adsorbed HIV (Lachgar *et al.*, 1998), and thereafter transferred virions to $CD4^+$ T cells (He *et al.*, 2008) but not if incubated with anti-Fy6 antibody. However, others have noted that HIV appears to bind to erythrocytes independent of DARC phenotype, suggesting that DARC may not be the only binding mechanism (Beck *et al.*, 2009).

An association between DARC genotype and HIV susceptibility was noted, with increased likelihood of infection, by as much as 40%, if the host was *FYB(ES)* homozygous, with subsequent and paradoxical slower CD4 decline (He *et al.*, 2008). It was calculated that up to 11% excess HIV infections in Africans might be as a result of this genotype. The authors suggested that the loss of erythroid DARC may reduce the pro-inflammatory state established during primary HIV infection thereby increasing the risk of sero-conversion by affecting circulating levels of inflammatory chemokines, including the HIV-suppressing CCL5. Conversely, absence of erythroid DARC would represent a loss of reservoir for HIV virions, and the continuous pro-inflammatory state induced by ongoing HIV infection may be ameliorated owing to loss of erythrocyte chemokine buffering activity and translating into slower disease progression. However there is little evidence to support this model and the effects of erythrocyte DARC on chemokine homeostasis are complex. Four other groups, (Walley *et al.*, 2009, Horne *et al.*, 2009, Winkler *et al.*, 2009, Julg *et al.*, 2009), were not able to reproduce the findings by He *et al.* The discrepancy was ascribed to the methods used to adjust for population admixture, as 30 to 40% African Americans are phenotypically DARC positive. Nevertheless, further work described in a large cohort

of African American subjects an association between leukopaenia and HIV progression: leukopaenic subjects of African ancestry homozygous for *FYB(ES)* had a survival advantage compared with all non-*FYB(ES)* study participants. This was found to be independent of CD4 count and viral load, which are known predictors of AIDS development and progression (Kulkarni *et al.*, 2009). In particular this survival benefit was conferred to those *FYB(ES)* homozygotes with lower white blood counts.

Recently, a relationship between *FYB(ES)*, leukopaenia and HIV infection was investigated (Ramsuran *et al.*, 2011) in 142 South African women at high risk of HIV infection. It appears that both loss of DARC expression on erythrocytes and a reduction in neutrophil count are risk factors for acquiring HIV. A 36% increase for each 1 x 10^9/L drop in the neutrophil count was noted in the risk of acquiring HIV. In particular those subjects typed as *-46* C/C (homozygous *FYB(ES)*) had a three times higher risk of contracting HIV. Taken together these findings suggest the prevalence of homozygous *FYB(ES)* modifies the risk of infection by HIV in that the reduction in neutrophil counts increases the risk of infection, but in contrast a survival advantage is given to HIV infected subjects with low neutrophil counts, thereby lengthening the duration of the infected state.

Following on from this work, another group examined the association of neutrophil counts in mothers and in new-borns at risk of infant perinatal HIV infection in the BAN cohort (Breastfeeding, Antiretrovirals, and Nutrition) study of 2369 mothers infected with HIV and their new-borns in Malawi (Kourtis *et al.*, 2012). Higher neutrophil counts in both mother and neonate were associated with a lower risk of perinatal HIV infection. The association of infant neutrophil counts with perinatal HIV

infection persisted after adjustment for maternal CD4 counts, treatment with co-trimoxazole during pregnancy, maternal viral load and infant's gender and birth weight. This further supports the notion that the neutropaenia seen in homozygous *FYB(ES)* individuals renders them at higher risk for HIV infections; however a mechanism for this association requires elucidation.

1.9.6.4 Other disease associations

There are associations of DARC genotype with other human diseases. The Fy(a–b–) phenotype in Africans co-segregates with sickle cell disease, another disorder associated with protection from malaria and conferring survival advantage in the heterozygous state. However one study found no effect of DARC genotype on sickle cell disease severity or changes in chemokines levels during vaso-occlusive crises (Schnog *et al.*, 2000). Similarly another group (Nebor *et al.*, 2010) found no correlation between Duffy serotype and end organ damage, although markers of haemolysis were higher in Duffy positive individuals, as were CXCL8 and CCL5. However Afenyi-Annan *et al.*, 2008, with more subjects, indicated that renal disease was more likely in Fy(a–b–) subjects. More recent investigators (Drasar *et al.*, 2013) noted markers of renal injury due to sickle cell disease to be more elevated in Duffy positive individuals and furthermore the development of leg ulcers was more likely in Duffy positive individuals. The number of hospital admissions and the length of hospital stay was lower in Fy(a–b–) individuals. These studies suggest an effect of higher leukocyte numbers, which are more activated in sickle cell disease (Lard *et al.*, 1999), leading to both more frequent sickling episodes, and consequently more end

organ damage. In sickle cell patients DARC expression on the erythrocytes is associated with the constitutive activation of leukocyte VLA-4, a counter-ligand for VCAM-1 on endothelial cells (Durpes *et al.*, 2011). Integrin activation is further enhanced by the presence of CXCL8 or CCL5 (Durpes *et al.*, 2011).

Higher CXCL8 levels were also measured in pregnant Fy(a–b–) pre-eclamptic women (Velzing-Aarts *et al.*, 2002a, Velzing-Aarts *et al.*, 2002b), with an increased number of Fy(a–b–) subjects having a history of pre-eclampsia when compared against Duffy positives. Higher susceptibility to asthma along with higher IgE levels observed in a group of patients of African origin were considered due, in part, to the Fy(a–b–) phenotype (Vergara *et al.*, 2008).

Blood transfusion is a predisposing condition for acute lung injury in the critically ill individuals, and mortality risk increases with further transfusions (Shaz *et al.*, 2011). Although allogeneic leukocytes have been implicated, leukoreduction has not alleviated these complications. Because the mortality increases with increasing age of the transfused red cells, it was suggested that the changes undergone by red cells in storage, the 'storage lesion' (Bessos and Seghatchian, 2005), may contribute to transfusion related morbidity. In a mouse model of systemic endotoxaemia followed by a secondary red cell transfusion challenge, (Mangalmurti *et al.*, 2009) aged red cells increased lung airspace chemokine concentrations and enhanced the lung microvascular permeability. In addition *in vitro* work done with human erythrocytes demonstrated reduced DARC expression and chemokine scavenging for CXCL1 and CCL2 but not CXCL8 occurred with increasing storage (Mangalmurti *et al.*, 2009). This group next used chimeric mouse models to investigate the effects of transfusing

red cells from DARC KO mice into wild-type animals, and noted more pronounced parameters of acute lung injury in comparison with wild type mice receiving wild type blood. These data suggest that reduced DARC expression on stored blood erythrocytes has decreased chemokine binding capacity, affecting local chemokine gradients and thereby promoting the entry of neutrophils into the pulmonary airspaces. It is of note that actual DARC expression on murine red cells was not assayed in this study owing to a lack of reliable anti-mouse DARC antibody.

From a clinical perspective, it is already established that African Americans have poorer survival compared to other groups treated in intensive care, due to a complex mix of altered co-morbidity profiles compared with the general population, and other socio-economic factors (Barnato *et al.*, 2008, Esper *et al.*, 2006b). Further work examining the significance of DARC in modulating inflammatory responses during acute lung injury compared the outcome between 127 patients studied under the ARDS Network (Kangelaris *et al.*, 2012), 67% of which were DARC negative. This study reports that there is a two-fold higher risk for mortality and likelihood for ongoing mechanical ventilation at 60 days in DARC negative patients. Taken together with the findings of Mangalmurti *et al.*, 2009 *FYB(ES)* individuals are at higher risk for acute lung injury following an insult, possibly as a result of loss of chemokine scavenging by DARC.

The absence of DARC on erythrocytes has demonstrable effects on chemokine levels in human subjects, and there is a very strong association between *FYB(ES)* genotype and neutropaenia. However mechanisms for this and disease associations have not been defined and it is possible that other factors may account for some observations.

1.10 Objectives

Chemokines are directly implicated in haematopoiesis, and the release of leukocytes from the bone marrow under homeostatic conditions and during periods of acute need such as inflammation is under the control of two chemokine-receptor axes, CXCL12-CXCR4 and ELR+ chemokines-CXCR2. The atypical chemokine receptor DARC (ACKR1), which binds among its many ligands also the ELR+ chemokines, is expressed within the bone marrow. A common human polymorphism with the promoter region of the *DARC* (ACKR1) gene results in the complete abolishment of its transcription in haematopoietic cells. This polymorphism is highly prevalent in Africa and is hypothesised to have arisen under natural selection to protect against *p. vivax* infection. It has also been strongly associated with reduced blood leukocyte counts in individuals homozygous for this polymorphism.

The aims of this thesis are to examine the role of erythrocyte DARC in haematopoiesis and dissect mechanisms giving rise to the neutropaenia in the absence of erythroid DARC. Given the abundance of erythroid cells in the bone marrow, it is hypothesised that loss of DARC expression in this compartment modulates the bone marrow micro-environment leading to altered kinetics in neutrophil mobilisation. I sought to study the impact of *FYB(ES)* on haematopoiesis, from stem cells to mature cells, and how chemokine signals might be altered by the absence of erythroid DARC. This was done using DARC-deficient mice as well as developing two new transgenic mouse models, expressing either *FYB(ES)* or *FYB* human polymorphisms of DARC in a murine-DARC KO background. Novel observations on skewed HPSC and granulocyte lineage

development in the DARC-deficient and FYB(ES) transgenic mice were further underlined by gene expression arrays and multiplex cytokine analysis. The impact of the Duffy-negative phenotype on survival from acute myeloid leukaemia was examined in a large multi-centre UK-based phase III study.

Chapter 2

The role of erythrocyte and endothelial DARC in haematopoiesis in reciprocal irradiation bone marrow chimeric mice

2.1 Materials and methods

2.1.1 Mice

All mice used were either C57Bl/6 (CD45.2) or BoyJ (CD45.1). DARC deficient mice (DARC KO) (Dawson *et al.*, 2000) mice were backcrossed for at least 12 generations onto a C57Bl/6 background. Mice were kept in a specific pathogen-free facility of the Biomedical Services Unit, University of Birmingham. All experimental procedures were approved by the Animal Ethics Committee, University of Birmingham and the Home Office, UK. All mice were used at 8–16 weeks of age. Within experiments, sex and aged matched and, if possible, littermate controls were used.

2.1.2 Bone marrow preparation for FACS analysis

Bone marrow was flushed from femurs and red cells were lysed using ACK lysis buffer where required. Cells were washed for 10 minutes (min) at 375g and were counted using a Cellometer automatic counter or in a Neubauer chamber under microscope. Cells were then added to either a 96 well plate or 1.5 ml tubes and blocked on ice for

fifteen minutes with 10% foetal calf serum and anti-mouse CD16/CD32 antibody, if appropriate.

2.1.3 Adoptive bone marrow transfers

The whole bone marrow was transplanted following lethal irradiation of murine recipients (9 Gy) by tail vein injection of 10^7 cells in 200μl PBS from either C57Bl/6 (WT) or DARC KO animals, with bone marrow transfers undertaken between WT and KO and *vice versa*, as well as KO to KO and WT to WT, to serve as radiation controls. Recipients received prophylactic endofloxacin (Baytril, Bayer AG, Germany) for a week prior to and after irradiation for all experiments.

The degree of donor chimerism, the expression of DARC on erythrocytes, was established by anti-mouse DARC antibody, directly conjugated to AF488 (kind gift of Prof Ulrich von Andrian, Boston USA) or anti mouse/rat DARC-APC (R&D systems, UK). Blood was collected for analysis whilst taking blood for neutrophil counting (see below). One million red cells were incubated with either 0.5μl of anti-mDARC-AF647 or 10μl of anti-mouse/rat DARC-APC for 30min, and then washed at 1000g for 10min. Samples were analysed using a BD FACS Calibur.

2.1.4 Peripheral blood cell counts

The full blood count was determined using an automated ABX Pentra 60 (HORIBA ABX S.A.S., Northampton, UK) blood counter.

Absolute and differential leukocyte counts were measured by collecting blood by tail bleed (not more than 7.5% of blood volume per week) into 100μl PBS + 10mM

EDTA. Fifty microlitres of the sample was transferred to a Trucount FACS tube containing a 20 μl PBS with 1μl of anti-Ly6G-PE (BD Bioscience, UK) using a reverse pipette technique. Subsequently the sample was incubated at room temperature for 30min and then red cells were lysed using 1x BD Pharmlyse (BD Bioscience, UK). Alternatively, blood samples with antibodies were incubated as described in ordinary polystyrene FACS tubes, and subsequent to lysis 20μl of CountBright (Invitrogen, UK) counting beads were added to the sample by reverse pipetting and frequent mixing. The samples were then analysed using a FACS Calibur, counting at least 2500 bead events, and the number of cells calculated according to the manufacturer's recommendation, as per the formula:

$$Neutrophils.\mu l^{-1} = \frac{number\ of\ cell\ events}{number\ of\ bead\ events} \times \frac{Beads\ added}{Volume\ of\ blood\ sampled}$$

The value for '*Volume of blood sampled*' was adjusted to compensate for varying volumes of blood obtained during tail-bleeding, e.g. total volume collected in 100μl of buffer was 150μl, therefore volume of blood sampled in the experimental tube 16.67μl.

2.1.5 Analysis of bone marrow populations

The following monoclonal antibodies were used for FACS analysis of bone marrow stem and progenitor cells: anti-mouse lineage panel-APC (BD Biosciences) or anti-mouse lineage panel-e450 (eBioscience), anti-c-Kit-APC-Cy7, anti-Sca-1-PE/Cy7 or anti-Sca-1-RPE, anti-CD127-Pacific Blue, anti-CD34-FITC, anti-CD16/CD32-PE/Cy5.5, biotinylated anti-CD135, anti-CD135-RPE, anti-CD127-e450 or APC, anti-VCAM-e450

and anti-CD62L-APC (all eBioscience, UK). Biotinylated antibodies were visualised with streptavidin-PE-Texas Red (BD Bioscience) or streptavidin-e450. The HSC population was defined as c-Kit$^+$, Sca-1$^+$ and lineage negative (LSK population), and at least 1x10^6 total bone marrow events were analysed per sample as per Ross *et al.*, 2008.

Antibodies used for myeloid surface antigen analysis included: anti-CD45-PerCP, anti-Ly6G-PE-Cy7, anti-Ly6C-FITC (BD Biosciences); anti-CD115-PE, anti-CD11b-e450, anti-CD11c-APC (eBioscience). Lymphoid populations were determined using anti-CD45-PerCP, anti-B220-FITC, anti-CD3-PE, anti-CD19-PECy7, anti-CD4-APC and anti-CD8-e450.

Erythroid precursors were examined using anti-CD71-PE and anti-Ter119-FITC (eBioscience), and directly labelled anti-mDARC-647. Gating was set using a method from Socolovsky *et al.*, 2001. Bone marrow cell populations were quantified and phenotyped using a CyAn ADP flow cytometer (Beckman Coulter, UK).

2.1.6 Preparation for flow cytometry

Staining was carried out in a rigid 96-well plate coated with heat-inactivated foetal calf serum (FCS, Sigma) on ice. Phosphate buffered saline without calcium or magnesium ions supplemented with either 1% bovine serum albumin (BSA) or 2% FCS was used as antibody diluent and wash solution. Cells were washed with 200μl wash solution at 375g for 4min at 4°C. Wash solution was removed by inversion of the plate. Cells were incubated with antibodies on ice for 30min to one hour depending on the antibody cocktail, in the dark. Following incubation, cells were washed twice

and re-suspended in 200μl wash solution, and transferred to polypropylene tubes. Fluorescence was then measured on an 11-parameter CyAn flow cytometer (Becton Dickinson).

In some experiments, cells stained with isotype control antibodies were used to determine the level of background non-specific binding. Compensation was performed using cells stained with each fluorochrome conjugated-antibody individually. Doublets were excluded by gating on the forward scatter versus pulse width. Debris and platelets were excluded from analysis by gating on forward and side scatter. Dead cells were identified by the use of either LIVE/DEAD Fixable Aqua Dead Cell Stain Kit, for 405 nm excitation, or LIVE/DEAD Fixable Near-IR Dead Cell Stain Kit, for 633 or 635 nm excitation (Life Technologies, UK), by first washing antibody stained cells in 200μl phosphate buffered saline (PBS) containing no proteins, twice, and then incubating cells on ice for 30min with the 1:1000 concentration of the relevant viability stain, after which cells were washed in PBS and re-suspended in wash buffer.

2.1.7 Statistical analysis

Statistical significance was determined for all analysis where $n<20$ with Mann-Whitney test, or unpaired Student t test for larger sample sizes: * $p<0.05$, ** $p<0.01$, *** $p<0.001$, **** $p<0.0001$. Relative or proportional data is presented as box-and-whisker plots showing minimum and maximum values, a horizontal line indicating the median, and the boxes represent the 25^{th} to 75^{th} percentiles. Absolute data values are presented as scattered-dot plots, with median. Where more than one population of cells is presented, bar graphs are used, with data presented as mean ± standard

deviation (SD). For purposes of clarity, numbers of animals studied per group are shown in some figures, or are described in the figure legend. Statistical tests were performed using Microsoft Excel 2013 (Redmond, USA), Graphpad Prism software version 5 (San Diego, USA) or SPSS (IBM, USA) version 21. According to experimental design, two way ANOVA with Bonferroni multiple comparisons was used to determine whether genotype was a significant source of variation. This statistical methodology and figure layout was used throughout this thesis, unless otherwise stated.

2.2 Results

2.2.1 Peripheral blood cell counts

To study the potential effects of DARC expression on neutrophil counts, reciprocal irradiation bone marrow chimeras were prepared as described in Material and Methods section, creating four groups of mice (**Figure 2.1**).

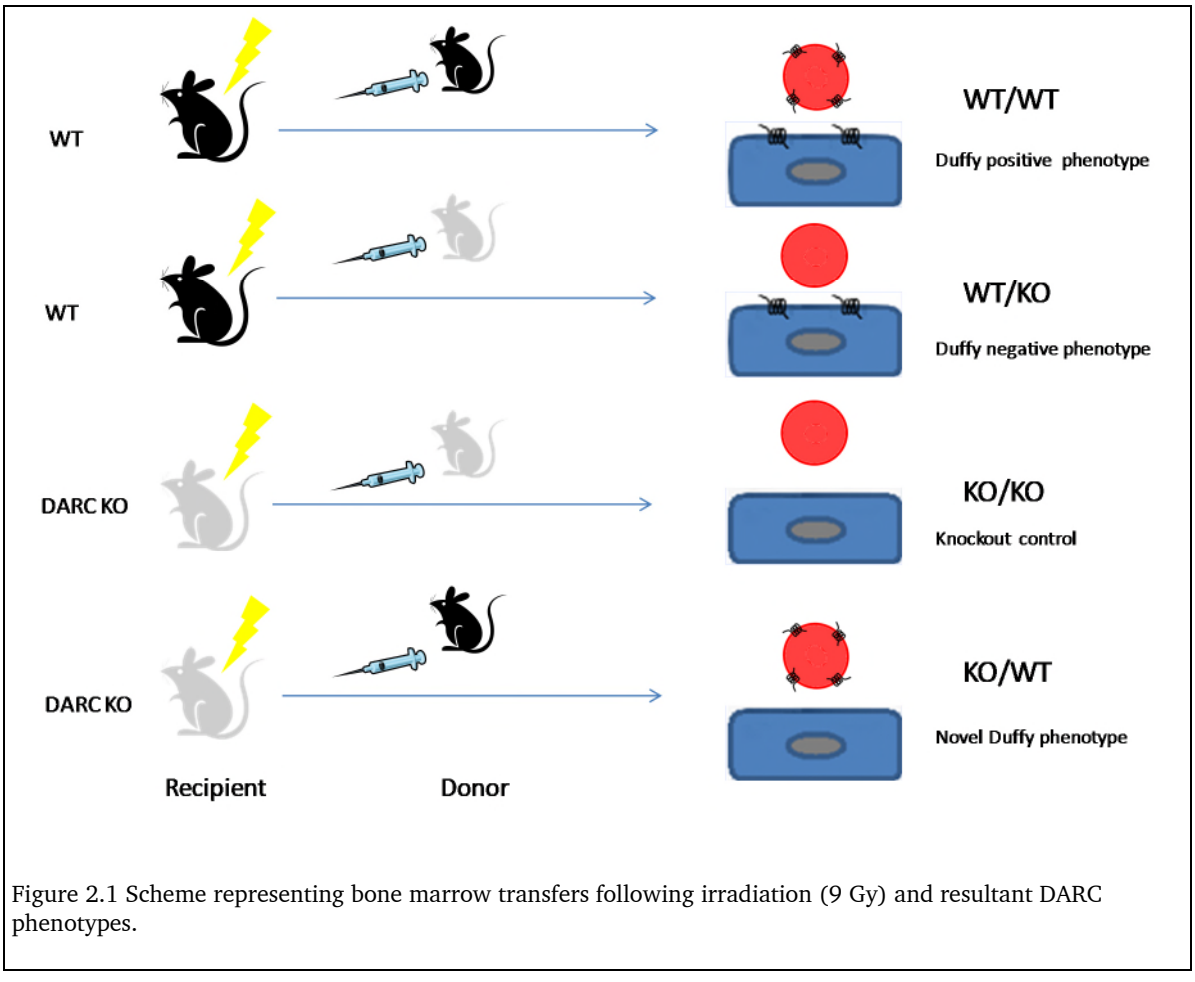

Figure 2.1 Scheme representing bone marrow transfers following irradiation (9 Gy) and resultant DARC phenotypes.

Chimeric mice reflecting the human Duffy negative phenotype ('WT-KO') had consistently lower neutrophil counts compared with all other DARC chimeric mice. Neutropaenia was detectable as early as 4 weeks post bone marrow transfer, and evident at 8 weeks post transfer, **Figure 2.2**. Thus neutropaenia set on already when the percentage of recipient erythrocytes in the blood was still approximately 40-60%, **Figure 2.2 b** and **c**.

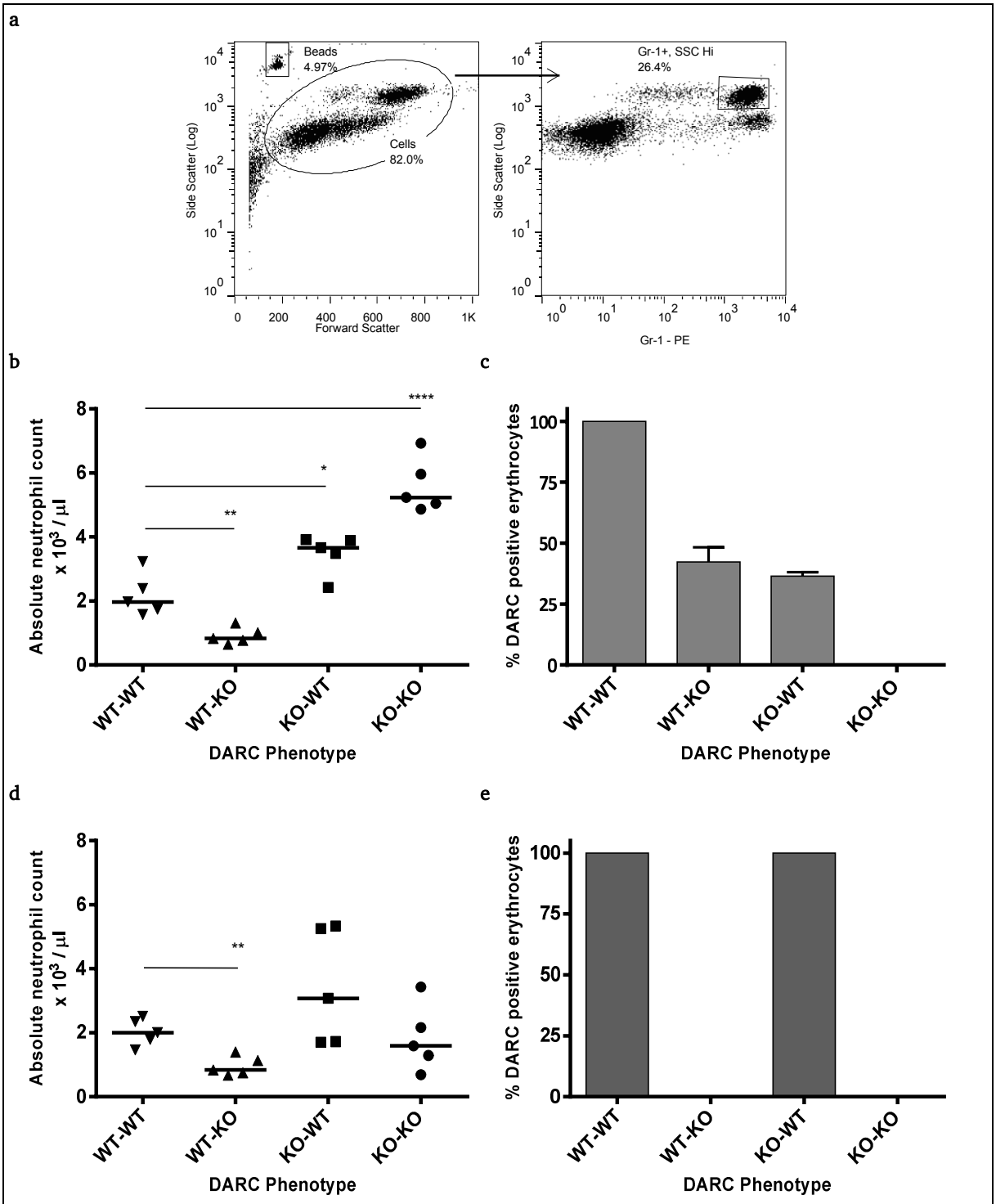

Figure 2.2 Enumeration of blood neutrophils in irradiation chimera. Representative gating (a) used for determination of neutrophil count at 4 weeks (b) and 8 weeks (d) post irradiation and bone marrow transfer. (c) & (e) DARC chimerism in peripheral blood measured as % of DARC positive erythrocytes at sampling times as in (b) & (d) respectively. Graphs show one out of two independent experiments with five mice each in each chimeric group. WT-WT (WT recipient, WT donor), WT-KO (WT recipient, DARC KO donor), KO-WT (DARC KO recipient, WT donor), KO-KO (KO recipient, KO donor). n=5 per group

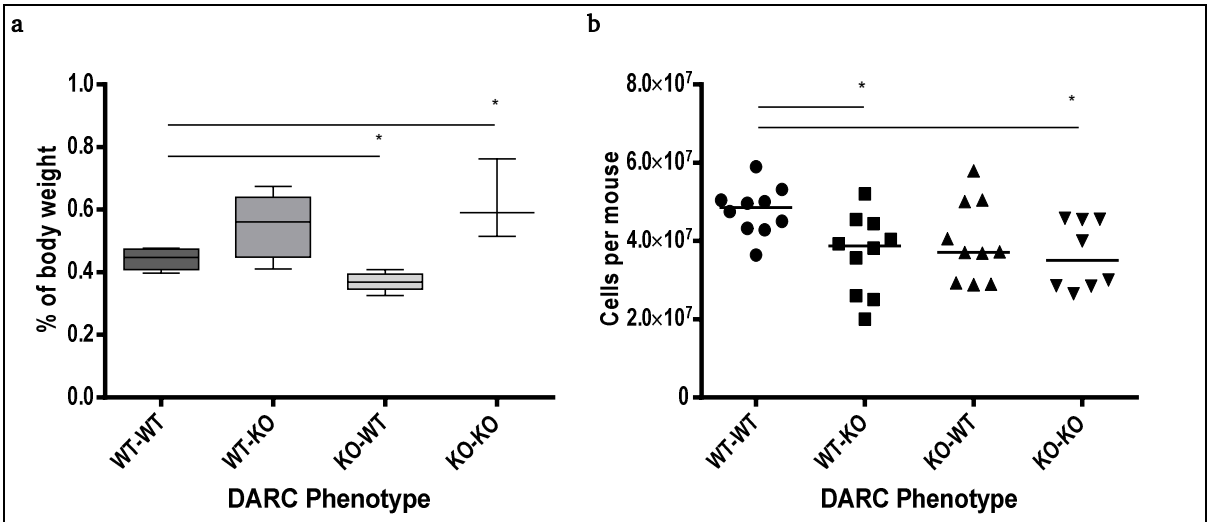

Figure 2.3 Spleen weights and bone marrow cell counts. Graph showing spleen weight as a percentage of total body weight, (a), n=5 per chimera group, except KO-KO n=3. Bone marrow total nucleated cell counts per two femurs, (b), data from two experiments, WT-WT n=10, WT-KO n=10, KO-WT n=10, KO-KO n=8

In mice lacking DARC on erythrocytes the spleen weights were mostly higher, but not significantly different, and bone marrow cellularity was reduced, **Figure 2.3**.

2.2.2 Myeloid analysis

Bone marrow neutrophils were elevated in chimeras lacking endothelial DARC, **Figure 2.4**, and although overall bone marrow and blood monocytes were not different, there was a significant increase in the proportion of non-classical monocytes in blood of the WT-KO chimeras. Myeloid cells as a proportion of total nucleated blood cells were higher in KO-WT and KO-KO mice but not significantly different (data not shown).

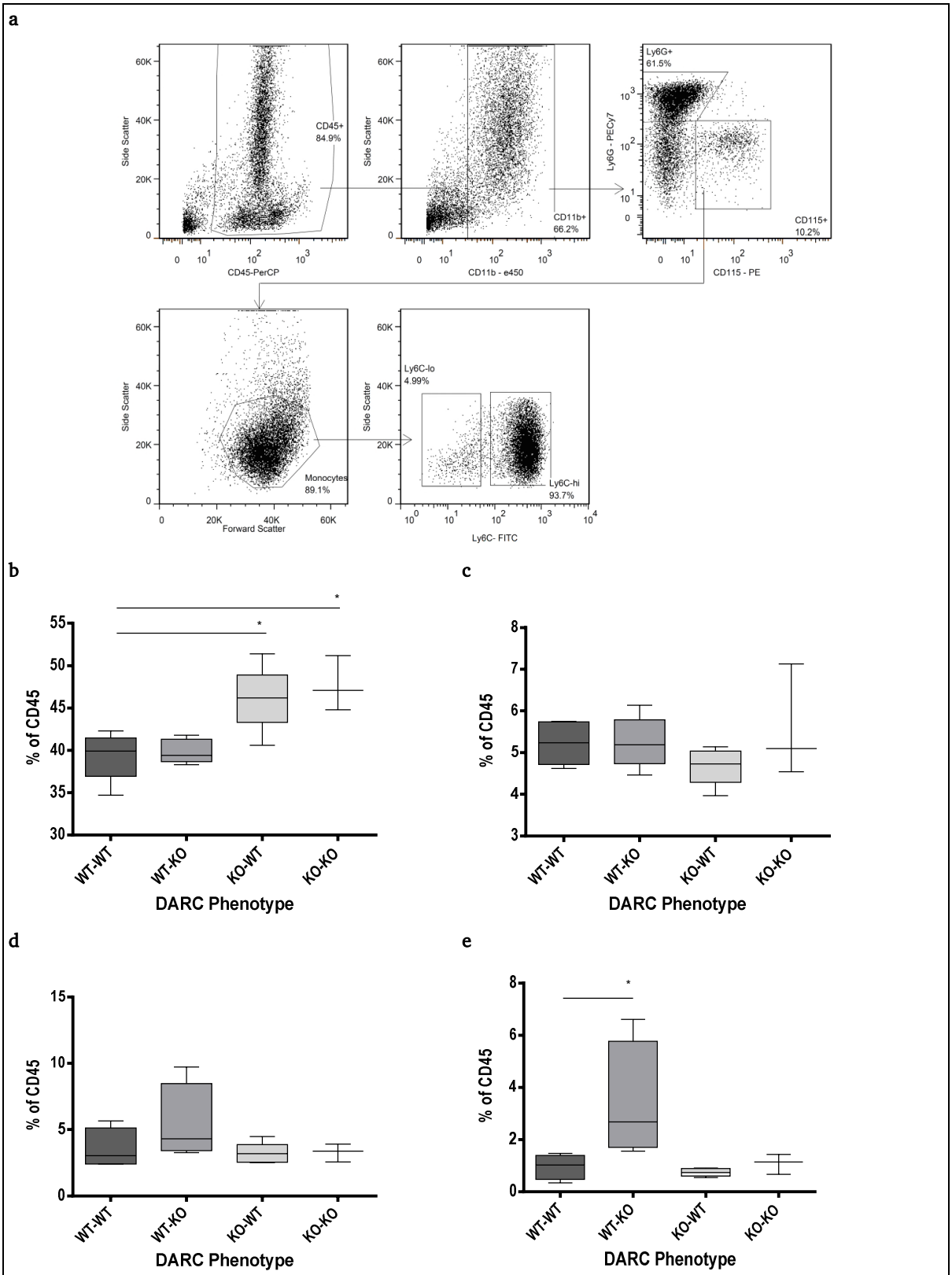

Figure 2.4 Analysis of myeloid cells in bone marrow and blood of chimeric mice. Representative gating (a). Proportions of myeloid cells in chimeric bone marrow (b) – neutrophils: $CD45^+$, $CD11b^+$ and $Ly6G^+$, and (c) Monocytes: $CD45^+$, $CD11b^+$, $Ly6G^{low/neg}$, and $CD115^+$. Blood total monocytes (d) and monocyte subgroups (e): non-classical monocytes: $CD45^+CD11b^+$, $Ly6G^{low/neg}$, $CD115^+$, $Ly6C^{low/neg}$ in blood. Monocyte subgroups in bone marrow were no different across chimera phenotypes (not shown). Experiment with n=5 mice per chimera group except KO-KO n=3

2.2.3 Lymphoid analysis

The proportions of lymphocyte subsets were also examined in the chimeric DARC mice, **Figure 2.5.** Relatively more T cells were present in the bone marrow of KO-WT and KO-KO mice, whereas fewer blood T cells were observed in the peripheral blood of WT-KO mice. Peripheral blood B cells were reduced in KO-WT chimeric mice.

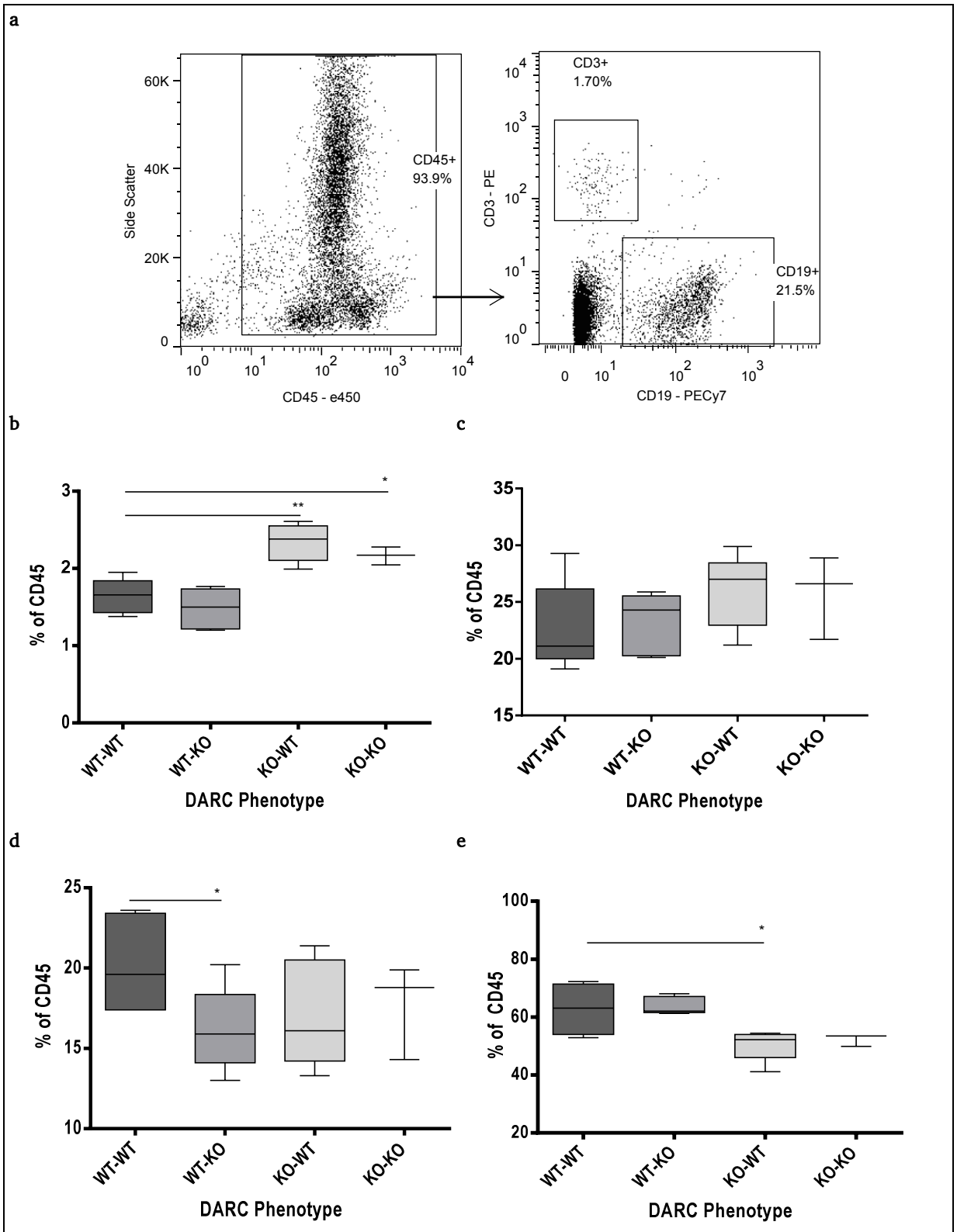

Figure 2.5 Analysis of lymphoid cells in bone marrow and blood of chimeric mice. Representative gating (a). Bone marrow T cells (b) and (c) B cells, and these respective populations in peripheral blood, (d) and (e). Experiment with n=5 mice per chimera group except KO-KO n=3.

2.2.4 Erythroid analysis

Ter119^{+} cells of the erythroid lineage, were significantly reduced in the bone marrow of WT-KO mice, **Figure 2.6**. KO-KO mice had fewer early erythroblasts, and KO-WT and KO-KO animals had significantly more late erythroblasts in the bone marrow, suggesting that more mature erythroid precursors were being retained in the bone marrow of these mice. Pro-erythroblasts were not significantly different across the chimeric groups (data not shown).

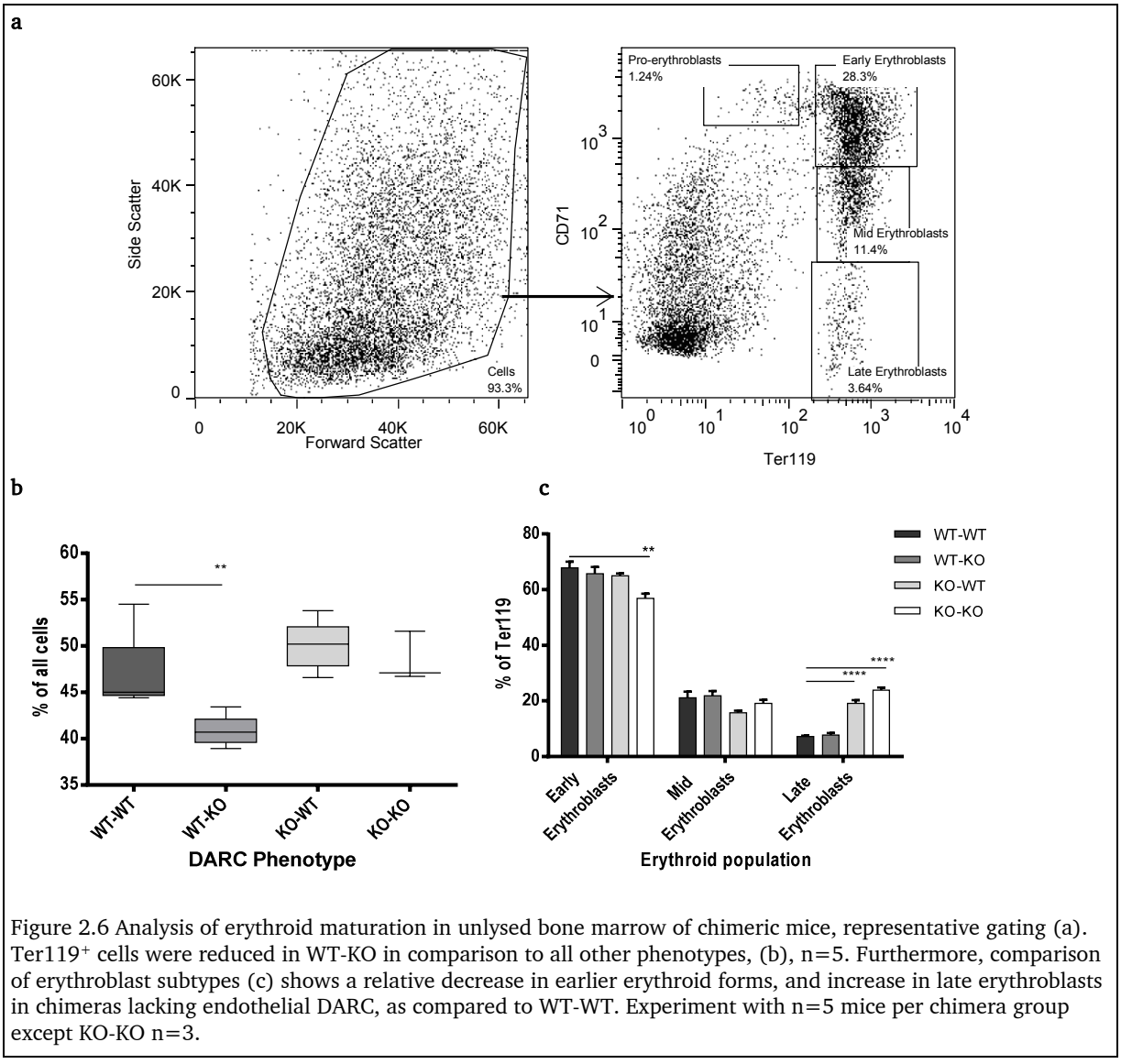

Figure 2.6 Analysis of erythroid maturation in unlysed bone marrow of chimeric mice, representative gating (a). Ter119^{+} cells were reduced in WT-KO in comparison to all other phenotypes, (b), n=5. Furthermore, comparison of erythroblast subtypes (c) shows a relative decrease in earlier erythroid forms, and increase in late erythroblasts in chimeras lacking endothelial DARC, as compared to WT-WT. Experiment with n=5 mice per chimera group except KO-KO n=3.

2.2.5 Stem and progenitor cell analysis

2.2.5.1 Myeloid Progenitors and LSK

In order to ascertain whether underlying HSPC alteration might be contributing to the observed phenotype, bone marrow myeloid progenitors and LSK cells from chimeric mice were examined, **Figure 2.7**. Myeloid progenitors were reduced in chimeric phenotype lacking erythroid DARC. This was as a result of pronounced reductions in GMP cells, **Figure 2.8**.

LSK populations were significantly increased in the KO-WT mice. In particular, the KO-WT and KO-KO mice have reduced numbers of multipotent progenitors, and correspondingly high early precursor numbers (LT- & ST- stem cells), although these were not significantly different in the KO-KO.

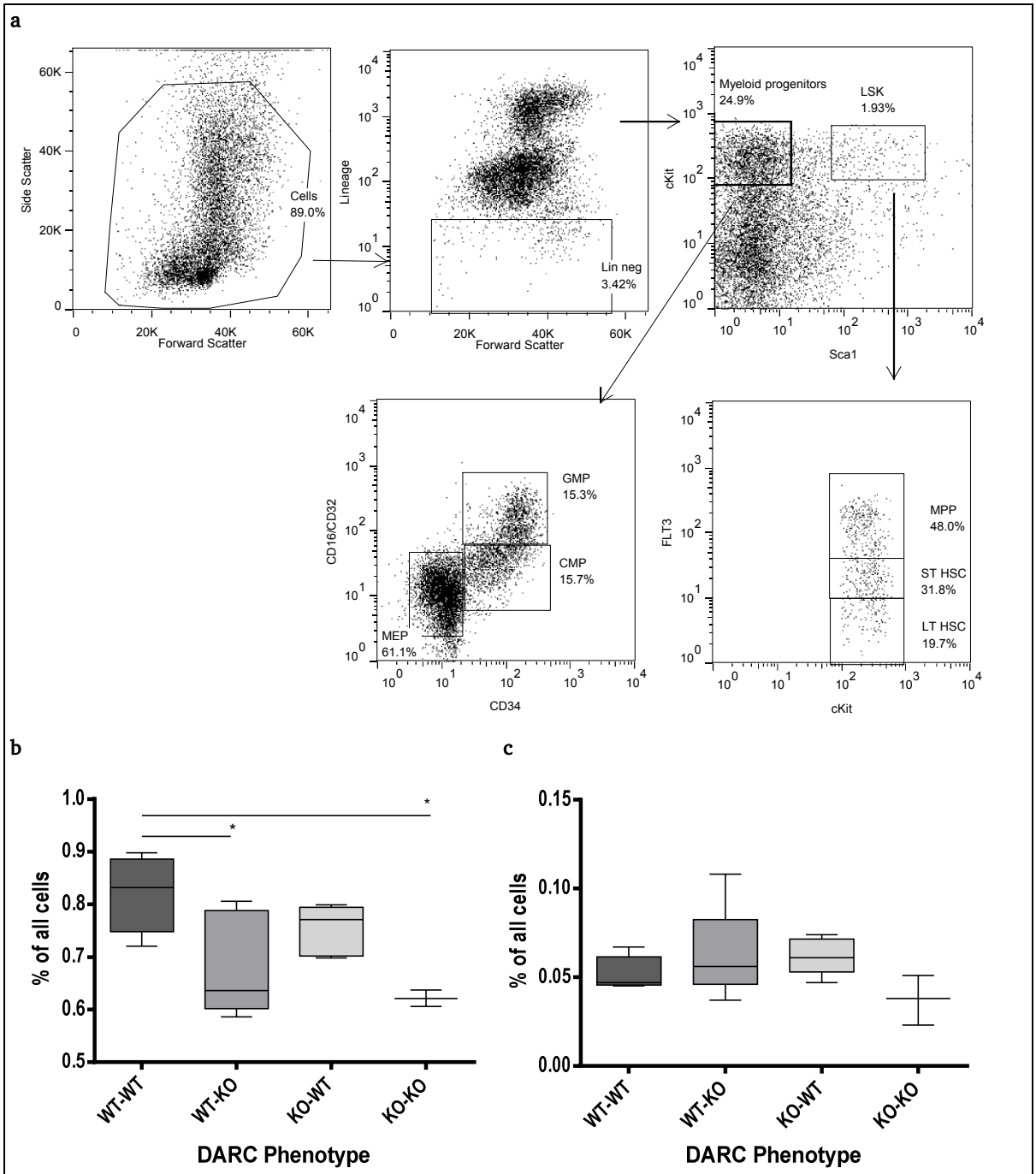

Figure 2.7 Progenitor and stem cell populations in bone marrow of chimeric mice, (a) representative gating. (b) Myeloid progenitors (Lin^- $cKit^+$ $Sca1^-$). (c) The stem cell enriched LSK fraction (Lin^- $cKit^+$ $Sca1^+$). Experiment with n=5 mice per chimera group except KO-KO n=3

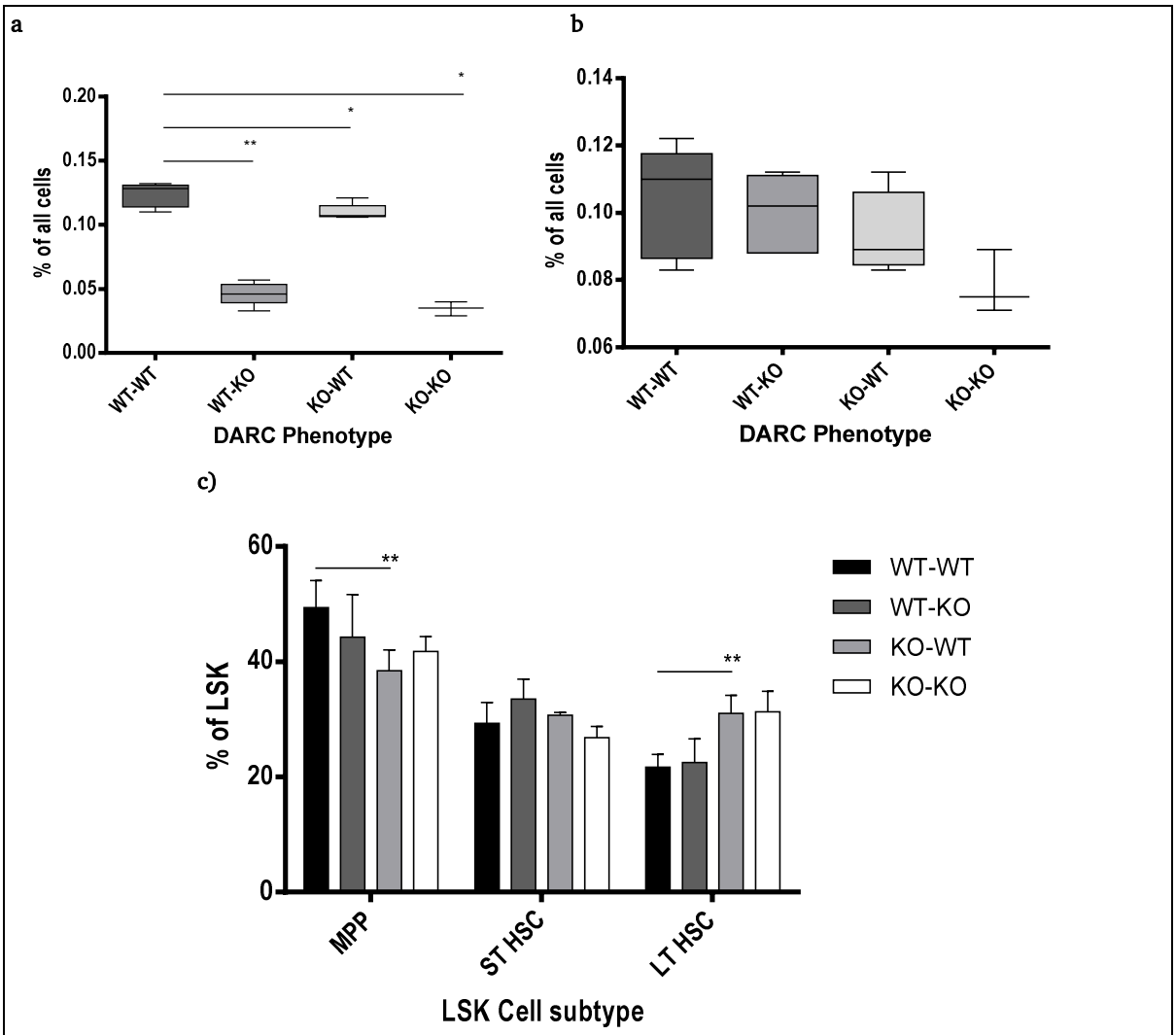

Figure 2.8. Progenitor and stem cell sub-populations in bone marrow of chimeric mice. Myeloid progenitor subtypes, GMP (Lin$^-$ cKit$^+$ Sca1$^-$ CD34$^+$ CD16/CD32^{high}) (a) and CMP (Lin$^-$ cKit$^+$ Sca1$^-$ CD34$^+$ CD16/CD32$^{low/neg}$) (b) were examined. The LSK population (c) was examined as per gating in Figure 2.7. MPP, multipotent progenitors (Lin$^-$ cKit$^+$ Sca1$^+$ Flt3^{high}), ST-HSC (Lin$^-$ cKit$^+$ Sca1$^+$ Flt3^{low}) and LT-HSC (Lin$^-$ cKit$^+$ Sca1$^+$ Flt3^{neg}). Experiment with n=5 mice per chimera group except KO-KO n=3

2.2.5.2 Multipotent progenitors

Multipotent progenitor populations (MPP) were analysed as per representative gating in **Figure 2.9**

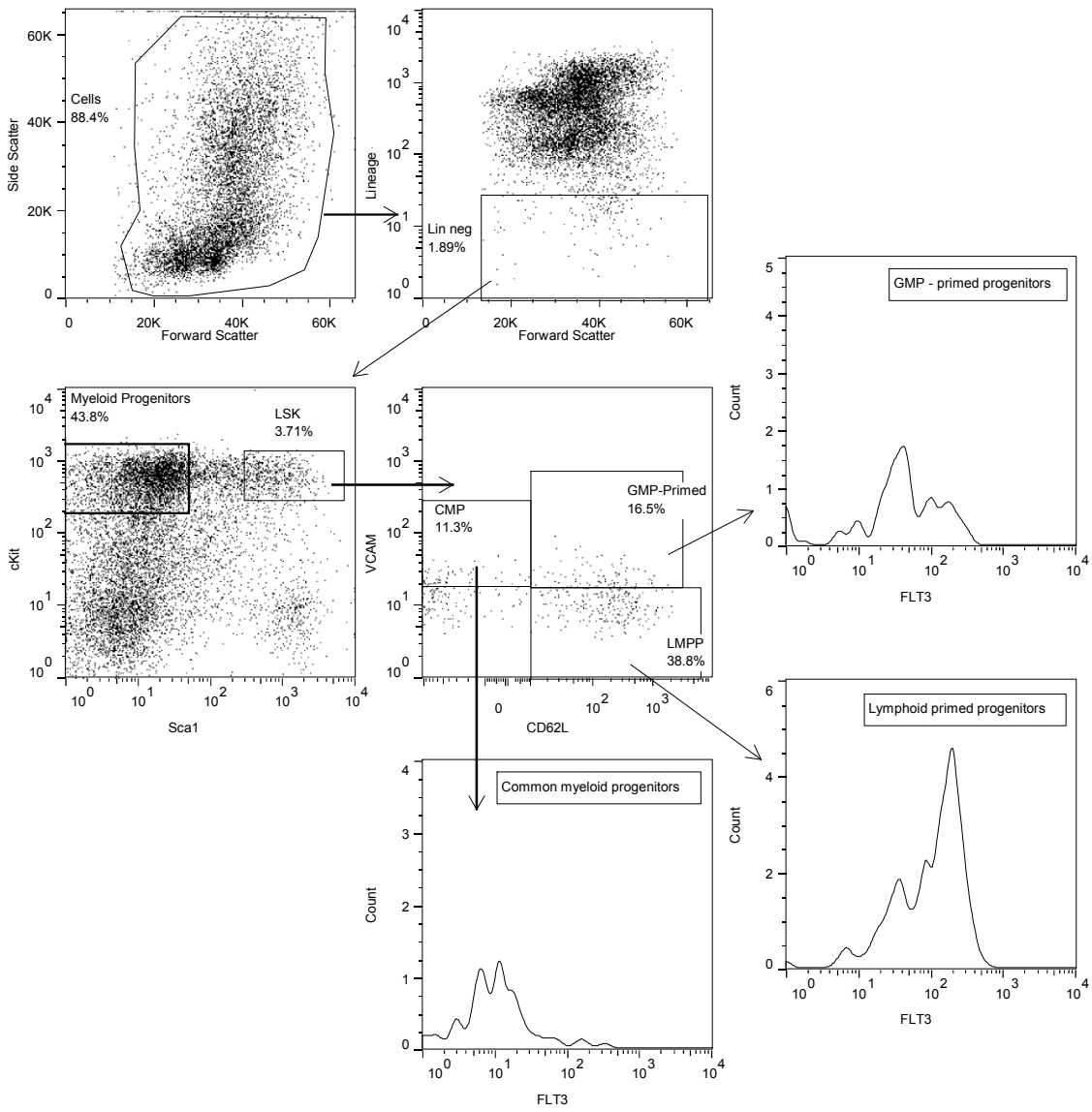

Figure 2.9 Representative gating for analysis of multipotent progenitors in bone marrow of chimeric mice. GMP-primed progenitors, Lin$^-$ cKit$^+$ Sca1$^+$ VCAM$^+$ CD62L$^+$ Flt3$^{low/mid}$; LMPP Lin$^-$ cKit$^+$ Sca1$^+$ VCAM$^+$ CD62L$^+$ Flt3^{high}, CMP Lin$^-$ cKit$^+$ Sca1$^+$ VCAM$^+$ CD62L$^+$ Flt3^{neg}.

Sub-division of the MPP contained with the LSK population, **Figure 2.10**, shows significant reductions in the GMP-primed progenitors in the MPP of the WT-KO mice. Conversely the KO-WT mice had increases in both the GMP-primed and LMPP progenitors. This was in parallel to the peripheral blood findings, where both neutrophils and lymphoid cells were altered in these phenotypes.

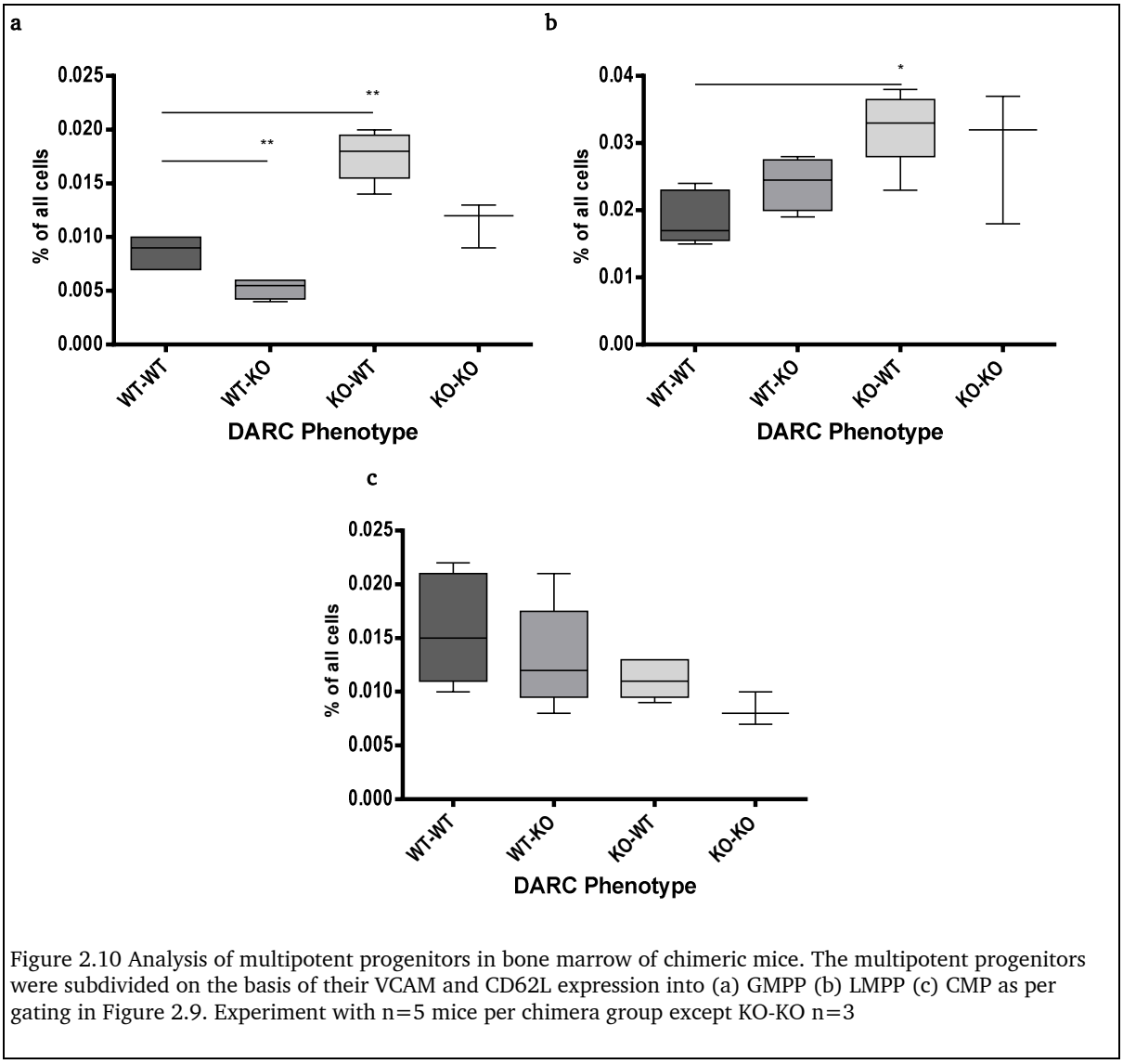

Figure 2.10 Analysis of multipotent progenitors in bone marrow of chimeric mice. The multipotent progenitors were subdivided on the basis of their VCAM and CD62L expression into (a) GMPP (b) LMPP (c) CMP as per gating in Figure 2.9. Experiment with n=5 mice per chimera group except KO-KO n=3

2.3 Discussion

The results in **Figure 2.3** are the first experimental demonstration of the association between the lack of erythroid DARC expression and reduced peripheral blood neutrophil counts (Nalls *et al.*, 2008, Reich *et al.*, 2009). Of note, neutropaenia occurred early in the bone marrow grafting period. Due to radio-resistance and long half-life of erythrocytes, erythroid engraftment leads to the complete exchange of erythrocytes only at approximately 60 days post-transplant. Neutropaenia occurred in WT-KO mice when half of their erythrocytes were still of recipient origin and thus still expressed DARC. These data are suggestive of an alteration within the bone marrow micro-environment due to early erythroid cell, and not peripheral erythrocytes, which may account for the reduced neutrophil count in the blood of WT-KO chimeras. A potential explanation for these findings may be that DARC on erythroid cells patterns chemokines within the bone marrow micro-environment thus affecting myelopoiesis. The localisation of erythroid cells in erythroblastic islands may lead to the optimum distribution or retention of chemokines for myeloid development.

The higher peripheral neutrophil counts in the KO-WT and KO-KO suggest a role for endothelial DARC in negatively regulating the release of cells from the bone marrow, or alternatively, a requirement for endothelial cell DARC to optimally direct neutrophil margination within the peripheral circulation or their homeostatic exit from the circulation into the peripheral tissues. In the bone marrow, KO-WT and KO-KO mice also had higher neutrophil proportions than WT-WT and WT-KO mice (**Figure 2.4a**) Therefore it is not likely that endothelial DARC is a negative regulator of

bone marrow release of neutrophils, but, on the contrary, may be required for the optimum release of neutrophils from the bone marrow, and also their margination or departure from the circulation into tissues.

It has been shown that in the peripheral tissues, the role of endothelial DARC is pro-inflammatory, by promoting the transmigration of leukocytes across the endothelium, whilst erythroid DARC is globally anti-inflammatory, by buffering chemokine levels and reducing leukocyte receptor sensitivity. Nevertheless chemokine reservoir function of erythrocyte DARC has also been suggested (Novitzky-Basso and Rot, 2012). It is attractive to speculate that, in line with the latter function, DARC expressed by the erythroid cells in the bone marrow may function to retain chemokines and pattern them whilst endothelial DARC in bone marrow vasculature may modulate the local distribution of ELR+ chemokines optimising their availability for homeostatic release of neutrophils into the circulation.

Other leukocyte populations such as total monocyte numbers were not altered in blood or bone marrow, although peripheral blood non-classical monocytes were significantly elevated in the WT-KO phenotype.

The KO-WT and KO-KO mice showed reductions in blood B cells as a proportion of all nucleated cells, which was significant in KO-KO mice. This may be due to the larger myeloid proportions seen in these mice, particularly since there is no significant difference in bone marrow B cells amongst the DARC phenotypes. The biological significance of the bone marrow T cell increase in the KO-WT and KO-KO is not clear, particularly given the transient nature of the mature T cells in the bone marrow.

Notably bone marrow erythroid cells were reduced in WT-KO, which may account for the slight reduction in overall bone marrow cellularity observed in this phenotype. Increased spleen size in mice without erythroid DARC may indicate a compensatory mechanism. In contrast to humans, the murine spleen is a haematopoietic organ under physiologic conditions, and these data suggests that bone marrow erythro- or haematopoiesis may be replaced by those in the spleen.

Examination of haematopoietic precursors revealed a reduction in myeloid progenitors in mice lacking erythrocyte DARC which was accounted for primarily by a substantial and significant reduction in GMPs. This suggests a role for the erythroid DARC in optimal myeloid development. This finding was further corroborated in the LSK stem-cell enriched fraction, which harbours earlier progenitors. In this population, GMP-primed progenitors were proportionally reduced, suggesting a lineage effect. CMP were not different, and there was an increase in lymphoid-primed multipotent progenitors in mice without endothelial DARC, which was significant in the KO-WT mice. The MPP group as a whole was reduced in chimeric mice lacking endothelial DARC. It is not known whether the absence of endothelial DARC affects the stem cell niche micro-environment, particularly the perivascular niche. There may be alterations in the expression of other adhesion molecules in the endothelium, or alternatively other changes in the micro-environment may modulate signals to transcription factors and other signalling pathways regulating cell lineage fates and HSC turnover, potentially explaining these findings. However this has no relevance to studies in humans as no populations are deficient in endothelial DARC.

Despite the utility of the irradiation bone marrow chimeras in demonstrating different roles for DARC expressed in haematopoietic and endothelial cells, there remain substantial drawbacks in using this method. Primarily, irradiation induces significant inflammation due to cellular damage. This may account for the increased baseline neutrophil counts in all animals compared with non-irradiated WT mice, and the higher counts in the KO-WT and KO-KO at 4 weeks after the graft. In addition, bone marrow studies requiring the setting of gates on lineage negative cells are affected by experimental variation, and the use of non-irradiated WT mice is not a suitable substitute. Furthermore, irradiation with 9 Gy, currently the maximal dose allowed under the Home Office guidelines, is insufficient to eradicate all the host cells, particularly dendritic cells and T cells, which may have subtle effects on the take and function of the bone marrow graft. Finally, irradiation causes animal suffering and a genetically modified animal model would reduce this harm, and animal numbers needed in the development of chimeras.

In order to study the contribution of erythrocyte DARC on haematopoiesis without the effects of inflammatory stimuli induced by irradiation, and to follow the animal husbandry principles of the 3Rs (replacement, reduction and refinement), we conceived a humanised mouse model reflecting two common human DARC polymorphisms. We set to produce transgenic mice expressing human DARC on the vascular endothelium but not on erythrocytes, as encoded by the *FYB(ES)* allele, or on both endothelium and erythrocytes, as encoded by *FYB* allele. We postulated that the establishment of such models would permit clearer dissection of the role of erythoid DARC in haematopoiesis.

Chapter 3

The development of *FYB(ES)* and *FYB* transgenic strains

3.1 Introduction

The FYB(ES) and FYB transgenic models were developed to study the role of erythroid DARC in haematopoiesis and investigate the mechanisms which may underlie the peripheral blood neutropaenia in chimeric mice lacking erythroid DARC. Furthermore it was postulated that the development of these strains would decrease technical experimental variations induced by irradiation as well as reduce animal use and suffering.

3.2 Materials and methods

3.2.1 Molecular Biology

3.2.1.1 DNA extraction from human blood

Human blood was taken from healthy volunteers following the ethical approval by the Ethics Committee of the School of Medical and Dental Sciences, University of Birmingham following informed consent. DNA was extracted using the DNeasy Blood & Tissue Kit (Qiagen). Briefly, blood samples were lysed with proteinase K, and the lysate centrifuged in a silica-based spin column which absorbs DNA, allowing the pass through of contaminants and enzyme inhibitors during two wash steps, after which DNA was eluted in ddH_2O.

3.2.1.2 Cloning of human DNA

Cloning was undertaken using the High Fidelity Phusion DNA polymerase (Thermo Scientific), which generates amplified genomic DNA of interest with a very low error rate. The following cloning primers were designed:

Forward Primer: ACA TGG TTT GAA CTG CCT TTC C

Reverse Primer: CCT CTG GGT AGA GGG TGA ATT TGC

3.2.1.3 DNA purification

DNA was purified using Fermentas GeneJET PCR Purification Kit. Briefly, DNA containing reaction was combined with a binding buffer (containing a chaotropic agent to denature proteins) and was put through a spin-column with a silica-based membrane after which an ethanol wash step removed impurities. Then DNA was eluted with a buffer.

3.2.1.4 Ligation into plasmid vector

The CloneJET PCR Cloning Kit (Thermo Scientific, UK) was used as per the manufacturer's instructions. The pJET1.2/blunt cloning vector contains a lethal gene which is disrupted by ligation of DNA insert into the cloning, permitting cells only with recombinant plasmids to propagate. Using the blunt-end protocol, reaction buffer, purified DNA, pJET1.2/blunt cloning vector and T4 DNA Ligase were combined on ice, vortex mixed, and incubated at room temperature for 5min, and then used for transformation of bacteria.

3.2.1.5 Bacterial transformation

Gold Efficiency α-Select Chemically Competent Cells (Bioline, UK) were used to incorporate and amplify the ligated plasmid vector. Briefly, cells were thawed on wet ice and 50μl of cell suspension was mixed with ligation mixture or control PCR product and incubated on ice for 30min, thereafter undergoing heat shock in 42°C water bath for 30 seconds, and then subsequently returned to ice for 2min. Then the transformation mixture was diluted in SOC medium: 2% tryptone, 0.5% Yeast extract,

0.4% glucose, 10mM NaCl, 2.5mM KCl, 10mM $MgCl_2$, 10 mM $MgSO_4$, and tubes were agitated for 60min at 37°C. SOC medium was used as it improves the transformation efficiency.

3.2.1.6 Plasmid DNA purification for clone selection

GeneJET Plasmid Miniprep Kit (Thermo Scientific, UK) was used to purify plasmid DNA from bacterial cultures. Briefly, cultured bacteria were pelleted and subjected to lysis with an alkali, releasing free plasmid DNA. The lysate was neutralised and centrifuged so that debris and precipitates were pelleted, and the supernatant containing plasmid DNA was added to a spin column containing a silica membrane which bound the plasmid DNA. The DNA was then washed with an ethanol containing buffer, and was then eluted with 50μl of the supplied elution buffer.

3.2.1.7 Restriction enzyme digestion for analysis

EcoRI restriction enzyme recognises G^AATTC sites and is predicted to cut the *DARC* gene sequence at position 1090 and 2996, giving 1090bp and 1906bp fragments. The reaction was prepared by mixing ddH_2O on ice, with 10x EcoRI Buffer, 1μg DNA, EcoRI 5u, and then incubated for 1-4 hours at 37°C. There after the product was run on 0.7% agarose electrophoretic gel for band analysis.

3.2.1.8 Restriction enzyme digestion for removal of vector

The restriction enzymes XhoI (recognises C^TCGAG), XbaI (T^CTAGA) and PvuI (CGAT^CG) do not cut *DARC* gene, and were used to remove the vector from the construct.

3.2.1.9 DARC KO genotyping

Tissue was lysed using 75μl of lysis buffer (25mM NaOH, 0.2 mM EDTA), for 45min at 95°C, after which 75μl of neutralisation buffer (40mM Tris-HCl, pH 5.5) was added, and the sample vortexed for 60 seconds.

Standard PCR conditions were: 1.2μl of 10x PCR buffer, 0.2mM dNTP, 1.5mM $MgCl_2$, 0.5μM Primer Duffy KO1, 1μM Primer Duffy KO2, 0.5μM of Primer Duffy Neo, ddH_2O, 0.25 units of *Taq* polymerase (Biotaq, Bioline, UK), 25-300ng of template in 1-2μl, run 37 cycles of 30s, 94°C; 30s, 60°C; 30s, 72°C, final 2min 72°C.

Sequences for primers were used from Dawson *et al.*, 2000 as below:

Duffy KO1: GCT AGA TGC CCT GAC TGT CC

Duffy KO2: CCA GTA GCC CAG GTT GCA TA

Duffy Neo: TAT GGC GCG CCA TCG ATC TC

The presence of a wild-type allele gives a 400bp product, whilst the *Neo* (DARC KO) allele gives a 300bp product.

3.2.1.10 Genotyping of hDARC transgenic mice

In order to genotype animals containing human DARC gene, primers were designed using Primer 3 (http://biotools.umassmed.edu/bioapps/primer3_www.cgi), using entire human *DARC* gene sequence. Results that detected murine targets were excluded. Potential primers were analysed using Eurofins Oligo Analysis Tool

(http://www.operon.com/tools/oligo-analysis-tool.aspx), to analyse potential self- and cross-primer hybridisation potential.

The following primers were selected:

Forward:	TGF62	TCA GCC GCC CTT CCA CTC CA
Reverse:	TGR402	TTA CCC CAC GCC CAC TGC CT

The reaction was optimised and standard PCR conditions for detection of human *DARC* gene were: 1x PCR buffer, 0.2mM dNTP, 1.5mM $MgCl_2$, 0.5μM of Primer TGF62, 0.5μM of Primer TGR402, ddH_2O, 0.25 units of *Taq* polymerase, 25-300ng of template in 1-2μl, run 37 cycles of 30s, 94°C; 30s, 69°C; 30s, 72°C, final 2min 72°C. The presence of human *DARC* corresponds with a product of 327bp. This primer pair does not distinguish between *FYB* and *FYB(ES)* alleles.

3.2.1.11 Human DARC Genotyping for Polymorphic Alleles

The detection of human DARC alleles was undertaken using the method described in Mullighan *et al.*, 1998. DNA was extracted using the Qiagen Blood DNA extraction kit. Four separate reactions were undertaken, containing the primers to detect *FYA*, *FYB*, wild-type GATA sequence in the GATA erythroid promoter region of DARC, and the *FYB(ES)* promoter region mutation. Human growth hormone (HGH) gene primers were used to control that the PCR mix amplified template.

Standard PCR conditions were: 1x PCR buffer, 0.2mM dNTP, 2mM $MgCl_2$, 0.56 μM Primer A, 0.56 μM Primer B, 0.2 μM HGH1, 0.2 μM HGH2, ddH_2O, 0.06μl of *Taq*

polymerase, 10-100ng of template in 1-2μl, run 37 cycles of 30s, 94°C; 30s, 60°C; 30s, 72°C, final 2min 72°C.

Primer mixes used:

FYA **expressed: FYA and Fy expressed**

FYB **expressed: FYB and Fy expressed**

FYB(ES)**: FyB and Fy Null**

All FY primer reactions give a 700 bp band while HGH primer reactions give a 345bp band on electrophoretic gel.

Primer sequences:

Fy expressed:	TCA TTA GTC CTT GGC TCT TAT
Fy null:	TCA TTA GTC CTT GGC TCT TAC
FYA:	GCT GCT TCC AGG TTG GCA C
FYB:	GCT GCT TCC AGG TTG GCA T

3.2.2 Assessment of mRNA levels and DARC gene expression

3.2.2.1 Sample preparation

Animals were culled by cervical dislocation, and organs were removed and preserved in RNAlater (Invitrogen).

3.2.2.2 RNA extraction

RNA was extracted from 20mg tissue pieces using an RNeasy kit (Qiagen), according to manufacturer's instructions. Briefly, tissue was added to 600μl Buffer RLT with β-mercaptoethanol, and homogenised using a rotor homogeniser, thereafter 350μl of 70% ethanol was added. The sample was applied to a column and centrifuged for 15s at 13000g to bind the sample to the column. The flow-through was discarded, 700μl of Buffer RW1 was added to the column, the sample was centrifuged for 15s at 13000g, and the flow-through discarded. Then 500μl of Buffer RPE was added to the column and the sample was centrifuged for 15s at 13000g after which the flow-through was discarded. A further 500μl of Buffer RPE was added and the sample was centrifuged for 2min at 13000g. The column was transferred to a new collection tube. Finally, 30μl RNase-free water was added to the column, and the sample was centrifuged for 1min at 13000g to elute the RNA.

Extracted RNA underwent DNA digestion, using the Promega RQ1 RNase-Free DNase kit as per manufacturer's instructions. Briefly, up to 8μl of RNA, 1μl RQ1 10x reaction buffer, 1 unit of RQ1 DNase per microgram of RNA were incubated at 37°C for 30min, after which 1μl of RQ1 DNase Stop Solution was added, and the mixture incubated at 65°C for 10min to inactivate the DNase. The reaction was scaled up to treat all RNA.

After DNA digestion, RNA underwent column clean-up as per RNeasy kit manufacturer's instructions. Briefly, the sample volume was adjusted to 100μl with RNase-free water, and 350μl of Buffer RLT and 250μl 100% ethanol were added. Following mixing by pipetting, the sample was transferred to an RNeasy Mini spin

column in a 2ml collection tube, and centrifuged for 15s at 8000g. The follow-through was discarded, 500μl of Buffer RPE was added to the column and the sample was centrifuged for 15s at 13000g after which the flow-through was discarded. A further 500μl of Buffer RPE was added and the sample was centrifuged for 2min at 13000g. The column was transferred to a new collection tube. Finally, 30μl RNase-free water was added to the column, and the sample was centrifuged for 1min at 13000g to elute the RNA, to be stored at -80°C until used.

3.2.2.3 First-strand cDNA synthesis (reverse transcription, RT)

The concentration of total RNA in each sample of purified RNA was determined using a spectrophotometer (Nanodrop 2000c, Thermo Scientific, UK) whereby the absorbance of each sample was measured at a wavelength of 260 nm (A_{260}). Distilled H_2O was used as a reference (0), since this was used to elute samples. RNA quality was determined from the A_{260}:A_{280}, indicating the degree of protein in the sample. Only samples giving values approximately 1.9-2.1 were used for RT.

RT was then performed using SuperScript VILO cDNA Synthesis Kit (Invitrogen Life Technologies, UK) according to the manufacturer's instructions. Briefly, a master mix was prepared with the following components for each reaction: 5x Vilo Reaction Mix 4μl, 10x SuperScript Enzyme Mix 2μl, RNA 1μg and RNase-free water to make up a reaction volume 20μl. Tube contents were mixed and incubated for 10min at 25°C, then 42°C for 60 min, and the reaction was terminated at 85°C for 5min. cDNA was stored at -20°C until used.

3.2.2.4 Measurement of gene expression by Quantitative Real Time PCR

Gene expression was measured utilising Applied Biosystems Taqman Gene expression system.

A master mix with 1x DARC Taqman Gene Expression assays with 1x Taqman Universal PCR Master Mix (Applied Biosystems, CA, USA), was added to wells of a 384 well plate along with test cDNA. Wells contained Taqman assays specific for human *DARC* and housekeeping gene *GAPDH* and/or *HPRT* according to previous optimisation experiments. The plate was loaded into an ABI 7900HT Real-time PCR System (Applied Biosystems) and run with the following program: 50°C for 2min, 95°C for 10min, and then 95°C for 15s, 60°C for 1min, for 40 cycles. Fluorescence analysis was performed utilising SDS v2.4 software (Applied Biosystems). The threshold was set manually at the logarithmic phase of the PCR reaction.

The threshold cycle (C_T) value obtained was then used to calculate the fold change in the expression of each gene relative to the housekeeping gene by using the $2^{-\Delta\Delta C_T}$ method, and the relative quantification was plotted. Genes which had a C_T value >40 were below the level of detection of the assay and were assigned an RQ value of zero. For measurement of relative gene expression, the reciprocal of the difference in C_T value between the target and housekeeping gene was used ($\frac{1}{\Delta C_T}$).

3.2.3 Flow Cytometry

3.2.3.1 Erythrocyte flow cytometry

Fluorescent antibody staining of erythrocytes (human or mouse) was undertaken by diluting whole blood so that $1x10^6$ erythrocytes were present in 100μl of wash buffer. Samples were incubated with heat inactivated FCS and purified anti-mouse or -human CD16/CD32, centrifuged at 375g for 10min, and then incubated with appropriate antibody mix, usually anti-murine DARC conjugated to Alex-Fluor 488 or Alexa-Fluor 647, and Ter119. Alternatively, erythrocytes were incubated with anti-Fy6 for 30min on at 4-8°C, and then washed, after which the sample was incubated with goat anti-mouse IgG-PE for 20min at 4-8°C. Cells were washed, re-suspended in wash buffer and transferred to polypropylene tubes.

3.2.4 Immunofluorescence

Frozen sections were acetone fixed for 20min at 4°C after cryosectioning and were rehydrated with PBS supplemented with 10% fetal calf serum and anti-mouse CD16/CD32 for 10min. Sections were incubated at room temperature in PBS supplemented with 1% bovine serum albumin for 10min, then washed for 5min in PBS. Secondary antibodies were incubated for 30min at room temperature. Sections were immersed in DAPI for 1min for nuclear staining, then mounted with Vectashield (Vector Labs) and kept in the dark at 4˚C.

Anti-Fy6 binding was detected with goat anti-mouse IgG2b Alexa Fluor 555. A Zeiss LSM 510 Meta confocal microscope (Zeiss) was used to visualise staining on sections.

Images were captured and processed using Zeiss LSM Image Examiner software (Zeiss).

3.2.5 Competition binding to human DARC of chemokines and the anti-Fy6 antibody

The method described by Tournamille *et al.*, 1997 was used with modifications. Briefly, blood was taken from Duffy-positive laboratory donors and 10^6 red cells were incubated with increasing concentrations (10^{-11} – 10^{-7} M) of cognate (CXCL8, mCXCL1) and non-cognate (hCCL21, mCXCL12) chemokines, in 100 μl PBS with 0.5% BSA for 1 hour at 37ºC and subsequently 1μl of anti-human Fy6 (mouse IgG2b, a kind gift from Dr M Uchikawa, Japanese Red Cross) for 30min, and finally 1μl of R-PE goat anti-mouse antibody added (Southern Biotech, USA). Cells were washed at 1000g for 10min and analysed on a FACS Calibur flow cytometer. Mean fluorescence index was read and IC_{50} calculated using GraphPad Prism software version 5.

3.3 Development of FYB(ES)TG murine model

The development of FYB(ES)TG murine model of the Duffy-negative phenotype was undertaken using the methods as described in Chaudhuri *et al.*, 2004, with a key difference that the human transgene was inserted into oocytes from DARC KO mice instead of wild-type mice. Importantly, the entire *DARC* gene including all potential regulatory regions were included, specifically incorporating 1kbp before and after the open reading frame of the main exon.

Initial design of the construct and cloning was performed by Dr MH Ulvmar. The work was continued as part of this thesis.

Following cloning from *FYB(ES)* homozygous donor and selection of suitable clones, 10ml of LB media with 100μg/ml of carbenicillin and ampicillin (CAM) in a universal container were cultured overnight at 37°C with bacterial colonies (designated clone 7(2)), after which 10μl from these cultures were added to further LB broth with CAM and allowed to grow over eight hours. Large scale amplification was undertaken using 500μl of bacterial culture in 500ml of LB broth with CAM. Plasmid DNA was extracted using Qiagen Maxiprep (Maxi) kit. The final elution was undertaken into 400μl of water. The amount of DNA in the preparation was routinely determined by measuring OD_{260} on a spectrophotometer, with a concentration of 1657ng/μl giving a total of 654.5μg for this amplification step.

Restriction analysis was undertaken utilising EcoRI restriction enzyme, which produced bands as expected, indicating the correct product had been amplified.

In order to remove the vector backbone, 2 samples of 10μg product were incubated with 20μl of 5x Tango buffer, Xba1 30 units (New England), Xho1 15 units (New England) PVU1 15units (Promega) and 65μl ddH_2O overnight 37°C (16 hours). Subsequently DNA from one digest was purified using Fermentas Purification Kit, with final total DNA 8μg.

Digested product was run on 0.7% agarose gel, and *FYB(ES) DARC* gene (a 3.2kbp product) was excised (**Figure 3.1 a & b**), cleaned up using Fermentas Gel Purification Kit, and analysed by EcoRI restriction enzyme digestion, giving two products (1906bp and 1090bp) as expected, (**Figure 3.1 c**) total DNA 2.44μg.

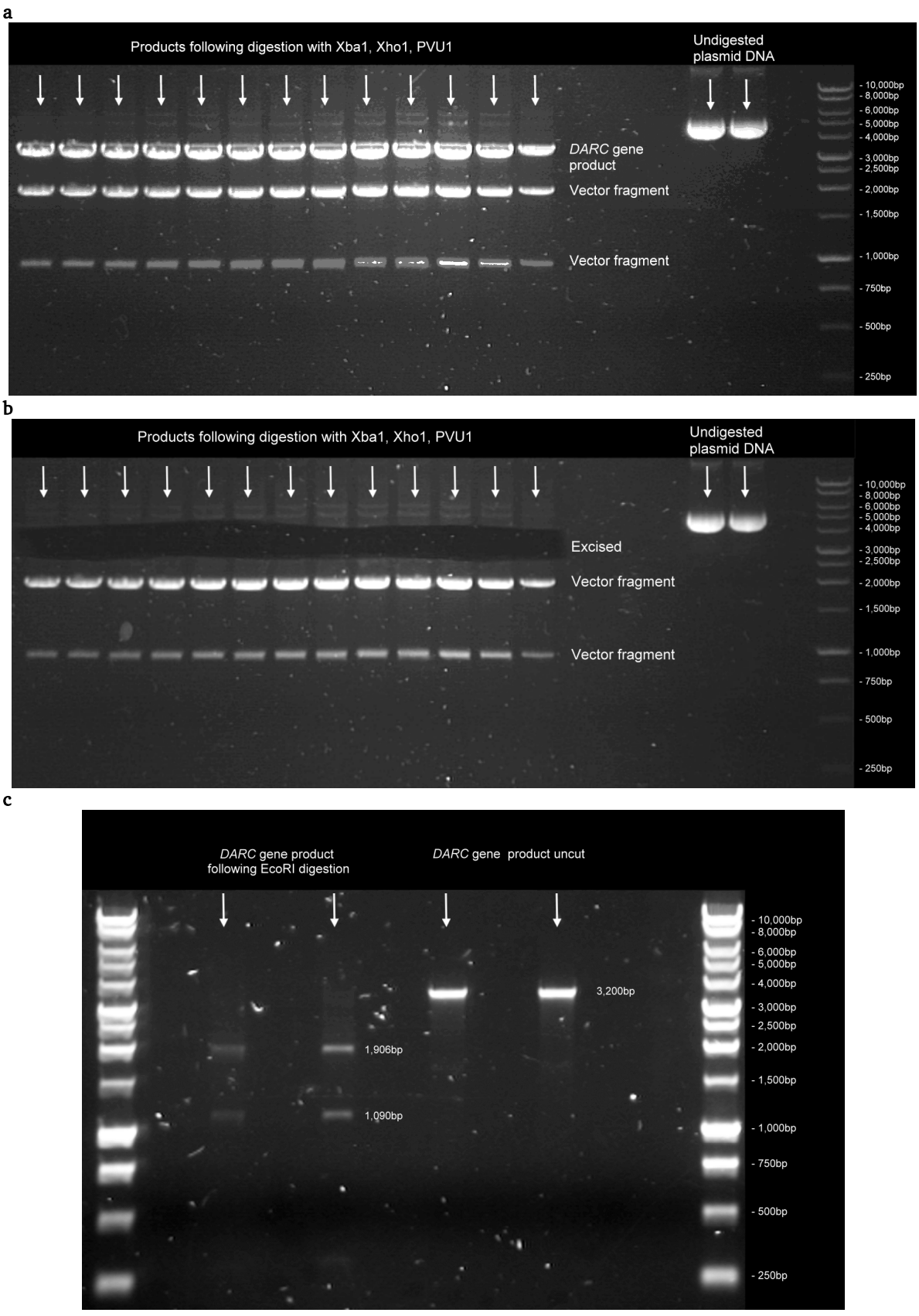

Figure 3.1 Representative 0.7% agarose gels following Xho1, Xba1, Pvu1 digestion of plasmid DNA (first 13 lanes) before excision of *DARC* gene product (a) and after (b), and restriction enzyme analysis of excised gene product by EcoRI (c).

The amplified gene product was fully sequenced using primers, which would cover the whole gene sequence. Sequencing was undertaken at the University of Birmingham School of Biosciences Sequencing Service. Sequence data were extracted using Sequence Scanner 1.0 (Applied Biosystems), and aligned with *DARC* gene sequence using NCBI BLAST (http://blast.ncbi.nlm.nih.gov/). Initial screening confirmed the presence of T-*46*C GATA-1 promoter mutation, and the presence of A at position 1142, indicating the *FYB(ES)* DARC allele was incorporated in the clone. No mutations leading to alterations in DARC protein sequence were detected.

Construct micro-injection into oocytes from super-ovulated DARC KO mice was undertaken by Dr Andrea Bacon.

3.4 Development of FYB Transgenic mouse strain

Donor blood was collected and DNA extracted by MH Ulvmar from a FYB homozygous donor. Cloning was undertaken using the High Fidelity Phusion DNA polymerase (Thermo Scientific) according to manufacturer's protocol, with template 50ng DNA per 100μl reaction.

Product was purified through Fermentas GeneJET PCR Purification Kit according to manufacturer's instructions, and eluted into 50μl AE Buffer, with a concentration of 21.9ng/μl as measured on Nandodrop. Gel electrophoresis on 0.7% agarose gel

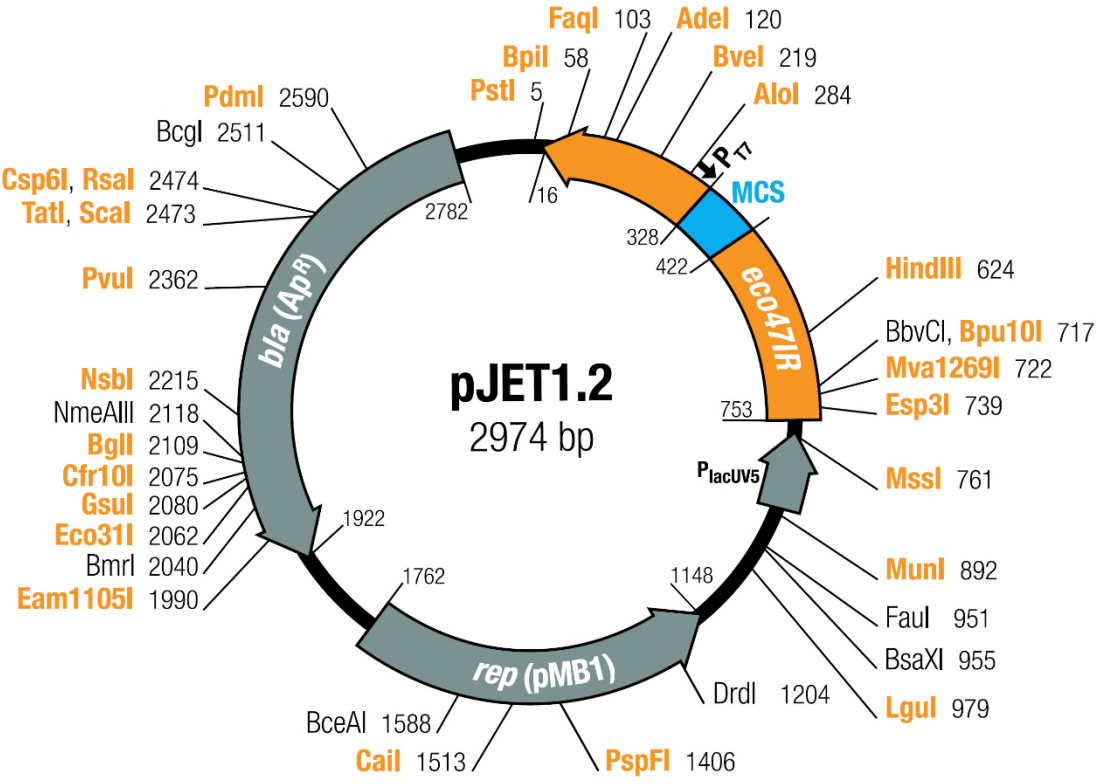

Figure 3.2. Layout of pJET1.2 plasmid. Restriction enzyme digestion sites are highlighted in bold orange font, followed by position on sequence cut.

revealed a single 3.2kbp product, consistent with amplified *DARC* gene.

Fifty nanograms of purified gene product was ligated into the pJET1.2/blunt Cloning vector **(Figure 3.2)**. Given the 3.2 kbp size of the product, a 3:1 product-to-vector ratio was used as per kit protocol.

Four microlitres of the ligation mixture containing cloned *DARC* gene and 2μl of ligation mixture and separately control PCR product (supplied with kit) were used directly for transformation of Alpha-Select Gold Efficiency bacteria, as per manufacturer's instructions.

Either 50μl or 100μl of transformation reaction was spread onto 10 LB agar plates containing 100μg/ml of carbernicillin and ampicillin (CAM). Cultures incorporating vector with control PCR product were run in parallel. Plates were incubated overnight at 37°C.

Individual colonies were picked and incubated overnight in 5ml cultures of LB broth at 37°C and agitated at 200 rpm.

Plasmid DNA was purified using the Thermo Scientific GeneJET Plasmid Miniprep Kit, from 2ml of overnight cultures, yielding between 2.5μg and 8.8μg of plasmid DNA.

Approximately 500ng of plasmid DNA was used for restriction enzyme analysis, undertaken utilising EcoRI restriction enzyme (Fermentas), which is predicted to cut product at position 1090 and 2996, giving a 1906 fragment and vector backbone. Gel electrophoresis on 0.7% agarose gel revealed the presence of predicted bands in 9 out of ten clones.

All clones were sequenced, and initial screening confirmed the absence of T-*46*C GATA promoter mutation, and the presence of A at position 1142, indicating the FYB DARC allele was incorporated in clones.

Clone 3 was selected, and fully sequenced. The following mutations were noted:

Position from beginning	Change in sequence
627	G/C
808	T deleted
3126	G/A
2635-2638	GTGT deleted

Table 3.1 Mutations detected in FYB construct C3. All were present in non-coding and non-regulatory regions.

As all mutations were located present outside coding and regulatory regions, it is unlikely that these mutations are of implication in the gene product.

Gene product was amplified as detailed for the *FYB(ES)* construct. Restriction analysis was undertaken utilising EcoRI restriction enzyme with 100ng of plasmid DNA, and expected bands were visualised with gel electrophoresis on 0.7% agarose gel. Repeat sequencing was undertaken, and no further mutations were noted in the amplified product. Vector excision was then performed as for the *FYB(ES)* construct.

Gene product (1μg) was provided to Dr Andrea Bacon for micro-injection into fertilised oocytes from DARC KO mice.

3.5 Results

3.5.1 FYB(ES) and FYB transgenic mouse strains

3.5.1.1 FYB(ES)TG founder screening

Screening for founders was undertaken through genotyping PCR utilising F62/R402 primers recognising only human *DARC* gene. One positive female founder was mated with DARC KO male and offspring were genotyped (**Figure 3.3**).

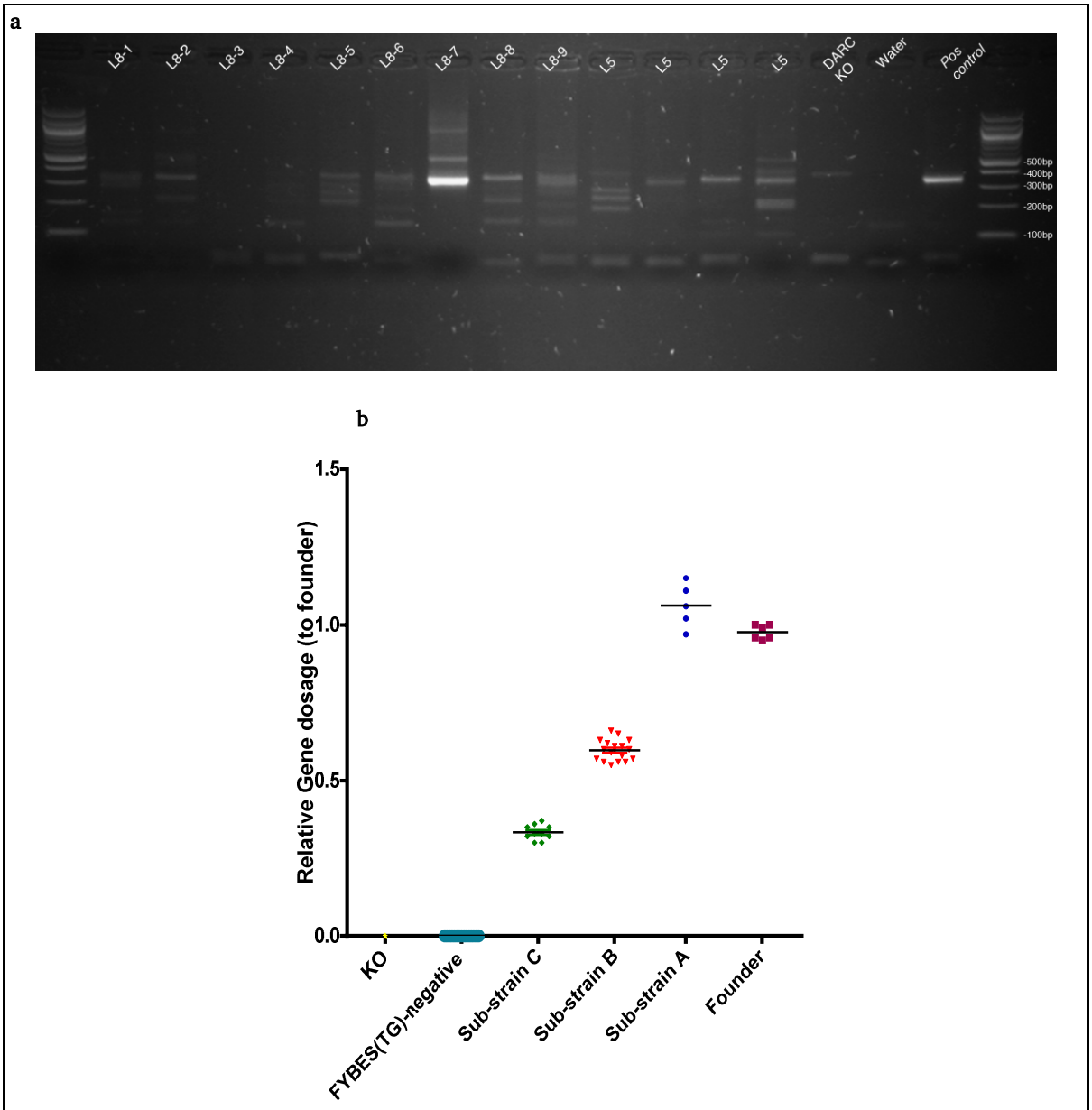

Figure 3.3 Agarose Gel electrophoresis of PCR products from potential FYB(ES)TG founders (a). Lane 'L8-7' is positive, other lanes exhibit background bands (see DARC KO and POS CONTROL lanes). RT-PCR of lysed tissue using Taqman primers confirmed the genotype, revealing three possibilities for genetic transmission of transgene (b).

Given the presence of background bands, RT-PCR based genotyping was undertaken using Taqman gene expression assays for human *DARC* and murine *GAPDH* in a multiplexed system **Figure 3.3b**. This also allowed the determination of relative gene dosage as per Wishart *et al.*, 2007 in offspring relative to the founder. Assuming that the founder animal has an arbitrary gene dosage of 1, dosages of approximately 1, 0.6

and 0.3 were detected. It is therefore likely that there are 3 insertions of *FYB(ES) DARC* transgene, two of which are likely in close chromosomal proximity (dosage=0.6) as breeding of this substrain does not lead to offspring with gene dosage of 0.3. Offspring of animals harbouring gene dosage 0.6 or 1.0 were used in all experiments.

3.5.1.2 Screening for FYBTG founder

Screening for founders was undertaken through the transgenic genotyping PCR using the same F62/R402 primers recognising only human *DARC* gene, as used for FYB(ES)TG. One positive male founder was mated with DARC KO female and offspring were genotyped, **Figure 3.4**.

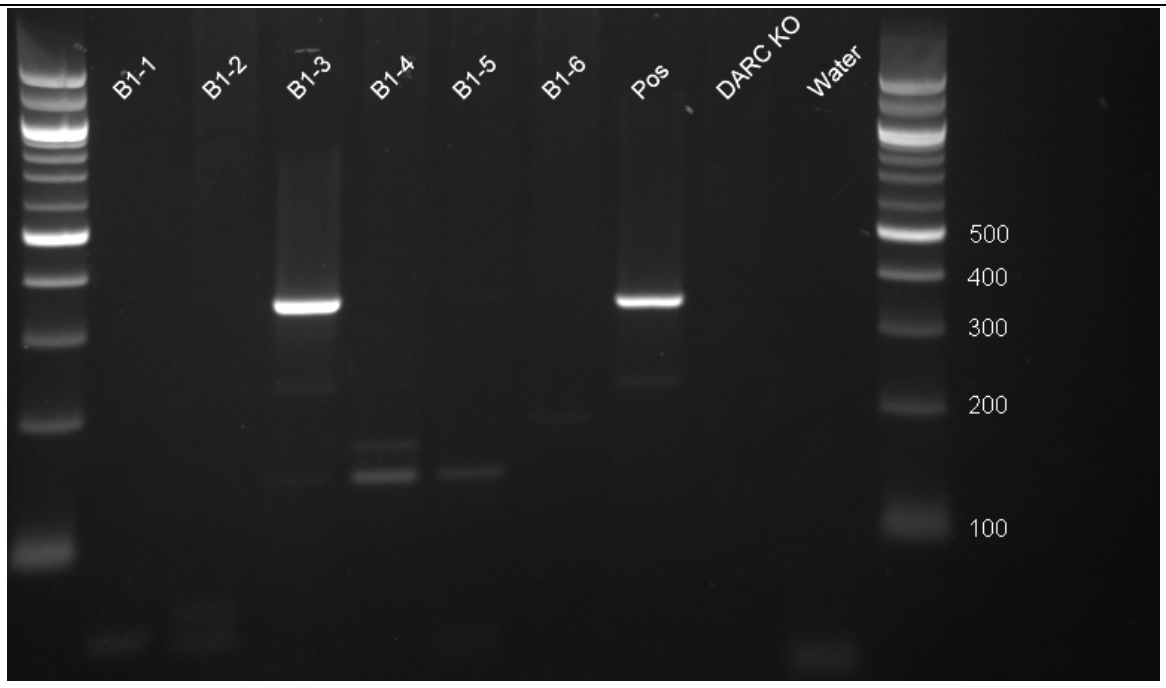

Figure 3.4 Agarose gel electrophoresis of PCR products from potential FYBTG founders. Lane 'B1-3' is positive, other lanes exhibit background bands (see DARC KO and POS CONTROL lanes). FYB Human donor used as positive control.

3.5.1.3 DARC gene expression

To determine whether genomic transmission correlated with gene transcription, RNA was extracted from organs and tissues of FYB(ES)TG and FYBTG mice and transcribed into cDNA, after which relative *DARC* gene expression was quantified against a house keeping gene *GAPDH*, **Figure 3.5a**. Notably DARC expression is relatively low in FYB(ES)TG bone marrow samples rather than absent, as probably the endothelial cells have been flushed out and account for the low level of DARC expression.

3.5.1.4 Erythrocyte DARC expression

Approximately 1 x 10^6 erythrocytes from DARC KO, FYB(ES)TG and appropriate positive control erythrocytes (either human FYB or C57Bl/6 wild-type) were incubated with anti-Fy6 (followed by anti-mouse fluorescent antibody) or directly lablled anti-murine DARC-488 and examined by flow cytometry. Neither of these antibodies bound to FYB(ES)TG erythrocytes (**Figure 3.5c** and **d**), indicating neither human nor murine DARC are present in normal conformations FYB(ES)TG erythroid cells. In contrast, anti-Fy6 incubation with FYBTG erythrocytes followed by secondary fluorescent antibody showed binding similar to human FYB erythrocytes.

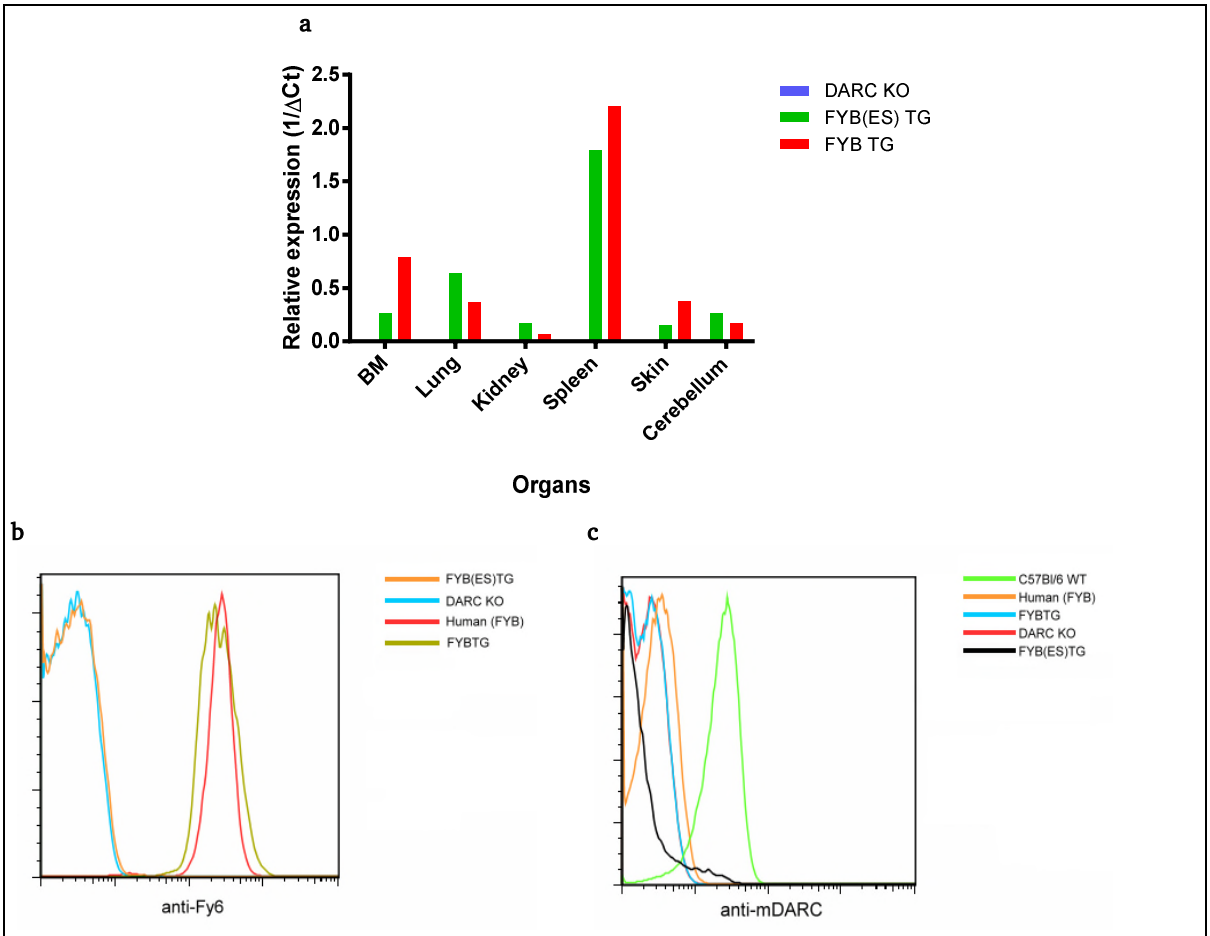

Figure 3.5 Relative *DARC* gene expression in humanised DARC FYB(ES)TG and FYBTG mice and genotype negative control tissues (a), results from one animal examined for each strain. Erythrocyte expression of human DARC was measured in FYB(ES)TG and FYBTG with anti-Fy6 antibody, with DARC KO and human DARC-positive controls (b), and erythroid cell antibody staining confirmed the absence of murine DARC (c). Graphs representative of erythroid DARC expression in at least 7 animals of respective strains

3.5.1.5 Detection of DARC expression in tissues by immunofluorescence

Acetone fixed frozen sections of human or murine spleen were incubated with anti-Fy6 antibody, followed by appropriate secondary antibody, which revealed positive staining in FYBTG and FYB(ES)TG in a distribution similar to human, along venules of red pulp and larger veins, **Figure 3.6b** and **e**, none of which was present in WT, **Figure 3.6f,** or DARC KO spleen (not shown).

Similarly, frozen section of human and FYB(ES)TG skin showed positive staining with anti-Fy6 antibody which were not present in WT, **Figure 3.6c** and **d**.

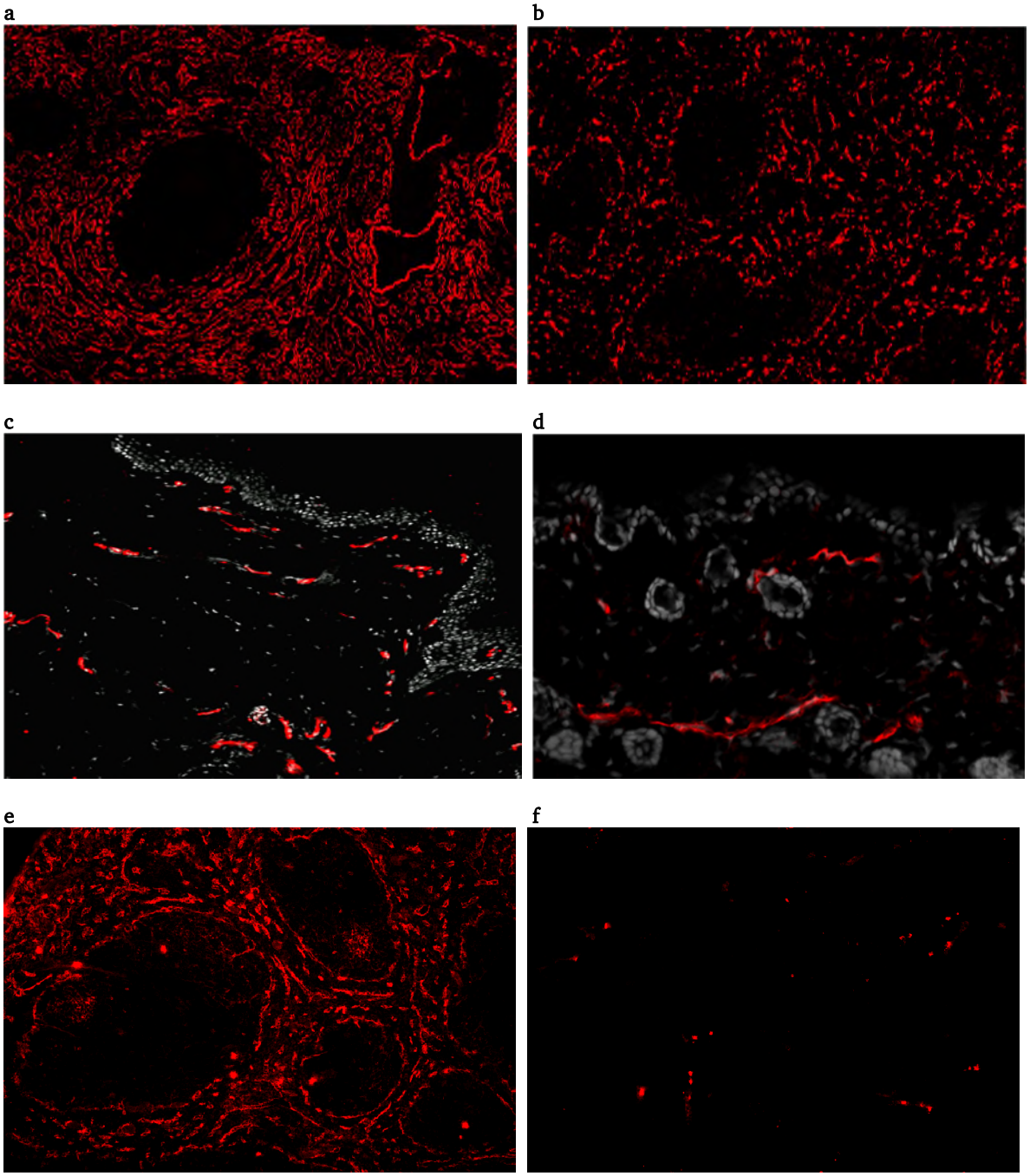

Figure 3.6 anti-Fy6 Immunofluorescent staining of (a) Human spleen 25x tile scan, (b) FYB(ES)TG spleen 40x tile scan, (c) human skin 25x, (d) FYB(ES)TG skin 40x, (e) FYBTG spleen 10x and (f) WT spleen 10x magnification. For this particular staining, goat anti-mouse IgG2b FAB2 Alex Fluor 555 was used, to reduce potential background in a 'mouse-on-mouse' system. Human DARC staining is highlighted along venules and the red pulp of the spleens, whereas in the skin sections it is most evident along the venous plexus and smaller vessels.

3.5.2 Binding of mouse chemokines to human DARC

It has been established that human chemokines bind to murine DARC (Luo *et al.*, 1997, Lee *et al.*, 2003b). To explore whether human DARC is a functional receptor for mouse chemokines we made use of the known cross-competition of chemokines and the anti-Fy6 antibody binding to human DARC (Tournamille *et al.*, 1997). Anti-Fy6 recognises an epitope within the chemokine binding pocket of DARC and does not recognise DARC ligated by a chemokine. Preincubation of human erythrocytes with increasing concentrations of murine CXCL1, a ligand for DARC, and with human CXCL8 (a positive control), lead to decreased anti-Fy6 binding. Conversely neither human CCL21 (not a DARC ligand, negative control), nor murine CXCL12 cross-competed for binding of anti-Fy6 antibody, **Figure 3.7**.

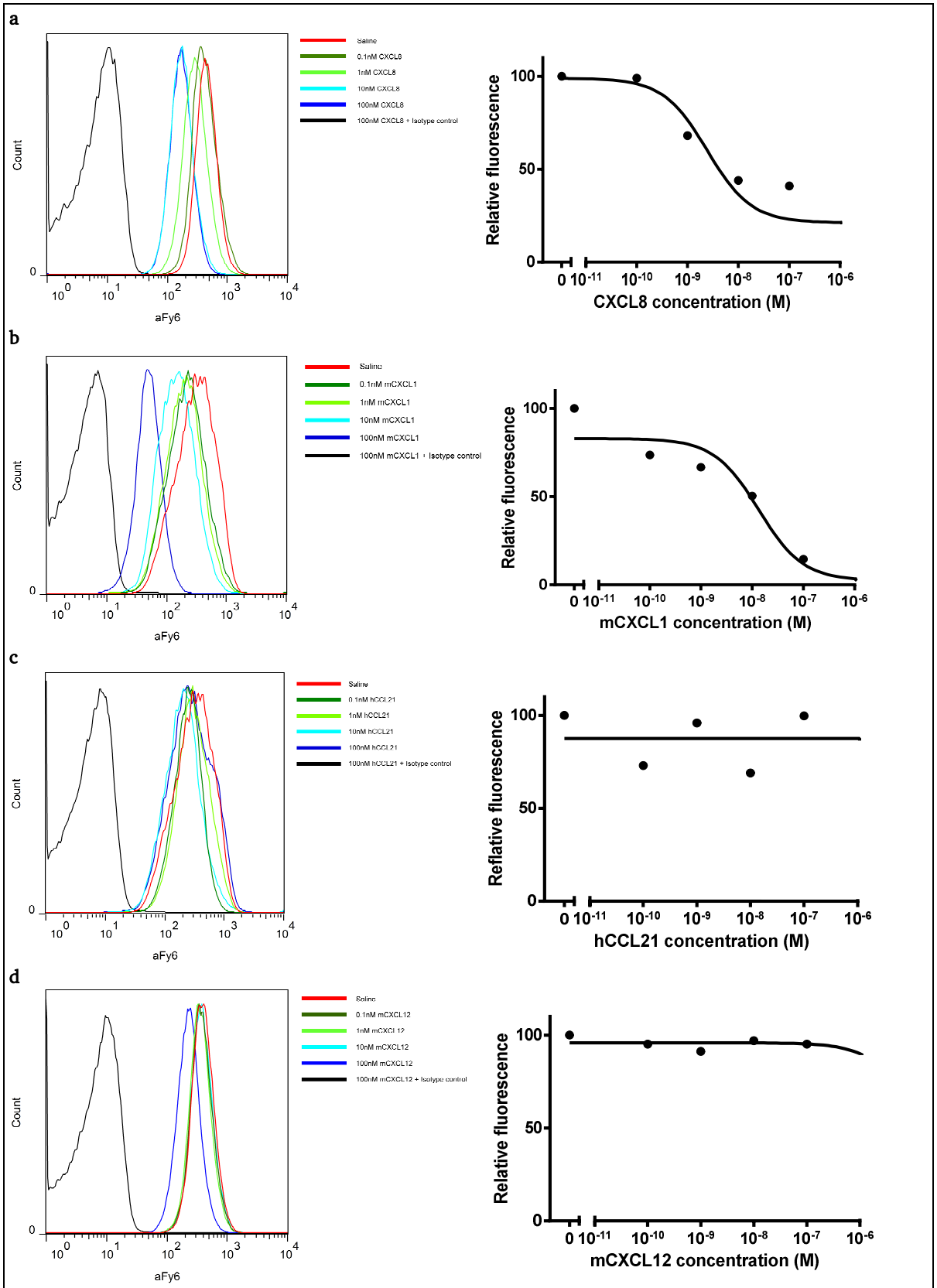

Figure 3.7 Chemokine-anti-Fy6 antibody binding competition assay. Human CXCL8 is a high affinity hDARC ligand (a), whilst hCCL21 is not (c). Anti-Fy6 fluorescence on human erythrocytes is not reduced following incubation with mCXCL12 (d) but is reduced with murine CXCL1 (b). Approximately $1x10^6$ DARC-positive erythrocytes in suspension with PBS + 0.5% BSA were incubated with PBS or chemokine, and then anti-Fy6 antibody (or isotype control where stated) was added, followed by secondary antibody and the samples washed. Along each FACS plot a non-linear curve of best fit for that experiment is shown.

3.6 Discussion

Two strains of mice were created to study the role of erythroid DARC and examine mechanisms leading to the peripheral neutropaenia seen in chimeras lacking erythroid DARC. The main human polymorphisms of DARC, *FYB(ES)* and *FYB*, were cloned and gene sequences amplified after which they were injected into the fertilised oocytes of DARC KO mice. Founders were screened and two new colonies established. DARC expression was determined by analysis of gene expression and immunofluorescence.

These results demonstrated that transgenic expression of the human DARC alleles *FYB(ES)* and *FYB* in a mouse host allowed for effective transcription and translation of the human DARC following the expression pattern similar to human. Both in homozygous human carriers of the *FYB(ES)* allele and mice of the FYB(ES)TG strain there is an absence of DARC expression on erythrocytes. Conversely, expression on the endothelium is maintained in both FYB(ES)TG and FYBTG strains as shown in spleen sections. Thus in FYBTG human DARC is expressed both in mouse endothelium and erythrocytes concordant with the human expression pattern in the carriers of the *FYB*

These models have been subsequently used for dissecting the role of DARC in specific compartments, namely bone marrow erythroid DARC, and blood erythrocyte DARC.

Given the abundance of erythroid cells in the bone marrow expressing DARC, a receptor for ELR+ chemokines, significant questions on the role of erythroid DARC on HSPC and granulocyte lineage development in the DARC-deficient and FYB(ES) transgenic mice remain. As discussed above, individuals of African ancestry have

changes in HSPC cell cycle kinetics and mobilisation, in particular relating to effects on HSPC gene expression and maturation, and the mechanisms for these changes are unknown. The relationship of these alterations in HSPC with peripheral blood leukopenia exhibited by Duffy negative humans and WT-KO chimeric mice requires mechanistic dissection and in particular the role, if any, of homeostatic and mobilising chemokines and cytokines within the bone marrow environment and peripheral blood. The DARC deficient, FYB(ES)TG and FYBTG mouse strains have been utilised in order to investigate these and related questions, as shown in Chapter 4.

Chapter 4

Haematopoietic phenotypes of DARC KO, FYB(ES)-transgenic and FYB-transgenic mice

4.1 Introduction

In order to ascertain the contribution of DARC on erythroid cells to the bone marrow homeostasis, the fundamental parameters of haematopoiesis were compared in WT, DARC KO, FYB(ES)TG and FYBTG mice. Owing to time limitations imposed by the development of the FYBTG mice, only a limited number of observations and not all parameters are available for this strain.

4.2 Materials and methods

The development of mouse strains used and the preparation of bone marrow for FACS analysis are detailed in Chapter 2.

4.2.1 Adoptive bone marrow transfers in irradiated hosts: competitive mixed chimerism

The whole bone marrow was transplanted following lethal irradiation (9 Gy) of BoyJ murine recipients expressing CD45.1 by tail vein injection of 10^7 cells in 200μl PBS. The experiment was setup such that competitor bone marrow cells, from either CD45.2 DARC KO or wild-type mice, were mixed with CD45.1xCD45.2 competitor cells. The injected cells were analysed to confirm correct mixing before injection.

The analysis of the degree of donor chimerism, and the expression of DARC on erythrocytes was undertaken as detailed in Chapter 2.

Peripheral blood cell counts were assayed at 6, 9 and 12 weeks post transfer by collecting blood by tail bleed in 100μl PBS + 10mM EDTA, and the proportions of competitor cells determined. Fifty microlitres of the sample was incubated using antibodies against Gr-1 (FITC), CD43 (PE), CD45.1 (PE-Cy5), CD11b (PE-Cy7), B220 (Pacific Blue), CD4 and CD8 (both on APC), and CD45.2 (APC-Cy7), all from eBioscience, UK. The samples were then analysed using a CyAn ADP flow cytometer (Dako, Ely, UK).

The LSK selected chimera experiment was conducted identically, except that bone marrow cells from either CD45.2 DARC KO or wild-type mice were FACS sorted (see section "4.2.3 FACS sorting") for LSK cells, and 500 cells from either CD45.2 DARC KO or wild-type were mixed with 10^6 CD45.1xCD45.2 competitor cells prior to injection into each irradiated host mouse. In this experiment, peripheral blood cell counts were assayed at 4, 8 and 16 weeks post transfer.

4.2.2 Peripheral blood cell counts

Absolute and differential leukocyte counts were determined as detailed in Chapter 2, but the following antibodies were used: 1μl of anti-Ly6G-PE, 1μl of CD11b-FITC, 1μl of CD3-APC antibodies (eBioscience, UK) and 1μl of anti-B220-PerCP (BD Bioscience, UK)

The total blood leukocyte count was calculated as the sum of the counts of $CD11b^+$, $CD3^+$ and $B220^+$ cells. This was correlated with the total white cell count obtained by the automated ABX Pentra 60 (**Figure 4.1**).

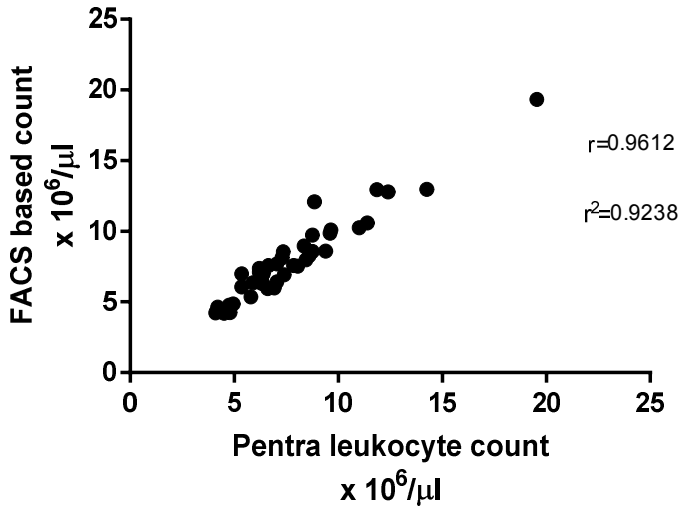

Figure 4.1 Correlation between total leukocyte counts obtained by FACS-based method using counting beads (y-axis) and Pentra automated cell analyser (x-axis), $p<0.0001$

4.2.3 FACS sorting for HSPC

Bone marrow of wild-type or DARC KO mice was flushed as described, and cells stained with lineage-APC (BD), CD34-FITC, CD16/CD32-Biotin, cKit-PE, Sca1-PECy7 (eBioscience) in 500μl buffer, for one hour on ice. Cells were washed twice and then incubated with streptavidin PE-Cy5.5 (Invitrogen) in 500μl buffer for 20 minutes on ice. The cells were sorted on a Mo-flow MultiLaser flow cytometer (Beckman Coulter) operated by Mr Roger Bird, an experienced technician. First, an enrichment step was undertaken, with gates set based on forward and side scatter characteristics for lineage negative and either GMP cells (lineage-negative, ckit-positive, Sca1-negative, CD34-positive, CD16/CD32 positive) or LSK cells (lineage-negative, ckit-positive, Sca1-positive). Then, the enriched populations then underwent a second 'purity' sorting step on the same gating profiles. Cells were collected in Eppendorf tubes and kept on ice. The final GMP and LSK populations were determined to be more than

94% pure. After sorting, Eppendorf tubes containing sorted cells were centrifuged at 5000g for 5min and the supernatant was carefully removed by pipette, after which the tubes were immediately placed on dry ice for storage at -80°C until used.

4.2.4 mRNA Microarray

RNA was extracted from FACS sorted GMP and LSK populations by Mr Stephen Kissane using Trizol (Life Technologies) as per manufacturer's directions. 25ng of each source sample RNA was labelled with Cy3 dye as per the protocol detailed in the Low Input Quick Amp Labelling Kit (Agilent Technologies). A specific activity of greater than 6.0 was confirmed by measurement of 260nm and 550nmwavelengths with a NanoDrop ND-1000 Spectrophotometer. 600ng of labelled RNA was hybridised for 16 hours to Agilent SurePrint G3 Human 8x60K microarray slides. After hybridisation slides were washed as per protocol, and scanned with a High Resolution C Scanner (Agilent Technologies), using a scan resolution of 3μm. Feature extraction was performed using Agilent Feature Extraction Software, with no background subtraction.

Scanned microarray images were analysed using Agilent's Feature Extraction software by Dr Wen Bin Li. Feature intensities were background-subtracted according to the normal-exponential convolution model (Silver *et al.*, 2009) and normalised using quantile normalisation (Bolstad *et al.*, 2003). Microarray annotation (GPL13497) was downloaded from GEO (http://www.ncbi.nlm.nih.gov/geo/). Differentially expressed genes were identified using limma (Smyth, 2004) with fold change >1.5 and $p<0.01$.

4.2.5 Low density gene array

Low density gene array cards (LDA), also known as microfluidic cards, were custom ordered from Applied Biosystems. Each assay contained gene-specific primers, probes and a reaction buffer for reverse transcription and real-time PCR. Gene expression of FACS sorted LSK and GMP cells from WT, DARC KO and FYB(ES)TG mice were analysed using a LDA containing 32 real-time PCR assays per sample (listed in Appendix 7.4 and 7.5,). Genes were selected from micro-array results based on their differential expression or importance in regulating HSPC development. In total, 29 genes were selected, and up to four samples per genotype were analysed in triplicate. Each card was designed such that a WT, DARC KO and FYB(ES)TG sample were analysed simultaneously. For some genes, real-time PCR assays contained primers designed within a single exon and would detect genomic DNA. Therefore RNA was treated with DNase to remove contaminating genomic DNA. Gene *18S* was selected as a positive control, and *GAPDH* and *HPRT* were used as housekeeping genes.

4.2.5.1 Bone marrow cell preparation and FACS sorting

Bone marrow cells from WT, DARC KO and FYB(ES)TG mice were prepared and FACS sorted as detailed in section 4.2.3, and at least 6000 LSK or GMP cells were collected per genotype.

4.2.5.2 RNA extraction from FACS sorted cells

RNA was extracted using the Qiagen RNeasy Micro Kit as per the manufacturer's instructions. Briefly, cell pellets were thawed at room temperature and loosened by

flicking, then disrupted by adding 75μl RLT buffer, and were homogenised by vortexing for 1min. 75μl 70% ethanol was added and mixed thoroughly by pipetting. The sample was transferred to an RNeasy MinElute spin column placed in a 2ml collection tube and centrifuged for 15s at 8000g, and the flow-through discarded. 700μl buffer RW1 was added to the spin column and centrifuged for 15s at 8000g, and the flow-through discarded. The spin column was placed in a new 2ml collection tube and 500μl buffer RPE was added, after which the column was centrifuged for 15s at 8000g, and the flow-through discarded. 500μl 80% ethanol was then added to the spin column. The spin column was placed in a new 2ml collection tube and centrifuged at full speed (16,000g) with the lid open, after which flow-through and collection tube were discarded. The spin column was placed in a new 1.5ml collection tube and 14μl RNase-free water was added to the spin column membrane. The lid was closed and the tube was centrifuged at full speed resulting in 12μl eluate containing RNA.

4.2.5.3 Digestion of contaminating genomic DNA

RNA was treated with DNase to remove contaminating genomic DNA. Briefly, the RNA eluate was mixed with 10μl buffer RDD and 2.5μl DNase I and made up to a total volume of 100μl. The mixture was incubated at room temperature for 10min. 350μl of buffer RLT was added and mixed, after which 250μl 100% ethanol was added and mixed by pipetting. The sample was transferred to an RNeasy MinElute spin column placed in a 2ml collection tube and centrifuged for 15s at 8000g and the flow-through discarded. The sample was then treated as detailed earlier (using buffer

RW1, 80% ethanol and RPE buffer) and a 12μl eluate containing RNA with genomic DNA removed was obtained.

4.2.5.4 First-strand cDNA synthesis (RT)

The concentration of total RNA was determined as detailed above and RT performed using SuperScript VILO cDNA Synthesis Kit (section 3.2.2.3).

4.2.5.5 Quantitative real-time PCR

Quantitative real-time PCR was performed as per the manufacturer's instructions. Briefly, 50μl of sample cDNA and 50μl of TaqMan Gene Expression Master Mix (Applied Biosystems) were thoroughly mixed and loaded into each port of the microfluidic card. The microfluidic card was centrifuged twice at 300g for 1min in a vertical Heraeus centrifuge fitted with the Heraeus custom buckets and card holders. The plate was sealed using a TaqMan Array Micro Fluidic Card Sealer (Applied Biosystems) and the filling strips were cut off. The card was then placed in an Applied Biosystems 7900HT Fast Real-Time PCR cycler. The cycling program was provided by the manufacturer by means of a configuration file; the conditions for real-time PCR were 50˚C for 2min, 95˚C for 10min then 40 cycles of 95˚C for 15s and 60˚C for 1min.

Fluorescence analysis was performed utilising SDS v2.4 software with a threshold set manually during the logarithmic phase of the PCR. The threshold cycle (C_T) value was then used to calculate the change in expression of each gene relative to the geometric mean of the housekeeping genes *GAPDH* and *HPRT* for WT samples (ΔC_T), resulting in a

$\Delta\Delta C_T$ value for DARC KO and FYB(ES)TG samples. The fold change of each gene relative to the housekeeping genes was obtained by the $2^{-\Delta\Delta^{C_T}}$ method, and the relative quantification was plotted. Genes which had a C_T value >40 were below assay detection level and were assigned an RQ value of zero. Statistical significance was calculated using the $\Delta\Delta C_T$ values and the unpaired Student t test.

4.2.6 Multiplex cytokine array and chemokine ELISA

For protein array measurement using Luminex-based platform (Luminex, USA), bone marrow supernatant was obtained from tibias and femurs of wild-type, DARC KO and FYB(ES)TG mice by centrifuging each bone with epiphysis cut-off in a 200μl pipette tip at 500g for 8 minutes, a method from Ergen *et al.*, 2012. The supernatant was pooled and protein contents quantified. Alternatively, for chemokine ELISA, both femurs were flushed in 1ml of PBS containing EDTA 2mM, and the supernatant removed by pipette after centrifugation at 3000g for 10 minutes. Afterwards, samples were stored at -80°C until assayed. Serum was obtained by allowing blood to clot for 2 hours following cardiac puncture of anaesthetised mice, and thereafter centrifuged at 10,000g for 10 minutes. Samples were stored at -80°C until assayed. Multiplex cytokine array assay was undertaken using Millipore mouse 32plex plates, as per the manufacturer's recommendations, washed with a magnetic plate washer, and analysed using a Biorad Bioplex 200 using the manufacturer's software. Analytes included G-CSF, CCL11 (eotaxin), GM-CSF, interferon gamma, IL-1A, IL-1B, IL-2, IL-3, IL-4, IL-5, IL-6, IL-7, IL-9, IL-10, IL-12P40, IL12P70, LIF, IL-13, CXCL5 (LIX), IL-5, IL-

17, CXCL10 (IP-10), CXCL1 (KC), CCL2 (MCP-1), CCL3 (MIP-1A), CCL4 (MIP-1B), CXCL9 (MIG), CXCL2 (MIP-2), CCL5 (RANTES), VEGF, TNF-Alpha.

CXCL12 ELISA was carried out using Mouse CXCL12 DuoSet according to the manufacturer's instructions (R&D Systems).

4.2.7 Bone marrow cell cultures

Methylcellulose supplemented with cytokines and growth factors as detailed below (M3434, Stem Cell, France) and penicillin 100iu/ml and streptomycin 100iu/ml was used for bone marrow colony assay. This medium was selected as it is formulated to support optimal growth of erythroid, granulocyte-macrophage and multi-potential murine myeloid progenitors. The methylcellulose in Iscove's medium contained fetal bovine serum and bovine albumin, recombinant human (rh) insulin, iron-saturated human transferrin, 2-mercaptoethanol, recombinant murine (rm) stem cell factor, rmIL-3, rmIL-6, rh-erythropoietin and other supplements not revealed by the supplier. Cells were grown in 35mm plates (Stem Cell, France) in triplicate in a humidified atmosphere with 5% CO_2. Cells were harvested from mouse bone marrow, red cell lysed and resuspended at a concentration of $2x10^5$/ml in buffer. Four hundred microlitres of this solution were added to 4ml of M3434 media using a 2ml syringe and blunt end needles (Stem Cell, France). The mixture was well mixed and bubbles allowed to disperse, whereupon 1.1ml of media was added to plates and evenly dispersed. Cells were grown for 7 days and then colonies were scored. Occasionally, colonies would be selected, mixed into 100μl of phosphate buffered saline, and cytospun for confirmation of colony type. Colonies were washed off with PBS, and

washed twice in 50ml conical tubes. The total number of cells present was counted with a disposable haemocytometer. In some experiments, the cells were incubated with fluorescent antibodies as previously described, and analysed by flow cytometry. In some experiments, 200,000 cells were also selected for re-culture, and were prepared as above. Two sequential re-platings were performed.

In addition, LSK cells were FACS-sorted as described previously, and suspended in 400μl. This mixture was added to 4ml of M3434 media and processed as described above.

4.2.8 Measurement of bone marrow cell proliferation by the BrdU incorporation assay

In order to assay cell proliferation of the bone marrow cell populations, the BD Bioscience APC BRDU flow kit (BD Bioscience, UK) was used as per the manufacturer's instructions. 5-bromo-2'-deoxyuridine (BrdU) is a thymidine analogue which is incorporated into DNA during cell cycle. Briefly, 1mg of BRDU as supplied in the kit was injected intra-peritoneally into wild-type, DARC KO or FYB(ES)TG mice and the animals were culled after 2 hours. Femurs were cleaned and flushed with PBS + 2% BSA + 2mM EDTA, and bone marrow was lineage depleted using the mouse lineage depletion kit from Miltenyi Biotec (Surrey, UK) as per the manufacturer's instructions. Bone marrow cells were incubated with biotinylated lineage antibodies, washed and incubated with magnetic beads linked to streptavidin, permitting removal of lineage positive cells after passage through a magnetic column. Subsequently lineage negative cells were washed and incubated with streptavidin e450, anti-c-Kit-

APC-Cy7, anti-Sca-1-PE/Cy7, anti-CD127-e450, anti-CD34-FITC, anti-CD16/CD32-PE/Cy5.5, anti-CD135-RPE (all eBioscience, UK), for one hour on ice. Cells were then washed, fixed and permeabilised, and then stained with anti-BRDU-APC before analysis by flow cytometry.

4.2.9 Measurement of bone marrow cell apoptosis by Annexin V staining

Rates of apoptosis were analysed in WT, DARC KO and FYB(ES)TG bone marrow cells by staining for Annexin V expression using the Annexin V-FITC Apoptosis Detection Kit I (BD Biosciences, UK) and 10X Annexin V Binding Buffer (BD Bisociences, UK) containing 0.1 M Hepes/NaOH (pH 7.4), 1.4M NaCl, 25mM $CaCl_2$ according to the manufacturer's protocol with modifications. Dead cells were detected using Sytox Blue (Life Technologies, UK), a nucleic acid stain which penetrates cells with damaged membranes but does not cross intact cell membranes.

Femurs were cleaned and flushed with PBS + 2% BSA + 2mM EDTA, red cells lysed and bone marrow cells were blocked with blocking buffer containing 10% FCS and anti-CD16/CD32 antibody on ice for 10min. Cells were then centrifuged at 300g for 10min twice and stained with anti-mouse lineage panel-e450, anti-cKit-PE and anti-Sca1-PE-Cy7 antibody cocktail in rigid 96 well plates for 45min on ice. Cells were then centrifuged at 300g for 10min and washed twice with ice-cold PBS, and 10^6 cells from each sample were resuspended in polypropylene tubes with 500μl 1x binding buffer (1 part 10x binding buffer diluted with 9 parts distilled water) and 2.5µl of Annexin V-FITC, and incubated in the dark on ice for 30min. Then 500μl binding buffer was

added and cells were kept on ice until analysed. Immediately prior to analysis, Sytox Blue was added at a final concentration of 1:50,000 to each tube, and samples were analysed by flow cytometry using a CyAn ADP flow cytometer within an hour of Annexin V staining. Unstained cells were used as negative controls, and positive controls were prepared by incubating 10^6 whole bone marrow cells in 500µl staining buffer at 60°C for one hour, which were then stained for Annexin V expression or Sytox Blue as detailed above.

4.2.10 Preparation of frozen bone marrow sections and immunofluorescence

Femora from wild-type, DARC KO or FYB(ES)TG mice were taken, cleaned and placed in 4% paraformaldehyde for 7 hours at 4°C following which they were rehydrated with 15% sucrose solution for 4 hours and subsequently 30% sucrose solution. Femora were sent by courier to the laboratory of Cesar Nombiela Arrieta (Boston, USA) where they were frozen and stored at -80C. Frozen tissues were sectioned using a CryoJane Tape-Transfer System (Leica Biosystems), transferred onto slides and stored at -80C. These were returned to Birmingham, UK for immunofluorescent staining.

Frozen sections were firstly rehydrated with PBS supplemented with 10% fetal calf serum for 10 min. Subsequently 100μl of purified mouse anti-rat CD31 antibody (eBioscience) at 1:50 concentration was incubated at room temperature with PBS supplemented with 1% bovine serum albumin for 30 minutes, then washed for 5 min in PBS. The sections were then incubated with donkey anti-rat Alex Fluor 647 (Life

Technologies) at 1:100 concentration for 30 minutes, and then were washed. CD11b and Gr-1 antibodies (eBioscience) both biotin conjugated (1:100) were incubated for 30 minutes, and the slides then washed. Finally streptavidin-555 (1:200, Life Technologies) and Ter119-FITC (1:100, eBioscience) were incubated for 30 minutes, after which the sections were washed and mounted in ProLong Gold Antifade Reagent with DAPI (Life Technologies).

A Zeiss LSM 510 Meta confocal microscope (Zeiss) was used to visualise staining of sections. Images were captured and processed using Zeiss LSM Image Examiner software (Zeiss).

4.2.11 Analysis and quantification of immunostained bone marrow sections

Bone marrow sections were captured at 25x and 40x magnifications. Images were analysed using *ImageJ* (http://rsb.info.nih.gov/ij/) software, which has the facility for automation of several procedural steps by the use of macros. This was undertaken as per Inman *et al.*, 2005. Briefly, the thresholds previously determined from a negative control slide were applied. This procedure converted the image from multiple 8-bit channels, each of which contains intensity data from 0 to 255 for a specific fluorophore, to multiple 1-bit channels containing only positive or negative values (0 or 1) for each fluorophore. The number of pixels of each colour was then automatically counted and presented as a proportion of the total number of pixels in the area under analysis. The percentage area of each colour in the area of interest was then calculated for each image.

Myeloid cell clustering was determined by standardising the image brightness such that all cells were visible in their entirety. The images were then thresholded and converted to binary images. Circles were drawn manually around individual or clustered myeloid cells, and the number of cells in each cluster noted. The mean number of myeloid cells per cluster was then determined.

4.2.12 Binding of radiolabelled CCL5 to erythroid cells

Five μCi of radioiodinated CCL5 was purchased from PerkinElmer, UK or Hartmann Analytic, Germany, depending on availability, and re-constituted in 200μl of PBS with 0.5% BSA. Unlysed bone marrow from WT or DARC KO mice was prepared as described above, and incubated with a cocktail of fluorescently labelled antibodies comprising anti-Ter119, CD71, CD11b and B220 (eBioscience). FACS sorting for erythroblasts was undertaken by gating on larger cells (higher FS), and a negative dump gate for $CD11b^+$ and $B220^+$ cells was used to minimise leukocyte contamination. Erythroblasts were selected as $Ter119^+$ and $CD71^+$ cells, and were collected into RPMI and transferred into 1.5ml Eppendorf tubes. Then 200nM ^{125}I-CCL5 was incubated with each sample in duplicate or triplicate (10^6 cells) depending on cell sorting yield. MDCK cells expressing D6 were used as control for binding and degradation of chemokines. A 'No Cells' tube was used as a negative control. After 3 or 18 hours of incubation at 37ºC with agitation in 200μl of RPMI, the samples were centrifuged at 300g for 5 min. The supernatant was removed, the pellet resuspended in RPMI, centrifuged again (supernatant added to Sample S) and then 200μl 10x PBS or 100iu/ml of heparin in 200μl of RPMI were added to the cell pellet

which was resuspended and incubated for either 3 minutes in PBS or for 10 minutes in heparin. After incubation, the sample was centrifuged, the supernatant removed (Sample W), the pellet resuspended in RPMI, centrifuged again (supernatant added to Sample W) and then the pellet was incubated with 200μl Triton-X 0.5% for 10min under agitation. After incubation, the sample was centrifuged, the supernatant removed (Sample C), the pellet resuspended in RPMI, centrifuged again (supernatant added to Sample C). Then 400μl of 20% TCA was added to all the supernatant tubes, and the samples incubated on ice for one hour. The tubes were then centrifuged at 16000g for 10min, and the supernatant placed into lidded tubes. The remaining pellets were resolved in 800μl NaOH 2N and 0.05% SDS before being transferred into lidded FACS tubes. A calibrated Packard Cobra gamma counter (PekinElmer, USA) was used to assay the samples. Background was subtracted from the resultant counts. To control for specific labelling of chemokine the ^{125}I-CCL5 starting material was assayed by TCA precipitation (**Figure 4.2**).

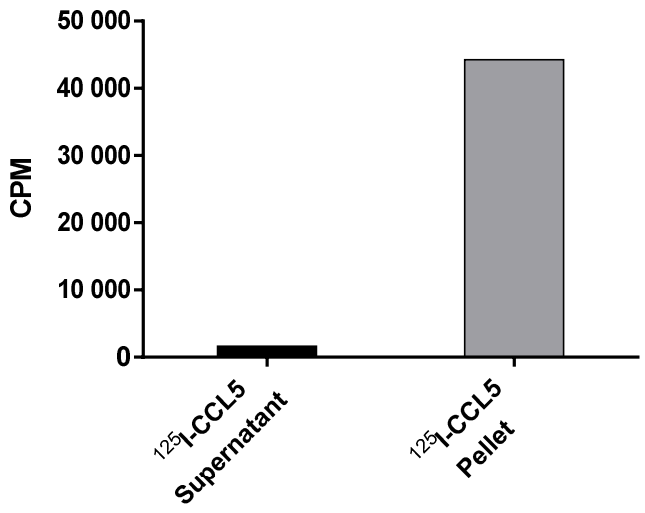

Figure 4.2 ^{125}I-CCL5 analysis of specificity for labelling.

4.3 Results

4.3.1 Fundamental parameters and peripheral blood counts

Principally DARC KO and FYB(ES)TG mice have larger spleens as a proportion of animal weight, **Figure 4.3a**, and FYBTG have spleen weights similar to WT mice. Coulter-counter-type analysis showed unchanged haemoglobin and platelets (in WT, DARC KO and FYB(ES)TG mice) but counts of leukocyte subsets were significantly reduced in the FYB(ES)TG, **Figure 4.4c-e**.

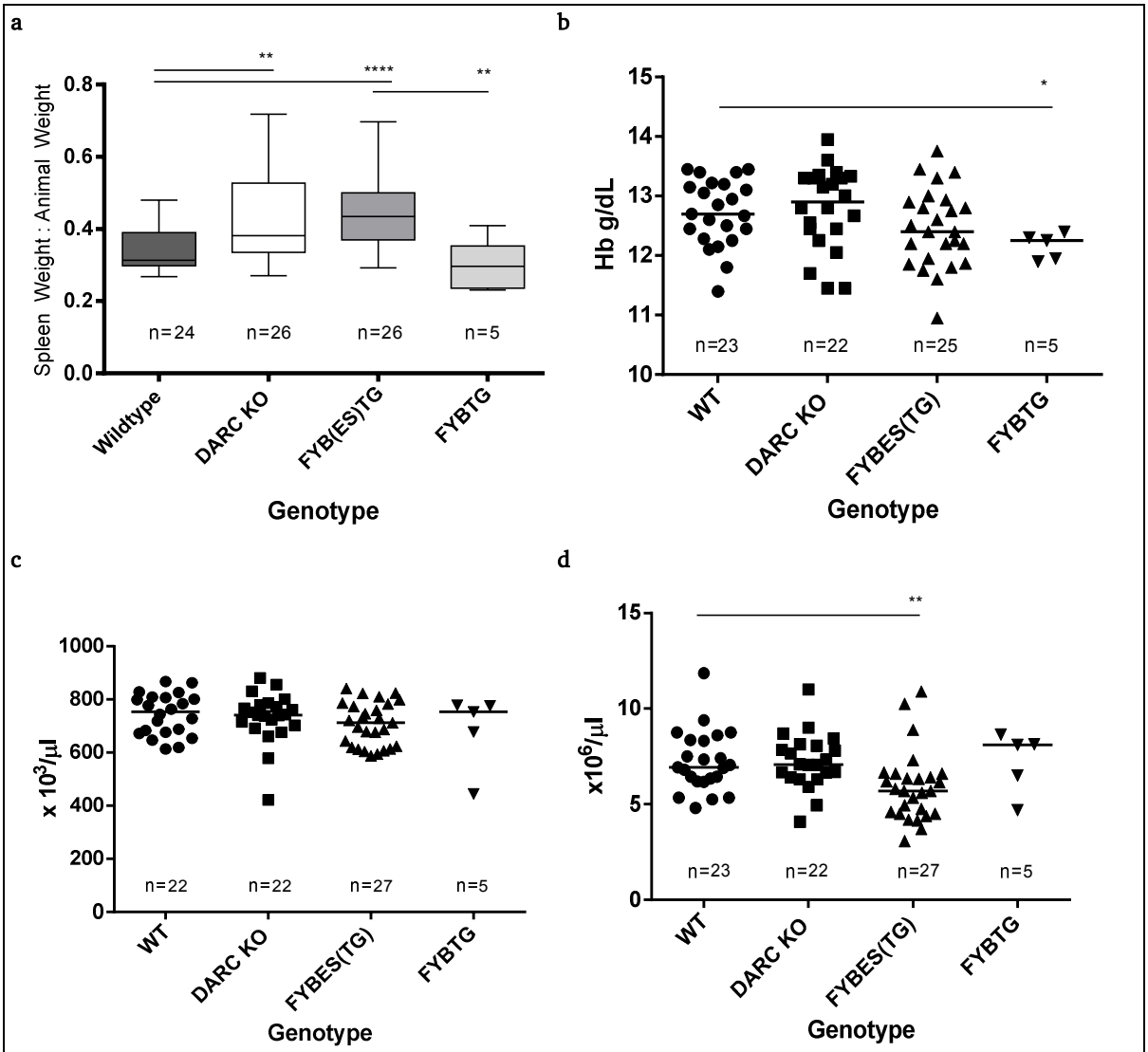

Figure 4.3 (a) relative spleen weights in wild-type, DARC KO, FYB(ES)TG and FYBTG. Readout from full blood count: (b) haemoglobin, (c) platelet count and d) white cell count.

Leukocyte differential count was determined by FACS using counting beads (**Figure 4.4**). The absolute neutrophil, $B220^{+}$ and $CD3^{+}$ lymphocyte counts were significantly reduced in FYB(ES)TG mice (**Figure 4.4b**). These measured parameters in FYBTG are similar to WT mice, suggesting that the absence of haematopoietic DARC is the principle effector of the changes observed in FYB(ES)TG. The reason for the lower haemoglobin in FYBTG is unclear; examining the peripheral blood parameters of more

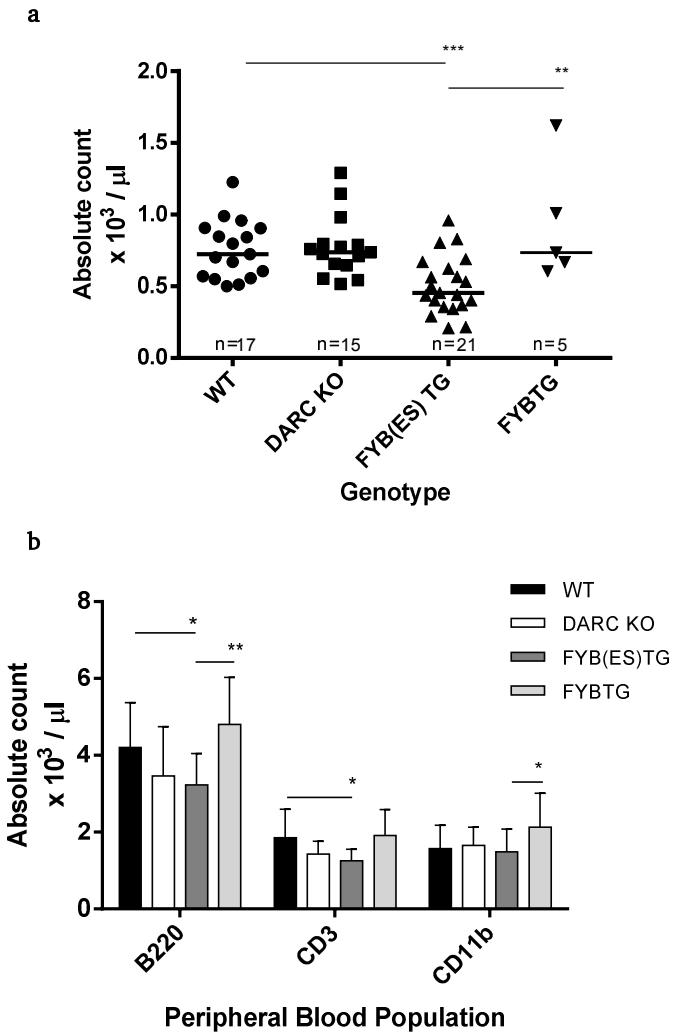

Figure 4.4 Differential blood leukocyte counts in WT, DARC KO, FYB(ES)TG and FYBTG mice. (a) Peripheral blood neutrophils by bead counting and (b) absolute counts of peripheral blood leukocytes divided into main cell types, WT n=12, DARC KO n=10, FYB(ES)TG n=10, FYBTG n=5.

animals may clarify this. It is of note that data comparing the peripheral blood counts between human Caucasian and African-ancestry groups showed similar a peripheral blood profile i.e. lower total WBC and lower neutrophils counts in individuals of African-ancestry (Bain, 1996).

4.3.1.1 The bone marrow myeloid cells

In order to further define the haematopoietic profile of the FYB(ES)TG and FYBTG phenotypes, bone marrow was examined by flow cytometry (**Figure 4.5**). Bone marrow cellularity was similar in FYBTG, FYB(ES)TG and WT mice, and slightly reduced in DARC KO (**Figure 4.5a**). Of note, bone marrow neutrophil ($CD45^+$ $CD11b^+$ $Ly6G^{hi}$) proportions were increased in DARC KO, and more so in FYB(ES)TG, but unchanged in FYBTG, compared to WT mice (**Figure 4.5b**). The proportion of bone marrow monocytes ($CD45^+$ $CD11b^+$ $Ly6G^{neg}$ $CD115^+$) were lower in FYB(ES)TG as compared to DARC KO mice, possibly as a result of their higher neutrophil proportions (**Figure 4.5c**). There was no difference in blood monocyte numbers (**Figure 4.5d**), however the subset of $Ly6C^{low}$ monocytes was notably increased in DARC KO and FYB(ES)TG mice (**Figure 4.5e**).

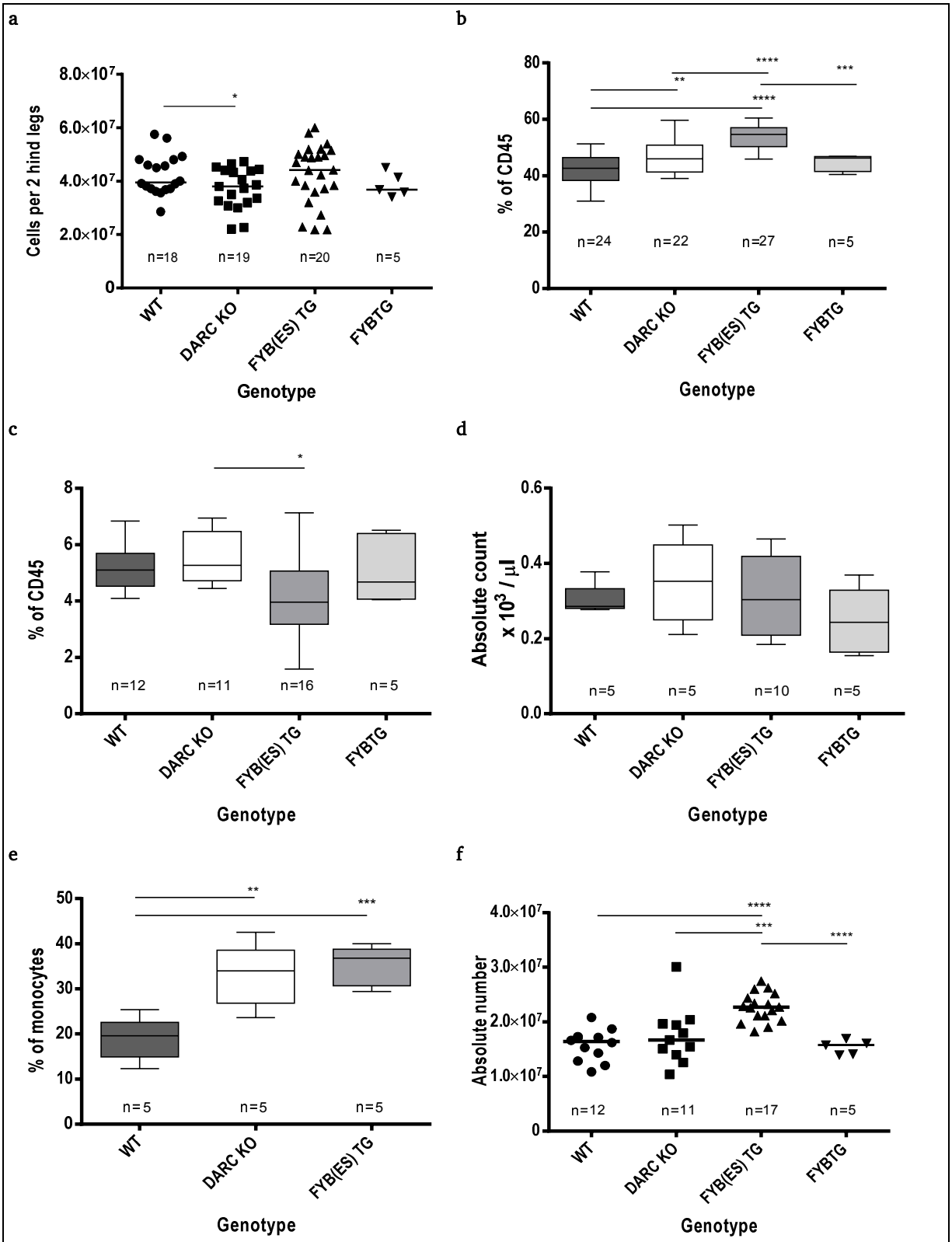

Figure 4.5 Bone marrow cellularity and myeloid cell composition. Bone marrow cellularity (a), relative proportions of bone marrow neutrophils (b), and monocytes (c). Examination of blood revealed no difference in monocyte numbers (d). There is an increase in Ly6C^{low} monocytes in DARC KO and FYB(ES)TG (e). Absolute bone marrow neutrophil numbers (f) suggests no difference between WT, DARC KO and FYBTG mice, although in FYB(ES)TG neutrophils are significantly elevated.

Absolute neutrophil numbers are substantially increased in the bone marrow of the FYB(ES)TG as compared to WT, DARC KO and FYBTG mice (**Figure 4.5f**).

Neutrophils in the bone marrow of DARC KO, FYB(ES)TG and FYBTG have lower CD11b expression (**Figure 4.6a**), whilst blood CD11b expression is unchanged in DARC KO compared to WT or FYBTG mice and is increased in FYB(ES)TG

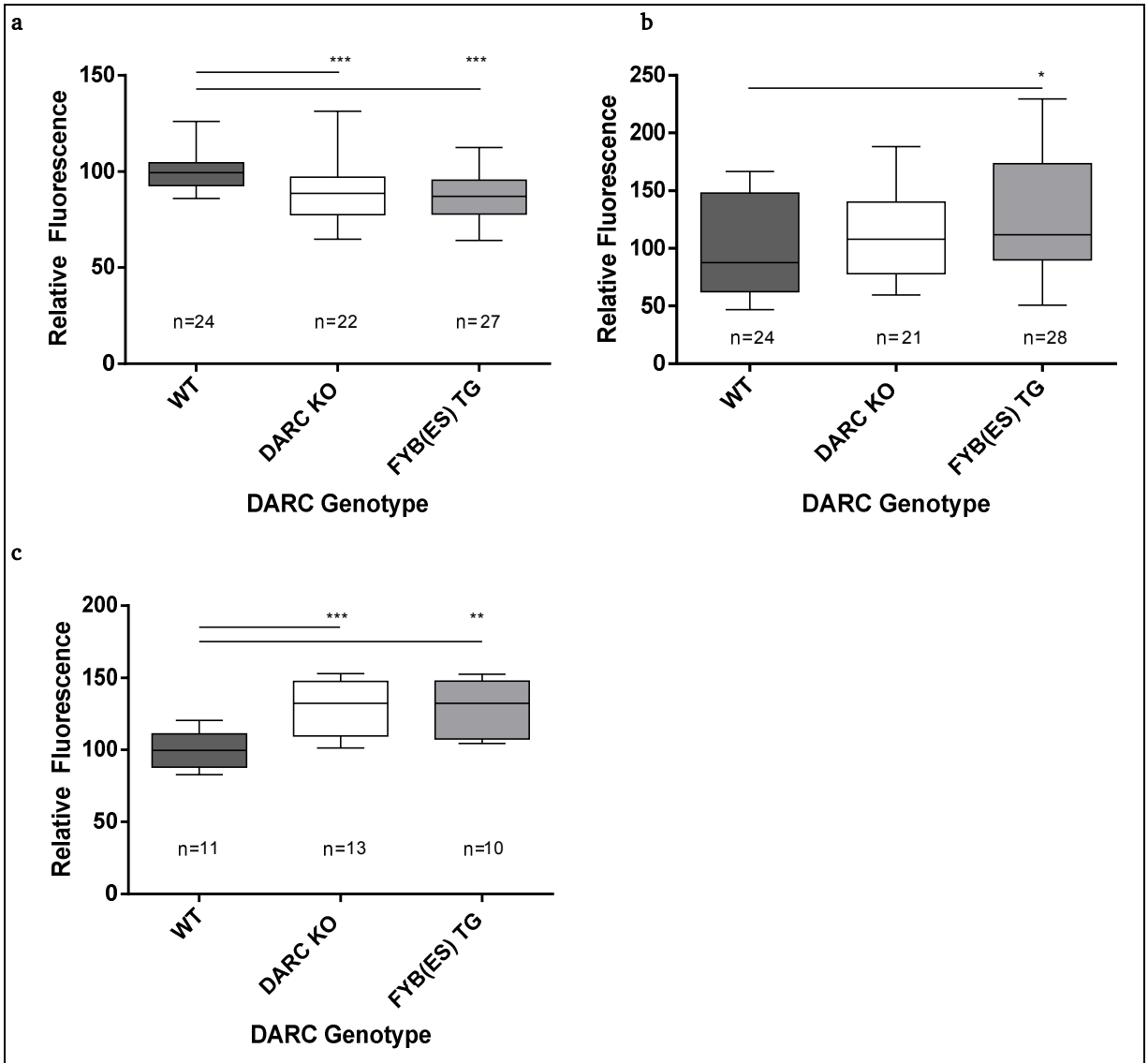

Figure 4.6 Expression of surface molecules on bone marrow and blood neutrophils. Absolute CD11b expression in bone marrow neutrophils ($FS^{Med\text{-}Hi}$ SSC^{Hi} $CD45^{+}$ $CD11b^{+}$ $Ly6G^{Hi}$) (a). (b) Blood neutrophils CD11b expression relative to WT: four experiments were combined, and expressed as percentage of WT for each experiment. (c) CD16/CD32 expression of bone marrow neutrophils (Live, $FS^{med\text{-}Hi}$, SSC^{Hi}).

(**Figure 4.6b**). The reasons for these contrasting phenotypes (bone marrow *vs.* blood) are not clear. However, increased systemic G-CSF as measured in DARC KO and FYB(ES)TG mice, may lead to upregulation of neutrophil adhesion molecules in the peripheral circulation (see section **4.4 Discussion**).

Furthermore, the expression of CD16/CD32, the FcγRIII and FcγRIIa, is higher on the neutrophils of the DARC KO, FYB(ES)TG and FYBTG bone marrow (**Figure 4.6c)**.

4.3.1.2 Spleen myeloid cells

Examination of the spleen myeloid cells (**Figure 4.7**) revealed no significant change in neutrophils in FYB(ES)TG, but their absolute numbers were increased due to the increase in spleen size.

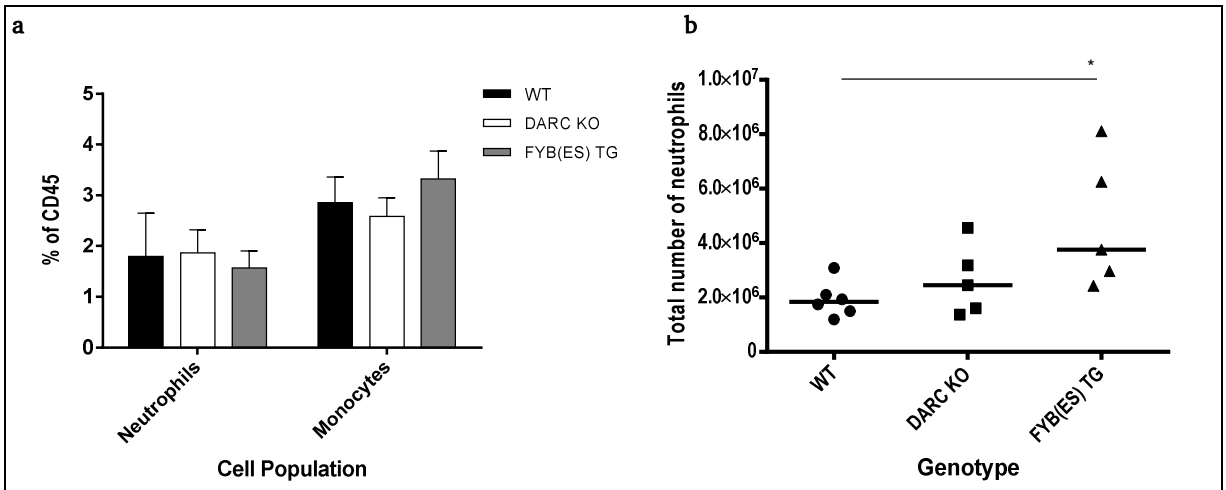

Figure 4.7 Spleen myeloid cell analysis. (a) Neutrophils and monocytes as a proportion of $CD45^+$ cells in the spleen; WT n=6, DARC KO n=5, FYB(ES)TG n=5. (b) Absolute neutrophil numbers in the spleen.

4.3.1.3 Lymphoid cells in bone marrow and spleen

B lymphocytes comprise approximately one-third of the murine bone marrow (Dogusan *et al.*, 2004); however in the DARC KO these proportions are reduced, probably given the expanded myeloid series (**Figure 4.8**). T Lymphocytes are also slightly reduced, possibly on the same basis. The FYB(ES)TG spleen harbours more B lymphocytes, proportionally, but fewer T lymphocytes. Given the substantial splenic enlargement in the FYB(ES)TG it is unlikely that this represents any actual reduction in lymphocyte numbers.

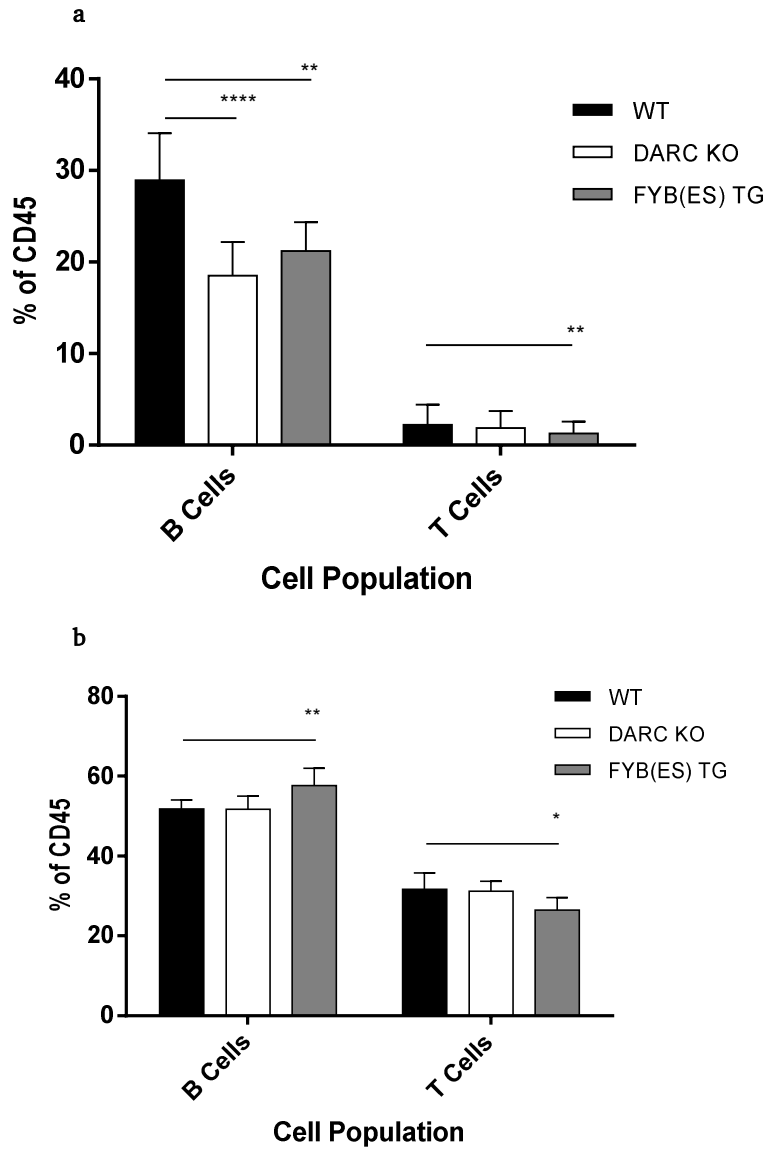

Figure 4.8 B and T Lymphocytes as a proportion of $CD45^{+}$ cells in the bone marrow (a), and the spleen (b). WT, n=12, DARC KO, n=12, FYB(ES)TG, n=6, in bone marrow, WT, n=11, DARC KO, n=11, FYB(ES)TG, n=6 in spleen.

FYBTG bone marrow analysis of total lymphoid cells (both B and T lymphocytes) show that lymphocytes are increased compared to FYB(ES)TG (**Figure 4.9**), with results for FYBTG similar to WT mice (data not shown).

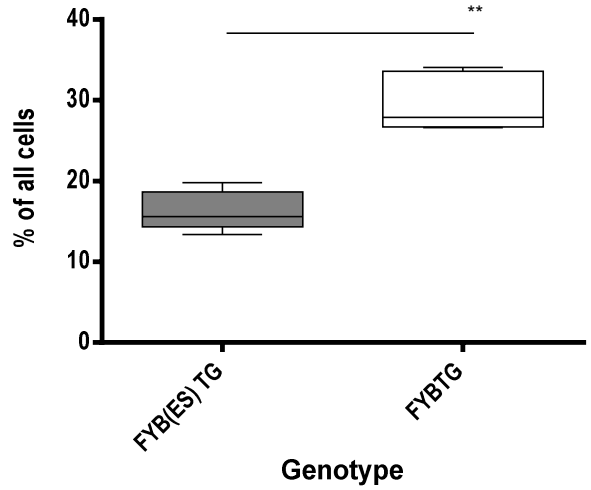

Figure 4.9 B and T Lymphocytes as a proportion of CD45$^+$ events in the bone marrow (CD3$^+$ and B220$^+$), results of preliminary experiment comparing FYB(ES)TG and FYBTG mice, n=5. Mean lymphoid proportions in FYBTG are similar to WT (data not shown, see Figure 4.8 for WT)

4.3.1.4 Bone marrow and splenic erythropoiesis

In order to account for the larger spleen seen in DARC KO and FYB(ES)TG mice compared to WT mice, erythroid proportions were examined in both bone marrow and spleen of these mice, with preliminary results for FYBTG shown (**Figure 4.10**). There was a significantly reduced erythropoietic component in both DARC KO and FYB(ES)TG bone marrow. Spleens of FYBTG mice in contrast show erythroid proportions comparable to WT mice. In FYB(ES)TG mice there was a significantly altered erythroblast maturation profile, with reduced early erythroblasts and more late erythroblasts. Within the spleen, erythropoiesis comprised a significantly large proportion of all cells in the FYB(ES)TG, although there was no difference in DARC KO compared to WT mice.

The maturation profile in the spleen was opposite to bone marrow with significantly more mid erythroblasts in the DARC KO and FYB(ES)TG mice spleens but only DARC KO showed significant difference in late erythroblasts, reduced in turn, suggesting that the spleen has fewer mature erythroblasts in DARC KO. This may be due to erythrocytes leaving the spleen into the blood sooner upon maturation.

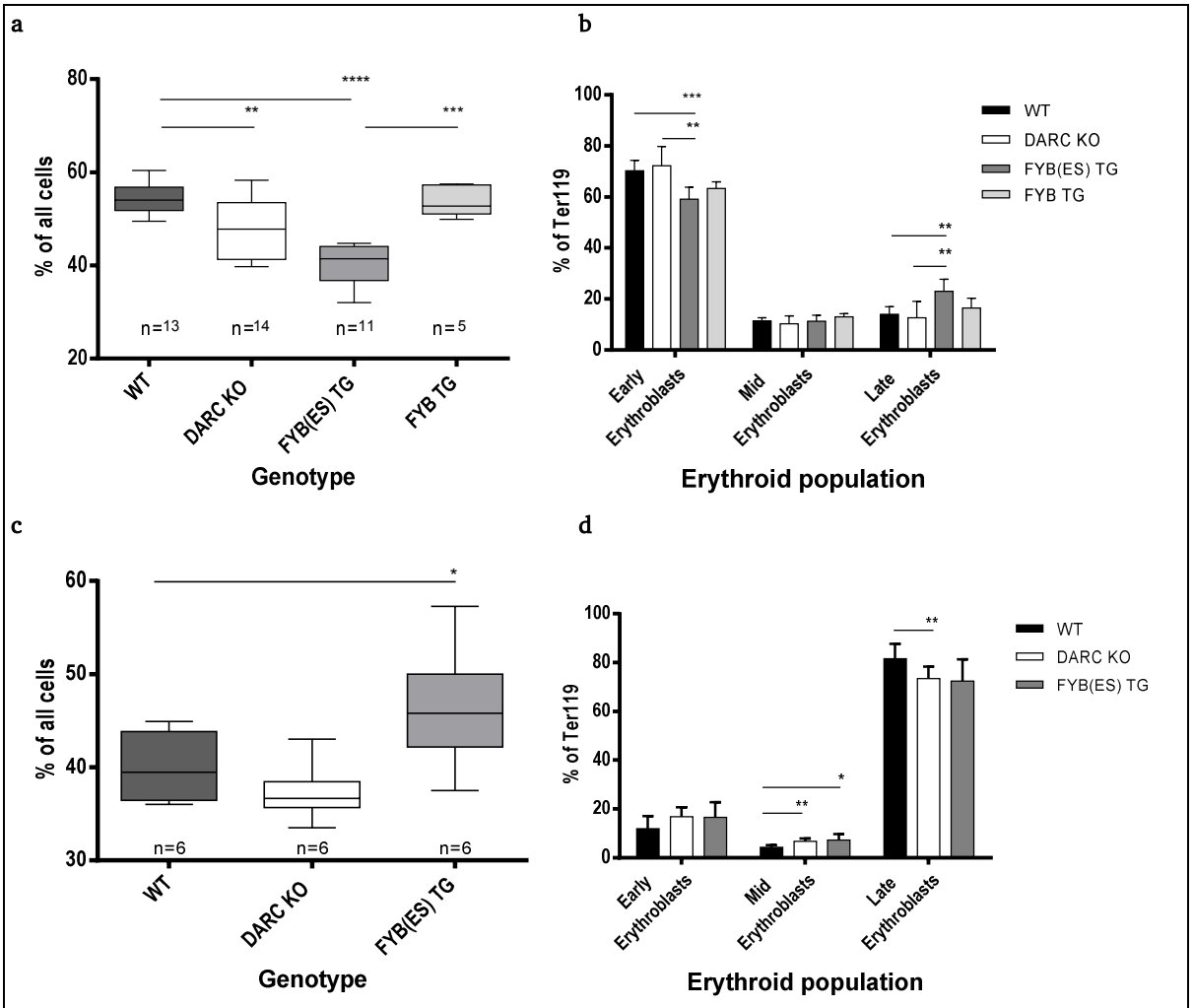

Figure 4.10 (a) Erythroid cells, as a proportion of all cells in unlysed bone marrow, (b) proportions of erythroid progenitors, as a proportion of all Ter119$^+$ cells, WT n=6, DARC KO n=6, FYB(ES)TG n=11, FYBTG n=5. (c) Splenic erythroid cells as a proportion of all unlysed cells, n=6 per genotype, and (d) proportions of splenic erythroid progenitors, as a proportion of all Ter119$^+$ cells, n=6 per genotype.

Since the spleen is a haematopoietic organ in mice, and given the differences in these profiles, the data could be interpreted as suggesting that the more prominent myeloid mass in the bone marrow directs a 'compensatory' erythropoiesis in the spleen of FYB(ES)TG mice. Alternatively the chemo- or cytokine profile may be less favourable towards bone marrow haematopoiesis. It is well known from human pathology that ineffective haematopoiesis or erythropoiesis gives rise to extramedullary haematopoiesis (Greer and Wintrobe, 2004), and splenomegaly is a feature of these conditions. Potentially a pro-granulocyte haematopoietic environment may lead to a translocation of erythropoiesis to the spleen in the maintenance of normal haemoglobin levels.

4.3.1.5 Bone marrow stem and progenitor cell profiles

Myeloid and lymphoid progenitors

FYB(ES)TG mice, and to a lesser extent DARC KO, have increased myeloid cells in the bone marrow but reduced lymphoid and erythroid cells, yet in the peripheral blood there is a relative neutropaenia in FYB(ES)TG compared to WT mice. However it is not clear whether this represents over-production of myeloid cells or a failure to release these cells under homeostatic conditions.

Examination of the HSPC populations revealed that myeloid progenitors are reduced in FYB(ES)TG and DARC KO mice, in particular due to reduction in GMP (**Figure 4.11**), which are reduced by approximately a third in both absolute and relative terms. MEP were also reduced implying altered maturation in the myeloid lineage.

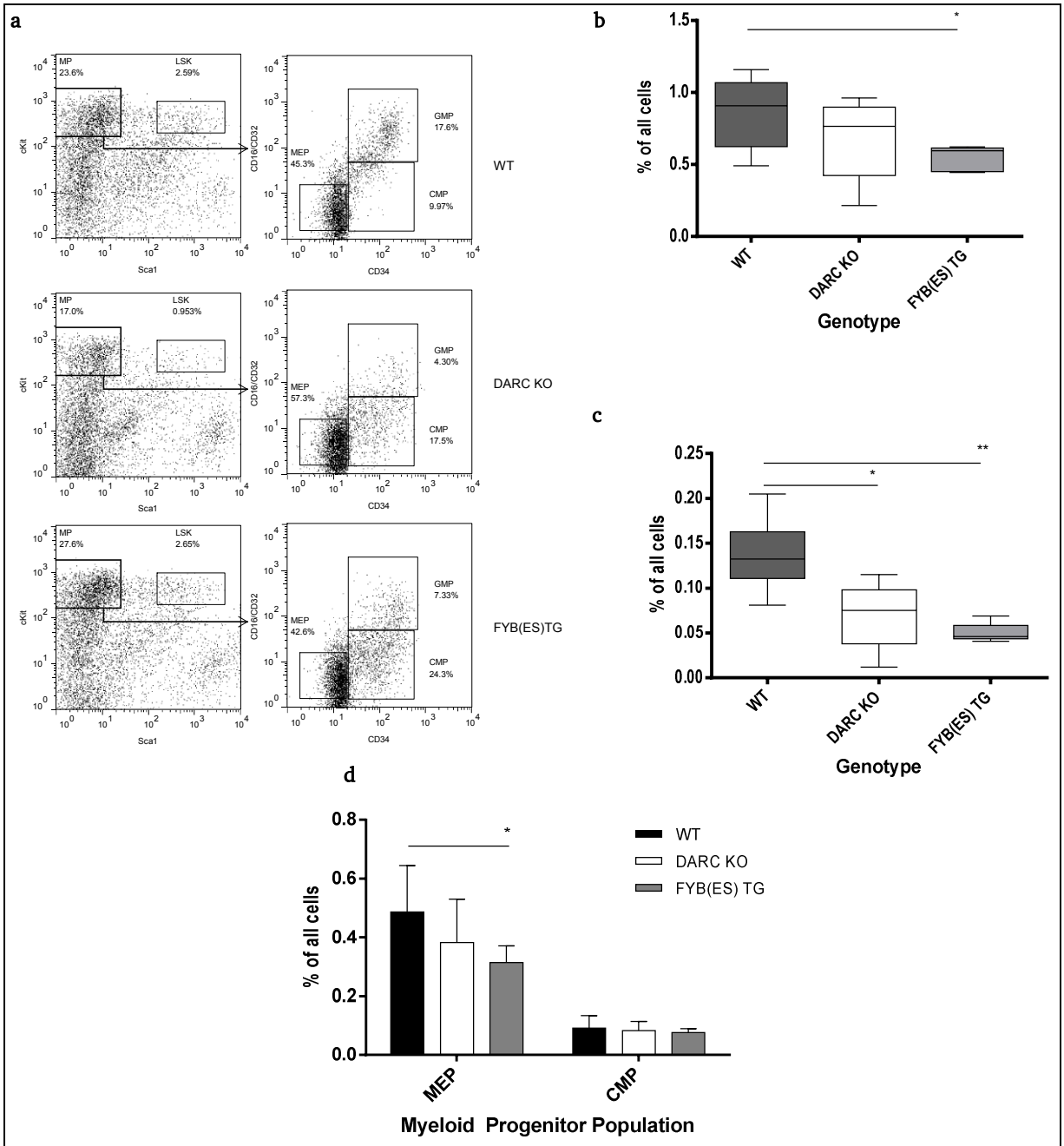

Figure 4.11 Analysis of myeloid progenitor cells. (a) Representative gating of lineage negative cells and myeloid progenitors in WT, DARC KO and FYB(ES)TG mice. (b) Myeloid progenitors in WT (n=6), DARC KO (n=5), FYB(ES)TG (n=5), (c) GMPs as a proportion of all cells in WT (n=6), DARC KO (n=5), FYB(ES)TG (n=5). (d) Other myeloid progenitor populations. Data from one experiment, representative of 4 independent experiments.

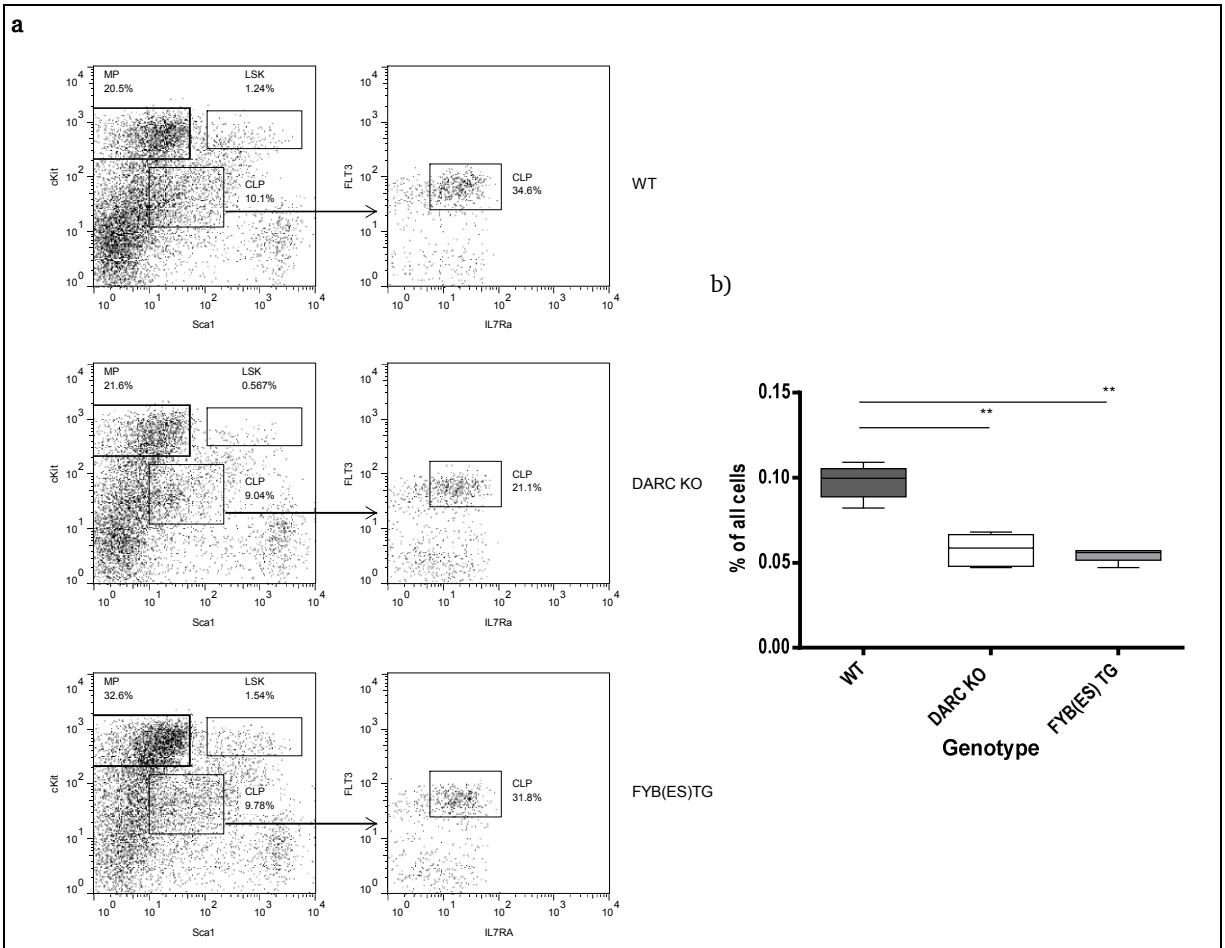

Figure 4.12 Analysis of lymphoid progenitor cells. (a) Representative gating of lineage negative cells and common lymphoid progenitor (CLP) region in WT, DARC KO and FYB(ES)TG mice. (b) CLP cells as a proportion of all cells. Data from one experiment (n=6 per genotype), representative of 3 independent experiments.

As a proportion of all cells, CLP (Lin^{-} $cKit^{+}$ $Sca1^{+}$ $IL7RA^{+}$ $Flt3^{Hi}$) were reduced in both DARC KO and FYB(ES)TG (**Figure 4.12**). In a preliminary experiment, (**Figure 4.13**), FYBTG had a GMP profile similar to WT mice, although myeloid progenitors were not different, and CMP were reduced in comparison to FYB(ES)TG. These results will require validation, but it is notable that the GMP difference between transgenic mice with and without erythroid DARC, show the same pattern as in chimeras, and WT and FYB(ES)TG respectively.

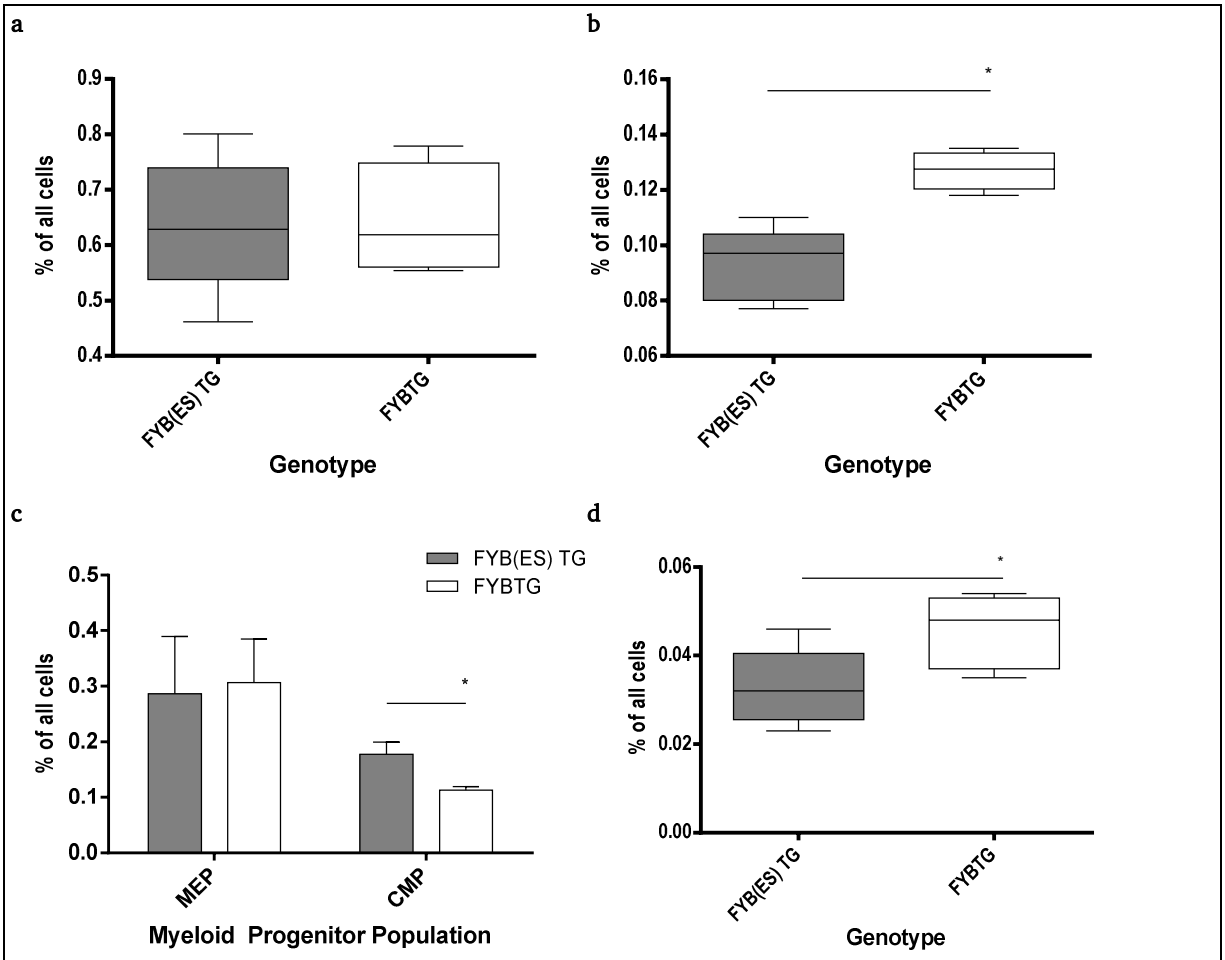

Figure 4.13 Preliminary analysis of sub-populations of myeloid progenitor cells as a proportion of all cells in FYB(ES)TG and FYBTG, n=5 per genotype. (a) Myeloid progenitors, (b) GMPs, (c) MEPs and CMPs, and (d) CLP.

LSK cells

DARC KO and FYB(ES)TG mice had reduced granulocyte progenitors and lymphoid progenitors, whereas preliminary analysis of FYBTG mice bone marrow appeared similar to WT mice. In order to determine where the reduced GMP and CLP might be due to alterations in MPP maturation, the LSK cells were examined. LSK cells were reduced in DARC KO and FYB(ES)TG, mainly due to a reduction in MPP cells, by approximately a third to a half in some cases. LT- & ST-HSC were not altered as a proportion of all cells (**Figure 4.14**).

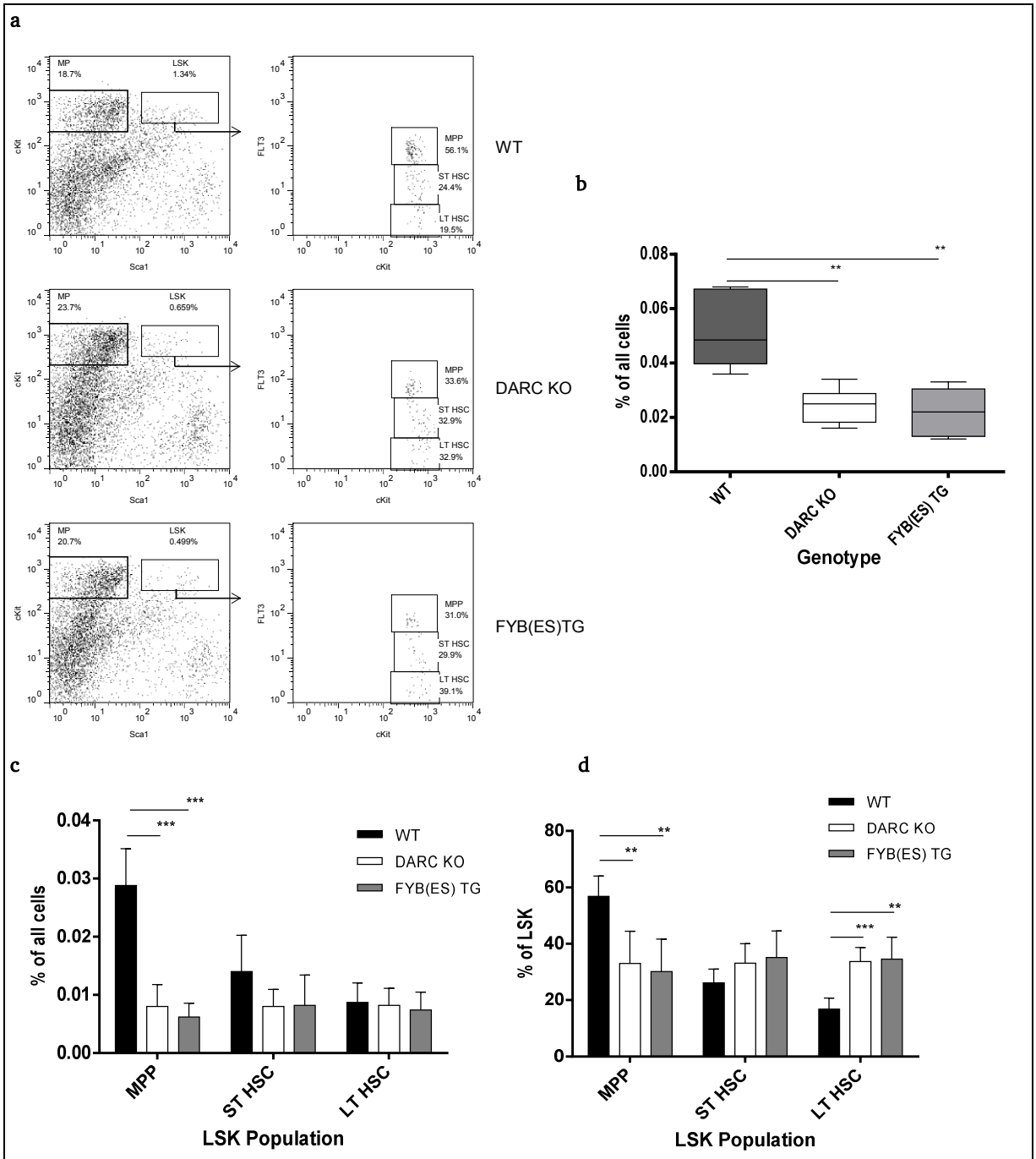

Figure 4.14 Analysis of LSK cells. (a) Representative gating of lineage negative cells and LSK region in WT, DARC KO and FYB(ES)TG mice. (b) LSK cells as a proportion of all cells. LSK populations as a proportion of (c) all cells; and (d) as a proportion of parent population. Data from one experiment (n=6 per genotype), representative of 4 independent experiments.

Preliminary examination of LSK cells in the FYBTG bone marrow (**Figure 4.15**) reveals that LSK cells are no different in proportions of total bone marrow compared to FYB(ES)TG mice. As a proportion of all cells, ST-HSC and LT-HSC were reduced and

MPP cells were not different in FYBTG mice. However as a proportion of LSK sub-groups, MPP cells in FYBTG mice are increased relative to FYB(ES)TG, and ST-HSC are reduced, and these findings are similar to those observed in WT mice. Verification of this finding and analysis of LSK sub-populations of FYBTG mice is required.

It is unclear as to the reasons why LSK cell proportions are not different in FYBTG mice comparison to those of FYB(ES)TG mice, given the prominent phenotypic similarity of FYBTG to WT mice.

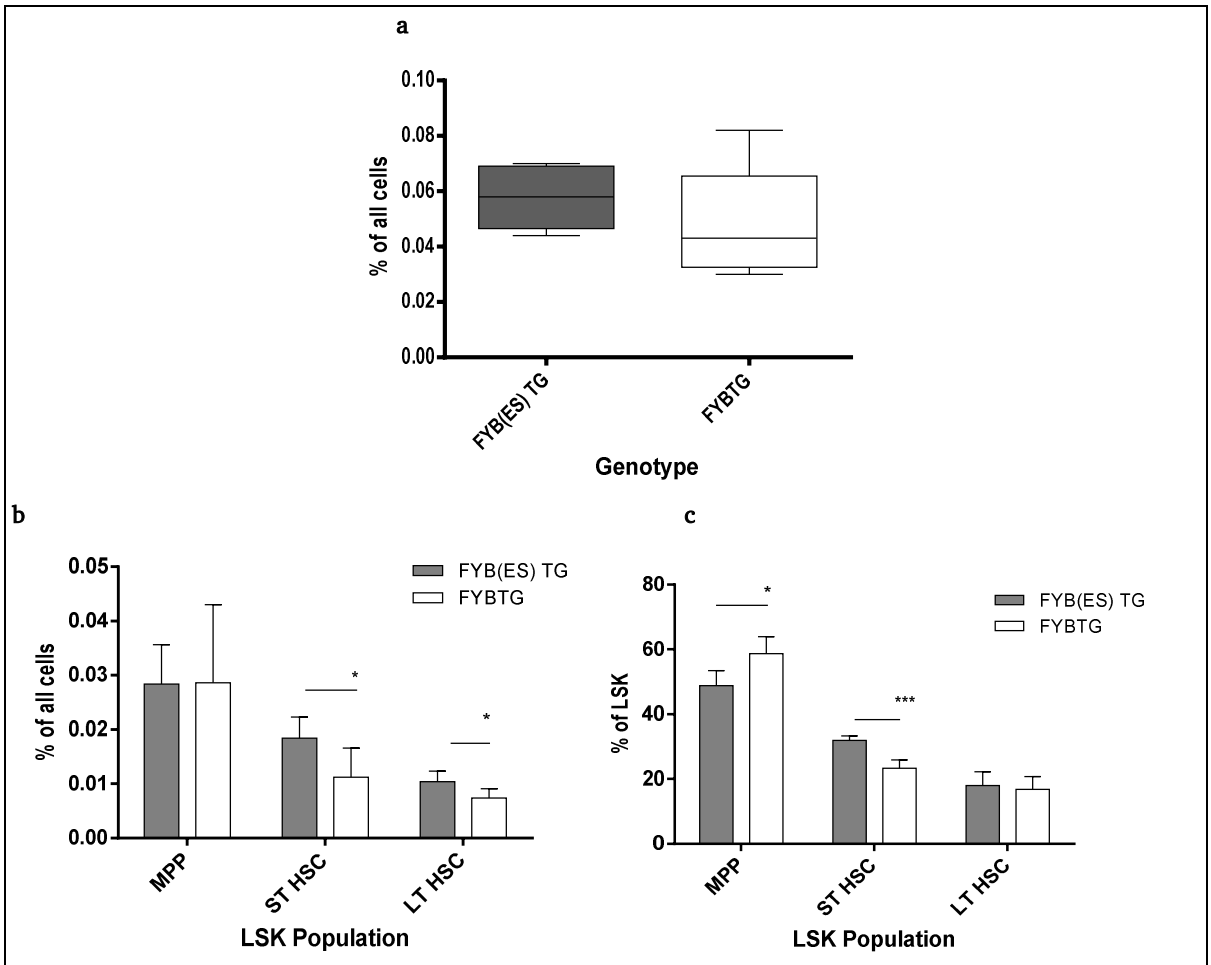

Figure 4.15 (a) LSK were unchanged between FYB(ES)TG and FYBTG mice, and (b) MPP were unchanged as a proportion of all cells, they were increased in FYBTG (c), similar to WT mice. Data from one experiment (n=5 per genotype), a preliminary experiment comparing FYB(ES)TG and FYBTG mice.

Multi-potent progenitors

As described earlier, MPP can be divided into three populations depending on VCAM-1, CD62L, and expression of FLT3, with a population with mainly GM potential, GMPP (VCAM-1^{+}, $CD62L^{+}$, $Flt3^{lo}$), a population with mainly lymphoid potential, termed LMPP (VCAM-1^{-}, $CD62L^{+}$, $Flt3^{Hi}$), and a CMP population with retained megakaryocytic-erythroid potential (VCAM-1^{+}, $CD62L^{-}$, $Flt3^{neg}$). DARC KO and FYB(ES)TG mice had a significant reduction in GMPP of approximately 50% whereas FYB(ES)TG also exhibited a reduction in CMP. This in concordance with both the reduced GMP and overall reduction in myeloid progenitors (**Figure 4.16**).

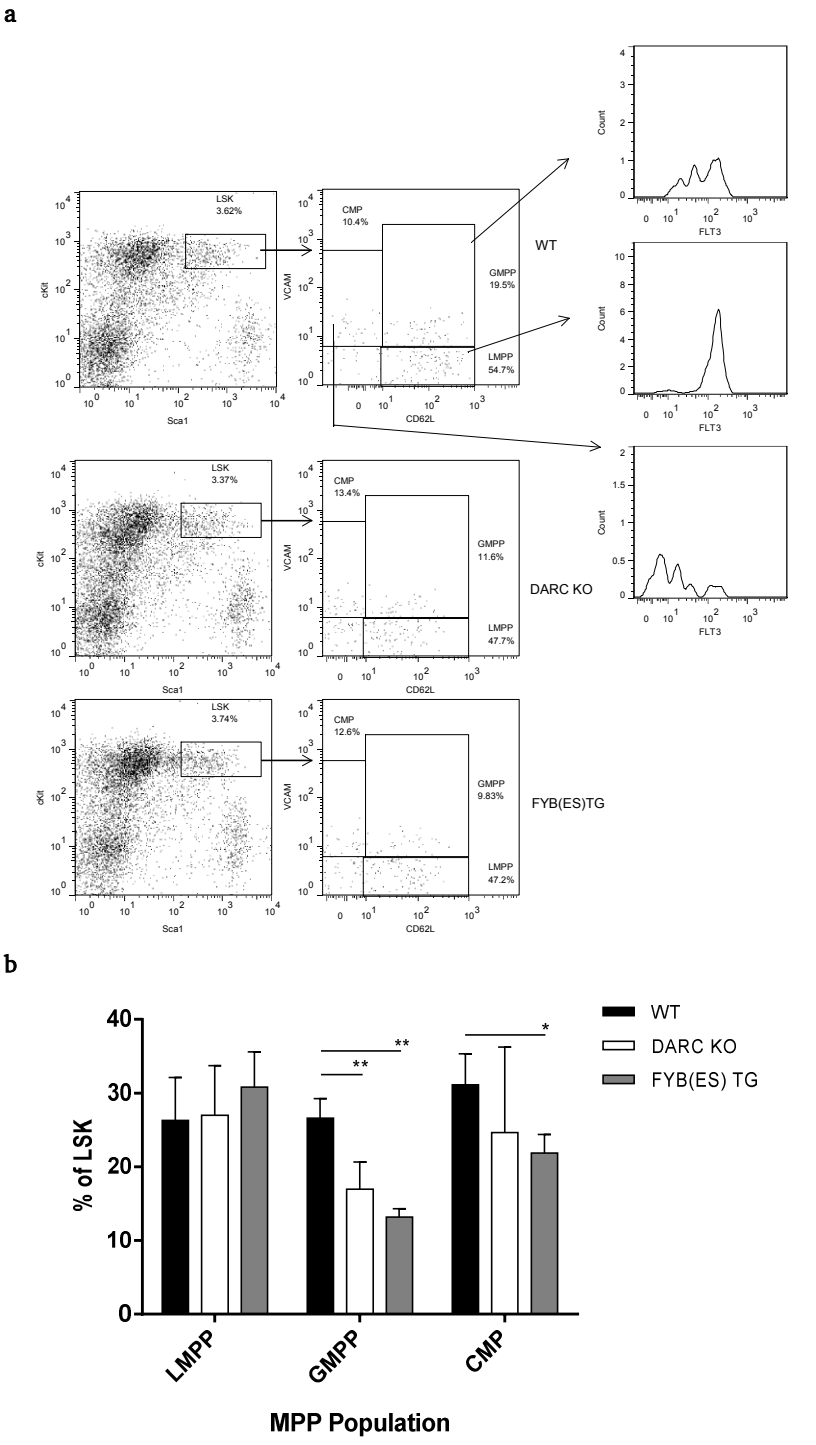

Figure 4.16 Analysis of multi-potent progenitor subtypes. (a) Representative gating of lineage negative cells and LSK region in WT, DARC KO and FYB(ES)TG mice. (b) Multipotent progenitors as a proportion of LSK cells. Data from one experiment (n=6 per genotype), representative of 3 independent experiments. CMP, common myeloid progenitors; GMPP, Granulocyte macrophage primed progenitors; LMPP, lymphoid multipotent progenitors.

A hitherto unexplained aspect of DARC expression is whether any stem or progenitor cells normally express this atypical chemokine receptor, at any stage of maturation. Conceivably, the altered myelopoiesis present in DARC KO and FYB(ES)TG may be due to DARC expression on HSPC playing a role in immobilising or internalising chemokines for normal development. Previous studies confirmed the absence of DARC expression on peripheral blood leukocytes (Dunstan, 1986). However, expression in HSPC has not previously been examined. Firstly, DARC expression was examined in developing erythroid cells in WT mice. From the pro-erythroblast stage, DARC expression could be detected (**Figure 4.17**), and was highest at earlier stages of maturation, thereafter declining slightly.

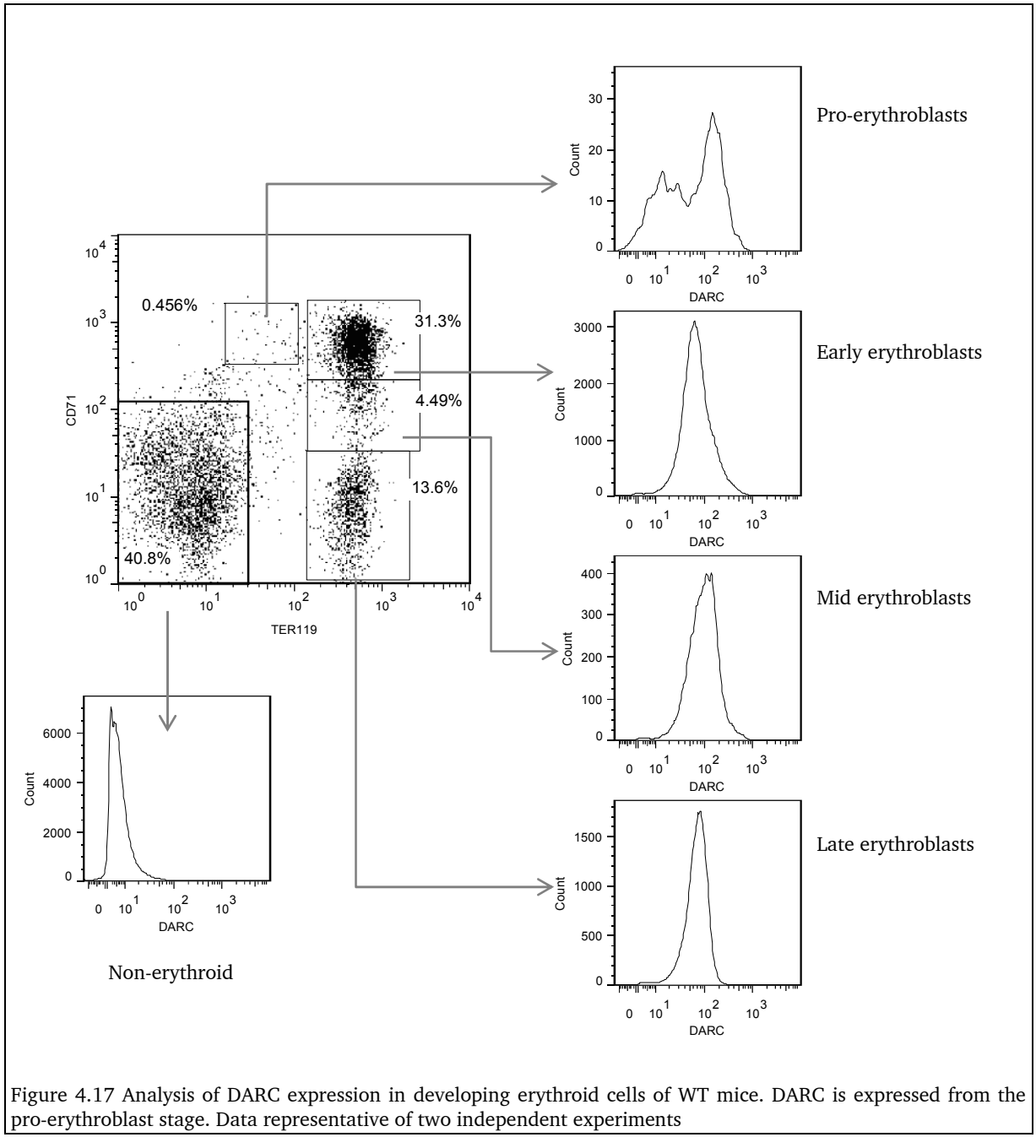

Figure 4.17 Analysis of DARC expression in developing erythroid cells of WT mice. DARC is expressed from the pro-erythroblast stage. Data representative of two independent experiments

The lineage negative fraction was subsequently examined, including LSK and myeloid progenitors. Neither LSK nor MEP, CMP or GMP expressed DARC (**Figure 4.18**). Other cell types, such as megakaryocytes and platelets, lymphoid and myeloid cells also did not express DARC protein (data not shown).

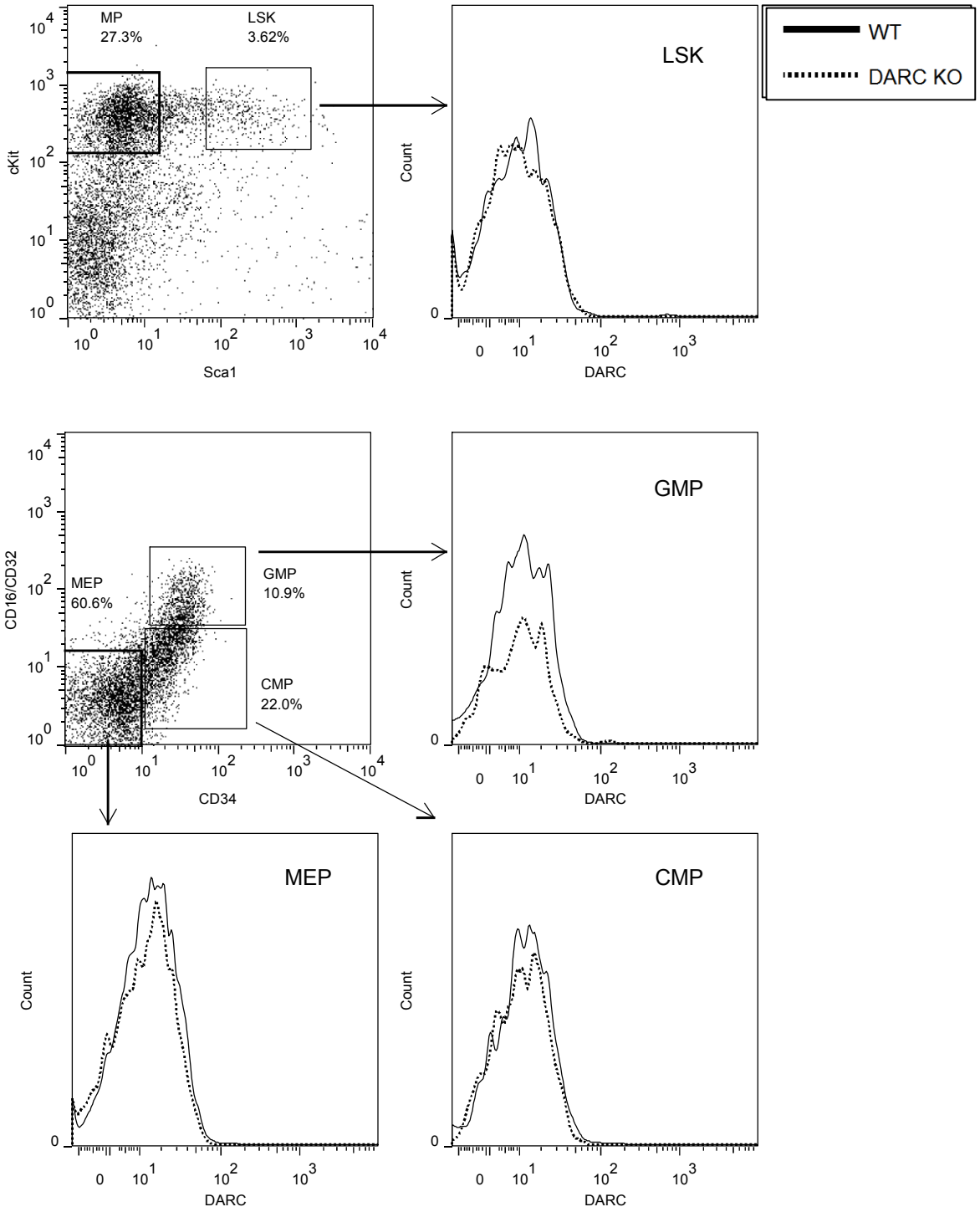

Figure 4.18 Examination of DARC expression in lineage negative cells of WT and DARC KO mice by flow cytometry. Data representative of two independent experiments

4.3.2 Bone marrow cultures

The *in vitro* short term haematopoietic cell culture system permits identification and determination of HSPC (Nishijima *et al.*, 1997), through the use of colony formation assays (Ito *et al.*, 2003). Cells are grown in methyl cellulose or other viscous medium, which reduces cell movement and permits individual proliferating cells to develop into colonies. The colonies containing differentiated cells, termed Colony Forming Units (CFU), are derived from single progenitor or stem cells. The CFU can be further classified according to the main differentiated cell type observed: CFU-GEMM are multi-lineage colonies containing granulocyte, erythrocyte, megakaryocyte and monocyte precursors, CFU-GM contain mainly granulocyte and monocyte precursors, and CFU-G or CFU-M, granulocyte and monocyte precursors only, respectively.

The proliferation potential of unfractionated DARC KO bone marrow cells was investigated utilising methyl cellulose cultures and compared to that of WT bone marrow cells. Owing to limitations of time and resources, DARC KO bone marrow cells were selected for investigation since these exhibited a similar phenotypic profile to FYB(ES)TG. Cultures were initially prepared with 20,000 nucleated bone marrow cells from WT and DARC KO mice following erythrocyte lysis (see representative images of colonies and constituent cells, **Figure 4.19**). Seven-day culture demonstrated that significantly fewer colonies, which were also less cellular, were present in cultures from DARC KO mice, (**Figure 4.20a, b**). Representative colonies were picked, cell suspensions cytospinned and analysed under the microscope to confirm identity (**Figure 4.20c**).

A potential alternative explanation for the reduction in colony numbers could be that relatively fewer LSK cells are present in the bone marrow of DARC KO mice, potentially leading to reduced numbers of CFU and cells (**Figure 4.20a**). Therefore subsequent cultures were undertaken starting from 500 FACS sorted LSK cells revealing an identical pattern, with DARC KO cultures producing significantly fewer colonies than their WT counterparts (**Figure 4.20b**). Colony scoring revealed a relative paucity of CFU-GM colonies, and which account for most of the deficit in total colony number grown from DARC KO LSK as compared to WT LSK **(Figure 4.20c**). Cell counts were also significantly reduced, indicating that the proliferative rate of the cells culture from DARC KO LSK was reduced (**Figure 4.20d**). Following the first 7 days of culture, colonies were washed off plates, cells resuspended and 20,000 cells were replated in triplicate. DARC KO cells demonstrated a significant increase in the number of resultant colonies and cell numbers (**Figure 4.20e**), compared to WT cells. Subsequent replating revealed no significant difference between WT and DARC KO colony numbers (data not shown).

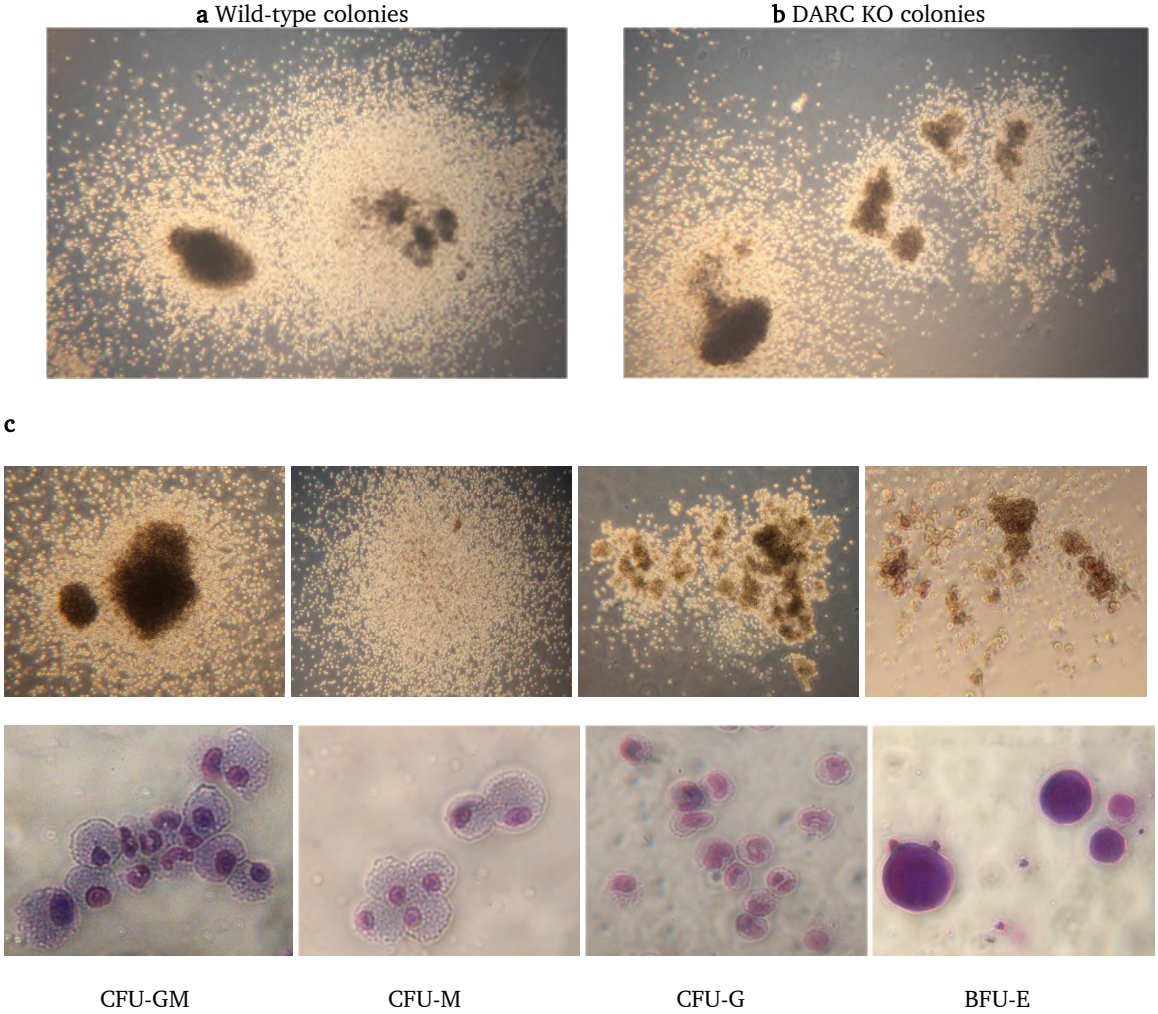

Figure 4.19 Images of colony appearances following 7 day culture of FACS sorted 500 LSK cells plated in semi-solid methycellulose medium (Methocult M3434), Wild-type (a), and DARC KO (b) at 10x magnification. Representative CFU-GM shown. (c) Representative colonies for CFU-GM, CFU-M and BFU-E, above, and corresponding images cytospin, below, of same colonies selected for further examination.

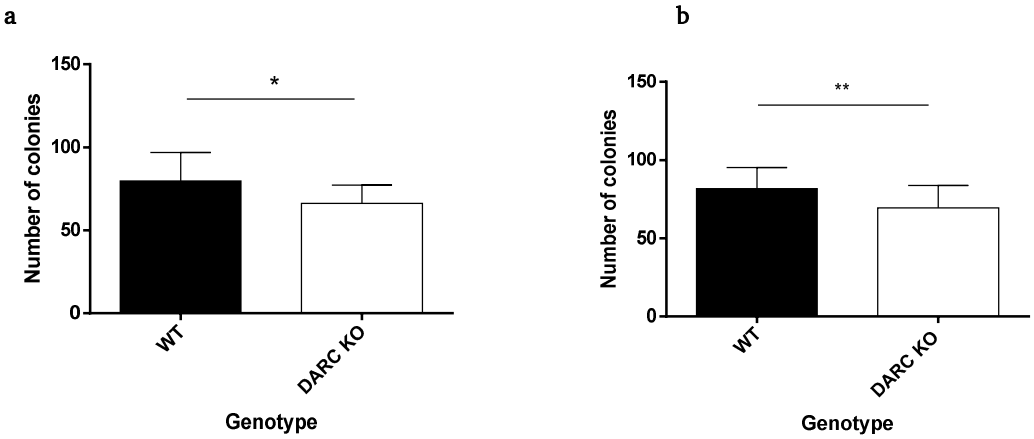

Figure 4.20 (a) Total number of CFU present after 7 days of culture of 20,000 bone marrow nucleated cells. Data presented as means and SD of 3 experiments, with triplicate cultures per genotype. Two-way ANOVA df(1,12) p=0.01 (b) Total number of CFU present after 7 days of culture of FACS sorted 500 LSK cells per plate, data presented as means and SD of 4 experiments with triplicate cultures per genotype. Two-way ANOVA df(1, 15) p=0.006

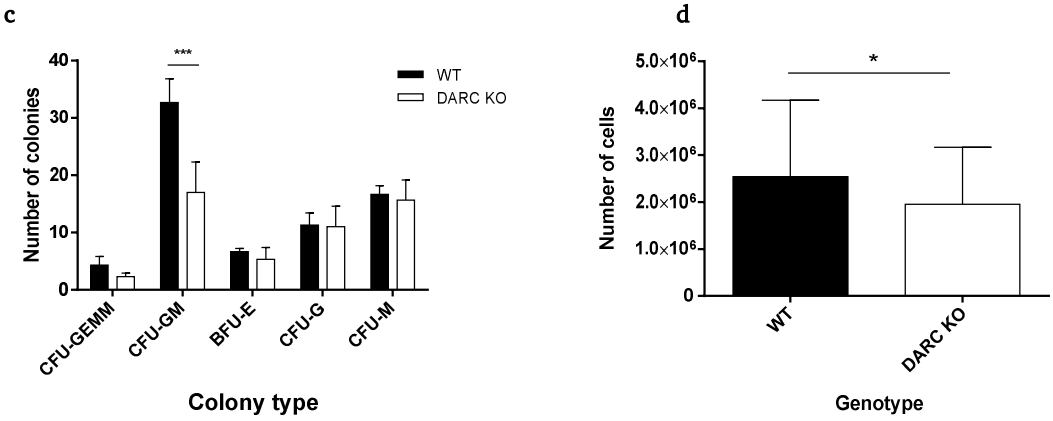

Figure 4.20(c) Distribution of colony types in cultures of 500 FACS sorted LSK per genotype. Data shown are results from one representative experiment, of 4 experiments, with triplicate cultures per genotype. Two-way ANOVA df(1, 15) p=0.0003, (d) Total cell count following 7 days cultures of 500 FACS sorted LSK per genotype. Data presented as means and SD of 3 experiments, with triplicate cultures per genotype. Two-way ANOVA df(1, 12) p=0.047.

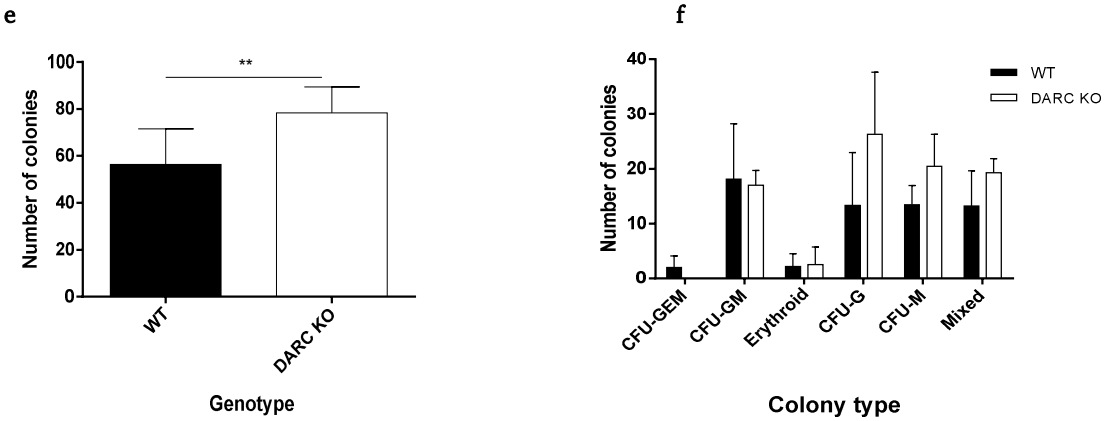

Figure 4.20 (e) Total number of CFU present after 7 days of culture of 20,000 replated cells from colonies arising during the culture of LSK cells. Data presented as means and SD of 3 experiments, with triplicate cultures per genotype. Two-way ANOVA df(1, 15) p=0.003. (f) Distribution of colony types after 7 days following replating of 20,000 cultured cells, no significant differences were observed in colony distributions by two-way ANOVA. Data shown are results from one representative experiment, of 3 experiments. Shown on all graphs is the statistical significance of genotype as an independent factor in ANOVA calculation.

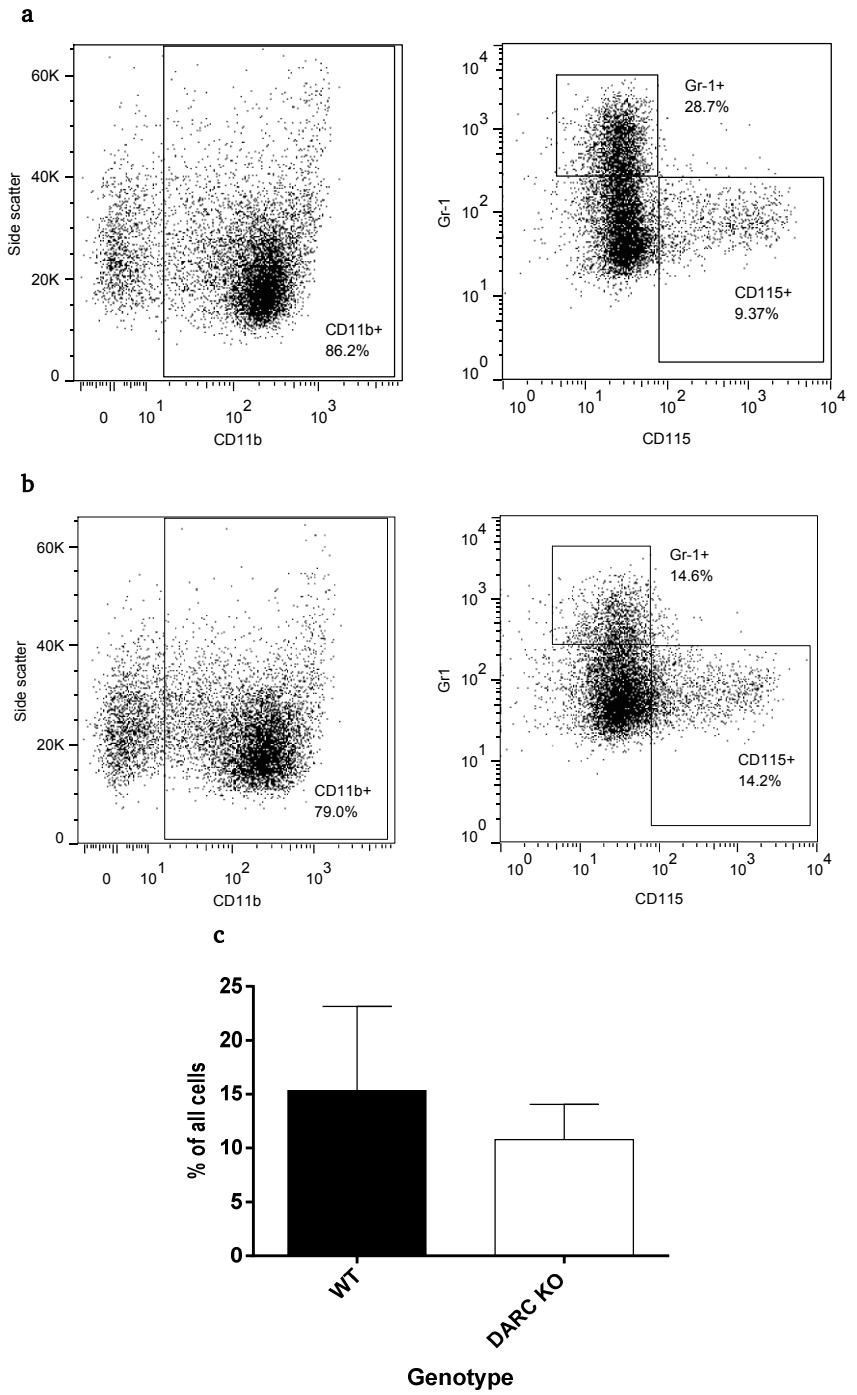

Figure 4.21 Representative myeloid profiles of cells from cultures of 500 FACS sorted LSK cells cultured for 7 days (a, b: wild-type, DARC KO, respectively). Proportions of myeloid cells from WT and DARC KO cultures, (c). Analysis of 4 cultures per genotype.

Flow cytometric analysis of culture cells revealed no significant difference in proportions of myeloid population (CD11b-positive, Ly6G-positive) between WT and DARC KO (**Figure 4.21**).

4.3.3 BrdU proliferation assay

In order to determine whether altered cell-cycle kinetics may be responsible for the reduced numbers of LSK cells in DARC KO and FYB(ES)TG mice, the BrdU uptake assay was undertaken as described in Methods. Briefly, BrdU, an analogue of the nucleotide thymidine was allowed to incorporate into DNA. Only cells entering and progressing through the S phase of the cell cycle incorporate BrdU into their newly synthesised DNA (Kobayashi *et al.*, 1998). The incorporated BrdU was detected with specific anti-BrdU fluorescent antibodies; the levels of cell-associated BrdU are then measured by flow cytometry permitting the determination of cells that are actively synthesizing DNA (Lacombe *et al.*, 1988, Dean *et al.*, 1984).

Experiments showed a significantly reduced BrdU uptake in the LSK cells and myeloid progenitor compartments of FYB(ES)TG mice (**Figure 4.22**). Apart from MEP, all myeloid progenitor subsets and LSK cells show reduced BrdU uptake suggesting reduced proliferation under homeostatic conditions.

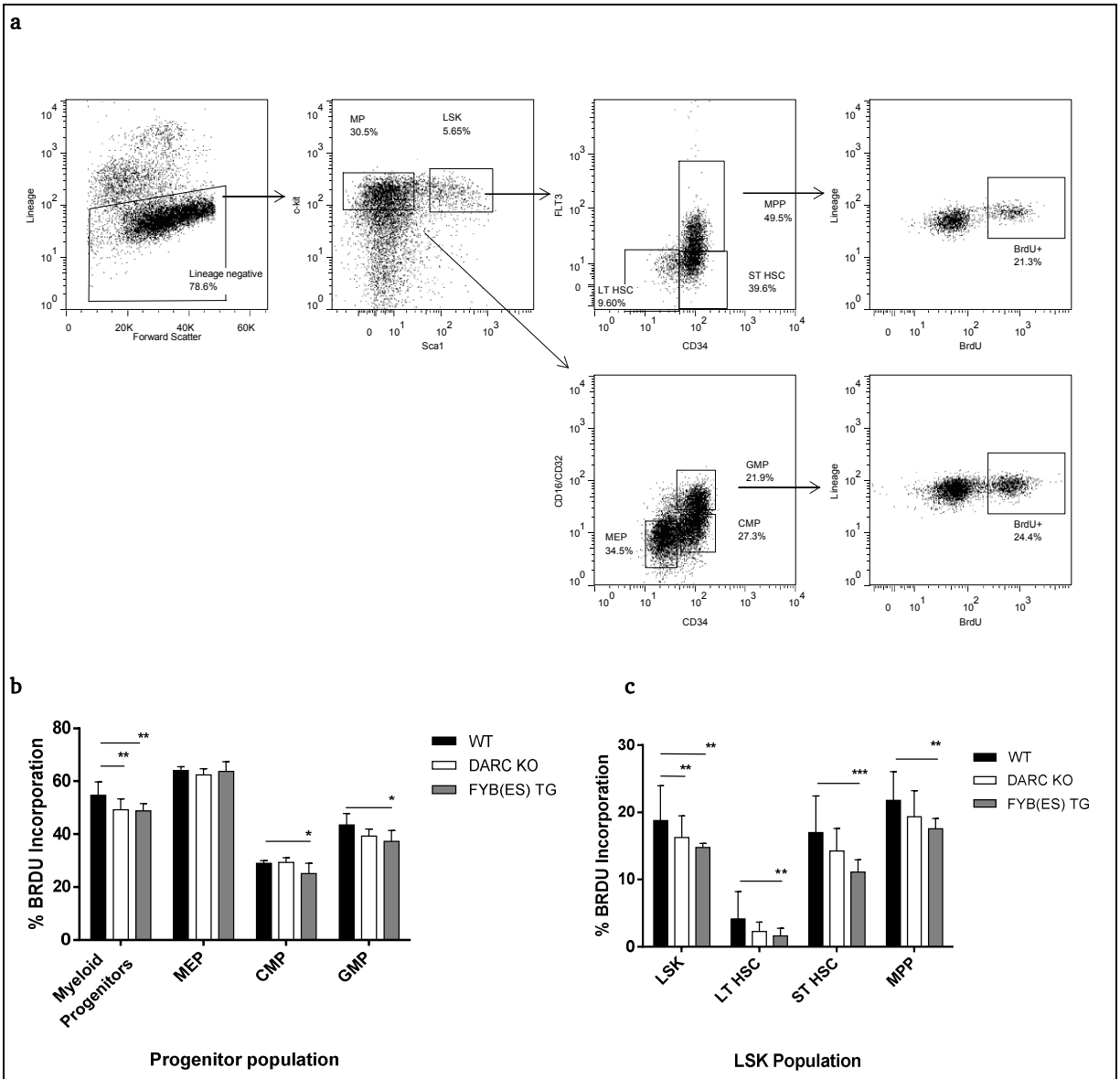

Figure 4.22 BrdU incorporation in myeloid progenitors and LSK cells of WT, DARC KO and FYB(ES)TG mice, representative gating (a). BrdU incorporation in (b) myeloid progenitors, divided by progenitor sub-type (myeloid progenitor two-way ANOVA df(2, 11) p=0.001), and (c) in LSK cells and subpopulations (LSK two-way ANOVA df(2, 11) p=0.001). Data presented as means and SD, n=5-7 per group. Shown on graphs is the statistical significance of genotype as an independent factor in ANOVA calculation.

4.3.4 Apoptosis

To investigate further potential mechanisms leading to reduced LSK and progenitor populations in the DARC KO and FYB(ES)TG mice, levels of apoptosis were examined in these cells by Annexin V staining as detailed in Methods. Apoptosis is a normal physiological process, which occurs in the maintenance of normal tissue growth and development, as well as in embryonic development (Horvitz, 1999). The underlying mechanisms of apoptosis involve an energy-dependent sequence of molecular events, which can be intrinsic (mitochondrial) or extrinsic, responding to receptor stimulation (Igney and Krammer, 2002). These converge on a final pathway, characterised by morphological features, such as the loss of plasma membrane integrity and condensation of the nucleus and cytoplasm (Hacker, 2000). Apoptotic cells show biochemical alterations such as DNA degradation, protein cross-linking and cleavage, and membrane changes that lead to their recognition by phagocytes (Hengartner, 2000). One of the earliest features of apoptosis is the translocation of the membrane phospholipid phosphatidylserine from the inner to the outer aspect of the cellular plasma membrane (Bratton *et al.*, 1997). These changes can be detected by Annexin V, which is a Ca^{2+} dependent phospholipid-binding protein with a high affinity for phosphatidylserine (Koopman *et al.*, 1994). Fluorochrome conjugated Annexin V staining occurs prior to the loss of membrane integrity, which takes place only at the later stages of cell death. Therefore cell viability dyes, such as Sytox Blue are used in conjunction, as viable cells with intact membrane exclude Sytox Blue, while the membranes of dead cells are permeable to Sytox Blue. Cells that are Annexin V-

positive and Sytox Blue positive are considered dead, whereas cells that are Annexin V-positive and Sytox Blue negative are deemed as entering apoptosis.

Experimental results reveal that myeloid progenitors and LSK cells from FYB(ES)TG and LSK cells from DARC KO mice are relatively resistant to apoptosis and necrosis (**Figure 4.23**).

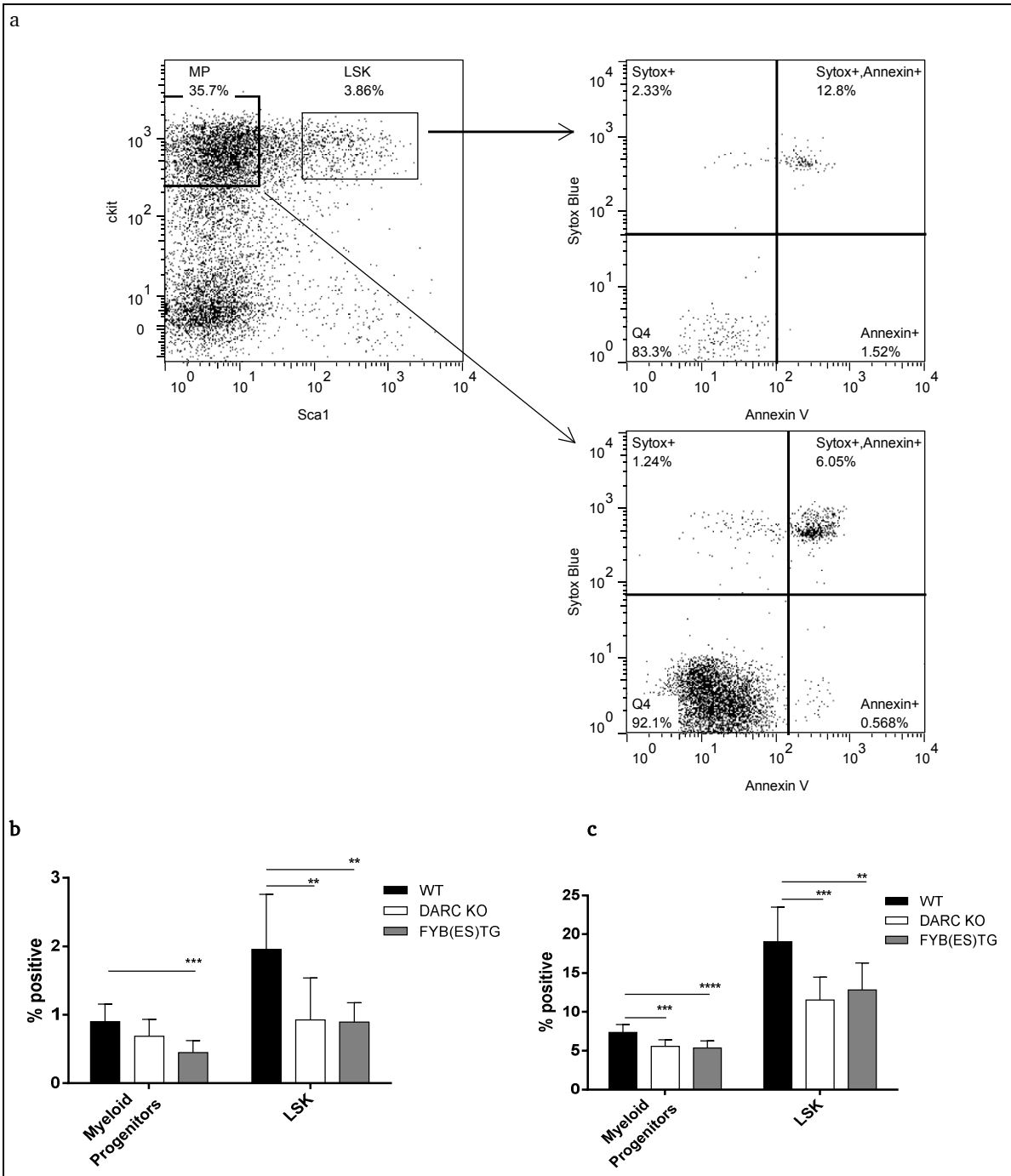

Figure 4.23 Apoptosis analysis of stem and progenitor cells in normal bone marrow from WT, DARC KO and FYB(ES)TG mice, (a) representative gating. The myeloid progenitor and LSK compartments were examined for rates of apoptosis (Annexin+ Sytox Blue–) and cell death (Annexin+ Sytox Blue+). (b) Graph showing proportions of apoptotic myeloid progenitors and LSK cells. (c) Graph showing proportions of dead cells in myeloid progenitors and LSK cells. n=9-11 per group.

4.3.5 Multiplex cytokine array analysis

FYB(ES)TG and DARC KO mice have reduced levels of both proliferation and apoptosis within the myeloid progenitors and LSK cells resulting in sum in reduced MPP and reduced GMP numbers. I hypothesised that changes in signalling molecules such as ELR+ chemokines in the bone marrow of DARC KO or FYB(ES)TG mice may lead to the bone marrow maturation profiles seen in these mice.

A function of DARC on erythrocytes is that of a chemokine sink or a reservoir, helping to potentially maintain chemokine gradients, and possibly also leukocyte sensitivity to them (Mei *et al.*, 2010). Since the large erythroid mass within the bone marrow expresses DARC, we aimed to determine the effect of differential erythroid DARC expression on chemokines and cytokines levels in the bone marrow supernatant of these mice. A 32-plex cytokine array panel of inflammatory chemokines and cytokines was used to investigate this question (**Figure 4.24**). In addition serum was chosen for similar analysis as it was desirable to determine the whole blood chemokine fraction.

Within the bone marrow supernatant, prepared as described in Methods, CCL11 was more clearly elevated, in both DARC KO and FYB(ES)TG, as was MIG (CXCL9). CXCL1 was reduced in DARC KO but not FYB(ES)TG. In the serum, the most significant result was the increase of G-CSF in both DARC KO and FYB(ES)TG. Furthermore CCL11 was elevated in the serum of FYB(ES)TG. There were no apparent differences in levels of CCL2, CCL5, CXCL1, CXCL5, CXCL9 and CXCL10.

The full panel of results is contained in Appendix 7.6 and 7.7

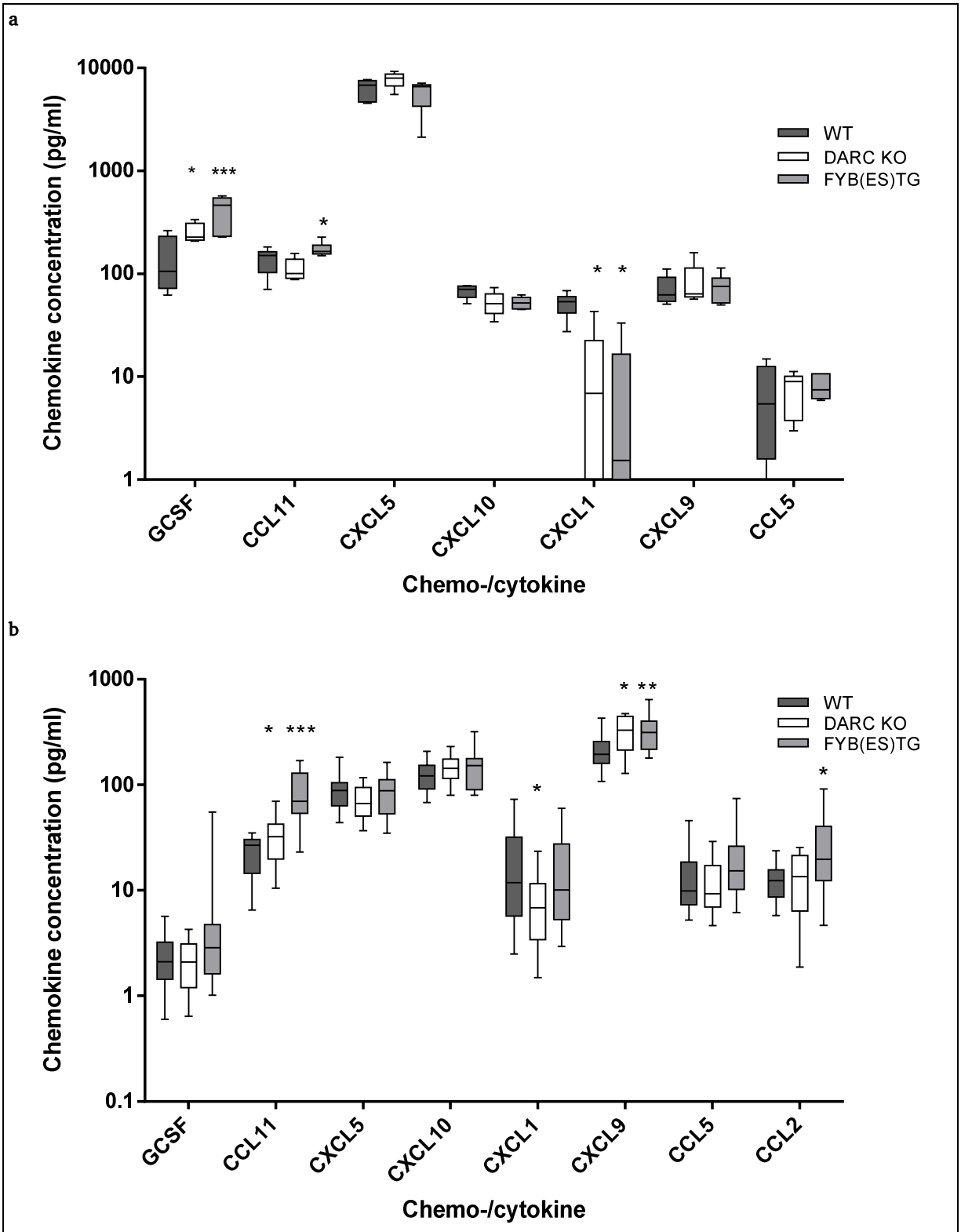

Figure 4.24 (a) Serum cyto- and chemokine analysis by multiplex cytokine array assay, in WT (n=6), DARC KO (n=6) and FYB(ES)TG (n=6) mice. (b) Bone marrow supernatant analysis by multiplex cytokine assay. WT (n=19), DARC KO (n=16) and FYB(ES)TG (n=16). Only DARC ligands or results with significant differences are shown. Mann-Whitney test used to calculate significance. See appendix for full panel of results.

4.3.6 Bone marrow competitive chimeras

Bone marrow competitive chimeras are tools utilised to measure, amongst others, differences in cellular proliferation and efficiency of engraftment. In addition, it was hypothesised that in a DARC replete environment, the engraftment of DARC positive cells may modify chemokine availability within the bone marrow and lead to a normalisation of the DARC KO and FYB(ES)TG myeloid maturation profiles. Typically cells can be introduced in a 50:50 or other ratio to determine proliferation potential and engraftment kinetics in-vivo. The DARC KO model was developed on a C57Bl/6 background with CD45.2 antigen expressed on leukocytes. Animal welfare considerations at the University of Birmingham Biomedical Services Unit limit the doses of gamma irradiation which can be used for myeloablation to a total of 9 Gy. In addition, while haematopoietic stem cells engraft and begin to differentiate towards mature cells, mature progenitors are required to maintain mature haematopoietic cell production temporarily, ensuring animal survival. For these reasons, a CD45.1xCD45.2 competitor within a CD45.1 host was used, such that residual host, competitor and donor proportions can be precisely determined. **Figure 4.25a** details general experimental procedure: CD45.1 BoyJ irradiated (2 x 4.5 Gy) hosts were injected with 10^6 bone marrow cells, which were 50% CD45.1xCD45.2 and either CD45.2 WT (designated WT-WT) or CD45.2KO (designated WT-KO), n=5 per group. Examining peripheral blood proportions by tail bleed revealed CD45.2 DARC KO had half the engraftment efficiency of CD45.2 WT. In addition **Figure 4.25b** demonstrates significantly increased spleen size in animals in the CD45.2 DARC KO group, and bone marrow cell counts were not different **Figure 4.25c**.

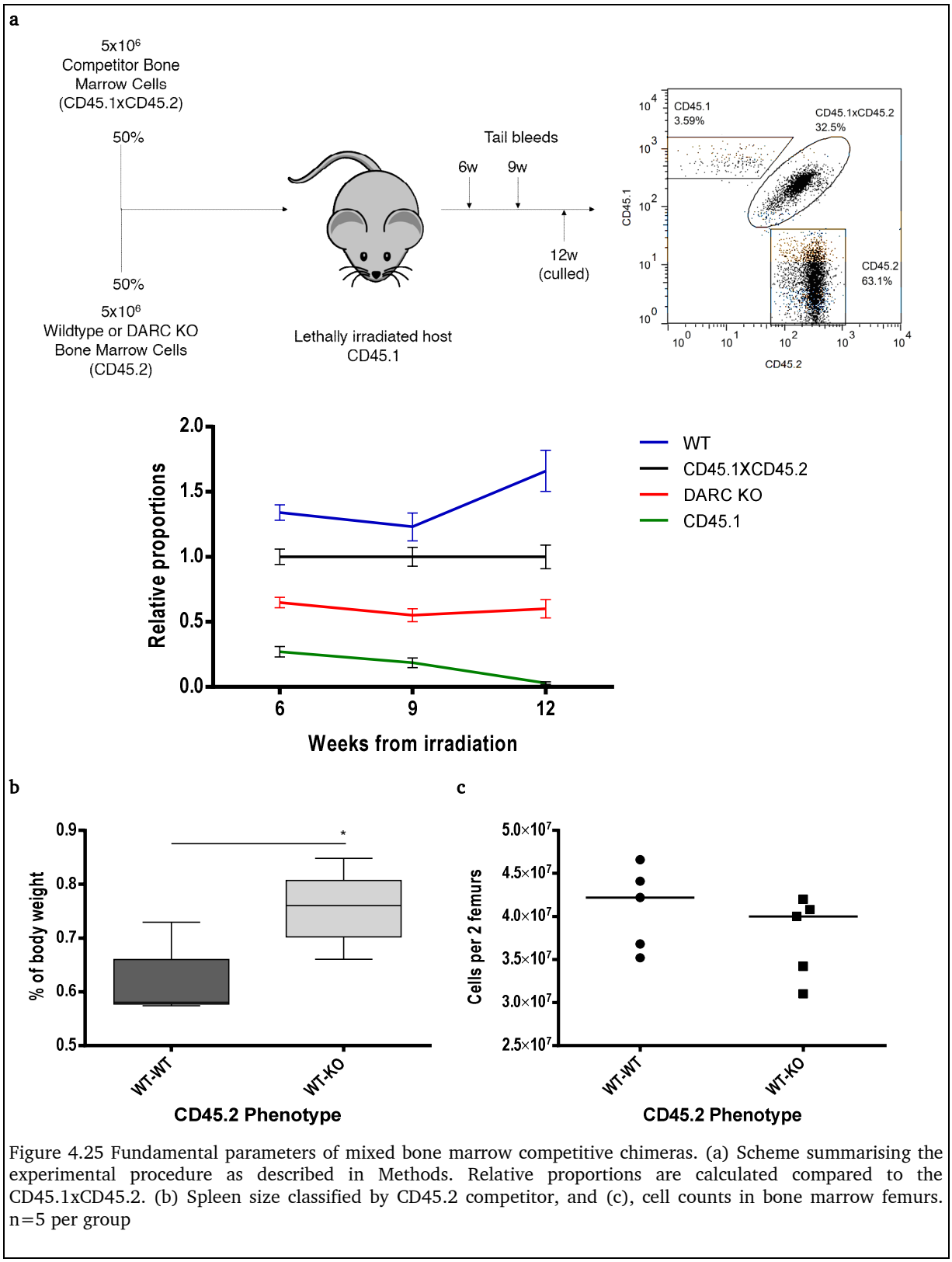

Figure 4.25 Fundamental parameters of mixed bone marrow competitive chimeras. (a) Scheme summarising the experimental procedure as described in Methods. Relative proportions are calculated compared to the CD45.1xCD45.2. (b) Spleen size classified by CD45.2 competitor, and (c), cell counts in bone marrow femurs. n=5 per group

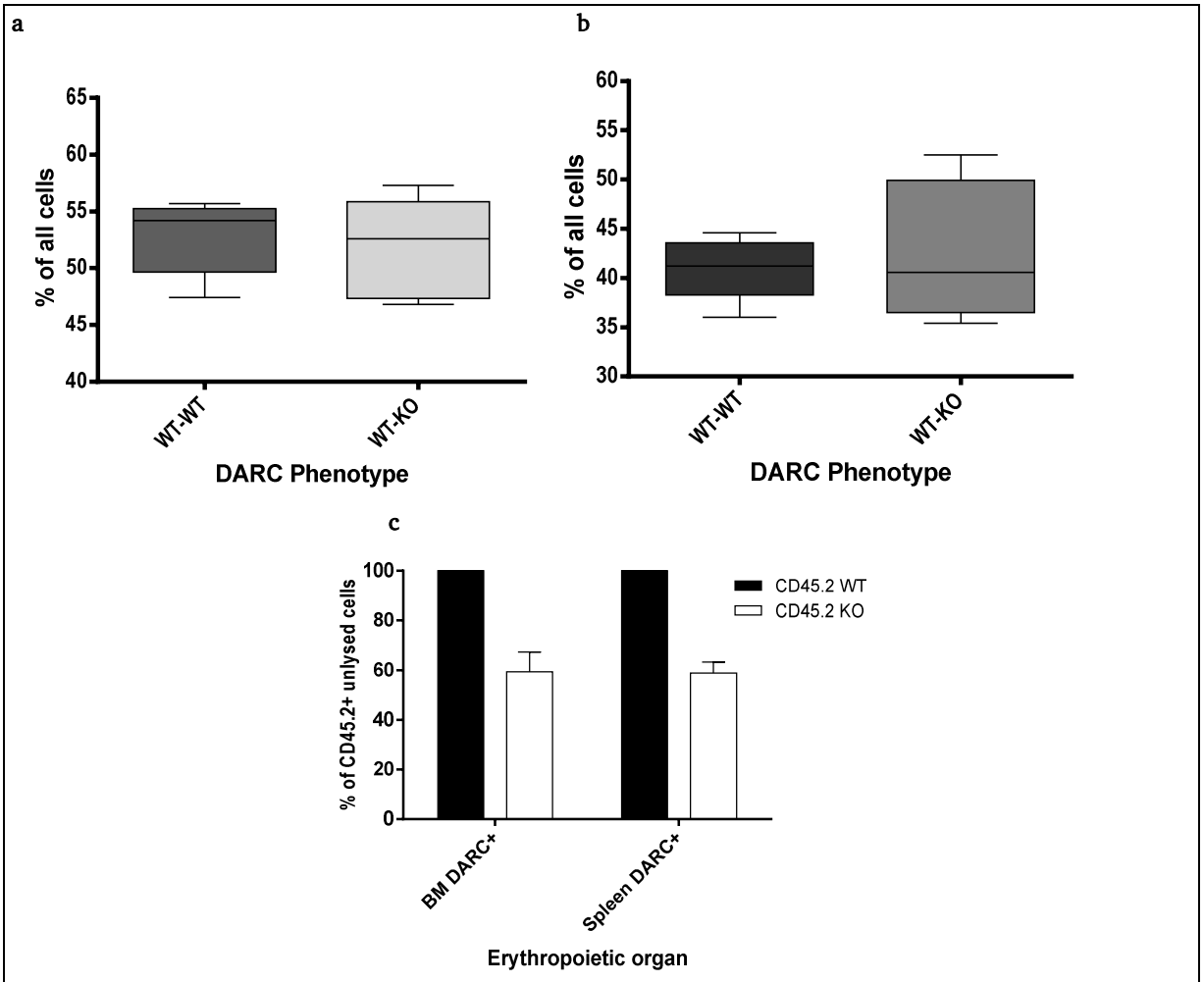

Figure 4.26 Erythroid cells as a proportion of all bone marrow and spleen cells in mixed bone marrow competitive chimeras, (a) bone marrow, and (b) spleen. Proportion of DARC-positive erythropoiesis in bone marrow and spleen, c). n=5 per group

There was no preferential relocation of erythropoiesis to the spleen (**Figure 4.26**), with no significant differences between the groups.

Total peripheral blood leukocyte, neutrophil and platelet counts and haemoglobin were not significantly different between the two groups (**Figure 4.27**).

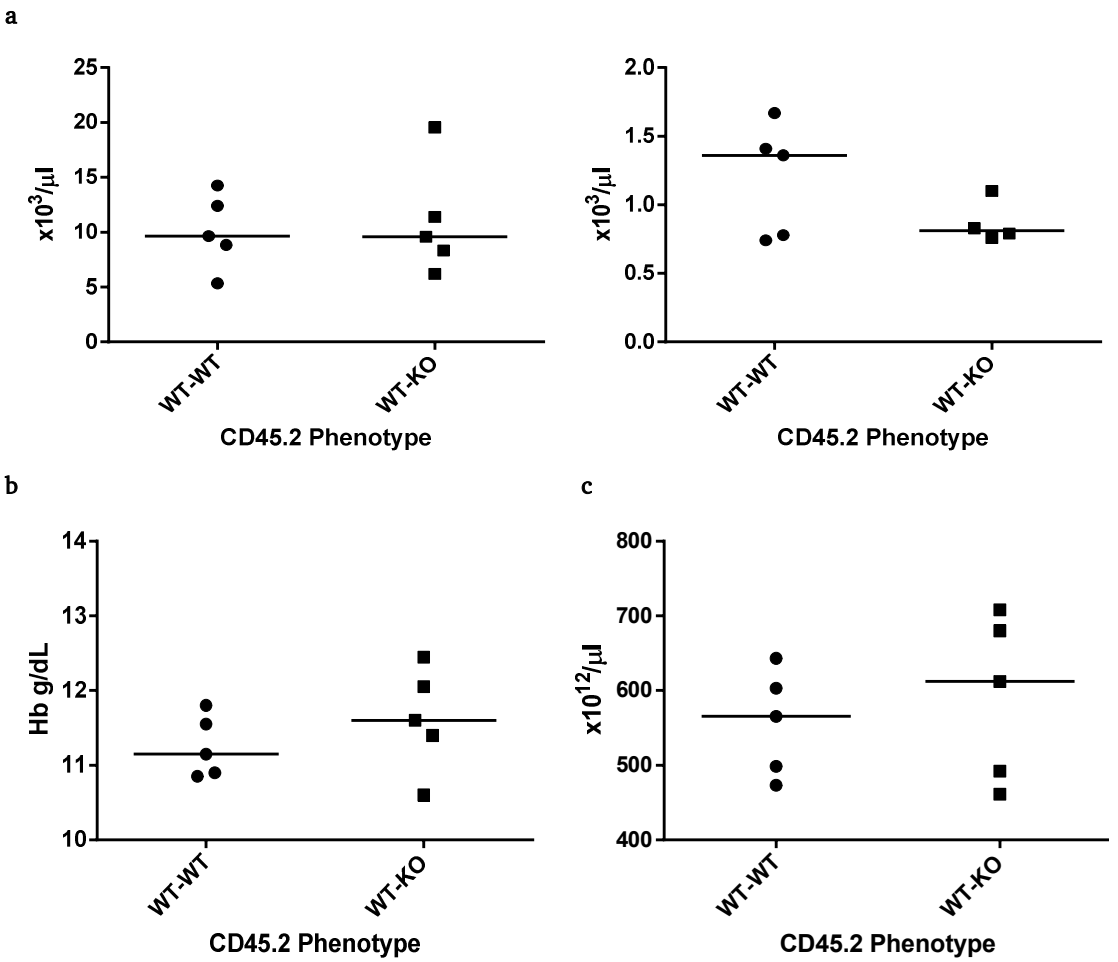

Figure 4.27 Complete blood count of mixed bone marrow competitive chimeras. Total leukocyte count (a), haemoglobin (c) and platelet count (d) from automated analyser. Neutrophil count by FACS-based bead counting method (b). n=5 per group.

As represented in **Figure 4.28**, relative to CD45.1xCD45.2, CD45.2 WT exceeded CD45.2KO at a ratio of 1.5-2:1, confirming that DARC KO cells have reduced proliferation compared to WT. There were no differences in peripheral blood cells populations between the two groups.

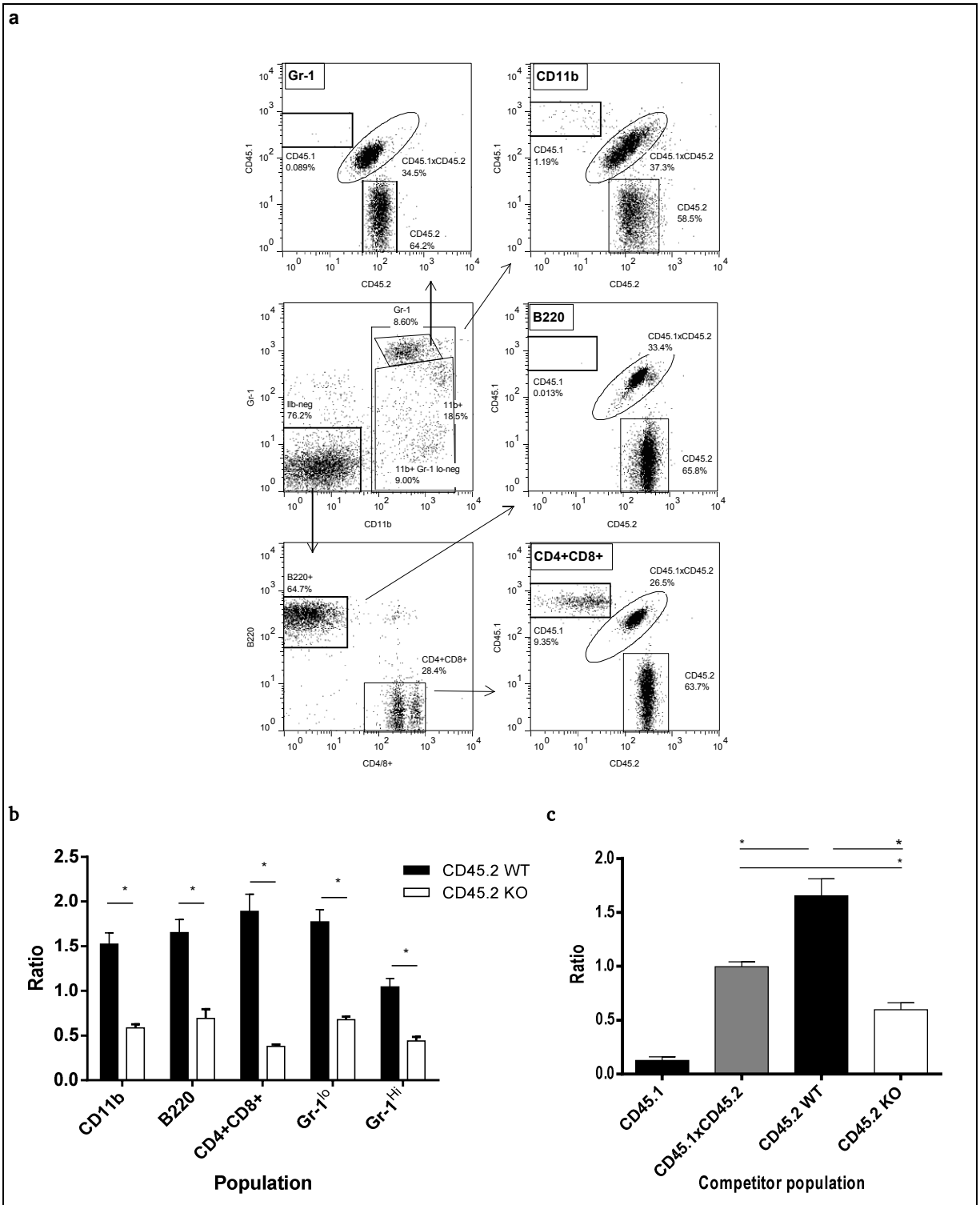

Figure 4.28 Analysis of blood leukocyte populations examined in mixed bone marrow competitive chimeras. Representative gating, (a). Live cells were gated for CD11b, Gr-1, B220, CD4/CD8 and then subgated for CD45.1 and CD45.2 expression. (b) CD45.1xCD45.2^{+} cells were assigned a ratio of 1 (i.e. 100%) within each mouse, and the proportion of CD45.2 cells (WT or KO) were computed. Shown are the relative contributions of CD45.2 WT or KO to CD45.1xCD45.2 competitors for each of the main blood leukocyte populations. (c) Competitor proportions (CD45.2 WT or KO) relative to CD45.1xCD45.2, averaged over 5 WT or 4KO samples.

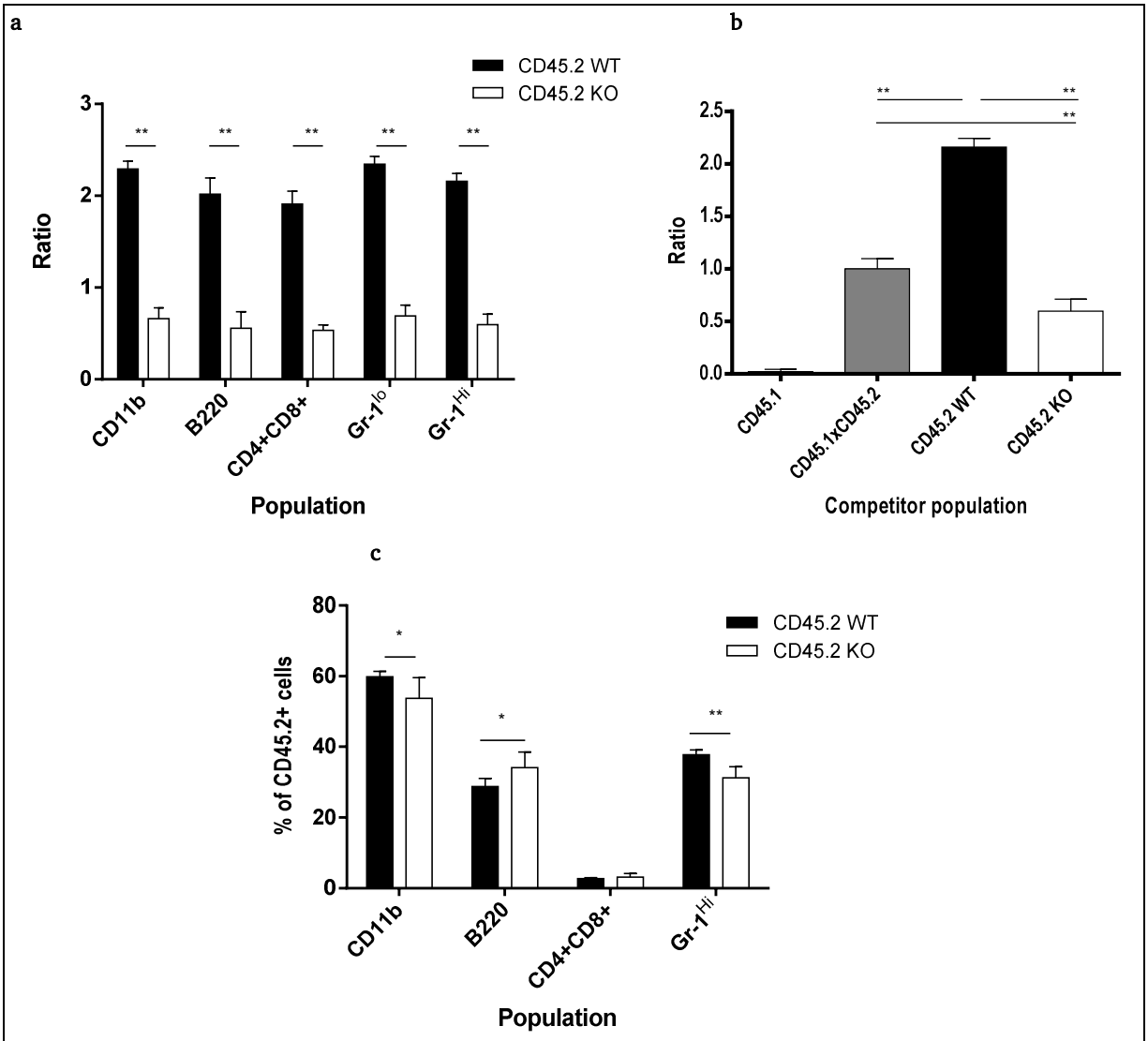

Figure 4.29 Analysis of bone marrow leukocyte populations examined in mixed bone marrow competitive chimeras. (a) Relative contributions of CD45.2 leukocyte populations compared to CD45.1xCD45.2 population in the bone marrow. (b) Overall CD45.2 contributions within the bone marrow relative to CD45.1xCD45.2. c) Proportions of principle bone marrow populations. n=5 per group

Figure 4.29 shows the results from the bone marrow analysis, which largely mirror those of the blood. **Figure 4.29c** shows that myeloid and neutrophil proportions of all cells in the CD45.2 DARC KO group (including CD45.1xCD45.2 as well as CD45.2 DARC KO) were relatively reduced, with a compensatory increase in $B220^{+}$ cells, a finding different to that seen in DARC KO or FYB(ES)TG,

Within the spleen (**Figure 4.30**) results were similar to those of the bone marrow, although the differences between CD45.2 WT and CD45.2 DARC KO were less pronounced. There was no significant difference in overall cellular proportions between the groups.

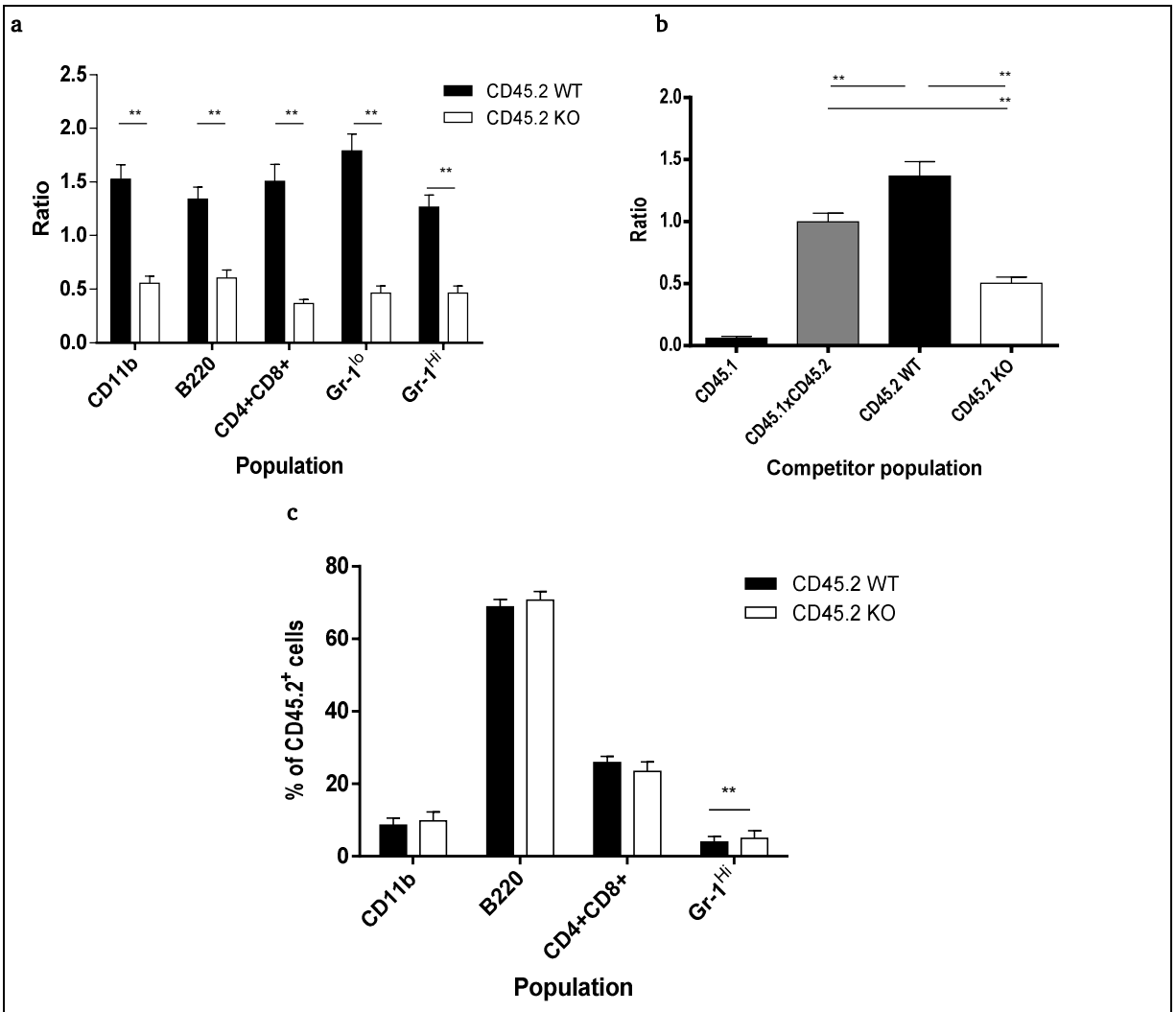

Figure 4.30 Analysis of spleen leukocyte populations examined in mixed bone marrow competitive chimeras. a) Relative contributions of CD45.2 compared to CD45.1xCD45.2 in the spleen. b) Overall CD45.2 contributions within the spleen relative to CD45.1xCD45.2. c) Proportions of principle spleen populations. n=5 per group.

Of interest, in-vivo introduction of the DARC KO haematopoietic stem cells and progenitors in a DARC replete system did not lead to normalisation of the myeloid progenitor profile, with a relative reduction in GMP cells in the DARC KO CD45.2 (**Figure 4.31**) and increase in CMP cells.

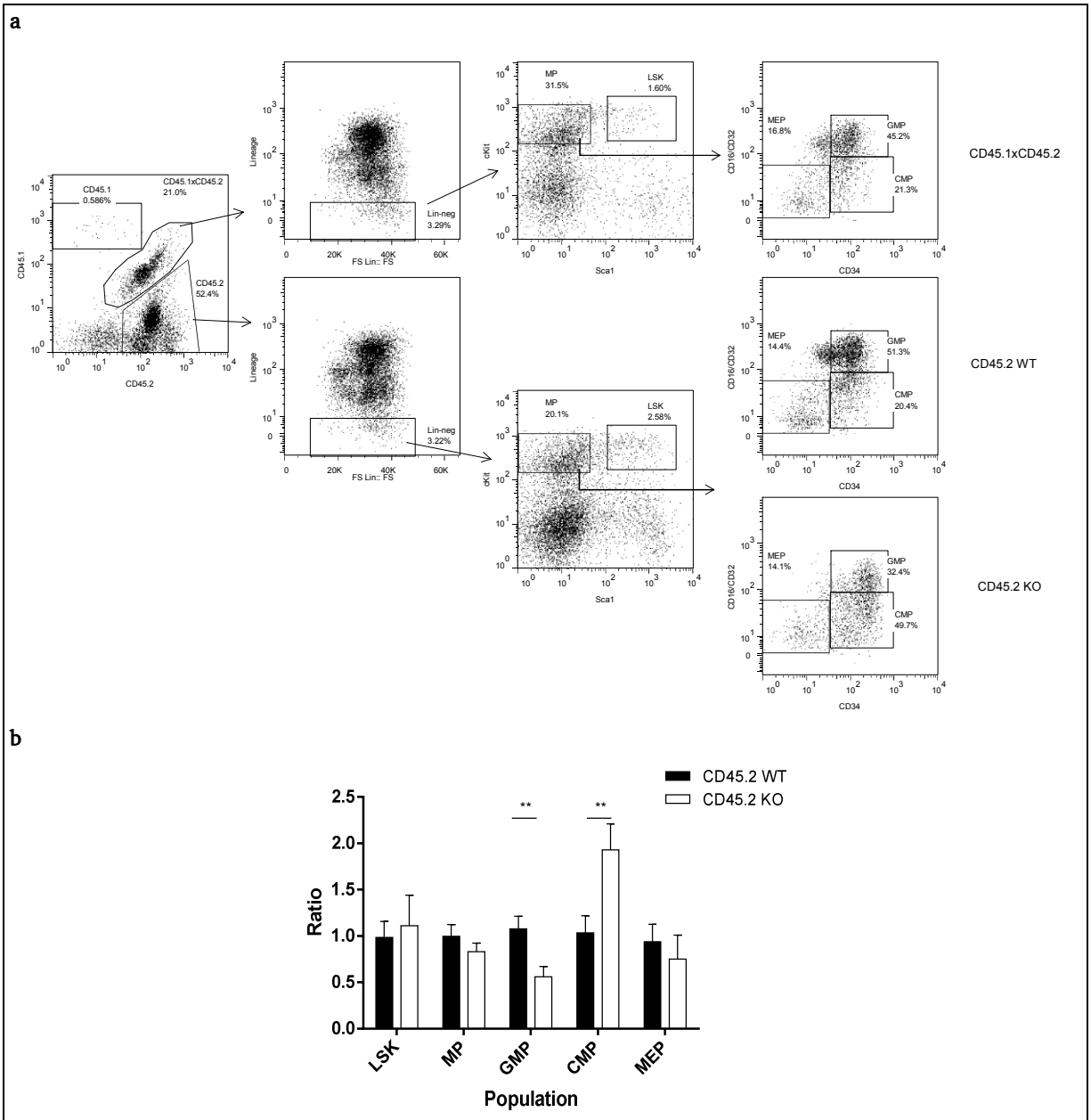

Figure 4.31 Bone marrow lineage$^-$negative populations examined in mixed bone marrow competitive chimeras, representative gating (a). Live cells were gated for CD45 expression, and then haematopoietic lineage$^-$negativity. There after subgates examining myeloid progenitors and their sub$^-$populations (GMP: CD34$^+$, CD16/CD32$^+$, CMP CD34$^+$, CD16/CD32 ^{low}, MEP CD34$^-$ CD16/CD32$^-$). b) CD45.1xCD45.2$^+$ cells were assigned a ratio of 1 (i.e. 100%) within each mouse, and the proportion of CD45.2 cells (WT or KO) were computed. Shown are the relative contributions of CD45.2 WT or KO to CD45.1xCD45.2 competitors for each of the main progenitor populations, (b). n=5 per group.

No statistically significant difference was noted in the ratio between CD45.2 WT and CD45.2 KO LSK cells. However, within this population, the CD45.2 DARC KO retained the original phenotype, demonstrating a reduction in MPP cells in absolute terms,

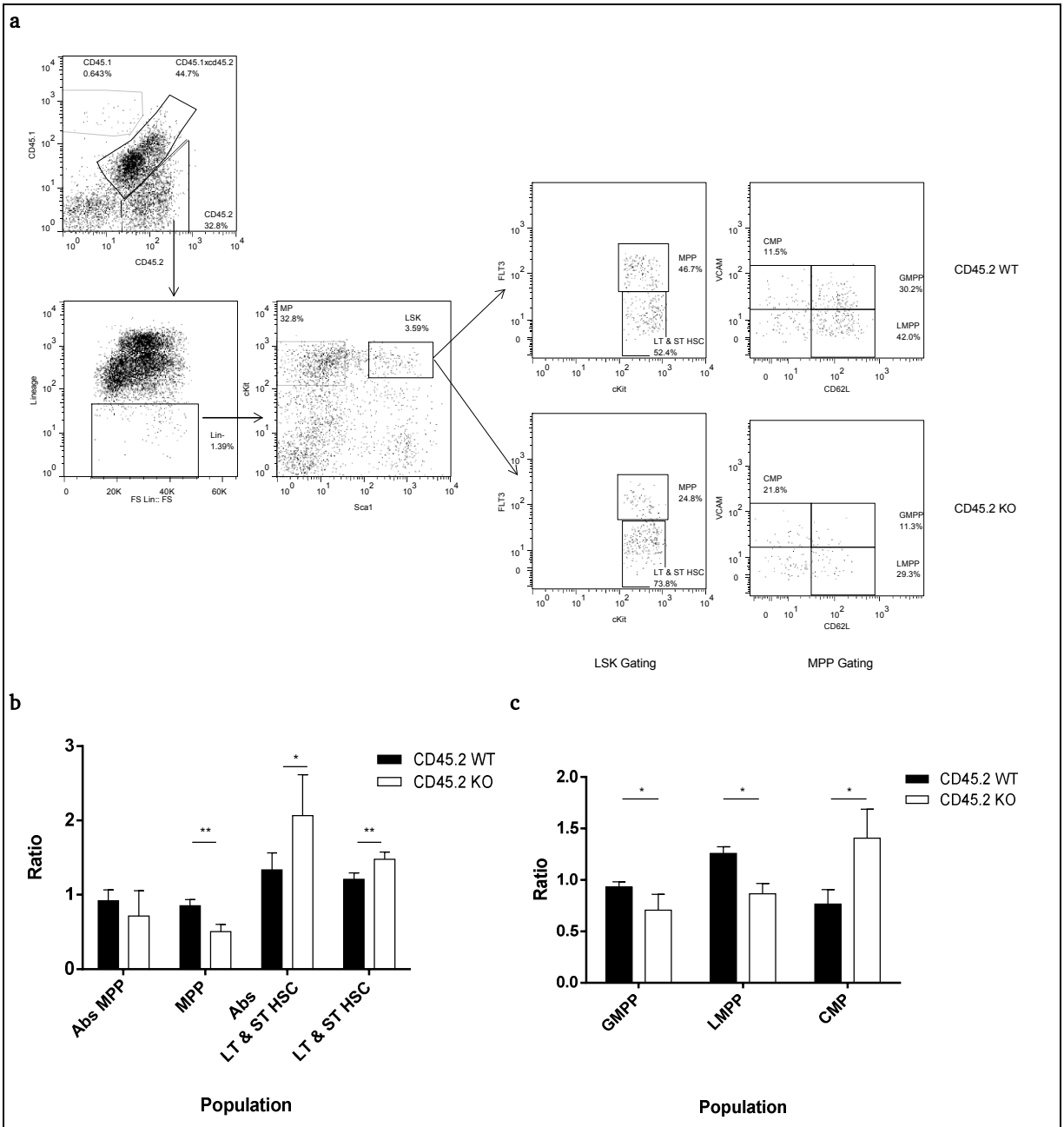

Figure 4.32 Bone marrow LSK sub-populations examined in mixed bone marrow competitive chimeras, representative gating (a). Live cells were gated for CD45 expression, and then haematopoietic lineage-negativity. There after subgates examining LSK compartment (cKit^{+}, Sca1^{+}) and the sub-populations (MPP: cKit^{+} FLT3^{Hi}, LT & ST HSC, cKit^{+} FLT3$^{-/low}$, GMPP VCAM^{+} CD62L^{+}, LMPP VCAM^{-} CD62L^{+}, CMP VCAM^{+} CD62L^{-}). (b) CD45.1xCD45.2+ cells were assigned a ratio of 1 within each mouse, and the proportion of CD45.2 cells (WT or KO) were computed. Shown are the relative contributions of CD45.2 WT or KO to CD45.1xCD45.2 competitors for each of the main HSPC populations. (c) Ratios of the MPP subpopulations. n=5 per group.

with a corresponding increase in LT + ST HSC in both absolute and relative terms (**Figure 4.32b**). The MPP population was similarly reduced due to the reduction in GMPP and increase in LMPP and CMP-progenitors (**Figure 4.32c**).

4.3.7 LSK-selected mixed competitive chimeras

Mixed chimera experiments confirmed that DARC KO bone marrow is less proliferative than wild-type bone marrow from the same murine strain. In addition, in vivo incubation of transferred bone marrow failed to normalise the reduced GMP and MPP profile in the CD45.2 DARC KO fraction. This may have been as a result of the reduced numbers of LSK cells and presence of relatively more mature progenitors, and insufficient time permitted for full engraftment of transplanted bone marrow. Therefore it was conceived that FACS sorted LSK cells, either CD45.2 WT or CD45.2 DARC KO would be injected into irradiated hosts with competitor cells so as to examine whether equal number of LSK cells injected and longer periods of maturation of LSK cells (LT-HSC, ST-HSC and MPP) in a DARC replete bone marrow environment would alter the maturation profile of the DARC KO bone marrow.

Figure 4.33a details general experimental procedure: CD45.1 BoyJ irradiated (2 x 4.5 Gy) hosts were injected with 500 FACS sorted LSK cells, either CD45.2 WT (animals designated WT-WT) or CD45.2KO (designated WT-KO), n=5 per group, with 10^6 competitor CD45.1xCD45.2 cells. Examining peripheral blood proportions by tail bleed revealed CD45.2 DARC KO had a higher proliferative rate compared to CD45.2 WT, on average. Blood was sampled by tail bleed at 28 and 56 days, and the animals were culled at 16 weeks post transfer.

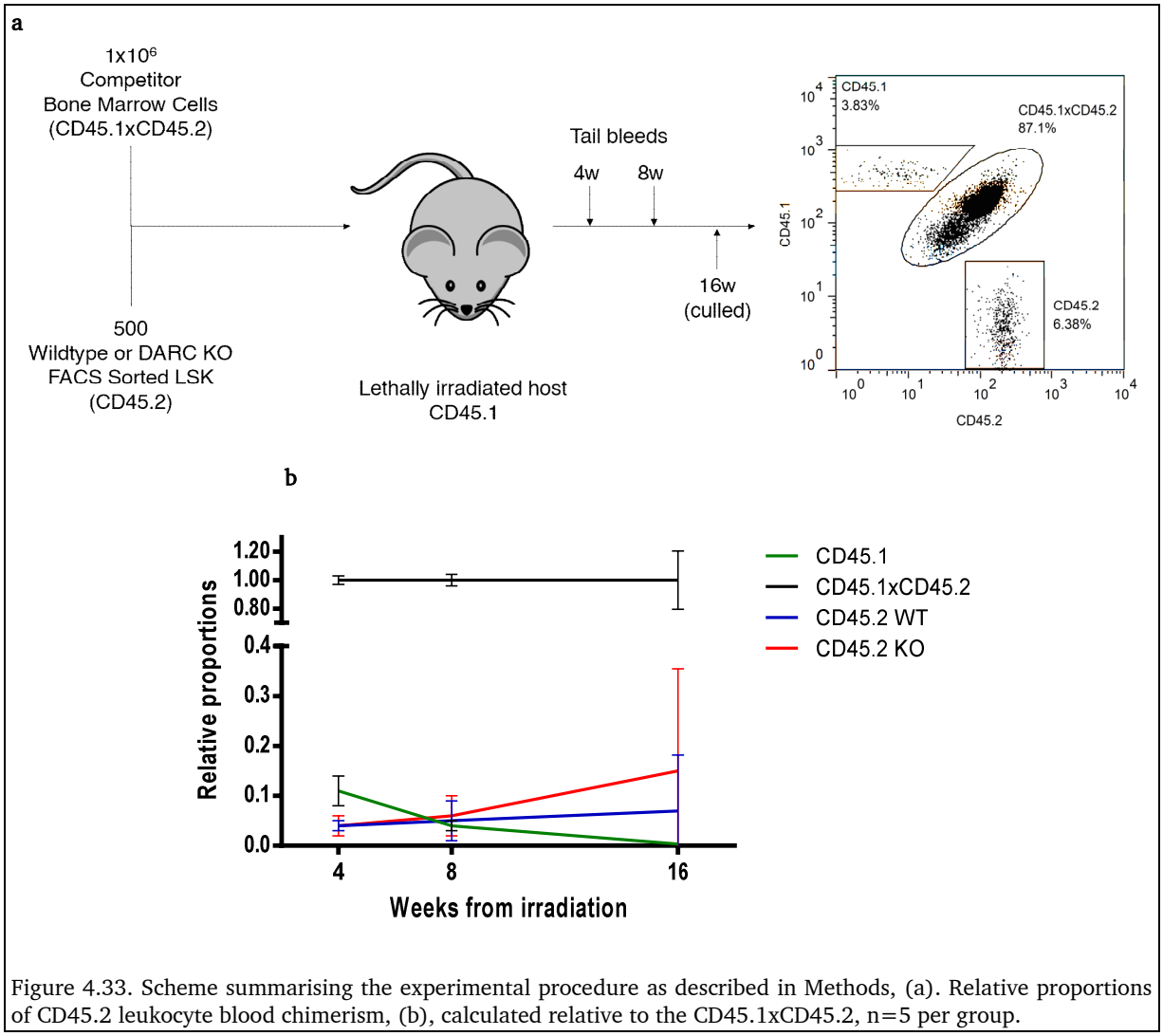

Figure 4.33. Scheme summarising the experimental procedure as described in Methods, (a). Relative proportions of CD45.2 leukocyte blood chimerism, (b), calculated relative to the CD45.1xCD45.2, n=5 per group.

The fundamental parameters of the chimeric mice were examined, and the blood leukocyte, bone marrow leukocyte and bone marrow HSPC populations were analysed. However substantial variation in WT and DARC KO CD45.2 population chimerism was noted (between <5 and 30%), for reasons that are not clear but may represent uneven mixing pre-injection, or clumping of LSK cells. The results of these analyses are contained in Chapter 6 Appendix, the reader is referred to Appendix section "7.8 LSK-selected mixed competitive chimeras".

Blood leukocyte proportions between CD45.2 WT and CD45.2 KO relative to CD45.1xCD45.2 competitor were not significantly different (**Figure 4.34a**) but in bone marrow there was an increased proportion of CD45.2 KO leukocytes. This would suggest that in the presence of a wholly DARC replete bone marrow environment, DARC KO LSK cells may receive sufficient cytokine signals to undergo increased proliferation. More likely however, similar to the *in vitro* colony assays, there may be more immature cells (LT-HSC and ST-HSC) contained in the DARC KO LSK population and these cells may subsequently lead to a greater output of mature cells. To clarify this further, future experiments could be undertaken using FACS sorted LT-HSC from WT and DARC KO, so that differences in LSK sub-populations between these mouse strains may be controlled for. In addition, FACS sorted MPP cells could be used instead of LSK to examine the progenitors produced by these cells and determine the exact contributions to mature bone marrow cell population by equal numbers of WT or DARC KO MPP cells.

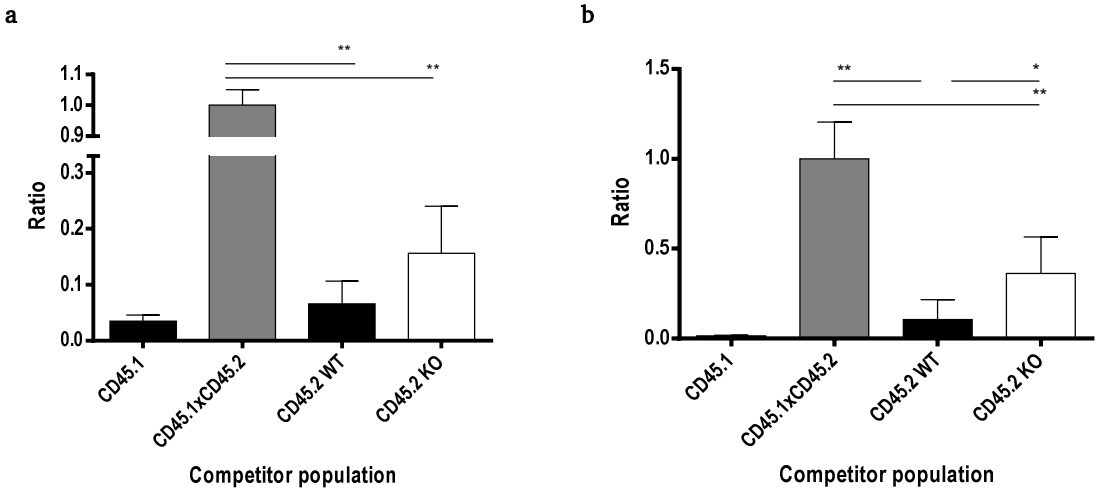

Figure 4.34 Analysis of blood and bone marrow leukocyte populations of mixed LSK-selected competitive chimeras. a) Blood leukocyte competitor proportions (CD45.2 WT or KO) relative to CD45.1xCD45.2, averaged over 5 CD45.2 WT or 4 CD45.2 KO samples. b) Bone marrow competitor proportions (CD45.2 WT or KO) relative to CD45.1xCD45.2, averaged over 5 CD45.2 WT or 4 CD45.2 KO samples.

4.3.8 Comparison of the morphological appearance of cryosectioned bone marrow in WT, DARC KO and FYB(ES)TG mice

In DARC KO and FYB(ES)TG mice, the relative proportions of bone marrow subsets are skewed towards myeloid differentiation. This may be reflected, in part, in changes in the localisation of developing myeloid cells, with reference to other cells and other myeloid cells. Therefore the distribution of maturing erythroid and myeloid cells might be altered in DARC KO and/or FYB(ES)TG mice in comparison to WT mice. Cryosections of paraformaldehyde fixed WT, DARC KO and FYB(ES)TG femora were used to examine the distribution of erythroid and myeloid cells in the bone marrow of these mice.

As can be seen in **Figure 4.35**, in sections from DARC KO and FYB(ES)TG bone marrows, there was an increase in the area of CD11b-positive immunofluorescence, with myeloid cells forming larger aggregates whereas erythroid cells were not significantly altered in comparison to their WT counterparts (**Figure 4.36**). In WT bone marrow, myeloid clusters contained a mean of 3.01 myeloid cells (2.38-3.66) in contrast to DARC KO bone marrow 6.38 (5-9.169) cells and FYB(ES)TG bone marrow 9.61 (5.89-12.74) cells. Thus it is possible that the absence of erythroid DARC affects the re-distribution of maturing myeloid cells, and may lead to their accumulation by altering the threshold for neutrophil release.

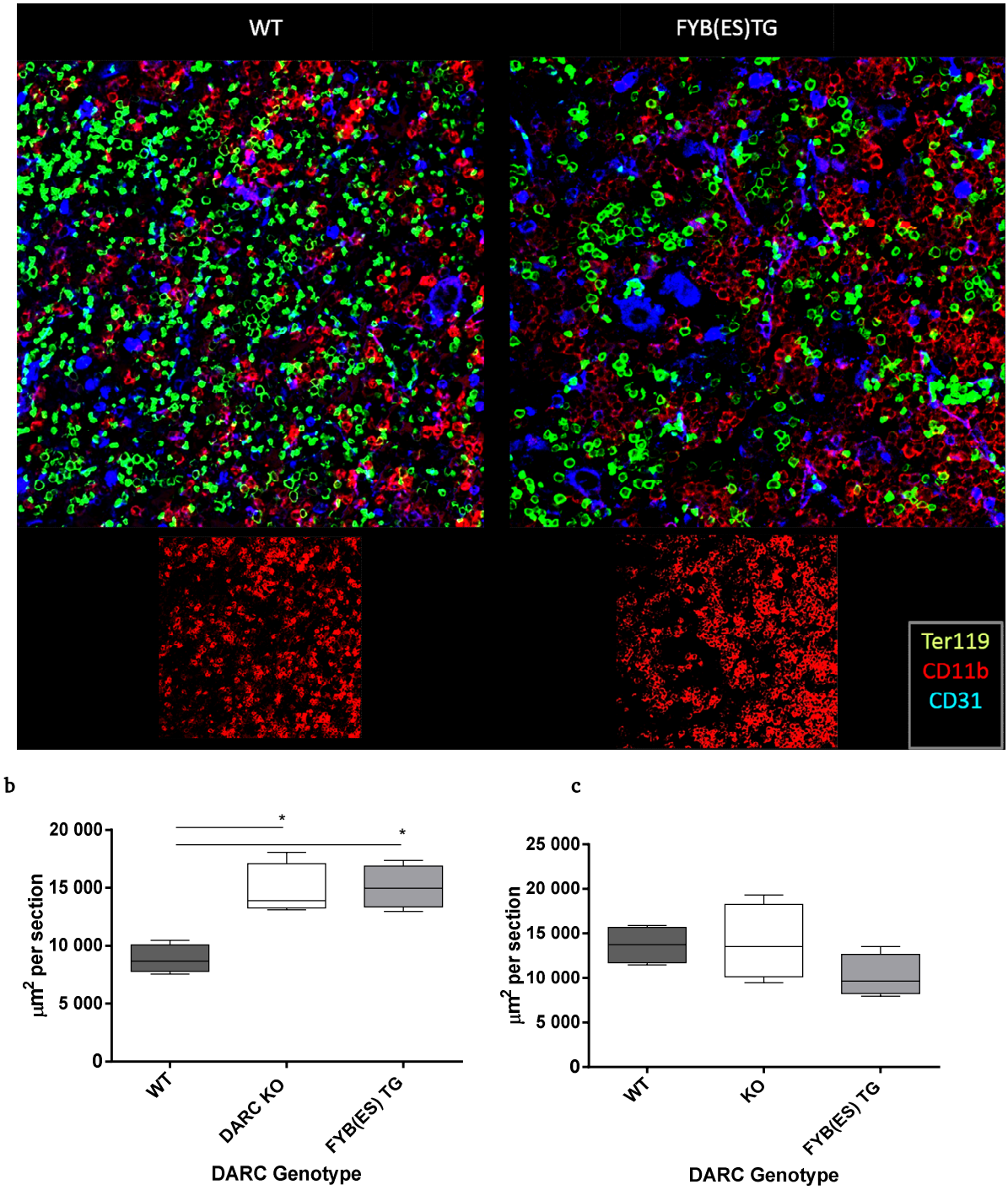

Figure 4.35 Representative immunofluorescent images of femur sections, highlighting Ter119, CD11b and CD31 positive cells, from wild-type and FYB(ES)TG mice, (a). The absolute area of positive staining for myeloid (b) and erythroid (c) cells was calculated from four representative areas of the femur sections. Images captured at 25x magnification.

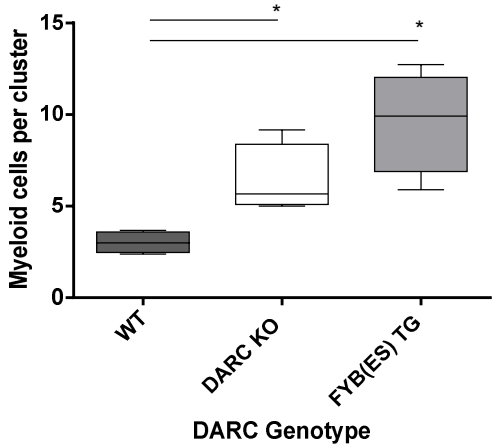

Figure 4.36 Analysis of myeloid cell clustering. Myeloid clustering was analysed by designating cell groupings as a myeloid cluster where cells were considered to be in a cluster if they were within a cell-width (ca. 10μm) of each other, and at least half of the nucleus was surrounded by red-stained ($CD11b^+$) cytoplasm.

4.3.9 Chemokine binding by DARC expressed on bone marrow erythroblasts

Whilst the role of DARC on the mature erythrocyte in the peripheral circulation has been suggested to be a chemokine sink, helping to buffer chemokine levels and potentially maintain cognate receptor sensitivity, the role if any of erythroid DARC in the bone marrow has remained completely obscure. ^{125}I-CCL5 was used to examine the chemokine binding of DARC on erythroblasts, and the contribution of DARC to chemokine levels in the bone marrow supernatants. A MDCK cell line expressing the atypical chemokine receptor D6 (ACKR2) which internalises chemokines and degrades them was used as a control.

Figure 4.37 and **Figure 4.38** show that DARC maintains higher levels of ^{125}I-CCL5 on erythroblast cell surface as well as in bone marrow supernatants, when DARC is present. There was no difference in the non-precipitable (degraded) chemokine

between the WT and DARC KO samples, across all three compartments studied (data not shown).

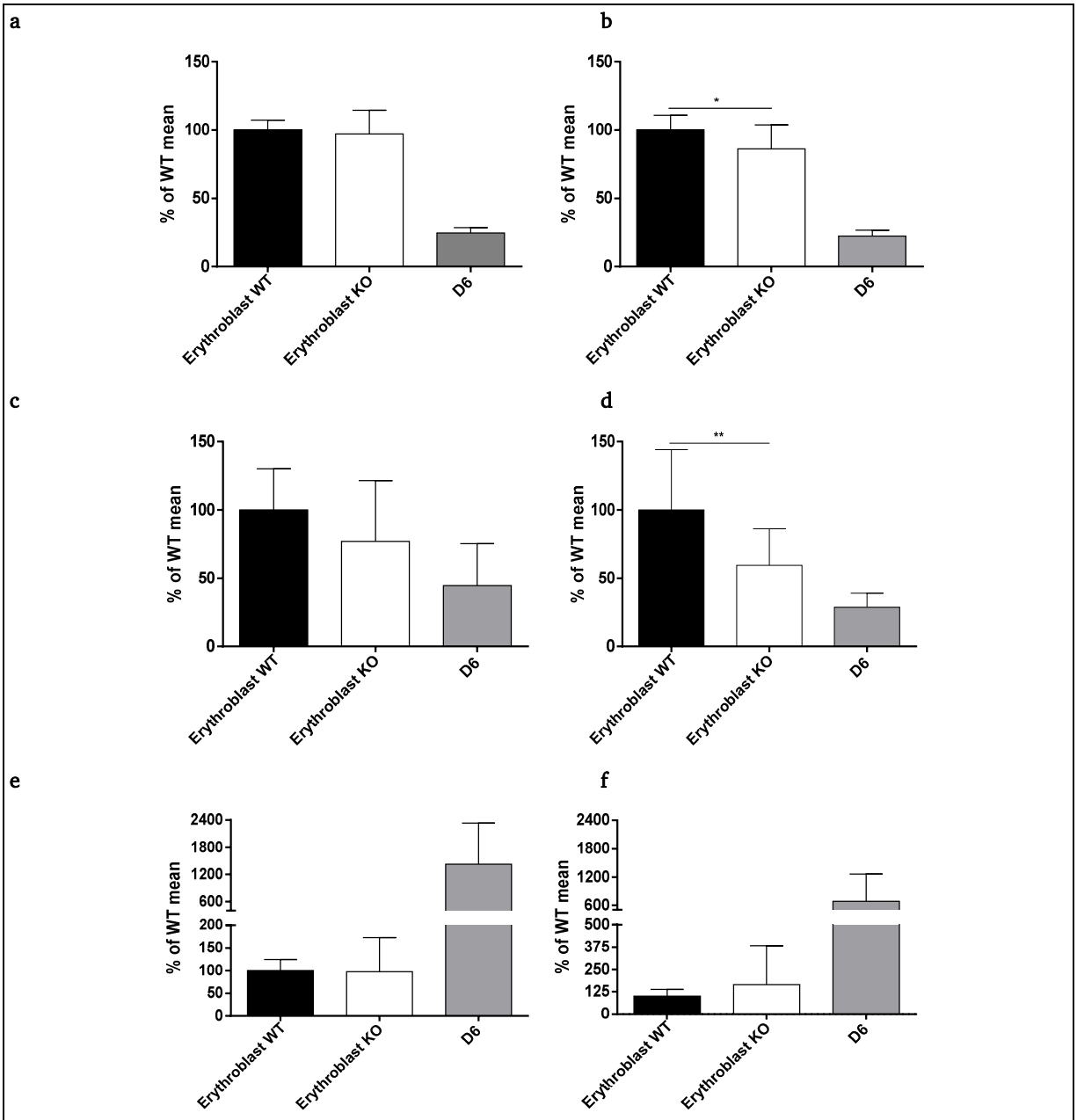

Figure 4.37 Representative graphs of ^{125}I-CCL5 binding assays. Following 3 hours of incubation there was no significant difference between WT and DARC KO erythroblast in the counts per minute (CPM) obtained in the supernatant (a) p= 0.98 (c), and intracellularly (e). Following 18 hours incubation, there was significantly more radiolabelled chemokine detectable in the wild-type supernatant (b) and cell surface (d), with no significant difference in the intracellular compartment (f). Analysis undertaken by combining 5 independent experiments, and calculating counts of KO relative to WT mean (WT=100%). Mann-Whitney test used to determine whether means significantly different. In some experiments WT and DARC KO whole bone marrow was studied in parallel, with similar results obtained to the erythroblast samples at 18 hour incubation; however the results were not significantly different.

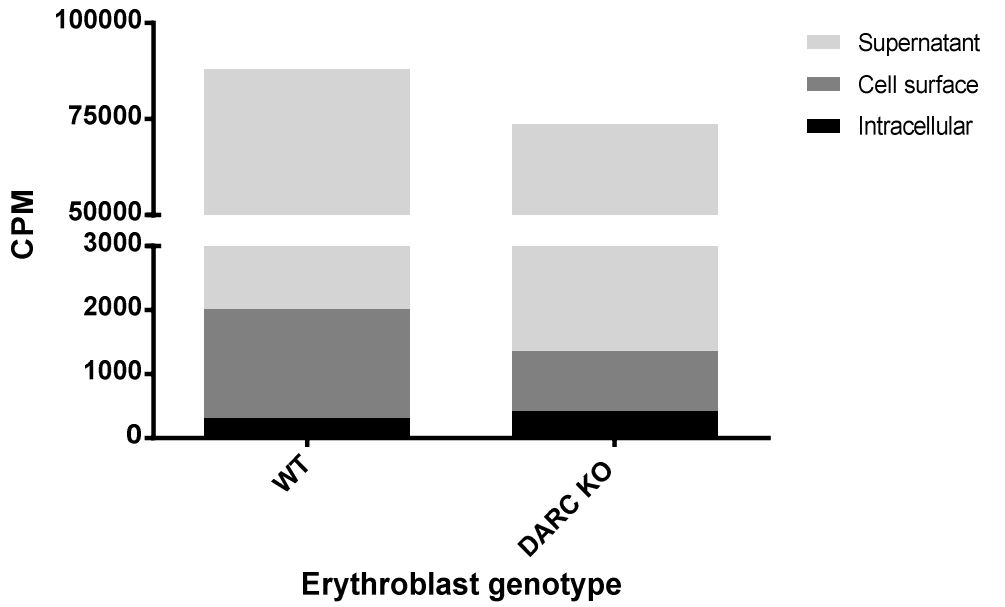

Figure 4.38 Combined mean CPM values for fractions assayed (supernatant, cell surface, intracellular) at the 18 hour time point from 5 independent experiments.

4.3.10 Microarray

Alterations in the maturation profile of HSC and progenitor cells as seen in the absence of erythroid DARC may occur in response to variations in the bone marrow micro-environment as a result of signalling pathway changes, potentially mediated by gene expression. An efficient method to screen for possibly hundreds of affected genes is the use of microarray technology, where differences in expression across thousands of genes can be determined.

GMP or LSK were FACS sorted (representative gating **Figure 4.39**) from either DARC KO or WT mice, and after RNA extraction gene expression changes were examined on an Agilent 8 spot chip. The on-line resource Immgen (http://www.immgen.org) was utilised to confirm normal gene expression patterns. The full list of results is presented in Appendix 7.2 (for LSK cells) and 7.3 (for GMP cells).

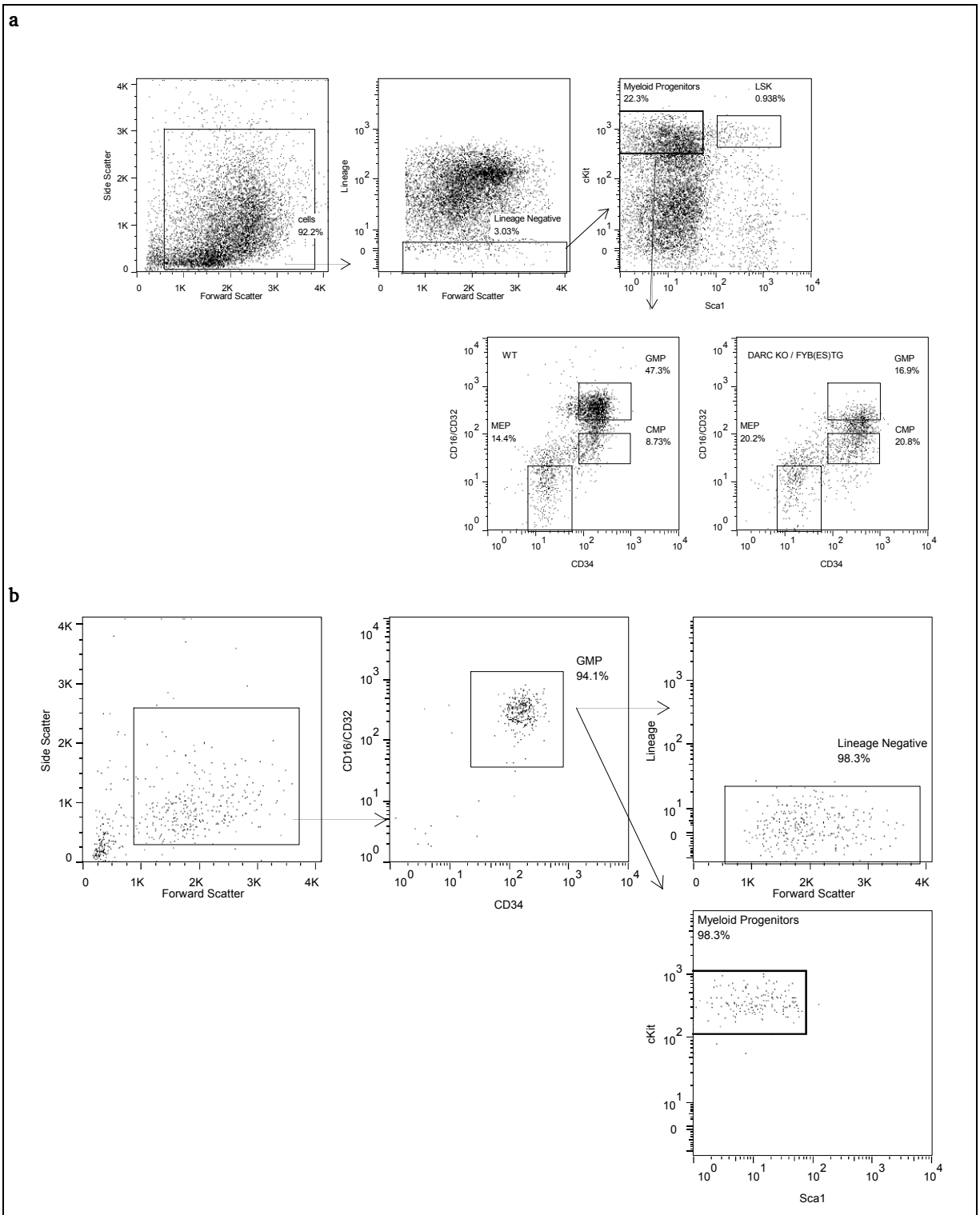

Figure 4.39 (a) Representative gating for FACS sorting strategy used for microarray experiment. Approximate purity, 94% (b).

4.3.10.1 LSK

Upregulated Genes

The most upregulated genes (**Table 4.1**) in the LSK cells of DARC KO mice were mainly genes expressed in maturing neutrophils and monocytes (*NGP, LTF, CAMP, S100A8, MMP8, CHI3L3, S100A9, IFITM6*), with minor expression of some genes typically found in erythroid precursors. *ALAS2* is an important gene in erythroid aminolevulinic acid synthesis, and *RETNLG* is highly expressed in maturing and mature granulocytes, as well as in adipose tissue.

In summary, genes typically expressed in maturing granulocytic populations were significantly upregulated in LSK cells of DARC KO mice.

Name	Symbol	Fold-change
neutrophilic granule protein	*NGP*	656.09
resistin like gamma	*RETNLG*	509.74
Lactotransferrin	*LTF*	418.15
cathelicidin antimicrobial peptide	*CAMP*	462.38
S100 calcium binding protein A8 (calgranulin A)	*S100A8*	351.33
matrix metallopeptidase 8	*MMP8*	210.62
chitinase 3-like 3	*CHI3L3*	176.46
aminolevulinic acid synthase 2, erythroid	*ALAS2*	182.53
S100 calcium binding protein A9 (calgranulin B)	*S100A9*	200.48
interferon induced transmembrane protein 6	*IFITM6*	131.22

Table 4.1 Ten most upregulated significant genes from microarray study for sorted LSK cells. Genes that were significantly more than 3-fold up or down regulated were selected for analysis (See appendix for full list of genes), $p<0.01$.

Down-regulated genes

Table 4.2 shows the ten most down regulated genes.

Name	Symbol	Fold-change
RNA component of mitochondrial RNAase P	*RMRP*	-11.7603
glutaredoxin 2 (thioltransferase)	*GLRX2*	-8.66415
histone cluster 1, H4d	*HIST1H4D*	-6.72826
histone cluster 1, H2ak	*HIST1H2AK*	-6.60662
ATP synthase F0 subunit 6	*ATP6*	-6.24427
histone cluster 1, H4c	*HIST1H4C*	-6.20175
histone cluster 1, H4j	*HIST1H4J*	-6.01895
histone cluster 1, H4k	*HIST1H4K*	-5.7852
phosphohistidine phosphatase 1	*PHPT1*	-4.50187
forkhead box D4	*FOXD4*	-3.72675

Table 4.2 Ten most downregulated significant genes from microarray study for sorted LSK cells. Genes that were significantly more than 3-fold up or down regulated were selected for analysis (See appendix for full list of genes), $p<0.01$.

Candidate transcription factors in LSK cells

Candidate transcription factors which might be involved in regulation of significant genes were determined utilising the on-line DiRE: Identification of Distant Regulatory. Elements of gene expression resource (http://dire.dcode.org) from (Gotea and Ovcharenko, 2008). C/EBPβ scores highest in importance in this analysis, highlighting the pro-granulocytic gene expression profile in DARC KO LSK cells as suggested by the most highly expressed genes from the microarray study.

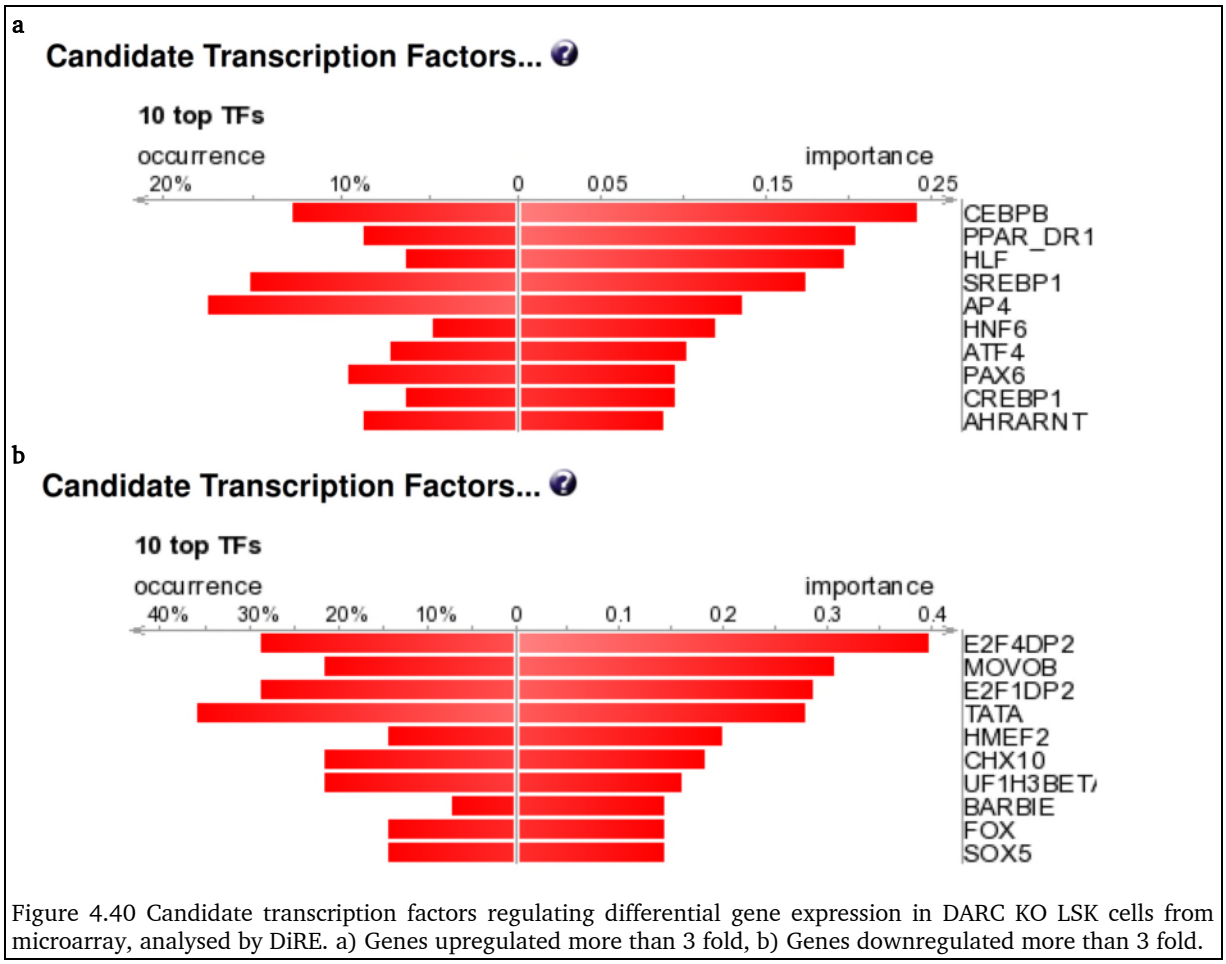

Figure 4.40 Candidate transcription factors regulating differential gene expression in DARC KO LSK cells from microarray, analysed by DiRE. a) Genes upregulated more than 3 fold, b) Genes downregulated more than 3 fold.

4.3.10.2 GMP

Upregulated Genes

The most upregulated genes in the GMP cells of DARC KO as compared to their WT counterparts were those normally expressed in lineage committed maturing erythroid progenitors and granulocytic precursors, in **Table 4.3**.

Of note, increased expression of one of these genes, *IFI202*, in HSC was shown to reduce the proliferation of myeloid cells and reduce the ability of constitutively *IFI202* expressing HSC to reconstitute irradiated mice (Ludlow *et al.*, 2008).

Name	Symbol	Fold-change
cathelicidin antimicrobial peptide	*CAMP*	1299.918
hemoglobin, beta adult major chain	*HBB-B1*	457.9743
S100 calcium binding protein A9 (calgranulin B)	*S100A9*	413.8867
resistin like gamma	*RETNLG*	285.2716
lactotransferrin	*LTF*	152.3321
neutrophilic granule protein	*NGP*	170.9426
hemoglobin alpha, adult chain 2	*HBA-A2*	181.9238
hemoglobin alpha, adult chain 1	*HBA-A1*	147.5344
hemoglobin, beta adult minor chain	*HBB-B2*	145.3437
interferon activated gene 202B	*IFI202B*	131.2353

Table 4.3 Ten most upregulated significant genes from microarray study for sorted GMP cells. Genes that were significantly more than 3-fold up or down regulated were selected for analysis (See appendix for full list of genes), $p<0.01$.

Down-regulated genes

Table 4.4 shows the ten most down regulated genes in GMP cells of DARC KO mice as compared to their WT counterparts.

Name	Symbol	Fold-change
IQ motif and Sec7 domain 3	*IQSEC3*	0.037595
dual specificity phosphatase 23	*DUSP23*	0.167913
keratin associated protein 5-4	*KRTAP5-4*	0.179302
apolipoprotein A-II	*APOA2*	0.220669
TOX high mobility group box family member 4	*TOX4*	0.251398
phosphoinositide-3-kinase interacting protein 1	*PIK3IP1*	0.2718
pleckstrin homology domain containing, family J member 1	*PLEKHJ1*	0.282339
integrin alpha 5 (fibronectin receptor alpha)	*ITGA5*	0.291348
tensin 4	*TNS4*	0.297402
v-maf musculoaponeurotic fibrosarcoma oncogene family, protein F (avian)	*MAFF*	0.299066

Table 4.4 Ten most downregulated significant genes from microarray study for sorted GMP cells. Genes that were significantly more than 3-fold up or down regulated were selected for analysis (See appendix for full list of genes), $p<0.01$.

Candidate transcription factors in GMP cells

Likely transcription factors were determined using DiRE, and results were as per **Figure 4.41**. Notably the C/EBP family of transcription factors is the most likely candidate for the up-regulation of genes in GMP of DARC KO mice, in similarity to LSK cells.

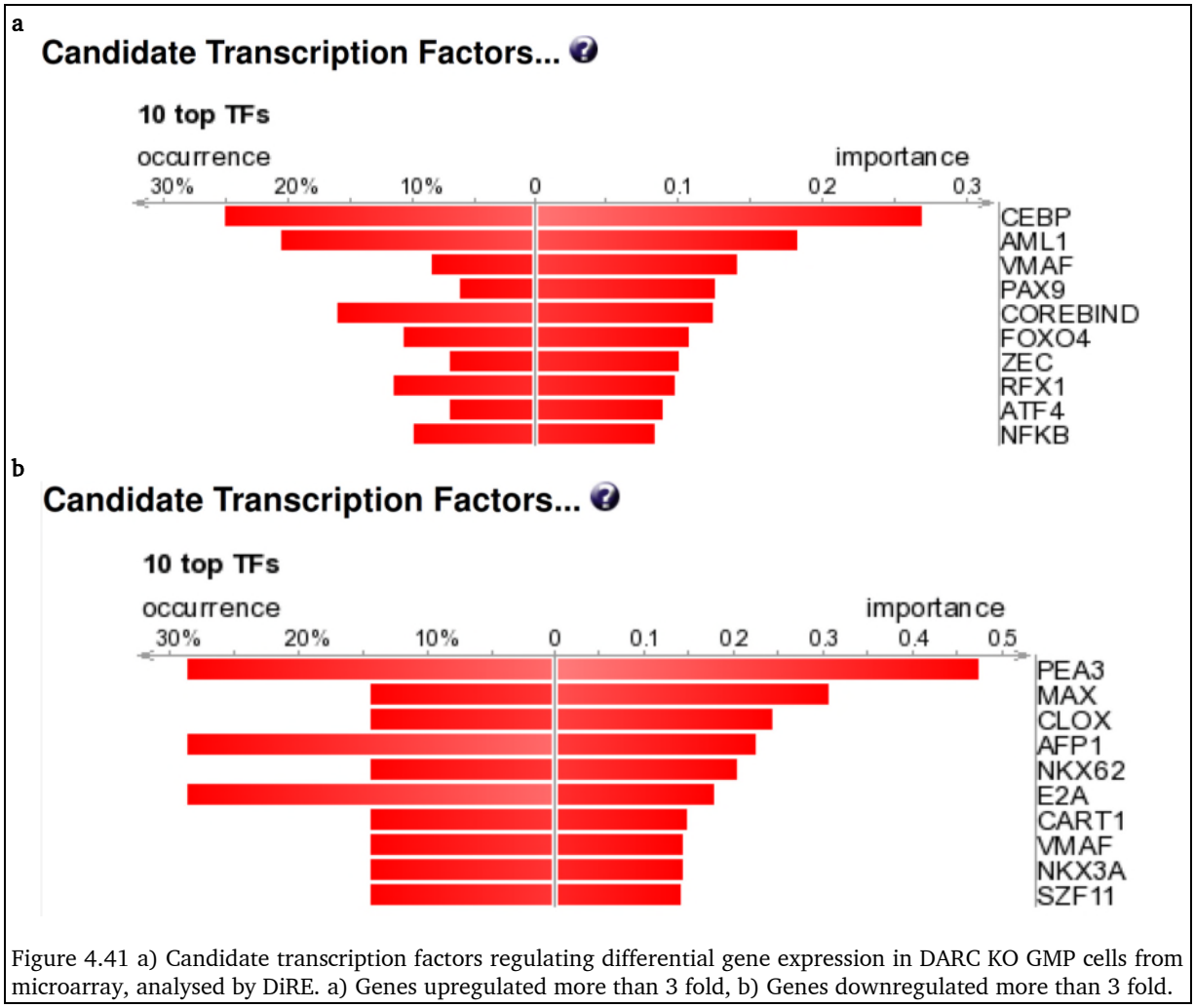

Figure 4.41 a) Candidate transcription factors regulating differential gene expression in DARC KO GMP cells from microarray, analysed by DiRE. a) Genes upregulated more than 3 fold, b) Genes downregulated more than 3 fold.

4.3.11 Low density gene array

A microfluidic card was designed to analyse expression of a panel of genes which included several significant genes from the microarray experiment and housekeeping genes. In addition, genes which have critical roles in granulocyte lineage differentiation from the pre-GMP stage to the GMP stage were included, as were those whose transcribed proteins (e.g. VCAM-1) were noted to be altered in surface expression in flow cytometry experiments of LSK and sub-populations. mRNA expression was determined by real-time PCR, and the expression of each gene was calculated relative to the levels of GAPDH. Of the three housekeeping genes included (*GAPDH, HPRT* and *18S*), *GAPDH* and *HPRT* were both selected (geometric means of their expression computed) for analysis as these showed little variation in expression between samples. RNA was detectable for all genes, and gene expression was assessed using RNA which was treated with DNase.

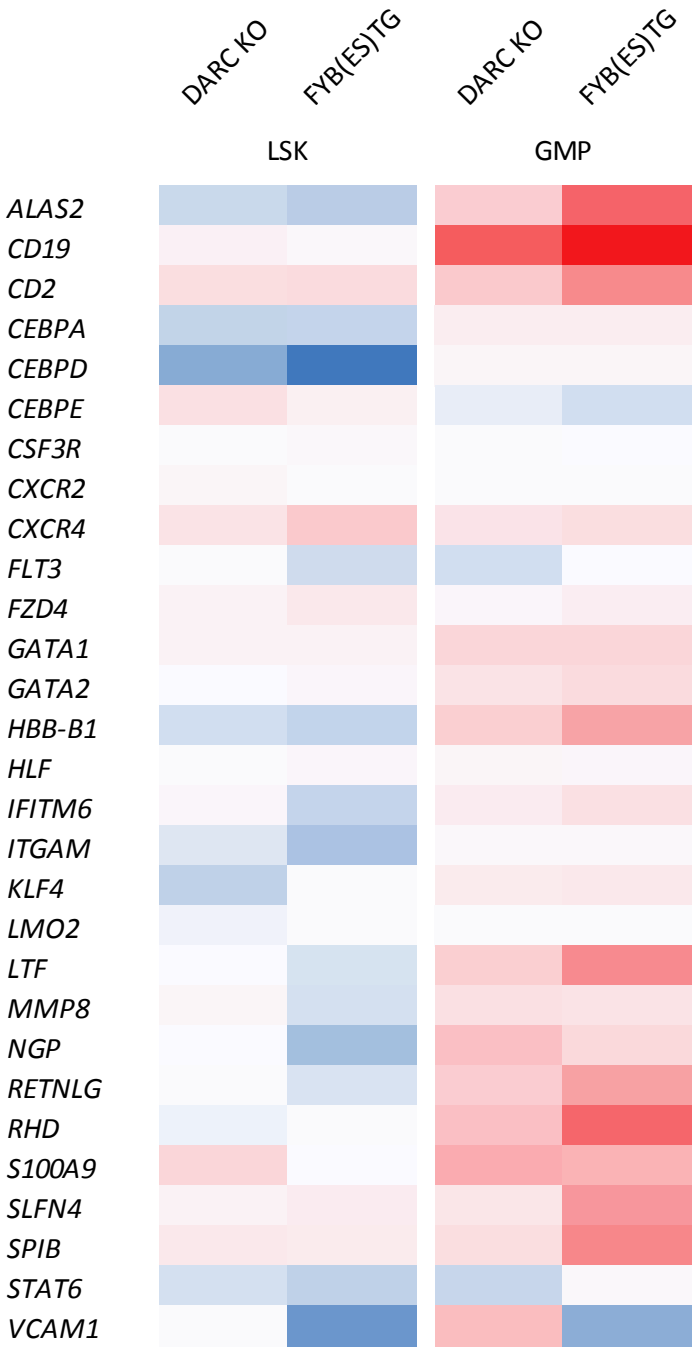

Figure 4.42 Heatmap of relative gene expression in LSK and GMP from DARC KO and FYB(ES)TG calculated from LDA results. Blue indicates reduced expression relative to WT, and red increased expression. The depth of colour correlates which intensity of gene expression change from WT mean (e.g. dark blue = strongly downregulated). Represented is the mean fold change relative to WT. LSK: WT n=5, DARC KO n=4 and FYB(ES)TG n=4; GMP: WT n=5, DARC KO n=4 and FYB(ES)TG n=3

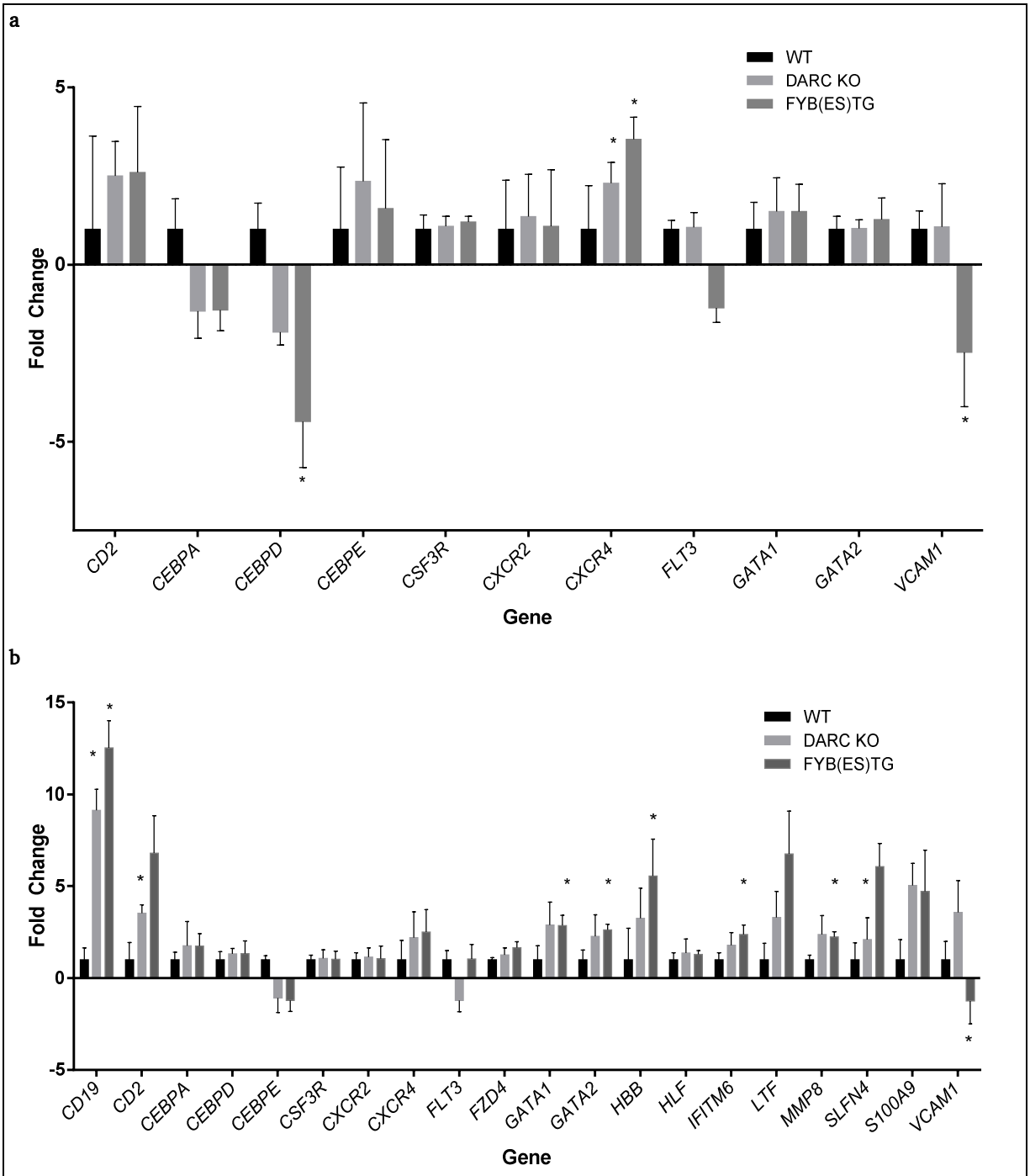

Figure 4.43 Differential expression of selected genes in LSK and GMP cells from WT, DARC KO and FYB(ES)TG mice, results from LDA: (a) selected genes from LSK analysis. WT n=5, DARC KO n=4 and FYB(ES)TG n=4 (b) selected genes from GMP analysis. Represented is the mean fold change relative to WT. WT n=5, DARC KO n=4 and FYB(ES)TG n=3. Statistical significance was calculated using Mann Whitney test, on ΔC_T values. Error bars represent the SD of ΔC_T values.

In LSK populations, CXCR4 was significantly up-regulated in FYB(ES)TG, and VCAM-1 down-regulated in FYB(ES)TG mice. Of note, flow cytometric analysis showed a reduction in VCAM-1^+ GMPP cell numbers in FYB(ES)TG mice. In addition, *CEBPD* was significantly down-regulated in FYB(ES)TG LSK. In contrast to the micro-array results, *LTF, MMP8, NGP* and *S100A9* did not differ from WT in expression.

GMP results indicated a number of differences compared to WT. Lymphoid genes appeared increased in expression by several fold in DARC KO and FYB(ES)TG GMP (*CD2, CD19*), and erythroid genes (*HBB, GATA1*) were also upregulated. Genes characteristic of maturing granulocytic precursors were upregulated (*LTF, MMP8, NGP* and *S100A9*) in GMP from both DARC KO and FYB(ES)TG mice. However genes in the C/EBP group were not differentially expressed. Interpretation of these data would suggest that the GMP have a more immature CMP-like gene expression profile, in combination with a more mature pro-granulocytic gene expression pattern. *GATA1* and *GATA2* were more expressed in FYB(ES)TG GMP cells, and the implication is unclear. Overexpression of GATA-2 leads to enforced cellular quiescence in HSC and progenitor cells with no change in apoptosis rates (Tipping *et al.*, 2009).

4.3.12 CXCR4-CXCL12 axis

Given the importance of the CXCR4-CXCL12 axis in modulating cellular released from the bone marrow, CXCL12 levels in bone marrow supernatants were examined by ELISA. These were similar between WT, DARC KO and FYB(ES)TG mice (**Figure 4.44**). In addition CXCR4 expression on mature neutrophils was not different across the three mouse strains. Therefore, the CXCR4-CXCL12 axis does not appear to play a

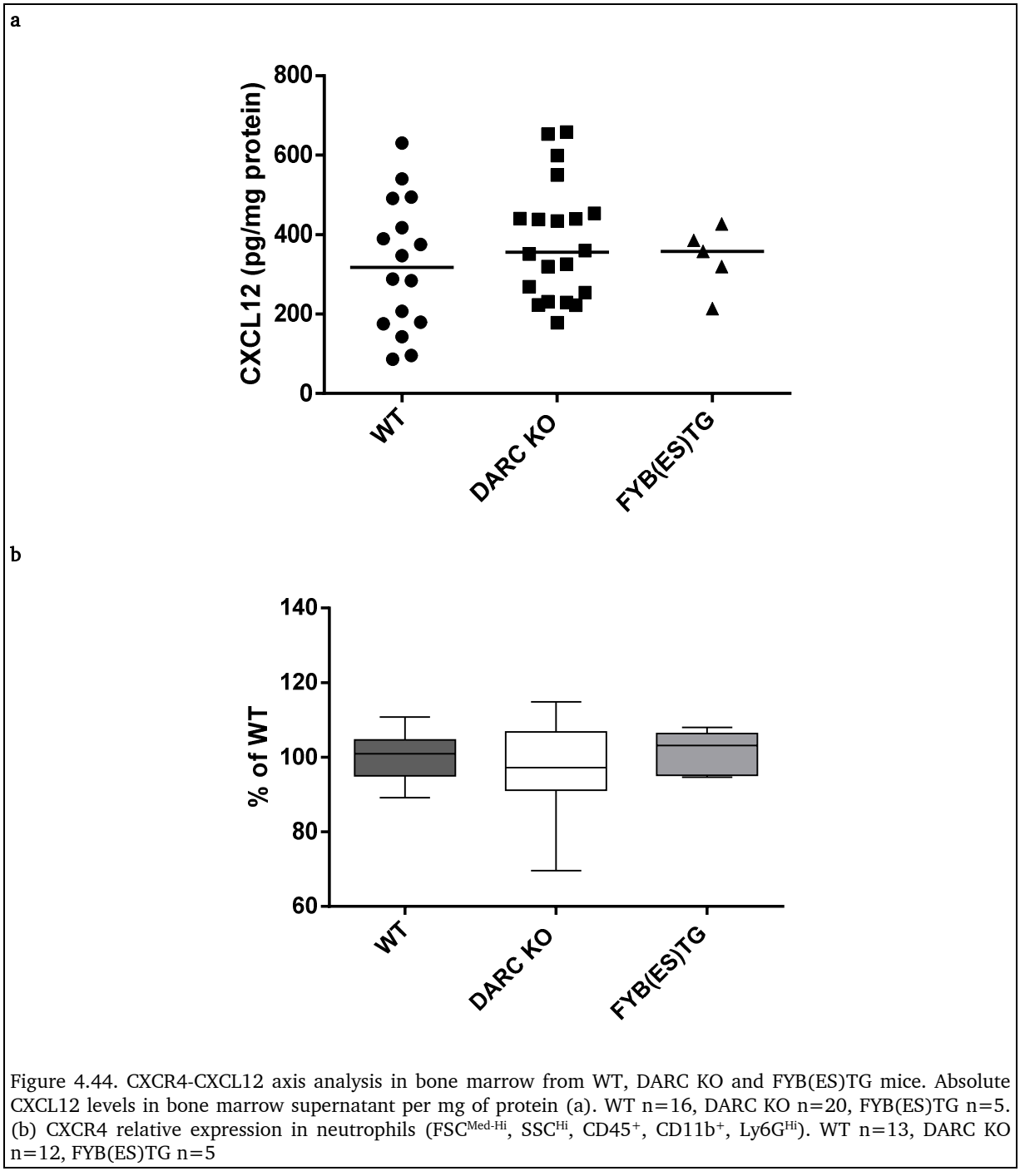

Figure 4.44. CXCR4-CXCL12 axis analysis in bone marrow from WT, DARC KO and FYB(ES)TG mice. Absolute CXCL12 levels in bone marrow supernatant per mg of protein (a). WT n=16, DARC KO n=20, FYB(ES)TG n=5. (b) CXCR4 relative expression in neutrophils (FSC^{Med-Hi}, SSC^{Hi}, $CD45^{+}$, $CD11b^{+}$, $Ly6G^{Hi}$). WT n=13, DARC KO n=12, FYB(ES)TG n=5

direct role in the increased neutrophil proportions presented in DARC KO and FYB(ES)TG mice.

4.4 Discussion

The primary aim of this work was to develop an animal model to represent the neutropaenia present in *FYB(ES)* homozygous Duffy-negative humans, and to use this model in the study of the mechanisms underpinning the neutropaenia. The FYB(ES)TG model is a humanised transgenic mouse expressing human DARC on the vascular endothelium and other locations but not erythrocytes similar to the human Duffy-negative phenotype, and exhibiting a 30-40% reduction in neutrophil counts compared to WT mice. As a control, the FYBTG mouse model was developed to establish whether the presence of erythroid human DARC in addition to endothelial human DARC would correct these changes. Accordingly, preliminary results from FYBTG mice demonstrate bone marrow and peripheral blood cell proportions and absolute counts similar to those in WT mice.

In DARC KO and FYB(ES)TG mice, increased proportions of neutrophils were found in the bone marrow, and in FYB(ES)TG was this was associated with reduced neutrophil count in the peripheral blood. The actual mechanism of the neutropaenia however is unclear. DARC KO animals have normal neutrophil counts as shown in this work and by others (Zarbock *et al.*, 2010). Preliminary results from FYBTG revealed a phenotype similar to WT mice, with normalisation of these parameters. In addition to differences in neutrophil numbers and distribution in blood and bone marrow of DARC KO and FYB(ES)TG mice, there may be changes in the nature of the neutrophils from these mice, particularly relating to levels of neutrophil activation. Blood neutrophil CD11b expression is increased in FYB(ES)TG and unchanged in DARC KO

as compared to WT mice. Increased CD11b expression and avidity for endothelial Ig receptors ICAM-1 and ICAM-2 plays a crucial role in immobilising neutrophils rolling along the vascular endothelium and promoting transmigration, as well as other important roles in chemotaxis and phagocytosis (Arnaout, 1990, Schymeinsky *et al.*, 2007). CD11b levels are increased by activation, being induced by complement C5a, chemokines, TNF and fMLP (Mazzone and Ricevuti, 1995). It is suggested that neutropaenia seen in clinical states such as systemic lupus erythematosus, diabetes mellitus and haemodialysis may reflect the observed increased CD11b expression in the neutrophils of these patients. This may imply that neutrophils from FYB(ES)TG may circulate in a more activated state and lead to the increased CD11b expression which may contribute to the neutropaenia seen in the FYB(ES)TG.

In addition, CD16/CD32 expression is increased in bone marrow neutrophils of both DARC KO and FYB(ES)TG mice. Work done in the murine myeloid cell line LGM-1 reveals increased G-CSF receptor signalling is associated with increased CD11b and FcγII (CD32) and FcγIII (CD16) receptor expression (Koay and Sartorelli, 1999). These Fcγ receptors are ligands for IgG, and mice express FcγII-B on neutrophils which leads to inhibitory signalling, whereas the FcγIII receptor is activating and leads to effects on phagocytosis and the secretion of chemoattractants (Nimmerjahn and Ravetch, 2008). Activation of FcγII receptor augments neutrophil adhesion through CD11b (Kusunoki *et al.*, 1994, Kocher *et al.*, 1997), suggesting a further pathway by which neutrophil proximity or margination to vascular endothelium is enhanced. Taken together this supports the notion that neutrophils from DARC KO and

FYB(ES)TG mice are more activated. Further functional experiments are required to determine the impact of this in responses to infectious stimuli.

One of the primary hypotheses of this work was that in the absence of erythroid DARC, an altered pattern of chemokines and cytokines necessary for optimal haematopoiesis develops. *In vitro* colony assays were done to test whether 'normalisation' of the growth environment of DARC KO bone marrow with ideal amounts of growth stimulants in culture could lead to normal CFU formation. The initial colony scoring results revealed a reduction in CFU numbers and cell counts, corresponding with a reduced homeostatic proliferation present in the bone marrow of DARC KO mice. In particular, the CFU-GM colony type was particularly reduced in numbers, reflecting a similar reduction in GMPs demonstrated in bone marrow FACS. Similar colony formation rates were obtained using unfractionated bone marrow cells, and FACS-sorted LSK cells. This suggests that the reduced colony output is not only as a result of fewer LSK cells present in DARC KO mice but due to a reduced cellular proliferation rate. Since cells from DARC KO may divide at a slower rate it is possible that cells differentiate more slowly in DARC KO, compared to WT, and hence more immature cells remain and are able to form more numerous colonies in subsequent replated DARC KO cultures. Alternatively, subsequent increases in cell counts and colony numbers on replating of DARC KO cultures compared to WT cultures may also suggest that proliferation rates may be responding to the optimal growth environment in the culture medium. Potential epigenetic changes present in the DARC KO LSK may be removed during the 7 days of incubation, leading to subsequent maximal growth rates. Further experiments to delineate potential mechanisms for these findings could

include culture of stem cells FACS sorted using the SLAM code (CD150, CD48), and single cell cultures, as well as examination for differences in receptor and gene expression between replatings. Of note, similar reductions in HSPC and myeloid progenitors from African American bone marrow harvests (Hsieh *et al.*, 2010) and reductions in CFU-GM colonies in *in vitro* assays from the bone marrow of individuals of African ancestry (Rezvani *et al.*, 2001) have been reported.

Reduced proliferation rates in DARC-negative haematopoiesis are further reflected in the BrdU uptake studies, which reveal a significant difference in BrdU incorporation and hence imply reduced proliferation in mice lacking erythroid DARC. This phenomenon is present in all HSPC compartments and therefore proliferation in itself does not account for the FYB(ES)TG mouse bone marrow phenotype. Population based cardiovascular studies have shown that participants of African ancestry have significantly longer telomeres in peripheral blood leukocytes (Hunt *et al.*, 2008), suggesting reduced cell divisions and reduced myeloid proliferation. This finding suggests that the absence of erythroid DARC reduces cellular proliferation rates in humans of African ancestry, most of whom are homozygous for *FYB(ES)*.

Rates of Annexin V binding were reduced in DARC KO and FYB(ES)TG, implying that lineage-negative cells from these genotypes are protected from apoptosis and cell death. Typically, cell populations exhibiting high proliferation would reflect lower rates of apoptosis. Inhibitors of apoptosis operate through several pathways, such NF-kB and RAS. In addition survival factors such as growth factors and cytokines, activate the JAK/Stat pathways and subsequently activate BCL-2. The bone marrow micro-environment in DARC KO and FYB(ES)TG models may possibly contribute to this

leading to aberrant cytokine signalling and activation of these pathways, thereby conveying protection from apoptosis. For example, fewer haematopoietic stem cells from mice overexpressing BCL-2 were in cell cycle and have lower apoptotic rates (Domen *et al.*, 2000). G-CSF ligation to the G-CSF receptor stimulates numerous signal transduction pathways, including STAT3, the Ras/Mek/Erk1/2 pathway(Tian *et al.*, 1994, de Koning *et al.*, 1998), leads to reduced apoptosis in neutrophils (Simon, 2001) and mobilised peripheral blood $CD34^{+}$ cells (Philpott *et al.*, 1997). Furthermore, G-CSF has recently been the subject of increased attention as a result of protective qualities it confers to injured organs expressing the G-CSF-R, such cardiac (Ma *et al.*, 2012), renal (Nogueira *et al.*, 2012) and neural (Doycheva *et al.*, 2013) tissues. These are not necessarily based on the recruitment of bone marrow derived progenitors to sites of injury. Recent work has shown that treatment with G-CSF induces expansion and increased quiescence of phenotypic HSCs, but leads to a HSC repopulating defect associated with induction of TLR expression and signalling (Schuettpelz *et al.*, 2014). The cited HSC repopulating defect induced by higher circulating systemic levels of G-CSF in DARC KO mice would also support the findings in the competitive chimera experiments, where rates of proliferation were reduced in CD45.2 DARC KO despite the introduction of DARC+ erythropoiesis. Taken together, this implies that reduced proliferation and apoptosis in lineage negative DARC KO and FYB(ES)TG cells are an induced effect possibly due to the chronically increased G-CSF levels detected in these genotypes using the multiplex cytokine array.

Whilst DARC binds to a number of inflammatory chemokines, none of these ligands is crucial for neutrophilic development: instead these are involved in the mobilisation

and recruitment of neutrophils from the bone marrow to site of inflammation. Conversely several cytokines are essential for neutrophil development including G-CSF, GM-CSF, M-CSF and IL3 (Liu *et al.*, 1996, Ward *et al.*, 2000). DARC KO and FYB(ES)TG mice have reduced serum CXCL1 and the binding studies using iodinated-CCL5 showed reduced binding to the DARC-negative erythroblast surface but also lower chemokine levels in the supernatants.

Suboptimal retention of mobilising chemokines (e.g. CXCL1, CXCL2, CXCL5) within the haematopoietic micro-environment due to loss of erythroid DARC may contribute to the increased neutrophil proportions found in the DARC KO and FYB(ES)TG bone marrow. It has been described that whilst total tissue chemokine levels may be normal, it is their availability in specific microenvironments and ability to form gradients which are necessary for the correct localisation of cells (Ulvmar *et al.*, 2014). This may explain why total chemokine levels were not dramatically altered in the bone marrow supernatant of DARC KO and FYB(ES)TG mice. Erythropoietic DARC may therefore be required for the optimal establishment of chemokine patterns which would direct developing and mature granulocytes towards the perivascular areas for release in to the circulation. A possible explanation for the neutropaenia of FYB(ES)TG may lie with distribution of presented chemokines on the bone marrow vascular endothelial cells, and reducing the release of cells into the blood. In addition, immunofluorescent imaging of bone marrow sections reveals an increased clustering of myeloid cells in DARC KO and FYB(ES)TG mice as compared to WT counterparts, suggesting an abnormal distribution of myeloid cells throughout the bone marrow. This effect may be extended to the circulation, where ELR+ chemokines may be

drawn to and presented primarily along the luminal surface of DARC expressing endothelial cells without erythroid DARC to provide a balanced distribution of these chemokines. In addition, effects on neutrophil CXCR2 by the abnormal distribution of cognate chemokines may be enhanced if the neutrophils have an activated phenotype. It has been shown that G-CSF increases responsiveness of neutrophils to CXCL2 binding to CXCR2, and induces the expression of CXCR2 (Nguyen-Jackson *et al.*, 2010). This may further contribute to neutrophil activation, and direction of neutrophils towards endothelial presented chemokines. The CXCR4 antagonist AMD3100 (Plerixafor) would be useful to examine this further, since it has been shown that the neutrophilia following the administration of this agent is due in significant part to demargination of leukocytes (Devi *et al.*, 2013). These findings do not fully explain the increased G-CSF levels seen in FYB(ES)TG, unless neutrophils remained in a state of sustained margination at steady-state, rather than entering the tissues to be taken up by macrophages and downregulate the IL-23-IL-17 axis. Furthermore, IL-17 was not detectable in multiplex cytokine array of serum from WT, DARC KO and FYB(ES)TG mice. This may be for technical reasons; however, detectably raised IL-17 levels in DARC KO or FYB(ES)TG serum would support hypothetical activation of IL-23-IL-17 axis as being important in explaining at least in part the observed increased G-CSF levels detected in these mice. Raised G-CSF levels have been reported in healthy volunteers of African descent (Mayr *et al.*, 2007), which supports the raised G-CSF as a secondary effect in the context of the neutropaenia seen in the FYB(ES)TG mice.

Raised levels of CCL11 were present in the bone marrow supernatant of DARC KO and FYB(ES)TG mice, and the serum of FYB(ES)TG mice. CCR3, the main receptor for CCL11, is reported to be expressed on bone marrow progenitors and increased CCL11 in vivo leads to increased number of bone marrow myeloid progenitors, directing haematopoiesis in a pro-myeloid direction (Peled *et al.*, 1998). CCL11 is chemotactic primarily for eosinophils which express CCR3, and has a central role in allergic responses, airway inflammation and human diseases such as asthma (Fulkerson *et al.*, 2006). Further important disease associations for CCL11 have been shown in CNS ageing (Villeda *et al.*, 2011) and inflammation, and inflammatory bowel disease (Rehman *et al.*, 2013). This chemokine has gained new prominence in studies of atherosclerosis (Emanuele *et al.*, 2006). Whilst CCR3, the main receptor for CCL11, is not present on monocytes, effects on monocytes are possibly mediated by antagonising the binding of cognate chemokines on CCR2 and CCR5 expressed by monocytes (Wang *et al.*, 2013). Increased levels of CCL11 may explain the increased non-classical ($Ly6C^{low}$) monocyte proportions seen in the blood of DARC KO and FYB(ES)TG (see **Figure 4.5e**). $Ly6C^{low}$ monocytes have important functions in 'patrolling' the vascular endothelium (Auffray *et al.*, 2009), and exhibit long-range crawling on the vascular endothelium, particularly in mesenteric and dermal vasculature with a postulated function of surveying and scavenging pathogens, lipids and dead cells. This monocyte subgroup has been shown to extravasate and be important during the early inflammatory response to *Listeria*, and differentiate into activated macrophages, with further roles in healing of damaged myocardium. Increases in vascular endothelium patrolling $Ly6C^{low}$ monocytes in DARC-negative

haematopoiesis may coincide with hypothesised increased FYB(ES)TG neutrophil margination. Further mechanistic work is required to determine the cause of the increased CCL11, and the possible link between this phenomenon and the noted increase in Ly6C^{low} monocytes, particularly since monocytes do not express CCR3. Given the known effects of CCL11 in directing haematopoiesis toward myeloid differentiation and proliferative effects on neutrophils, this chemokine may be contributing to the myeloid hyperplasia seen in FYB(ES)TG.

Changes in the bone marrow environment in the absence of erythropoietic DARC leading to differences in cellular proportions, distribution and turnover were hypothesised to induce alterations in gene expression within the HSPC compartment. The micro-array results of GMP cells suggested that the cells collected from DARC KO and FYB(ES)TG had increased expression of markers normally low in these granulocyte-macrophage precursors. Several erythroid and lymphoid genes showed increased expression, implying that the gene expression profile was more CMP-like, and more immature. LSK cells however had increased expression of several markers usually found in mature neutrophils, which could suggest a scenario of enhanced pro-neutrophilic differentiation, in response to external factors, but in the context of reduced cell divisions which could lead to ongoing immature gene expression profiles.

This may also explain the relative reduction in GMP, as these may begin to express more mature myeloid markers (e.g. CD11b) and hence slip into the lineage gating. In other words, the GMP of DARC KO and FYB(ES)TG are likely CMP-type cells with early high CD16/CD32 expression, and possibly interplay of CCL11 and G-CSF is accelerating myeloid-neutrophilic maturation. MPP cells directed towards GMP

development (GMPP) were similarly reduced which may be due to similar mechanism. It remains unclear whether the GMPP are truly reduced, or appear so due to premature altered surface marker expression changes and hence do not appear as the expected immunophenotype of GMPP. Given the robust myeloid output within the bone marrow of DARC KO and FYB(ES)TG, the latter may be the likely explanation. A further alternative explanation, which is supported by some of the LDA results (high expression of lymphoid genes) is that GMPP are truly reduced, and the deficiency is compensated by some LMPP being directed toward GMP differentiation, which is a known ability of this cell group, as described earlier.

Whereas CXCR4 gene expression was significantly increased in the LSK of DARC KO and FYB(ES)TG compared to WT as shown in the LDA results, this was not present in GMP of the same mice. This would suggest that LSK cells are more likely to be retained in the bone marrow, although this retention signal is decreasing at the GMP stage. CXCR4 is required for the quiescence of HSC (Nie *et al.*, 2008), and it is conceivable that increased expression may be associated with augmented CXCR4 signalling leading to increased HSC quiescence and correlate with the reduced BrdU uptake seen in LSK of DARC KO and FYB(ES)TG. In contrast, as stated above, G-CSF stimulation leads to a transient upregulation of CXCR4 followed by reduction in CXCR4 surface expression on HSPC. DARC KO and FYB(ES)TG mice demonstrate elevated G-CSF levels and the effects of chronic G-CSF exposure on HSPC CXCR4 expression are not known. It is possible that the raised CXCR4 expression in LSK cells acts to counter-balance the elevated G-CSF levels in these mice.

In contrast, VCAM-1 expression was significantly decreased in the LSK of DARC KO and FYB(ES)TG. Mice lacking VCAM-1 show increased numbers of circulating HSPC (Ulyanova *et al.*, 2005). It has been described that VCAM-1 expression is reduced by the accumulation of neutrophils in the bone marrow, whose proteases (neutrophil elastase and cathepsin G) directly cleave VCAM-1 (Levesque *et al.*, 2001), although some controversy exists as to whether proteases are essential for HSPC mobilisation, as described above. Nevertheless, G-CSF treatment has been shown to be associated with reduction in VCAM-1 expression in wild-type mice (Levesque *et al.*, 2004). Whether the raised G-CSF levels or increased bone marrow neutrophil number present in DARC KO and FYB(ES)TG are the cause of the reduced VCAM-1 levels will require further study.

As described above, surface CXCR4 expression on mature bone marrow neutrophils is low compared to intracellular levels, and aged neutrophils have increased CXCR4 expression which contributes to their homing to the bone marrow for clearance (Martin *et al.*, 2003). Neutrophil surface CXCR4 expression was the same in WT, DARC KO and FYB(ES)TG mice. This would suggest than there is no preferential homing for aged neutrophils in the bone marrow of DARC KO and FYB(ES)TG, implying that is not the cause of increased bone marrow neutrophils in these mice. In contrast to the known association with bone marrow neutrophil accumulation and G-CSF induced reductions in CXCL12 during mobilisation, DARC KO and FYB(ES)TG mice had similar CXCL12 levels in the bone marrow supernatant to WT mice. The effects of chronic G-CSF stimulation on bone marrow CXCL12 levels are not known, and it is possible that eventually a compensatory increase in CXCL12 develops. From a

technical perspective ELISA of whole bone marrow supernatant may not detect differential localisation of CXCL12.

Given the altered bone marrow environment in DARC KO and FYB(ES)TG mice as shown by the changes in various cytokine and chemokine levels, it is possible that these lead to epigenetic modifications, with implications for gene expression in daughter HSPC. For example, chronic G-CSF stimulation is associated with persistent HSC re-population defects (Schuettpelz *et al.*, 2014). Some results from the mixed chimera experiments, such as persistence of reduced GMP profile may be due to epigenetic changes within DARC KO stem cells persisting despite localisation within DARC replete bone marrow. This assumption is supported by the *in vitro* colony assays showing reduced proliferation of DARC deficient bone marrow or LSK cells in an optimal growth environment. It is possible that this contributes to the persistent DARC KO phenotype of the CD45.2 DARC KO within the mixed chimera.

The loss of CXCR2 expression in mice leads to a phenotype characterised by increased bone marrow neutrophils, reduction in erythroid cells and neutrophilia. However mixed chimeric mice with both WT and CXCR2 KO bone marrow show increased CXCR2 deficient neutrophils in the bone marrow and a reduction of these neutrophils in the blood. This is explained by the presence of WT neutrophils normalising the peripheral IL23-IL17 'sensor' of neutrophil deficiency and reducing the production of cytokines (such as G-CSF) which would increase their mobilisation as seen in CXCR2 KO mice (Eash *et al.*, 2010). This would suggest that CXCR2 deficient neutrophils under normal conditions have a mobilisation defect. This phenotype shows some similarities to the FYB(ES)TG phenotype, and the mixed bone marrow chimera

experiment was also associated with a reduction in the proportion of DARC KO neutrophils; however this affected all peripheral blood cells including lymphocytes to a similar degree. This further reinforces the notion that loss of haematopoietic DARC leads not only, if at all, to a neutrophil mobilisation defect but leads also to significant changes in gene expression in HSPC and mature cells, and that restoration of cytokine and chemokine profiles to wild-type levels is not sufficient to return the phenotype to normal.

Whilst this work has focused primarily on the role of the *FYB(ES)* polymorphism in causing a peripheral blood neutropaenia, a potential limitation of using a murine model to study this effect applies. Primarily, the major component of the murine blood is lymphocytes, whereas in human neutrophils comprise more than 50% of blood leukocytes. The reduction in blood B lymphocytes in the FYB(ES)TG mouse may represent a G-CSF effect, since increased G-CSF levels have a suppressive effect on B-lymphopoiesis (Winkler *et al.*, 2013), or be representative of the reduced proliferation in the steady state in FYB(ES)TG mice. The latter possibility is less likely, considering that DARC KO mice have no such reduction in blood lymphocytes. A similar reduction is noted for blood T lymphocytes in FYB(ES)TG mice. It may be possible that lymphocytes in FYB(ES)TG may be preferentially re-locating to other sites, such as the spleen.

Further work would be required to determine whether the differences in progenitor receptor expression, development and cell turnover rates seen in FYB(ES)TG mice translate to alterations in neutrophil function, chemokine receptor sensitivity and protection from apoptosis. In addition functional work examining neutrophil

mobilisation and response of the FYB(ES)TG (and FYBTG) murine model to infection and inflammation may give further insight into the role of DARC modulating cellular mobilisation from the bone marrow and directing responding cells to inflamed tissues. Finally the FYBTG mouse will require full characterisation to confirm the preliminary findings and determine cell proliferation and gene expression changes.

Therefore, in summary, the FYB(ES)TG mouse model recapitulates the human Duffy-negative phenotype, by showing that the loss of erythroid DARC directly leads to peripheral blood neutropaenia, and is supported by irradiation chimera experiments with the same effect. The reduced neutrophil count seen in FYB(ES)TG mice and, by extension, in humans with ethnic neutropaenia, may be due to increased margination as originally theorised due to abnormal neutrophil localisation within the bone marrow and blood. Feedback to the bone marrow by way of G-CSF signalling may lead to increased pro-myeloid haematopoietic maturation, and accumulating aggregations of myeloid cells therein due to suboptimal patterning of chemokines. The increased levels of G-CSF would also increase HSPC quiescence, yet contribute to anti-apoptotic signalling, leading to fewer cell divisions and in humans potentially protect from the development of acute myeloid leukaemia (see Chapter 5).

Chapter 5

The Role of DARC in Cancer Survival

5.1 Introduction

The potential importance of ethnicity in the outcome of cancer therapy is receiving increasing attention (Bhatia, 2011, Artinyan *et al.*, 2010). Persons of African ancestry fare worse in analyses of health outcomes compared with many other populations, with recent data from the United States indicating higher overall cancer death rates for African Americans (SEER Program database, 2012). Poor cancer survival in ethnic minority groups has been ascribed to be due to a complex mix of biological and socio-economic factors, such as access to health-care, cancer surveillance, educational opportunity and cultural factors (Bach *et al.*, 2002). The inference of biological factors however is intriguing. These include differences in disease biology, such as a higher incidence of poor risk disease (Kadan-Lottick *et al.*, 2003, Woodward *et al.*, 2006), different metabolism of drugs due to genetic polymorphisms (McLeod *et al.*, 1994), or susceptibility to side effects (Hasan *et al.*, 2004) in some ethnic minority groups.

There has been recent interest in a potential role for DARC on cancer development and outcome of cancer therapy. African American men have higher incidence of prostate cancer (Hsing and Devesa, 2001, DeSantis *et al.*, 2013), and increased likelihood of more aggressive disease as well as higher death rates, compared to Caucasian Americans.

Studies have examined potential associations between DARC phenotype or ethnic neutropaenia and cancer survival. An initial clinical study failed to demonstrate an association between Duffy phenotype within a Jamaican population, and prostate cancer risk, although the authors identified a number of confounding risk factors (Elson *et al.*, 2011). A further study investigated a possible association between neutrophil count and prostate cancer risk and severity (Sadeghi *et al.*, 2012) in African American men. An association was noted between blood absolute neutrophil count $<1.5x10^6$/ml and Gleason score, an indicator of prostate cancer prognosis based on histological degree of tissue abnormality, at prostatectomy. Although only 18 individuals (5%) of 336 African American men in this study demonstrated a neutrophil count $<1.5x10^6$/ml, the result is of interest, as it suggests a potential functional effect of Duffy negative phenotype by way of bone marrow myeloid cell effects, instead of direct blood chemokine effects. This may represent a complex interaction, as neutrophils are known to have anti-tumour potential through cytotoxicity against tumour cells, and cause damage to vascular endothelium through oxidants and proteolytic enzymes (Di Carlo *et al.*, 2001). In contrast substantial evidence now shows significant pro-tumour actions of neutrophils, including promoting tumour angiogenesis (Tazzyman *et al.*, 2009). It remains unclear what causes the conversion of neutrophil function from tumour suppressive to tumour promoting, although G-CSF and IL-6, which could be produced by tumour cells and/or stromal cells in malignant tumours (Shojaei *et al.*, 2007), are potential candidates for modulating neutrophils to induce their tumour-promoting function (Yan *et al.*, 2013). It has been previously described that G-CSF levels are elevated in

Duffy negative individuals (Mayr *et al.*, 2007), although no link between systemic and intra-tumour GCSF levels and neutrophil-tumour effects have been demonstrated. In contradiction to findings demonstrating a link between prostate cancer severity and neutropaenia, in gastric (Jin *et al.*, 2013) and colon cancer (Michael *et al.*, 2006), melanoma (Schmidt *et al.*, 2007), nasopharyngeal carcinoma (He *et al.*, 2012), mesothelioma (Kao *et al.*, 2010) and advanced non-small cell lung cancer (Teramukai *et al.*, 2009), higher neutrophil levels and/or higher neutrophil-to-lymphocyte ratios are associated with poorer survival.

Treatment of leukaemia (myeloid or lymphoid) with combination chemotherapeutic agents induces periods of profound immunosuppression, in conjunction with the immunosuppressive effects of the underlying malignant disorder. A major cause for presentation in these disorders and treatment related mortality remains infection, particularly therapy-associated bacterial neutropaenic sepsis (Creutzig *et al.*, 2004). Susceptibility to infection in individuals of African ancestry has been a contentious issue. A study demonstrating substantial anti-microbial effects by neutrophils against tuberculosis infection, also noted that the likelihood of acquiring this disease appeared to correlate inversely with neutrophil counts (Martineau *et al.*, 2007). Study subjects of African origin tended to have lower neutrophil counts and the highest incidence of tuberculosis infection, compared with other groups (including South Asians) in the South London cohort. Furthermore, US registry data revealed an increased incidence of severe sepsis and consequent organ dysfunction in individuals of African ancestry (Mayr *et al.*, 2010). However this analysis of registry data is affected by potential confounders which include socio-economic factors and access to healthcare,

particularly in a health-care system with a substantial private-care component (Robbins *et al.*, 2009). In a more controlled analysis Duffy-negative African Americans admitted to intensive care units for treatment of acute lung injury have twice the mortality of Duffy-positive subjects of the same ethnicity (Kangelaris *et al.*, 2012). This finding would support an underlying biological effect of the Duffy negative phenotype on response to severe infection/inflammation, relating to the loss of erythrocyte function as a sink or reservoir of inflammatory chemokines rather than neutropaenia. In addition chronic co-morbidities such as diabetes and hypertension which are more common (Harris, 1990, Lloyd-Jones *et al.*, 2009) in African Americans and require high-quality medical management (affected by access to healthcare), as well as disparities in disease prevention may contribute to the increased rates of sepsis (Esper *et al.*, 2006a, Dombrovskiy *et al.*, 2007). It is not possible however to isolate the individual components leading to the observed effect.

Regarding outcome following treatment for malignancy, a significant reduction in survival in children of African American background has been reported following treatment for acute myeloid leukaemia, due primarily to an increased mortality from infectious complications (Aplenc *et al.*, 2006). In addition an inferior outcome for women of African ancestry has been reported following treatment for breast cancer and this may have been due to treatment delay secondary to neutropaenia (Smith *et al.*, 2005, Hershman *et al.*, 2003). It is clear that the identification of the relative roles of genetic or environmental factors in determining the basis of any association between ethnicity and cancer outcome therefore remains challenging.

The role of ethnicity and *DARC* genotype on the outcome of acute myeloid leukaemia in patients entered into UK clinical trials for acute myeloid leukaemia was investigated. The UK National Health Service is an open access health care system and therefore limits potential environmental confounding factors.

Collaboration was established with Prof AK Burnett, head of the MRC AML trials group, who kindly agreed to provide extracted DNA from stored bone marrow aspirate samples of patients with acute myeloid leukaemia treated as per trial protocol.

5.2 Materials and methods

DNA was extracted by Dr Amanda Gilkes (Cardiff, UK) with the Qiagen Blood DNA extraction kit. Extracted DNA was diluted to a concentration of 25ng/μl and stored at -80^{o}C until used. Human DARC allele genotyping was done by method in section 1.1.12 ('Human DARC Genotyping for Polymorphic Alleles') using allele-specific primers (Mullighan *et al.*, 1998). DNA was available from 54 patients whose ethnic origin was described as Black or Asian. Twenty-eight subjects of self-described Asian ancestry were genotyped for the presence of *FYB(ES)*, along with 25 subjects of self-described African origin.

5.3 Results

Five year outcome data were available for 2967 patients entered into the UK MRC AML15 trial (designed for patients under the age of 60) between May 2002 and January 2009 and 1811 patients in the NCRI AML16 trial (designed for patients over the age of 60) between August 2006 and May 2012. Only patients treated with intensive chemotherapy are included in this comparison. Follow-up is complete for AML15 to 1st January 2012, and for AML16 to 1st January 2013. Ethnic origin was self-described by the patient at the time of trial entry. The results of the genotyping are given in **Table 5.1**. The homozygous prevalence of *FYB(ES)* within Caucasian subjects is 0.07-0.1% (Reich *et al.*, 2009, Reid and Lomas-Francis, 2004) and this group was not genotyped but assumed to carry *FYA* or *FYB* alleles.

Genotype	African ancestry	Asian
FyA*FyA	0	18
FyA*FyB	2	5
FyB*FyB	1	3
FyBES*FyBES	15	0
FyBES*FyA	2	0
FyBES*FyB	3	0
N/A	2	2
TOTAL	**25**	**28**

Table 5.1 Genotyping results of non-Caucasian subjects from MRC AML15 trial for the three principal *DARC* alleles.

Approximately 61% percent of patients self-described as of African ancestry were homozygous for the point mutation terminating transcription of DARC protein in erythroid cells. None of the Asian patients harboured this polymorphism, and 64% were homozygous for *FYA*, the allele more commonly found across Asian populations.

a)

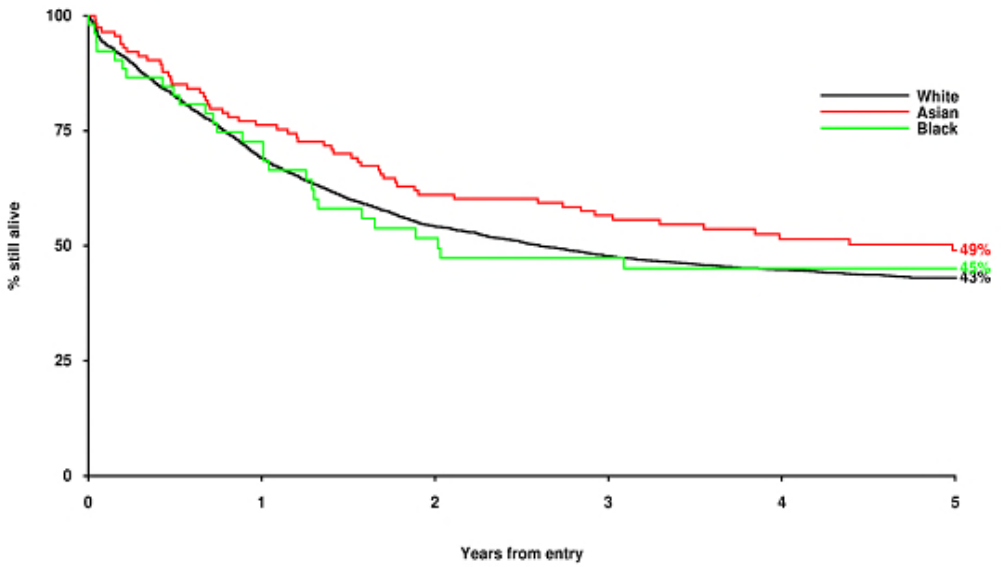

b)

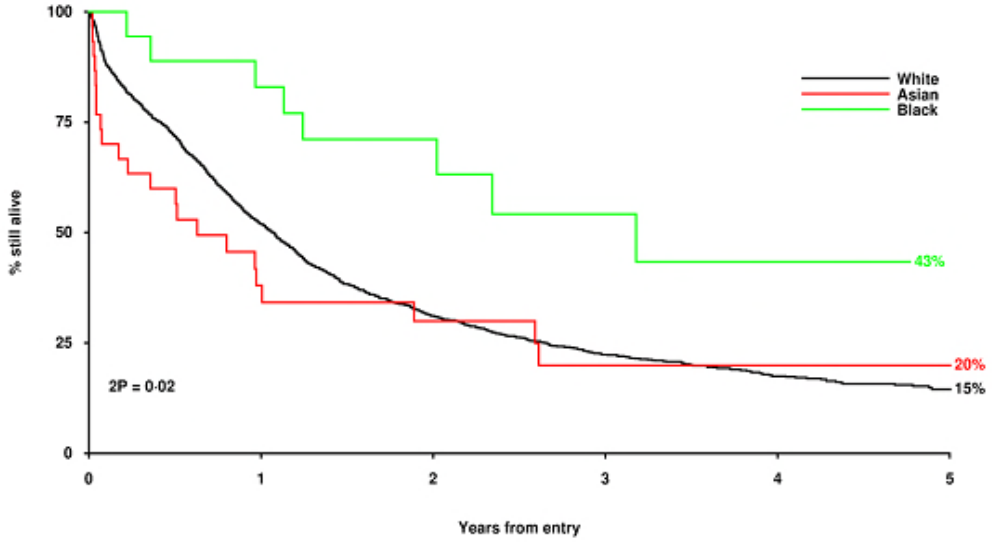

Figure 5.1 Overall 5 year survival in AML15 and AML16 studies. (a) 5 year survival from trial entry divided by ethnicity for AML15. 2814 white patients had 1628 events, 114 Asian patients had 59 events and 52 black patients had 27 events. Overall survival for black patients was not different compared to white patients, p=0.3
(b) 5 year survival from trial entry divided by ethnicity for AML16. 1763 white patients had 1298 events, 30 Asian patients had 22 events and 18 black patients had 8 events. Overall survival for black patients was superior compared to white patients, p=0.02

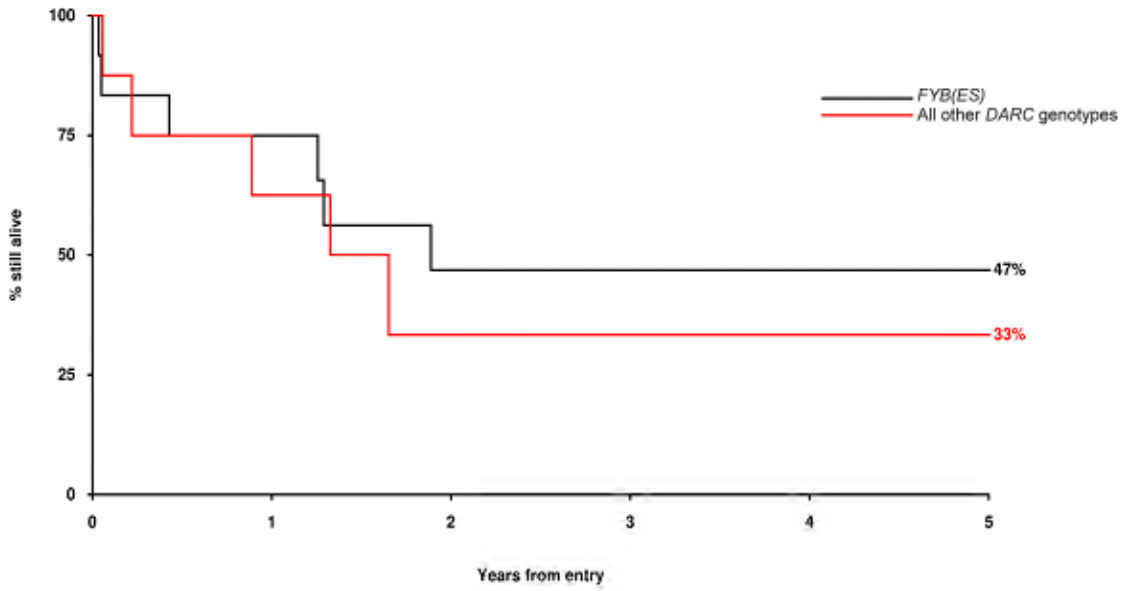

Figure 5.2 5 year survival from trial entry divided by *DARC* genotype in Black patients for AML15. Twelve patients homozygous for *FYB(ES)* experienced 6 events, whereas 8 Duffy positive individuals had 8 events. Overall survival was not different between the genotypes, p=0.7

No differences in risk of early death or 5-year survival were observed between the three ethnic groups, Asian, Black and White in AML15 (p=0.3) (**Figure 5.1a**); in the AML16 trial for older patients, those in the Black ethnic group had better outcomes (p=0.02) (**Figure 5.1b)**. The outcome for 'Duffy negative' and 'Duffy positive' individuals within the Black ethnic group in AML15 was not significantly different (HR 1.30, 95% CI (0.39-4.40), p=0.7) although numbers are too small to draw any definitive conclusion (**Figure 5.2**).

5.4 Discussion

Ethnic minority origin did not adversely influence clinical outcome in this large national study of AML treatment. A similar observation has been found in a paediatric AML cohort when healthcare access is equalised (Pui *et al.*, 2012). This is of particular interest as the intensive chemotherapy regimens used during AML treatment are associated with frequent and prolonged episodes of neutropaenia. The failure to observe any influence of Duffy negative phenotype on clinical outcome suggests that the moderately reduced neutrophil counts seen in ethnic neutropaenia may be sufficient to protect patients on peripheral blood recovery following myeloablative chemotherapy. Other factors such as the duration of severe neutropaenia, and the biological characteristics of the malignancy may play a more important role in AML survival.

Data from the SEER program database also indicate a lower incidence of acute myeloid leukaemia in African Americans compared to Caucasians across the same age group stratifications (2012). Whilst this needs to be shown in a prospective study, data from a cardiovascular study (Hunt *et al.*, 2008) found longer telomeres in individuals of the African American group, as discussed above. This suggests that myeloid cells in these individuals may have undergone fewer cell divisions and are 'younger'. AML is an illness affecting older individuals (Cartwright and Staines, 1992), and the probability of accumulating genetic damage increases with cell divisions. Telomeres help to reduce the genomic instability which leads to cancer development and shorten

with successive cell divisions (O'Sullivan and Karlseder, 2010). It is possible that this mechanism may contribute to the lower incidence of AML in this population group, although other gene polymorphism may play a role.

Limitations of the present study include small numbers of individuals which are of the ethnic minority type, restricting statistical power to large differences in outcome. In addition, patients of the ethnic minority cohort tended to be of younger age, which in itself confers superior survival, as biologic factors such as lower likelihood of resistant disease and better tolerability of intensive chemotherapeutic regimes are more relevant.

Better powered studies are likely to provide clearer results. Most clinical trials involving acute myeloid leukaemia treatment are small, incorporating a few centres. In addition, countries with substantial African ancestry populations and the resources to undertake studies with the collection of high quality data are limited to the United States. A future study to examine the role of DARC, ethnic neutropaenia and survival from acute myeloid leukaemia might correct for socio-economic confounding factors by including individuals only of African ancestry. In the USA, approximately 20% of these individuals are not homozygous for the 'Duffy negative' promoter mutation (Reich *et al.*, 2009), and would therefore be a more suitable control group. Furthermore this would control for other confounders such as those which might potentially have been introduced in this study by immigration, for example, where better outcome in first generation immigrants has been reported (Siemerink *et al.*, 2011, Keegan *et al.*, 2010).

Chapter 6

Conclusion

The existence of DARC as a blood group antigen has been established for over half a century, and subsequently its indispensable role for vivax malaria infection became apparent. Over the last twenty years, functional aspects of the role of DARC in inflammation and infection have been gradually dissected, with more recent findings suggesting it may function to regulate peripheral blood neutrophil counts.

Both haematopoiesis and the release of leukocytes from the bone marrow are under the control of two chemokine-receptor axes, involving CXCR4 and CXCR2. The ligands of CXCR2 bind to DARC, and in this work, I have shown that loss of haematopoietic DARC has implications for haematopoiesis in homeostasis.

The study of peripheral blood reconstitution in irradiation chimeras showed that the introduction of DARC-deficient haematopoiesis in wildtype hosts lead to peripheral blood neutropenia. This inspired the development of two mouse models, FYB(ES)TG and FYBTG, that express two polymorphic variants of the human *DARC* gene, and which allowed the analysis of haematopoiesis in these models and in DARC deficient mice. Only FYB(ES)TG mice, which harbour a polymorphism of DARC where transcription is abolished in the erythroid cells, display blood neutropenia, similar to both humans homozygous for this polymorphism, and the irradiation chimeric mice with DARC-deficient bone marrow. Preliminary results from FYBTG mice, where human DARC is expressed both on erythroid and endothelial cells, show that DARC

expression on erythroid cells leads to peripheral neutrophil counts similar to WT mice. DARC expressed by cells of the erythroblast lineage may have a role in modulating neutrophil release from the bone marrow, and in promoting optimal and orderly granulopoiesis. This is substantiated by the larger numbers of neutrophils in the bone marrow of FYB(ES)TG mice, and their development in larger aggregates. HSPC and granulocytic lineage development were skewed in these mice as determined from gene expression studies of these cells and enumeration of their progenitors, showing that a pro-granulocytic gene expression profile was associated with reduced numbers of precursors, possibly due to accelerated differentiation and the bypassing of developmental stages.

The loss of erythroid DARC may alter the availability and distribution of ELR+ and other chemokines within the bone marrow microenvironment. Work in this thesis shows that erythrocyte DARC increased the concentration of cognate chemokine in the supernatant and on the cell surface of erythroblasts. This supports the hypothesis that DARC serves to maintain the availability of chemokines in the bone marrow. Analysis of the bone marrow supernatant and peripheral blood of FYB(ES)TG mice showed increased concentration of G-CSF, possibly as a response to the blood neutropenia and contributing to the increased granulopoiesis observed in the bone marrow. Unexpectedly CCL11, a chemokine traditionally associated with allergic responses, was found to be highly expressed in the bone marrow and blood of FYB(ES)TG mice. Further work is required to determine whether this is due to a loss of erythroid DARC receptor buffering, or is a secondary response to the neutropenia. For example, mass spectrometry analysis may determine whether this is the intact molecule, or a digested

form detected by the assay. Erythrocyte DARC may serve to protect CCL11 from degradation and in the absence of DARC it may digested by proteinases.

Changes in neutrophil surface molecule expression suggest a more activated neutrophil phenotype in FYB(ES)TG mice, and there may also be implications for CXCR2 receptor responsiveness. Reductions in availability of ELR+ chemokines due to their altered bone marrow distribution in the absence of DARC may affect CXCR2 responsiveness and may contribute to the accumulation of neutrophils in the bone marrow of these mice, and impair their release. Labelled neutrophil transfer experiments could help determine whether this is the case or whether more mature neutrophils have returned and accumulated in the bone marrow following their release into the circulation. In addition administration of CXCR4 antagonists, G-CSF and sympathomimetics to FYB(ES)TG mice could help to establish the release kinetics of neutrophils from the bone marrow and their distribution in the marginated pool.

The gene expression signature of precursor LSK and myeloid progenitor bone marrow cells from FYB(ES)TG is not only pro-granulocytic, but also with signs of errant differentiation, with high expression of genes typically associated with other lineages. This is associated with reduced proliferation and protection from apoptosis seen in LSK and myeloid progenitors in FYB(ES)TG mice, and further work is required to determine whether the restoration of erythroid DARC expression would revert these to wildtype levels. Genetic manipulation using viral vectors to induce DARC expression in erythroblasts of FYB(ES)TG mice may provide significant further information in this regard. Furthermore, irradiation mixed chimeric mice harbouring both DARC-replete and DARC-deficient haematopoiesis in a WT host did not lead to a

normalisation of DARC KO proliferation kinetics and progenitor maturation profiles, underscoring possible epigenetic changes on haematopoietic stem cells developing in a DARC deficient bone marrow. Serial transplantation experiments of the LT-HSC may confirm this hypothesis, and studies of DNA methylation and microRNA would provide further valuable information to determine the role of epigenetic phenomena regulating gene expression in the HSPC of FYB(ES)TG mice.

Circulating lower number but more activated neutrophils in FYB(ES)TG mice may alter immune responses to infection and inflammation, and the investigation of the outcomes of FYB(ES)TG mice in models of infection may give further indication as to whether the *FYBES* polymorphism has implications for the study of clinical infections in Africans.

Treatment of acute myeloid leukaemia is associated with prolonged periods of neutropenia. Examination of the results of leukaemia survival within large UK trials determined that *FYB(ES)* homozygous individuals did not experience inferior outcomes. In particular, black individuals of all DARC genotypes in one study (which enrolled patients over 60 years of age) had better survival 5 years post leukaemia diagnosis. The reasons for this are unclear, but the main conclusion to be drawn is that the reduced neutrophil counts present in *FYB(ES)* homozygous individuals are not detrimental and are sufficiently protective during the recovery following myeloablative chemotherapy.

In summary, this work has shown a new role for haematopoietic DARC, which supports the availability of cognate chemokines in the bone marrow environment, and

may serve to promote the availability of chemokines for optimal haematopoiesis and neutrophil release from the bone marrow, possibly by modulating the ELR+ chemokine-CXCR2 axis. Both erythroblast and endothelial DARC may function in concert to promote orderly neutrophil development and release into the circulation. Finally, this is the first functional demonstration that the loss of haematopoietic DARC leads to the neutropenia seen in *FYB(ES)* homozygous humans.

Chapter 7

Appendix

7.1 Annotated *DARC* gene sequence

The human *DARC* gene sequence is presented below with annotations. The translated amino acid sequence is present in capitals immediately below respective codons. The 500bp upstream and 1kbp downstream of the sequence included in *FYB(ES)* and *FYB* transgene constructs is not shown.

7.1.1 Key

Colour highlighting code: Military green=plasmid DNA (excised); yellow=regulatory elements, red=mutation, exons=blue, grey= terminal nucleotides, pink=restriction enzyme analysis sites.

7.1.1.1 Polymorphic mutations

The main polymorphic mutations are presented below for illustrative purposes.

Fy(a+b-): Gly (GGT) Fy(a-b+): Asp(GAT)

GATA motif: TTA TCT mutation TTA CCT

7.1.2 *DARC* sequence

-512 ctcgagtttttcagcaagatacatggcttttgaactgcctttccttggatc

-481 cagttcaaggggatggaggagcagtgagagtcagccgcccttccactccaatttcccagc

-421 acctcccttatctctgcctcacaagtcacccagccccccctctttccttccttgtgcttg

-381 aagaatctctccttgctggaaagccccctgttttctcaatctccctttccacttcggtaa

-321 aatctctacttgctggaaagccccctgttttctcaatctccctttccacttcggtaaaat

-261 gcccactttctggtccccacctttttcctgagtgtagtcccaaccagccaaatccaacct

-201 caaaacaggaagaccccaaggccagtgacccccataggcctgaggcttgtgcaggcagtgg

-141 gcgtggggtaaggcttcctgatgcccccctgtccctgcccagaacctgatggccctcatta

-81 gtccttggcttcttaccttggaagcacaggcgctgacagccgtcccagcccttctgtctgc

-21 gggcctgaaccaaacggtgccatggggaactgtctgcacagggtgagtatggggccaggc

M G N C L H R

40 cccagagtcccttatccctatgcccctcatttcccgtgctgtttgcccctcagtctttat

100 atctcttccttttcctcctcatcttttctcccttcctgctttttttcctcttccttcaaag

160 tctttttccttctctccttcctatgctagcctcctagctccctcttgtgtccctcccttt

220 gcctttgagtcagttccatcctggtctcttggtgccttttccttctgaccttgcactgct

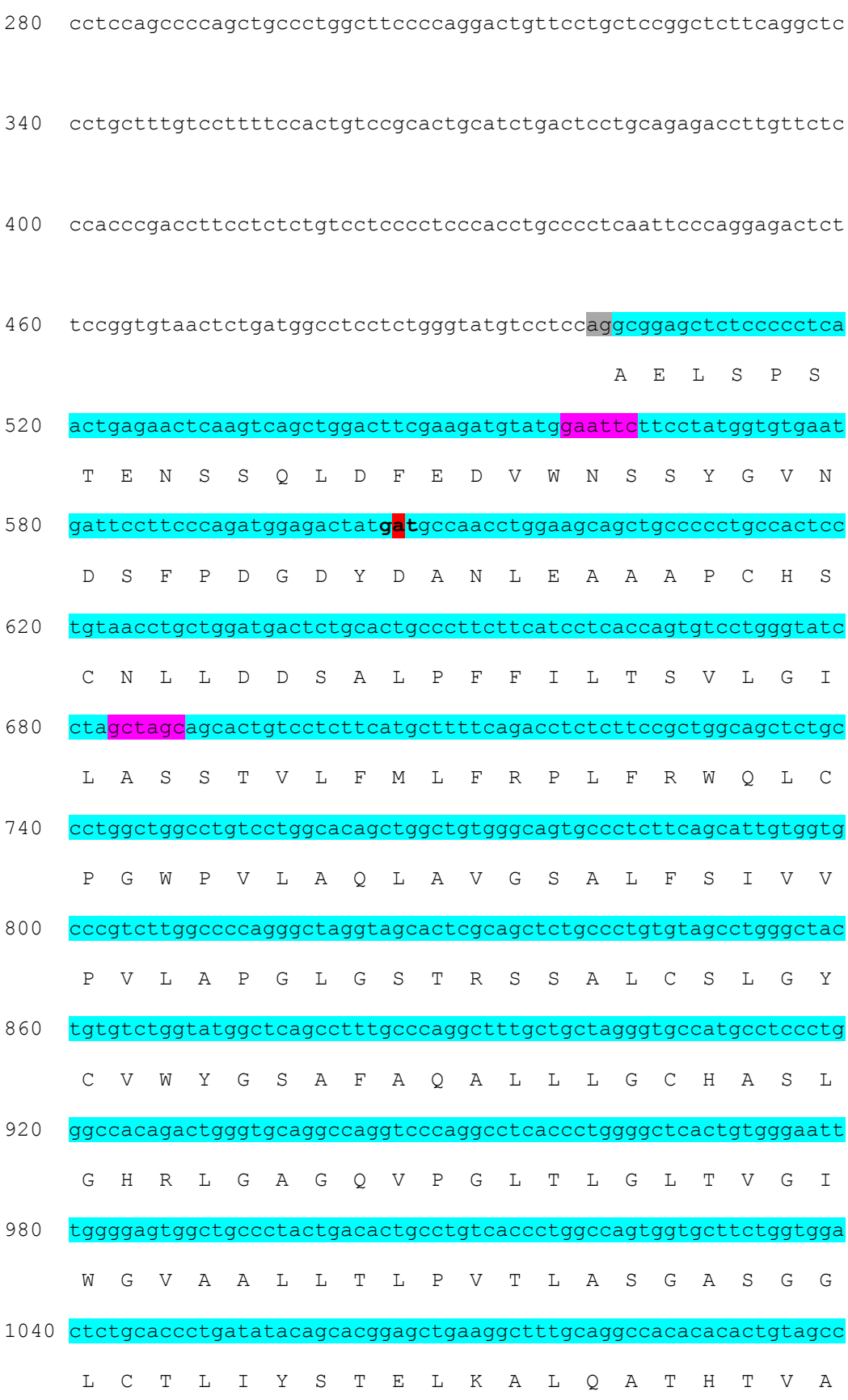
280 cctccagccccagctgccctggcttccccaggactgttcctgctccggctcttcaggctc
340 cctgctttgtccttttccactgtccgcactgcatctgactcctgcagagaccttgttctc
400 ccacccgaccttcctctctgtcctcccctcccacctgcccctcaattcccaggagactct
460 tccggtgtaactctgatggcctcctctgggtatgtcctccaggcggagctctcccctca
A E L S P S
520 actgagaactcaagtcagctggacttcgaagatgtatggaattcttcctatggtgtgaat
T E N S S Q L D F E D V W N S S Y G V N
580 gattccttcccagatggagactatgatgccaacctggaagcagctgccccctgccactcc
D S F P D G D Y D A N L E A A A P C H S
620 tgtaacctgctggatgactctgcactgcccttcttcatcctcaccagtgtcctgggtatc
C N L L D D S A L P F F I L T S V L G I
680 ctagctagcagcactgtcctcttcatgcttttcagacctctcttccgctggcagctctgc
L A S S T V L F M L F R P L F R W Q L C
740 cctggctggcctgtcctggcacagctggctgtgggcagtgccctcttcagcattgtggtg
P G W P V L A Q L A V G S A L F S I V V
800 cccgtcttggccccagggctaggtagcactcgcagctctgccctgtgtagcctgggctac
P V L A P G L G S T R S S A L C S L G Y
860 tgtgtctggtatggctcagcctttgcccaggctttgctgctagggtgccatgcctccctg
C V W Y G S A F A Q A L L L G C H A S L
920 ggccacagactgggtgcaggccaggtcccaggcctcaccctggggctcactgtgggaatt
G H R L G A G Q V P G L T L G L T V G I
980 tggggagtggctgccctactgacactgcctgtcaccctggccagtggtgcttctggtgga
W G V A A L L T L P V T L A S G A S G G
1040 ctctgcaccctgatatacagcacggagctgaaggctttgcaggccacacacactgtagcc
L C T L I Y S T E L K A L Q A T H T V A

1100 tgtcttgccatctttgtcttgttgccattgggtttgtttggagccaaggggctgaagaag

C L A I F V L L P L G L F G A K G L K K

1160 gcattgggtatggggccaggcccctggatgaatatcctgtgggcctggtttatttctgg

A L G M G P G P W M N I L W A W F I F W

1220 tggcctcatggggtggttctaggactggatttcctggtgaggtccaagctgttgctgttg

W P H G V V L G L D F L V R S K L L L L

1280 tcaacatgtctggcccagcaggctctggacctgctgctgaacctggcagaagccctggca

S T C L A Q Q A L D L L L N L A E A L A

1340 a**ttttgcactg**tgtggctacgcccctgctcctcgccctattctgccaccaggccacccgc

I L H C V A T P L L L A L F C H Q A T R

1400 accctcttgccctctctgcccctccctgaaggatggtcttctcatctggacacccttggga

T L L P S L P L P E G W S S H L D T L G

1460 agcaaatcctagttctcttcccacctgtcaacctgaattaaagtctacactgcctttgtg

S K S

1520 aagcgggtggtttcttattttgtctggggagaagaaggagaatggagagagagacatttt

1680 tatgtcagactttcttgccagtgtctgcttctatagctggcttgggaagaaggtgaatga

1740 tgaataaataccctcagggtacacagatgttctcttgaggtgtggggtcacggccatctc

1800 aagggagaagagaagaggaaccagagcatgaggggagtcattaaaccaaaaaaaacagaa

1860 gggatggcttagctggaaaaaaagctgttctgggaagcaaatggaataggaactcaaact

1920 gagagataaacagtgaagagtgatgacaaagcccagagcaataccacctccccctgtcca

1980 acctgcccagcctctgtcttctgtctcctctctggctttgtttagtgattaggacagtgg

2040 tggggaaggtgaaagaagcatcccaggggatgttactcagttcagggaacatatcaaggt

2100 aatttaaaaagccacttcctgggagtcatctctcccaggttcctcagcatgacctgaatg

2160 tgcgtgcgtgtgtgtgtgtgtgtgtgtgtacacatctgtttctcgatctgttagaatcta

2220 cctttatgttagatgtatgcatgtaaaaacatatgtccacccatgagcttgcatctctgt

2280 cagcacctgaactgcgcacacctgtgcgtgtgcactgacttttctcaggacccaaacccc

2340 cactcaattctgcactcatccctgttcacaggatatagaatcgggatttatgactcactc

2400 cttacccaaatgagttttctttaccctggtttttaagcctagtcttttctgtgtaggatg

2460 tgtggagggaagaaaagatcaagaagttgtgaagggtggagaaacttgaaggggggaggcc

2520 ctgatttgattcatcttctgcttggaattcccgaatttccctttcagaatctcagcttt

2580 tgaaataaacctttatttcccacatacatctttccttccaccttccacacaataccccaa

2640 tcccctgggcacctttttcccaacccctgattctctggctgcttaatcatgacctttgag

2700 atttttctcagtctctacctacccaagtttagatggctggaaggacagaaacccctcctc

2760 atcaggggcacagcttttaccaccaagagcaaattcaccctctacccaagaggatctttctaga

7.2 Microarray data: LSK

Table 7.1 Significant ($p<0.01$) differentially up- and down-regulated genes in DARC KO LSK cells from microarray study.

Fold-change	Symbol	Name	Parametric p-value	t-value
656.09	*NGP*	neutrophilic granule protein	0.00053	9.773863
509.74	*RETNLG*	resistin like gamma	1.19E-05	24.91421
462.38	*CAMP*	cathelicidin antimicrobial peptide	0.000169	12.99951
418.15	*LTF*	lactotransferrin	0.000193	12.58048
351.33	*S100A8*	S100 calcium binding protein A8 (calgranulin A)	0.000645	9.304109
290.63	*CAMP*	cathelicidin antimicrobial peptide	2.68E-05	20.44101
210.62	*MMP8*	matrix metallopeptidase 8	2.03E-05	21.87719
200.48	*S100A9*	S100 calcium binding protein A9 (calgranulin B)	0.00085	8.676108
182.53	*ALAS2*	aminolevulinic acid synthase 2, erythroid	0.000154	13.29547
176.46	*CHI3L3*	chitinase 3-like 3	0.000285	11.42115
131.22	*IFITM6*	interferon induced transmembrane protein 6	0.000614	9.421482
102.05	*AHSP*	alpha hemoglobin stabilizing protein	0.000974	8.381289
96.26	*HP*	haptoglobin	0.00074	8.986058
92.35	*HBB-B2*	hemoglobin, beta adult minor chain	0.002499	6.572798
91.57	*SLC4A1*	solute carrier family 4 (anion exchanger), member 1	4.09E-05	18.43689
86.88	*ITGB2L*	integrin beta 2-like	0.003455	6.034561
84.14	*RHD*	Rh blood group, D antigen	9.97E-05	14.81026
83.34	*CD300LF*	CD300 antigen like family member F	8.97E-05	15.20151
64.79	*C3*	complement component 3	0.000223	12.13369
55.94	*FN1*	fibronectin 1	0.00197	6.993227
48.57	*SLC38A5*	solute carrier family 38, member 5	0.000684	9.167096
46.30	*CD300LF*	CD300 antigen like family member F	0.000263	11.64906

Fold-change	Symbol	Name	Parametric p-value	t-value
41.27	*CEBPE*	CCAAT/enhancer binding protein (C/EBP), epsilon	0.000206	12.38332
40.34	*HBB-B1*	hemoglobin, beta adult major chain	0.000189	12.64351
39.69	*FAM46C*	family with sequence similarity 46, member C	0.000296	11.31384
37.30	*LCN2*	lipocalin 2	0.000861	8.64718
33.21	*ERMAP*	erythroblast membrane-associated protein	0.000269	11.57775
30.61	*PILRA*	paired immunoglobin-like type 2 receptor alpha	0.000711	9.076722
30.17	*ITLN1*	intelectin 1 (galactofuranose binding)	0.000426	10.32706
26.76	*GDA*	guanine deaminase	0.000239	11.92209
26.47	*AQP1*	aquaporin 1	0.000658	9.257144
25.67	*PI16*	peptidase inhibitor 16	0.006276	5.138434
25.43	*IFI202B*	interferon activated gene 202B	0.001034	8.255027
23.33	*RHOU*	ras homolog gene family, member U	0.000237	11.94988
21.97	*LGALS3*	lectin, galactose binding, soluble 3	0.002935	6.300563
20.63	*HDC*	histidine decarboxylase	0.006479	5.093721
20.32	*MRGPRA2A*	MAS-related GPR, member A2A	0.000668	9.222977
19.58	*SPNA1*	spectrin alpha 1	0.000225	12.11429
19.40	*PLBD1*	phospholipase B domain containing 1	0.008732	4.689462
17.93	*MMRN1*	multimerin 1	0.005711	5.272437
17.71	*CCL6*	chemokine (C-C motif) ligand 6	0.000563	9.629102
15.89	*C3*	complement component 3	0.002858	6.345243
15.67	*VPREB3*	pre-B lymphocyte gene 3	0.000311	11.17124
14.66	*CXCR2*	chemokine (C-X-C motif) receptor 2	0.001126	8.077367
14.55	*MRGPRA2B*	MAS-related GPR, member A2B	0.001429	7.598519
14.13	*ZDHHC22*	zinc finger, DHHC-type containing 22	0.002787	6.38746
14.07	*PROK2*	prokineticin 2	0.004893	5.49812
14.02	*ST3GAL5*	ST3 beta-galactoside alpha-2,3-sialyltransferase 5	0.000484	9.998391
13.95	*LILRA6*	leukocyte immunoglobulin-like receptor, subfamily A (with TM domain), member 6	0.000403	10.46906
13.72	*FPR1*	formyl peptide receptor 1	0.000362	10.75792

Fold-change	Symbol	Name	Parametric p-value	t-value
13.60	*GPR77*	G protein-coupled receptor 77	0.002215	6.783315
13.21	*PRAM1*	PML-RAR alpha-regulated adaptor molecule 1	0.009999	4.514087
13.12	*GDA*	guanine deaminase	0.000985	8.357811
12.70	*GPR77*	G protein-coupled receptor 77	0.001586	7.397091
12.67	*PROM1*	prominin 1	0.000868	8.629861
12.53	*LILRA6*	leukocyte immunoglobulin-like receptor, subfamily A (with TM domain), member 6	0.000658	9.258265
11.83	*MEFV*	Mediterranean fever	0.006395	5.112074
11.73	*PILRA*	paired immunoglobin-like type 2 receptor alpha	0.002195	6.79945
11.64	*GYPA*	glycophorin A	0.000601	9.470268
11.29	*FECH*	ferrochelatase	0.000673	9.203285
11.19	*MKRN1*	makorin, ring finger protein, 1	0.00495	5.481013
11.08	*ADD2*	adducin 2 (beta)	0.002198	6.796708
10.98	*NHSL2*	NHS-like 2	0.000766	8.908844
10.69	*MOGAT2*	monoacylglycerol O-acyltransferase 2	0.003763	5.899321
10.62	*PIRA7*	paired-Ig-like receptor A7	0.000635	9.34147
10.51	*FCGR4*	Fc receptor, IgG, low affinity IV	0.006676	5.052028
10.15	*ALDH3B1*	aldehyde dehydrogenase 3 family, member B1	0.003212	6.15272
9.94	*BC100530*	cDNA sequence BC100530	0.000799	8.814366
9.70	*OLFR71*	olfactory receptor 71	0.001139	8.052764
9.58	*CD177*	CD177 antigen	0.001275	7.824199
9.56	*ANKRD22*	ankyrin repeat domain 22	0.001705	7.260434
9.04	*CYP4F18*	cytochrome P450, family 4, subfamily f, polypeptide 18	0.00518	5.41417
9.02	*CD300LD*	CD300 molecule-like family member d	0.00183	7.128654
8.90	*CDR2*	cerebellar degeneration-related 2	0.004731	5.548193
8.86	*S100A6*	S100 calcium binding protein A6 (calcyclin)	0.00318	6.169041
8.79	*MGLL*	monoglyceride lipase	0.009592	4.567357
8.14	*IRG1*	immunoresponsive gene 1	0.004082	5.772525
8.11	*MGLL*	monoglyceride lipase	0.009761	4.544912

Fold-change	Symbol	Name	Parametric p-value	t-value
7.99	*STFA2*	stefin A2	0.004083	5.771989
7.64	*TSPAN33*	tetraspanin 33	0.00233	6.693964
7.52	*CRISPLD2*	cysteine-rich secretory protein LCCL domain containing 2	0.002803	6.377471
7.51	*BUTR1*	butyrophilin related 1	0.002471	6.592366
7.49	*SEMA4A*	sema domain, immunoglobulin domain (Ig), transmembrane domain (TM) and short cytoplasmic domain, (semaphorin) 4A	0.006486	5.092214
7.44	*IL5*	interleukin 5	0.003143	6.187864
7.30	*SLC2A4*	solute carrier family 2 (facilitated glucose transporter), member 4	0.001741	7.220597
7.22	*SLC6A9*	solute carrier family 6 (neurotransmitter transporter, glycine), member 9	0.003596	5.970779
6.97	*AMICA1*	adhesion molecule, interacts with CXADR antigen 1	0.006076	5.184082
6.82	*STFA2L1*	stefin A2 like 1	0.004413	5.653066
6.67	*APOL11B*	apolipoprotein L 11b	0.003045	6.239866
6.58	*CEACAM2*	carcinoembryonic antigen-related cell adhesion molecule 2	0.003437	6.04305
6.52	*PIRA11*	paired-Ig-like receptor A11	0.001563	7.425016
6.43	*CES2G*	carboxylesterase 2G	0.004788	5.530295
6.35	*C5AR1*	complement component 5a receptor 1	0.001505	7.496983
6.14	*CCR2*	chemokine (C-C motif) receptor 2	0.006387	5.113681
6.00	*SLPI*	secretory leukocyte peptidase inhibitor	0.003315	6.101331
5.96	*LOC100042072*	y-linked testis-specific protein 1-like	0.001764	7.196521
5.87	*GATA1*	GATA binding protein 1	0.007391	4.912188
5.73	*NCAM1*	neural cell adhesion molecule 1	0.001757	7.203295
5.59	*PRKCB*	protein kinase C, beta	0.008444	4.733778
5.59	*KLRA22*	killer cell lectin-like receptor subfamily A, member 22	0.004061	5.780442
5.55	*BMX*	BMX non-receptor tyrosine kinase	0.002982	6.274377
5.38	*STFA1*	stefin A1	0.002172	6.817774
5.37	*E2F2*	E2F transcription factor 2	0.005701	5.27512
5.31	*ARID3A*	AT rich interactive domain 3A (BRIGHT-like)	0.008777	4.682838
5.28	*SIGLECH*	sialic acid binding Ig-like lectin H	0.005164	5.418602

Fold-change	Symbol	Name	Parametric p-value	t-value
5.20	*GSN*	gelsolin	0.006702	5.046551
5.20	*GSN*	gelsolin	0.005622	5.295092
4.98	*GRHL2*	grainyhead-like 2 (Drosophila)	0.004273	5.702184
4.86	*ERMAP*	erythroblast membrane-associated protein	0.005854	5.237082
4.66	*SLC25A37*	solute carrier family 25, member 37	0.007211	4.94583
4.64	*RAB44*	RAB44, member RAS oncogene family	0.007148	4.95783
4.53	*ADAM19*	a disintegrin and metallopeptidase domain 19 (meltrin beta)	0.00494	5.484002
4.41	*CRISPLD2*	cysteine-rich secretory protein LCCL domain containing 2	0.003676	5.936147
4.32	*FCNB*	ficolin B	0.003419	6.051379
4.30	*IL28RA*	interleukin 28 receptor alpha	0.007671	4.861939
4.29	*INPP5J*	inositol polyphosphate 5-phosphatase J	0.005039	5.454589
4.26	*SEPX1*	selenoprotein X 1	0.004484	5.628984
4.16	*ABCB10*	ATP-binding cassette, sub-family B (MDR/TAP), member 10	0.008563	4.715185
4.13	*UBE2O*	ubiquitin-conjugating enzyme E2O	0.00742	4.906859
3.92	*SPHK1*	sphingosine kinase 1	0.004673	5.566827
3.90	*NUDT4*	nudix (nucleoside diphosphate linked moiety X)-type motif 4	0.005419	5.348224
3.87	*FDFT1*	farnesyl diphosphate farnesyl transferase 1	0.008921	4.66149
3.65	*MMP25*	matrix metallopeptidase 25	0.00815	4.780797
3.64	*LTB4R1*	leukotriene B4 receptor 1	0.0065	5.089202
3.60	*PYGL*	liver glycogen phosphorylase	0.00958	4.569028
3.59	*OLFR1441*	olfactory receptor 1441	0.008834	4.674291
3.42	*ABCA13*	ATP-binding cassette, sub-family A (ABC1), member 13	0.008607	4.708414
3.31	*CLDN15*	claudin 15	0.008081	4.792024
3.24	*MFHAS1*	malignant fibrous histiocytoma amplified sequence 1	0.009891	4.52793
-3.36	*WFDC2*	WAP four-disulfide core domain 2	0.007201	-4.94784
-3.73	*FOXD4*	forkhead box D4	0.008692	-4.69562
-3.73	*GRCC10*	gene rich cluster, C10 gene	0.008033	-4.80003
-4.50	*PHPT1*	phosphohistidine phosphatase 1	0.006165	-5.16354

Fold-change	Symbol	Name	Parametric p-value	t-value
-5.78	*HIST1H4K*	histone cluster 1, H4k	0.007418	-4.90731
-6.02	*HIST1H4J*	histone cluster 1, H4j	0.006094	-5.17991
-6.20	*HIST1H4C*	histone cluster 1, H4c	0.003784	-5.89037
-6.24	*ATP6*	ATP synthase F0 subunit 6	0.008363	-4.74638
-6.61	*HIST1H2AK*	histone cluster 1, H2ak	0.007039	-4.979
-6.73	*HIST1H4D*	histone cluster 1, H4d	0.007439	-4.90354
-8.67	*GLRX2*	glutaredoxin 2 (thioltransferase)	0.002577	-6.52025
-11.76	*RMRP*	RNA component of mitochondrial RNAase P	0.008392	-4.74194

7.3 Microarray data: GMP

Table 7.2 Significant ($p<0.01$) differentially up- and down-regulated genes in DARC KO GMP cells from microarray study.

Fold-change	Symbol	Name	Para-metric p-value	t-value
1299.918	*CAMP*	cathelicidin antimicrobial peptide	0.000267	12.03715
357.0088	*CAMP*	cathelicidin antimicrobial peptide	0.000781	9.139834
457.9743	*HBB-B1*	hemoglobin, beta adult major chain	9.68E-05	15.57128
413.8867	*S100A9*	S100 calcium binding protein A9 (calgranulin B)	0.000393	10.9049
285.2716	*RETNLG*	resistin like gamma	9.56E-06	27.84513
152.3321	*LTF*	lactotransferrin	0.000973	8.63404
170.9426	*NGP*	neutrophilic granule protein	7.27E-05	16.73881
181.9238	*HBA-A2*	hemoglobin alpha, adult chain 2	0.000138	14.22782
147.5344	*HBA-A1*	hemoglobin alpha, adult chain 1	0.000379	11.01015
145.3437	*HBB-B2*	hemoglobin, beta adult minor chain	0.001385	7.87226
131.2353	*IFI202B*	interferon activated gene 202B	3.89E-05	19.58281
106.59	*IFI202B*	interferon activated gene 202B	0.000969	8.641521
86.83853	*ALAS2*	aminolevulinic acid synthase 2, erythroid	4.13E-05	19.29982
75.28579	*RHD*	Rh blood group, D antigen	0.000637	9.634034
59.75624	*CHI3L3*	chitinase 3-like 3	0.001134	8.296324
47.22655	*BETA-S*	hemoglobin subunit beta-1-like	0.009394	4.675196
73.45551	*AHSP*	alpha hemoglobin stabilizing protein	0.000875	8.87404
43.09595	*ITGB2L*	integrin beta 2-like	0.001164	8.239638
55.74978	*S100A8*	S100 calcium binding protein A8 (calgranulin A)	0.000536	10.07249
34.11875	*SIRPB1B*	signal-regulatory protein beta 1B	0.004677	5.683285
44.93004	*AQP1*	aquaporin 1	0.000136	14.27863
45.46432	*SNCA*	synuclein, alpha	1.29E-05	25.81321
35.87348	*PLBD1*	phospholipase B domain containing 1	0.001791	7.356988

Fold-change	Symbol	Name	Para-metric p-value	t-value
29.34044	*MMP8*	matrix metallopeptidase 8	0.000303	11.65928
28.47696	*FAM46C*	family with sequence similarity 46, member C	0.000554	9.987735
24.60934	*AA467197*	expressed sequence AA467197	0.002566	6.686838
26.36377	*ST3GAL5*	ST3 beta-galactoside alpha-2,3-sialyltransferase 5	0.000703	9.392834
25.1563	*ITLN1*	intelectin 1 (galactofuranose binding)	0.000212	12.76592
22.2565	*SLC4A1*	solute carrier family 4 (anion exchanger), member 1	7.07E-05	16.85385
21.6894	*GM5483*	predicted gene 5483	0.005589	5.410939
21.06786	*FPR2*	formyl peptide receptor 2	3.81E-05	19.69363
17.9257	*SLC38A5*	solute carrier family 38, member 5	0.001709	7.449092
16.68893	*IGJ*	immunoglobulin joining chain	0.001035	8.496598
14.69588	*CHI3L1*	chitinase 3-like 1	0.001346	7.931548
14.35971	*ZDHHC22*	zinc finger, DHHC-type containing 22	0.00094	8.710488
14.1952	*GM6522*	chitinase 3-like 3 pseudogene	0.005608	5.406029
13.01874	*RSAD2*	radical S-adenosyl methionine domain containing 2	0.000576	9.889326
12.571	*CTSE*	cathepsin E	0.000807	9.062293
12.33174	*FCER1A*	Fc receptor, IgE, high affinity I, alpha polypeptide	0.009578	4.649321
12.24198	*SCRG1*	scrapie responsive gene 1	0.003213	6.294758
11.55962	*STFA2L1*	stefin A2 like 1	0.003603	6.102583
11.47234	*ERMAP*	erythroblast membrane-associated protein	0.00182	7.326602
11.39002	*ADAM8*	a disintegrin and metallopeptidase domain 8	0.004594	5.711323
11.23685	*PDZK1IP1*	PDZK1 interacting protein 1	9.89E-05	15.48478
10.93351	*VPREB3*	pre-B lymphocyte gene 3	0.003101	6.355228
10.88412	*PLA2G7*	phospholipase A2, group VII (platelet-activating factor acetylhydrolase, plasma)	0.005259	5.502926
10.65692	*PF4*	platelet factor 4	0.002139	7.019331
10.63031	*CTLA2A*	cytotoxic T lymphocyte-associated protein 2 alpha	0.000526	10.11961
9.953441	*SIRPB1A*	signal-regulatory protein beta 1A	0.004855	5.625248
9.59762	*FPR1*	formyl peptide receptor 1	0.001424	7.815444
9.510684	*RPS24*	ribosomal protein S24	0.009377	4.677611
9.190772	*NUF2*	NUF2, NDC80 kinetochore complex component, homolog (S. cerevisiae)	0.000183	13.25005

Fold-change	Symbol	Name	Para-metric p-value	t-value
8.585921	*F2R*	coagulation factor II (thrombin) receptor	0.004637	5.696916
8.176762	*EPOR*	erythropoietin receptor	0.003268	6.265991
8.142974	*ADD2*	adducin 2 (beta)	0.005439	5.451817
8.100505	*ART4*	ADP-ribosyltransferase 4	0.006744	5.135146
8.050571	*FHDC1*	FH2 domain containing 1	0.001097	8.367229
7.960679	*LILRB3*	leukocyte immunoglobulin-like receptor, subfamily B (with TM and ITIM domains), member 3	0.002715	6.58647
7.875625	*S100A6*	S100 calcium binding protein A6 (calcyclin)	0.00116	8.245976
7.709034	*TUG1*	taurine upregulated gene 1	0.009717	4.630084
7.67796	*IFITM6*	interferon induced transmembrane protein 6	0.000406	10.81775
7.646765	*ANKRD22*	ankyrin repeat domain 22	0.009668	4.636809
7.634908	*MGLL*	monoglyceride lipase	0.005811	5.352971
7.275156	*GM14548*	predicted gene 14548	0.007643	4.95762
6.933328	*FGR*	Gardner-Rasheed feline sarcoma viral (Fgr) oncogene homolog	0.000691	9.433297
6.856131	*EPB4.9*	erythrocyte protein band 4.9	0.000262	12.10256
6.85518	*LTB*	lymphotoxin B	0.000977	8.622916
6.815796	*PIRA7*	paired-Ig-like receptor A7	0.008112	4.874806
6.787061	*MS4A1*	membrane-spanning 4-domains, subfamily A, member 1	0.008867	4.752922
6.661626	*SIRPB1A*	signal-regulatory protein beta 1A	0.003237	6.282154
6.552838	*BST1*	bone marrow stromal cell antigen 1	0.002795	6.535483
6.288875	*ITLN1*	intelectin 1 (galactofuranose binding)	0.004301	5.815522
6.235769	*TSPAN33*	tetraspanin 33	0.000852	8.936726
6.223626	*GM11428*	predicted gene 11428	0.00131	7.988815
6.188198	*CES2G*	carboxylesterase 2G	0.006538	5.179828
6.134249	*SLC14A1*	solute carrier family 14 (urea transporter), member 1	0.00052	10.15174
6.115285	*GYPA*	glycophorin A	0.000548	10.01633
6.10157	*LY6D*	lymphocyte antigen 6 complex, locus D	0.001674	7.489839
5.771065	*GM10693*	predicted pseudogene 10693	0.002977	6.425451
5.731663	*APOL8*	apolipoprotein L 8	0.00311	6.350174
5.704967	*LILRA6*	leukocyte immunoglobulin-like receptor, subfamily A (with TM domain), member 6	0.007009	5.079888

Fold-change	Symbol	Name	Para-metric p-value	t-value
5.577841	*LILRA6*	leukocyte immunoglobulin-like receptor, subfamily A (with TM domain), member 6	0.001467	7.754438
5.527655	*PEX11C*	peroxisomal biogenesis factor 11 gamma	0.00651	5.18603
5.445753	*ISG20*	interferon-stimulated protein	0.000431	10.65207
5.346245	*SLC6A9*	solute carrier family 6 (neurotransmitter transporter, glycine), member 9	0.000293	11.75981
5.306081	*KEL*	Kell blood group	0.000527	10.11501
5.200905	*NR3C1*	nuclear receptor subfamily 3, group C, member 1	0.007717	4.944135
4.976604	*OLFR312*	olfactory receptor 312	0.007077	5.066086
4.945319	*NUF2*	NUF2, NDC80 kinetochore complex component, homolog (S. cerevisiae)	0.000451	10.52732
4.811501	*PDZK1IP1*	PDZK1 interacting protein 1	0.007654	4.955631
4.726137	*GM10872*	predicted gene 10872	0.003688	6.064157
4.537062	*GM6792*	predicted gene 6792	0.005667	5.390139
4.505204	*SLC6A9*	solute carrier family 6 (neurotransmitter transporter, glycine), member 9	0.000745	9.252588
4.449686	*BUTR1*	butyrophilin related 1	0.001224	8.131262
4.371499	*ANK1*	ankyrin 1, erythroid	0.002371	6.829628
4.302823	*GDPD2*	glycerophosphodiester phosphodiesterase domain containing 2	0.005765	5.364622
4.280243	*GM13152*	predicted gene 13152	0.004684	5.681189
4.240546	*IL28RA*	interleukin 28 receptor alpha	0.007963	4.900524
4.226138	*LHX3*	LIM homeobox protein 3	0.009458	4.666083
4.219845	*ALOXE3*	arachidonate lipoxygenase 3	0.004133	5.878972
4.21471	*DDX23*	DEAD (Asp-Glu-Ala-Asp) box polypeptide 23	0.006675	5.149905
4.153978	*CEACAM10*	carcinoembryonic antigen-related cell adhesion molecule 10	0.003582	6.112173
4.139992	*ABCG4*	ATP-binding cassette, sub-family G (WHITE), member 4	0.004543	5.728862
4.131521	*PIRA11*	paired-Ig-like receptor A11	0.004306	5.813411
4.102952	*CTLA2B*	cytotoxic T lymphocyte-associated protein 2 beta	0.001084	8.394606
4.089062	*GATA1*	GATA binding protein 1	0.00051	10.20381
4.025715	*ROBO3*	roundabout homolog 3 (Drosophila)	0.009763	4.623886
3.964432	*ZFPM1*	zinc finger protein, multitype 1	0.005106	5.547805
3.937079	*ITLN1*	intelectin 1 (galactofuranose binding)	0.000565	9.935122
3.892899	*ZFPM1*	zinc finger protein, multitype 1	0.005468	5.443795

Fold-change	Symbol	Name	Para-metric p-value	t-value
3.887415	*OLFR141*	olfactory receptor 141	0.007145	5.052507
3.85886	*GFI1B*	growth factor independent 1B	0.003611	6.099124
3.847685	*ABCG4*	ATP-binding cassette, sub-family G (WHITE), member 4	0.007938	4.904821
3.825118	*IL1RL1*	interleukin 1 receptor-like 1	0.003996	5.933315
3.814264	*GM5196*	chromobox homolog 3 pseudogene	0.000875	8.875132
3.769203	*GM14325*	predicted gene 14325	0.002415	6.795574
3.686704	*DNAJC10*	DnaJ (Hsp40) homolog, subfamily C, member 10	0.000891	8.834269
3.668078	*RHBDL1*	rhomboid, veinlet-like 1 (Drosophila)	0.003584	6.111452
3.657873	*RAB37*	RAB37, member of RAS oncogene family	0.004393	5.7819
3.605121	*SLC26A3*	solute carrier family 26, member 3	0.008435	4.821096
3.582563	*MCF2L*	mcf.2 transforming sequence-like	0.002204	6.963535
3.563904	*SOWAHA*	sosondowah ankyrin repeat domain family member A	0.009244	4.696747
3.557407	*CAPZA1*	capping protein (actin filament) muscle Z-line, alpha 1	0.000745	9.252409
3.544677	*RAB37*	RAB37, member of RAS oncogene family	0.006401	5.210577
3.52069	*ZFP931*	zinc finger protein 931	0.003989	5.936077
3.488917	*JHDM1D*	jumonji C domain-containing histone demethylase 1 homolog D (S. cerevisiae)	0.001638	7.533139
3.455098	*TGM2*	transglutaminase 2, C polypeptide	0.006133	5.273187
3.454203	*IFI27L2A*	interferon, alpha-inducible protein 27 like 2A	0.002659	6.623242
3.417496	*S1PR1*	sphingosine-1-phosphate receptor 1	0.0067	5.144599
3.366178	*VANGL1*	vang-like 1 (van gogh, Drosophila)	0.007853	4.919775
3.339354	*GM14308*	predicted gene 14308	0.004606	5.707319
3.299323	*CBX3*	chromobox homolog 3 (Drosophila HP1 gamma)	0.004037	5.916708
3.270372	*CRISPLD2*	cysteine-rich secretory protein LCCL domain containing 2	0.007736	4.940638
3.268583	*GM14391*	predicted gene 14391	0.002439	6.777796
3.261638	*GM14393*	predicted gene 14393	0.002685	6.605611
3.255634	*DYNLT1C*	dynein light chain Tctex-type 1C	0.004405	5.777552
3.251284	*BLVRB*	biliverdin reductase B (flavin reductase (NADPH))	0.001543	7.652174
3.208248	*CD2*	CD2 antigen	0.003035	6.392073
3.168414	*CCL6*	chemokine (C-C motif) ligand 6	0.004434	5.767308

Fold-change	Symbol	Name	Para-metric p-value	t-value
3.123637	*CXCR2*	chemokine (C-X-C motif) receptor 2	0.001238	8.107056
3.094544	*MORF4L2*	mortality factor 4 like 2	0.001393	7.860706
3.05565	*SYCN*	syncollin	0.009643	4.640287
3.051958	*EIF4A2*	eukaryotic translation initiation factor 4A2	0.002634	6.64011
3.031052	*EPB4.2*	erythrocyte protein band 4.2	0.001773	7.377047
3.030024	*RPS6KA2*	ribosomal protein S6 kinase, polypeptide 2	0.004352	5.796808
3.025964	*GM14411*	predicted gene 14411	0.005173	5.528067
3.006443	*CELF6*	CUGBP, Elav-like family member 6	0.007861	4.918383
-3.16358	*DTX3*	deltex 3 homolog (Drosophila)	0.008567	-4.79988
-3.23963	*WDR72*	WD repeat domain 72	0.001943	-7.20008
-3.34374	*MAFF*	v-maf musculoaponeurotic fibrosarcoma oncogene family, protein F (avian)	0.009851	-4.612
-3.36245	*TNS4*	tensin 4	0.001719	-7.43767
-3.43232	*ITGA5*	integrin alpha 5 (fibronectin receptor alpha)	0.008099	-4.87707
-3.54184	*PLEKHJ1*	pleckstrin homology domain containing, family J member 1	0.006987	-5.08441
-3.67918	*PIK3IP1*	phosphoinositide-3-kinase interacting protein 1	0.009348	-4.68184
-3.97775	*TOX4*	TOX high mobility group box family member 4	0.009536	-4.65523
-4.53167	*APOA2*	apolipoprotein A-II	0.001706	-7.45248
-5.57718	*KRTAP5-4*	keratin associated protein 5-4	0.000589	-9.83038
-5.95546	*DUSP23*	dual specificity phosphatase 23	0.001725	-7.43057
-26.5995	*IQSEC3*	IQ motif and Sec7 domain 3	0.002505	-6.72976

7.4 LSK Low-density array results

Table 7.3 Gene expression results from low-density array of DARC KO and FYB(ES)TG LSK cells. Significance calculated by upaired two way Student t test.

Gene	WT		DARC KO			FYB(ES)TG		
	Mean Fold Change	Standard Deviation	Mean Fold Change	Standard Deviation	t-test	Mean Fold Change	Standard Deviation	t-test
18S	1	0.76	0.89	0.63	n	0.79	0.21	n
ALAS2	1	5.26	0.80	5.08	n	0.73	4.58	n
CD19	1	2.86	1.53	3.44	n	1.24	1.47	n
CD2	1	2.63	2.51	0.97	n	2.60	1.86	n
C/EBPA	1	0.86	0.76	0.78	n	0.78	0.58	n
C/EBPΔ	1	0.74	0.52	0.36	n	0.23	1.29	*
C/EBPE	1	1.75	2.35	2.21	n	1.58	1.95	n
CSF3R	1	0.40	1.08	0.28	n	1.21	0.16	n
CXCR2	1	1.38	1.35	1.20	n	1.08	1.60	n
CXCR4	1	1.23	2.30	0.59	*	3.54	0.62	*
FLT3	1	0.25	1.06	0.42	n	0.82	0.41	n
FZD4	1	0.56	1.45	0.92	n	2.03	1.37	n
GAPDH	1	0.18	1.04	0.20	n	1.02	0.08	n
GATA1	1	0.76	1.50	0.95	n	1.50	0.76	n
GATA2	1	0.36	1.02	0.25	n	1.27	0.61	n
HBB-B1	1	5.08	0.82	4.50	n	0.77	5.96	n
HLF	1	0.28	1.12	0.35	n	1.27	0.06	*
HPRT	1	0.23	0.96	0.23	n	0.95	0.11	n
IFITM6	1	2.22	1.29	2.96	n	0.77	3.87	n
ITGAM	1	1.33	0.88	0.83	n	0.67	0.79	n
KLF4	1	1.07	0.76	0.86	n	1.08	1.17	n
LMO2	1	0.29	0.96	0.16	n	1.05	0.16	n
LTF	1	3.01	1.03	4.14	n	0.85	3.14	n
MMP8	1	3.05	1.37	3.37	n	0.84	3.24	n
NGP	1	3.06	1.05	5.00	n	0.64	3.31	n
RETNLG	1	3.93	1.11	3.37	n	0.86	2.27	n
RHD	1	2.77	0.95	2.14	n	1.05	3.30	n
S100A9	1	2.51	2.90	2.98	n	1.04	2.63	n
SLFN4	1	5.00	1.50	3.94	n	1.76	2.72	n
SPIB	1	1.39	2.04	1.83	n	1.84	2.26	n
STAT6	1	0.76	0.85	0.40	n	0.76	0.24	n
VCAM1	1	0.54	1.07	1.24	n	0.41	1.55	*

7.5 GMP Low-density array results

Table 7.4 Gene expression results from low-density array of DARC KO and FYB(ES)TG GMP cells. Significance calculated by upaired two way Student t test.

Gene	WT		DARC KO			FYB(ES)TG		
	Mean Fold Change	Standard Deviation	Mean Fold Change	Standard Deviation	t-test	Mean Fold Change	Standard Deviation	t-test
18S	1	0.30	1.59	0.70	ns	1.27	0.26	ns
ALAS2	1	1.39	3.34	1.59	ns	8.72	2.10	ns
CD19	1	0.64	9.13	1.14	**	12.53	1.48	*
CD2	1	0.94	3.54	0.45	*	6.79	2.05	ns
C/EBPA	1	0.40	1.76	1.32	ns	1.74	0.68	ns
C/EBPΔ	1	0.44	1.31	0.30	ns	1.32	0.70	ns
C/EBPE	1	0.21	0.92	0.79	ns	0.83	0.62	ns
CSF3R	1	0.24	1.07	0.47	ns	1.02	0.45	ns
CXCR2	1	0.38	1.14	0.49	ns	1.06	0.69	ns
CXCR4	1	1.06	2.19	1.42	ns	2.51	1.23	ns
FLT3	1	0.49	0.83	0.62	ns	1.04	0.80	ns
FZD4	1	0.12	1.25	0.39	ns	1.66	0.31	*
GAPDH	1	0.14	1.03	0.10	ns	0.99	0.09	ns
GATA1	1	0.76	2.88	1.24	ns	2.86	0.56	*
GATA2	1	0.52	2.27	1.17	ns	2.63	0.31	**
HBB-B1	1	1.71	3.25	1.64	ns	5.55	2.02	*
HLF	1	0.38	1.36	0.77	ns	1.28	0.20	ns
HPRT	1	0.20	1.03	0.13	ns	1.04	0.07	ns
IFITM6	1	0.38	1.79	0.69	ns	2.37	0.53	*
ITGAM	1	0.37	1.24	0.47	ns	1.16	0.23	ns
KLF4	1	0.76	1.88	0.67	ns	1.96	0.45	ns
LMO2	1	0.13	1.11	0.26	ns	1.13	0.25	ns
LTF	1	0.90	3.30	1.43	ns	6.76	2.33	ns
MMP8	1	0.24	2.37	1.03	ns	2.24	0.28	*
NGP	1	0.42	4.00	1.26	ns	2.81	1.41	ns
RETNLG	1	0.82	3.39	1.41	ns	5.60	2.13	ns
RHD	1	1.22	3.99	1.92	ns	8.56	2.01	ns
S100A9	1	1.09	5.04	1.20	*	4.72	2.25	ns
SLFN4	1	0.92	2.09	1.19	ns	6.06	2.20	ns
SPIB	1	1.06	2.57	1.03	ns	6.95	2.03	ns
STAT6	1	0.04	0.78	2.37	ns	1.25	0.32	ns
VCAM1	1	0.80	4.20	1.74	ns	0.55	0.46	*

7.6 Complete multiplex chemokine and cytokine results – serum

Table 7.5 Results of all analytes from multiplex chemokine and cytokine assay of serum from WT, DARC KO and FYB(ES)TG mice.

Sig, significance, calculated by Mann Whitney test

Analyte	WT		DARC KO			FYB(ES)TG		
	Mean Pg/mg	Range Pg/mg	Mean Pg/mg	Range Pg/mg	Sig	Mean Pg/mg	Range Pg/mg	Sig
G-CSF	138.62	61.84-262.71	254.80	207.32-336.42	*	414.83	226.90-569.39	***
GM-CSF	0	0	0	0	ns	0	0	ns
M-CSF	0	0	0	0	ns	0	0	ns
IFN-GAMMA	0	0	0	0	ns	0	0	ns
IL-1ALPHA	552.05	61.69-2086	133.55	78.05-277.85	ns	134.77	65.41-348.61	ns
IL-1BETA	0	0	0	0	ns	0	0	ns
IL-2	0	0	0	0	ns	0	0	ns
IL-3	0	0	0	0	ns	0	0	ns
IL-4	0	0	0	0	ns	0	0	ns
IL-5	0	0	0	0	ns	0	0	ns
IL-6	0	0	0	0	ns	0	0	ns
IL-9	92.10	0-258.87	62.32	37.18-107.56	ns	54.11	0-82.05	ns
IL-10	0	0	0	0	ns	0	0	ns
IL-12P40	0	0	0	0	ns	0	0	ns
IL-12P70	0	0	0	0	ns	0	0	ns
IL-13	49.12	0-144.53	29.42	0-79.99	ns	37.88	0-73.20	ns
IL-15	0	0	0	0	ns	0	0	ns
IL-17	0	0	0	0	ns	0	0	ns
LIF	0	0	0	0	ns	0	0	ns
CXCL1	51.13	27.45-68.58	12.05	0-42.93	*	7.89	0-33.30	*
CXCL2	0	0	0	0	ns	0	0	ns
CXCL5	6255.19	4568.77-7701.04	7770.51	5540.02-9310.13	ns	5758.88	2126.58-7120.32	ns
CXCL9	71.15	50.84-110.74	82.13	56.88-159.97	ns	75.17	49.81-113.87	ns
CXCL10	67.69	51.20-76.97	52.27	34.06-73.60	ns	52.46	44.83-62.42	ns
CCL2	0	0	0	0	ns	0	0	ns
CCL3	0	0	0	0	ns	0	0	ns
CCL4	0	0	0	0	ns	0	0	ns
CCL5	6.60	0-14.83	7.32	2.97-11.20	ns	8.05	5.88-10.65	ns
CCL11	137.62	70.51-182.25	111.61	88.01-157.55	ns	173.88	150.15-227.74	*
VEGF	0	0	0	0	ns	0	0	ns
TNF-ALPHA	0	0	0	0	ns	0	0	ns

7.7 Complete multiplex chemokine and cytokine results – bone marrow supernatant

Table 7.6 Results of all analytes from multiplex chemokine and cytokine assay of bone marrow supernatant from WT, DARC KO and FYB(ES)TG mice.

Sig, significance, calculated by Mann Whitney test

Analyte	WT		DARC KO			FYB(ES)TG		
	Mean pg/mg	Range pg/mg	Mean pg/mg	Range pg/mg	Sig	Mean pg/mg	Range pg/mg	Sig
G-CSF	2.41	0.60-5.67	2.22	0.64-4.26	ns	6.31	1.02-55.38	ns
GM-CSF	11.94	0-28.12	13.44	0-36.52	ns	23.72	0-65.85	*
M-CSF	7.3	0-21.98	5.67	0.06-15.56	ns	14.53	0-65.19	ns
IFN-GAMMA	57.02	0-286.40	28.01	0-151.72	ns	59.98	0-271.35	ns
IL-1ALPHA	104.64	0-347.15	59.60	4.35-271.84	ns	123.05	8.88-354.56	ns
IL-1BETA	0	0	0	0	ns	0	0	ns
IL-2	0	0	0	0	ns	0	0	ns
IL-3	0	0	0	0	ns	0	0	ns
IL-4	0	0	0	0	ns	0	0	ns
IL-5	0	0	0	0	ns	0	0	ns
IL-6	19.31	0-32.54	6.95	0-33.71	ns	19.17	0-84.51	ns
IL-9	0	0	0	0	ns	0	0	ns
IL-10	0	0	0	0	ns	0	0	ns
IL-12P40	0	0	0	0	ns	0	0	ns
IL-12P70	0	0	0	0	ns	0	0	ns
IL-13	140.65	0-209.32	139.55	37.14-306.91	ns	212.21	26.72-429.08	*
IL-15	0	0	0	0	ns	0	0	ns
IL-17	0	0	0	0	ns	0	0	ns
LIF	0	0	0	0	ns	0	0	ns
CXCL1	18.76	2.5-73.34	7.87	1.49-23.59	*	17.31	2.94-59.98	ns
CXCL2	65.72	0-121.75	66.12	0-136.61	ns	76.04	0-203.91	*
CXCL5	88.32	43.89-182.96	72.21	36.85-117.42	ns	90.19	34.76-163.37	ns
CXCL9	214.01	107.23-428.56	309.26	128.58-473.73	*	326.81	179.48-643.76	**
CXCL10	125.27	68.21-208.65	145.04	79.95-230.65	ns	155.22	79.59-320.24	
CCL2	11.28	0-23.79	12.14	0-25.59	ns	24.10	0-91.36	*
CCL3	12.76	1.32-26.41	9.48	0-36.67	ns	26.03	2.99-78.92	*
CCL4	16.21	1.72-25.44	13.56	0-32.92	ns	22.95	4.08-55.96	ns
CCL5	15.82	5.22-45.93	12.55	4.64-29.17	ns	20.79	6.14-74.41	ns
CCL11	23.22	6.5-34.99	32.69	10.50-69.73	*	86.12	23.08-169.67	*****
VEGF	0	0	0	0	ns	0	0	ns
TNF-ALPHA	0	0	0	0	ns	0	0	ns

7.8 LSK-selected mixed competitive chimeras

The experiment was conducted as per scheme in Figure 4.33. Owing to major variation in the CD45.2 populations the validity of this data is unclear, but it is included here for reference purposes.

Results in **Figure 7.1a** & **b** demonstrate no significant difference spleen size in animals between groups, and bone marrow cell count, respectively.

Peripheral leukocyte counts were not different between the two groups, although neutrophil counts were lower in the WT-KO group, both in absolute terms and as a proportion of all leukocytes, **Figure 7.2**. Haemoglobin and platelet counts were not significantly different between the two groups, **Figure 7.2**.

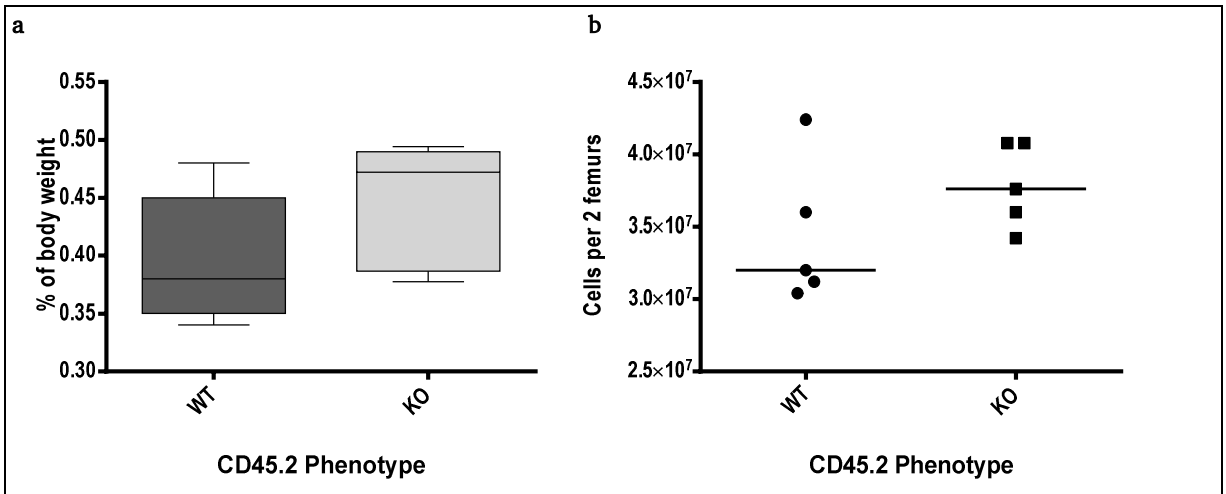

Figure 7.1. Fundamental parameters of mixed LSK-selected competitive chimeras (a) Spleen size classified by CD45.2 competitor, and (b), cell counts in bone marrow femurs. n=5 per group

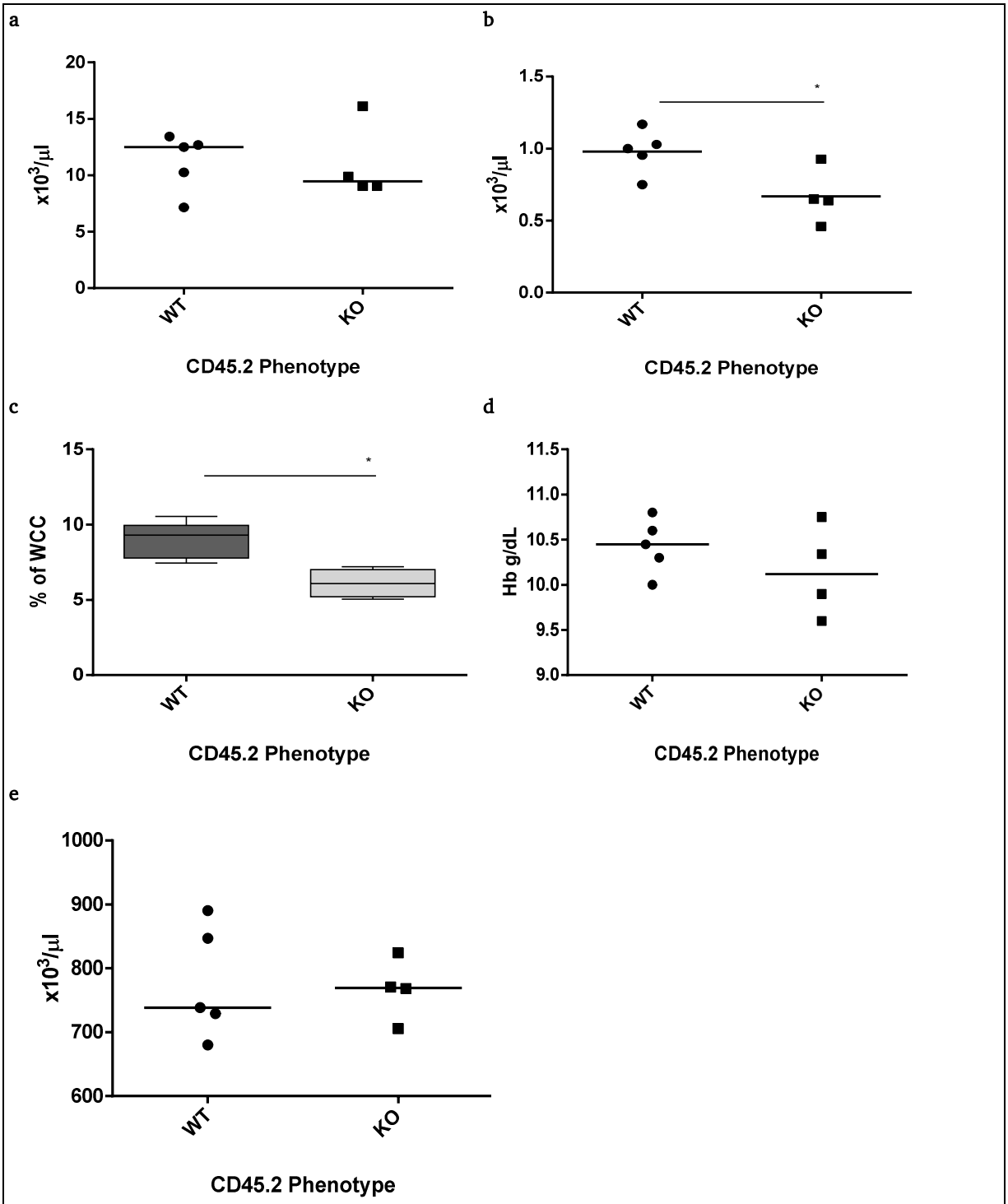

Figure 7.2 Complete blood count of mixed LSK-selected competitive chimeras. Total white cell count (a), neutrophil count (b), neutrophil proportions of white cell counts (c), haemoglobin (d) and platelet count (e), from automated analyser. WT-WT n=5, WT-KO n=4

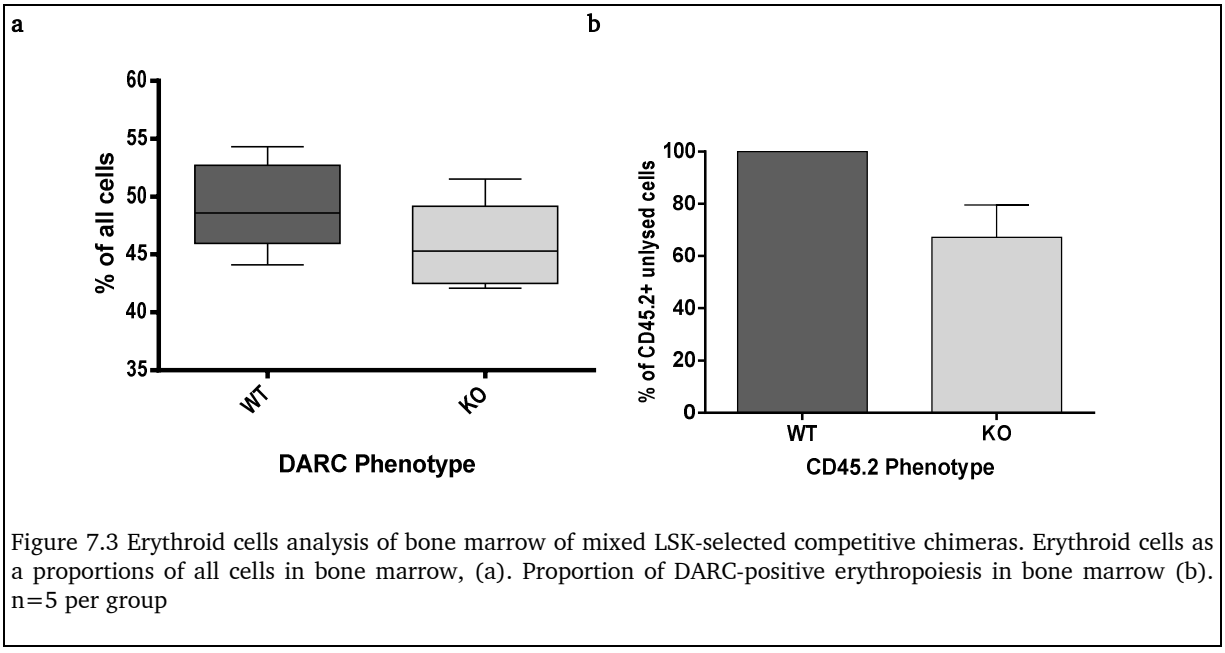

Figure 7.3 Erythroid cells analysis of bone marrow of mixed LSK-selected competitive chimeras. Erythroid cells as a proportions of all cells in bone marrow, (a). Proportion of DARC-positive erythropoiesis in bone marrow (b). n=5 per group

Bone marrow erythroid proportions were not different between the two groups, and in the WT-KO group, DARC negative erythropoiesis accounted on average for approximately 40% of the total erythropoiesis, **Figure 7.3**.

Although neutrophil numbers were lower in WT-KO, **Figure 7.4**, relative to CD45.1xCD45.2, myeloid cells including in particular Gr-1^{Hi} cells proliferated faster in CD45.2 DARC KO bone marrow fraction. Overall CD45.2 proportions between WT and KO were not different relative to CD45.1xCD45.2, largely due to significant variation between mice, with some animals harbouring <5% CD45.2 DARC KO peripheral blood CD45+ cells, and other in excess of 20%. Reasons for this are unclear, but could possibly represent uneven mixing pre-injection, or clumping of LSK cells

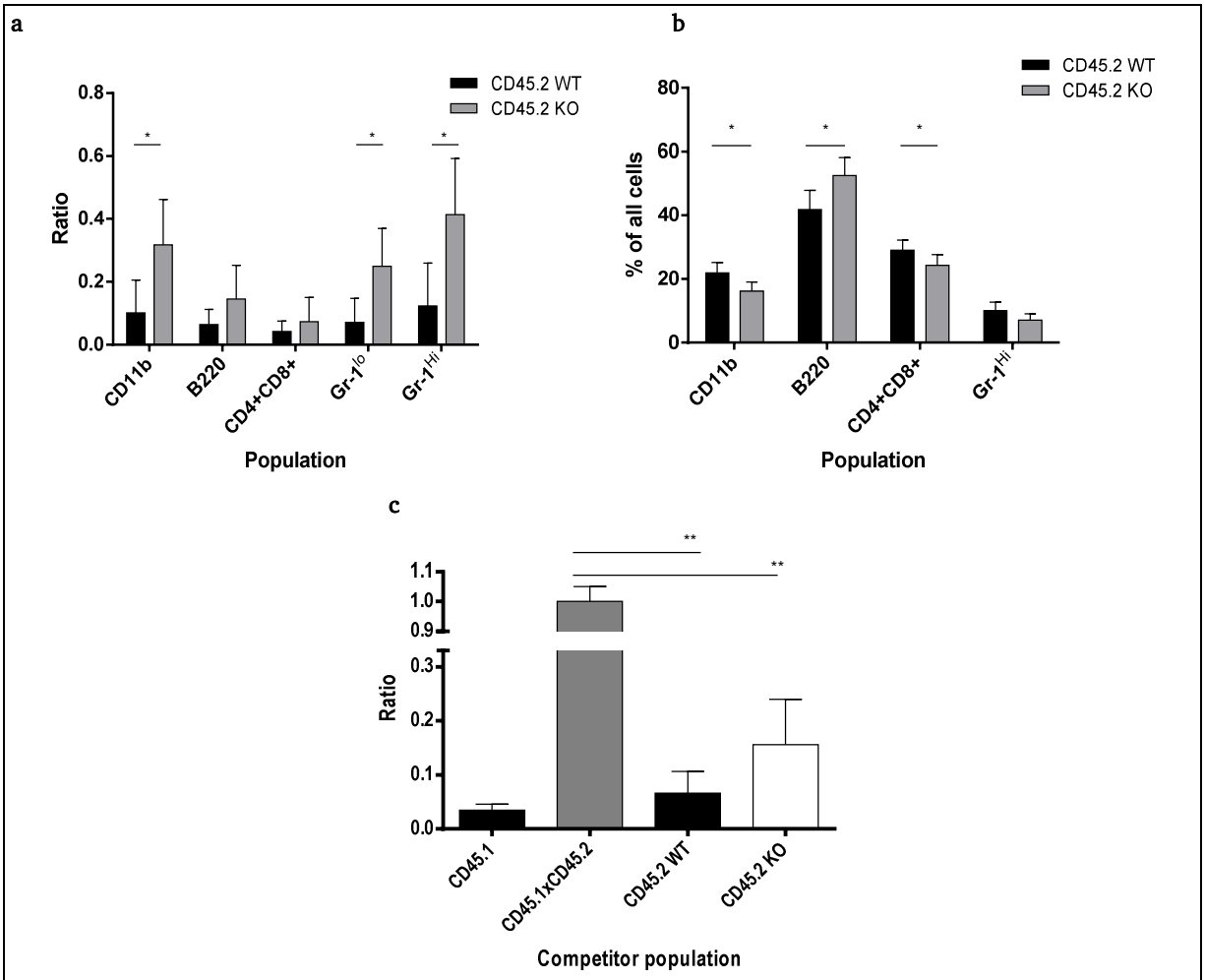

Figure 7.4 Analysis of blood leukocyte populations of mixed LSK-selected competitive chimeras. See Figure 4.28 for representative gating of blood populations examined in mixing chimeras.
(a) CD45.1xCD45.2+ cells were assigned a ratio of 1 (i.e. 100%) within each mouse, and the proportion of CD45.2 cells (WT or KO) were computed. Shown are the relative contributions of CD45.2 WT or KO to CD45.1xCD45.2 competitors for each of the main blood leukocyte populations. (b) Proportions of leukocyte populations in blood, for CD45.2 WT or KO. c) Competitor proportions (CD45.2 WT or KO) relative to CD45.1xCD45.2, averaged over 5 WT or 4KO samples. n=5 per group

Similarly in the bone marrow CD45.2 DARC KO proportions relative to CD45.2 WT were increased, although the large variance between individual animals meant these results were not significantly different, and also in total cell populations, **Figure 7.5a, b**. However overall, there was a relatively higher CD45.2 DARC KO component compared to CD45.2 WT (**Figure 7.5c**).

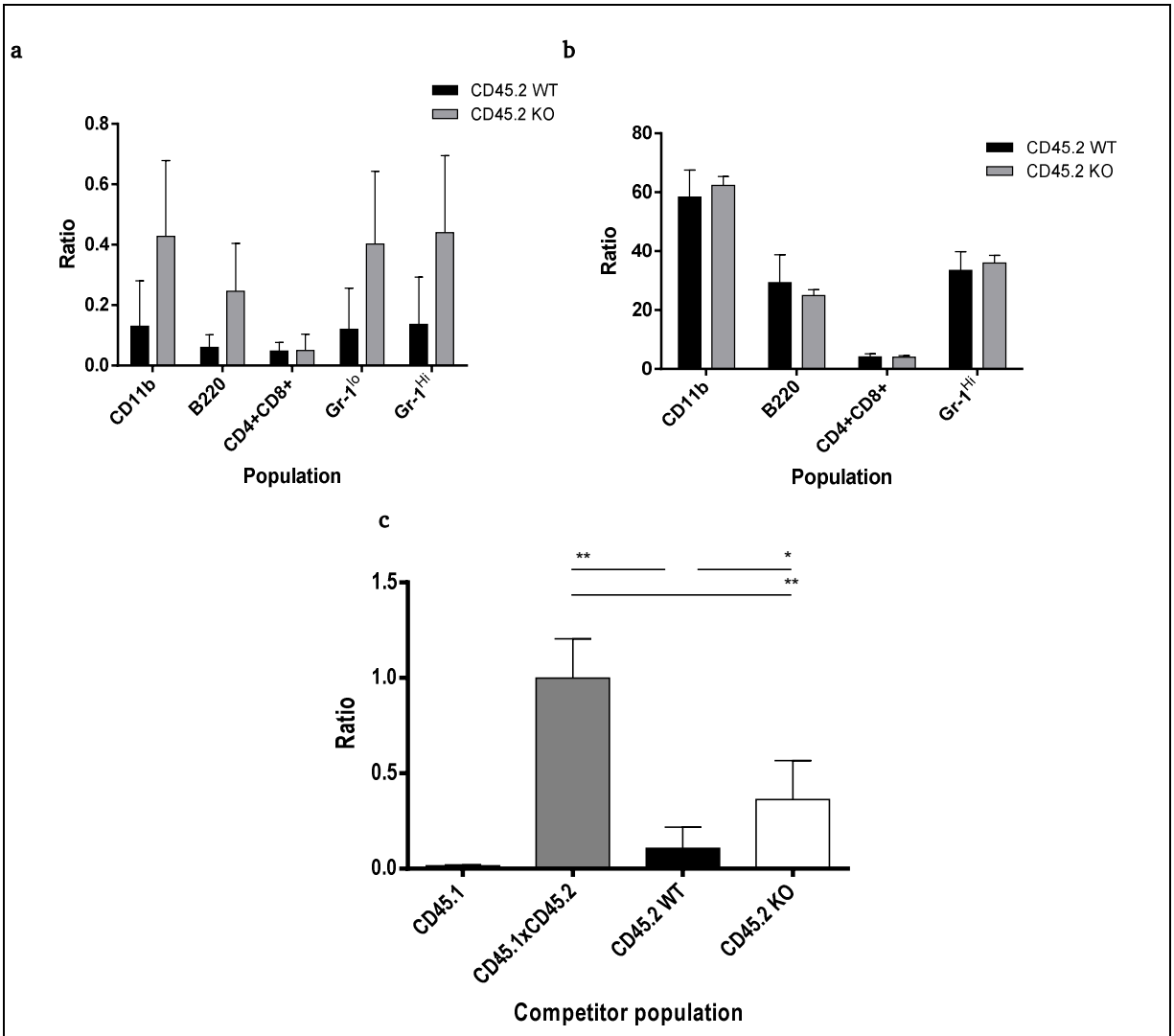

Figure 7.5 Analysis of bone marrow leukocyte populations of mixed LSK-selected competitive chimeras. (a) Relative contributions of CD45.2 compared to CD45.1xCD45.2 in the bone marrow. (b) Proportions of principle bone marrow populations. (c) Overall CD45.2 contributions within the bone marrow relative to CD45.1xCD45.2. n=5 per group.

Examination of the bone marrow progenitors revealed no significant differences in progenitor profiles, particularly for GMP and LSK. However, these data should be interpreted with caution since there was large variance, and visually the GMP populations appeared reduced in CD45.2 DARC KO, although the difference from CD45.2 WT was modest. This would imply that HSC and progenitor cells have possibly been exposed to a wild-type DARC environment for sufficient period to

modify some of the maturation profiles in the DARC KO haematopoietic component (**Figure 7.6**).

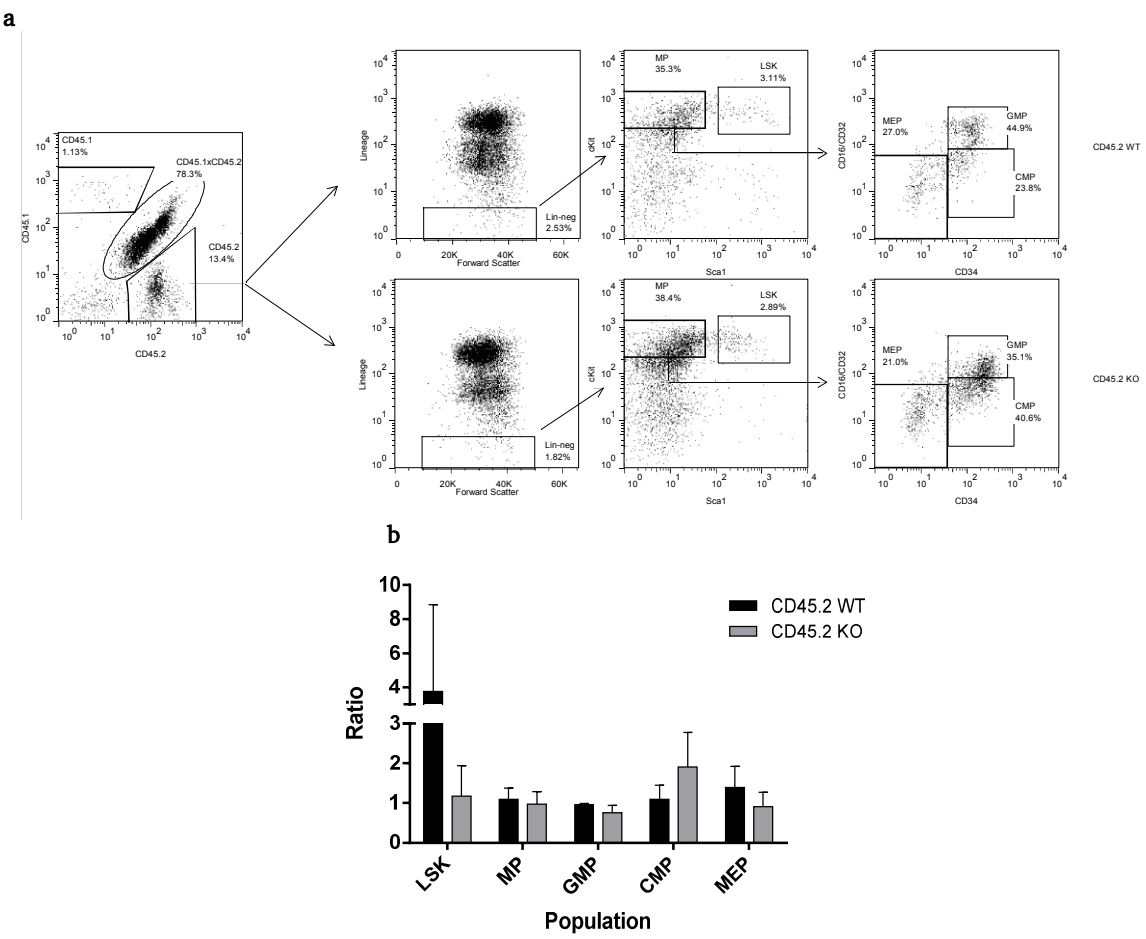

Figure 7.6 Bone marrow lineage-negative populations (LSK and myeloid progenitors) of LSK selected chimeras. Representative gating, (a). Live cells were gated for CD45 expression, and then haematopoietic lineage-negativity. There after subgates examining myeloid progenitors and their sub-populations (GMP: $CD34^{+}$, $CD16/CD32^{+}$, CMP $CD34^{+}$, $CD16/CD32^{low}$, MEP $CD34^{-}$ $CD16/CD32^{-}$). b) $CD45.1xCD45.2^{+}$ cells were assigned a ratio of 1 (i.e. 100%) within each mouse, and the proportion of CD45.2 cells (WT or KO) were computed. Shown are the relative contributions of CD45.2 WT or KO to CD45.1xCD45.2 competitors for each of the main blood leukocyte populations. Data from two animals from the WT-WT group was excluded as CD45.2 chimerism was <5% and hence HSPC data is not considered reliable owing to low cell numbers. n=3-5 per group.

Similarly, there was no significant difference in LSK sub-populations between the two study groups (**Figure 7.7**). However, maturation profiles were significantly different from normal WT mice, with reduced numbers of MPP in both CD45.2 WT and CD45.2 DARC KO. Reasons for this are not clear.

Transplanted HSC establish localised areas of haematopoiesis which is comprised of progenitors from that HSC, forming islands of maturing transplanted cells arising from single HSC. This might partly explain the retention of the reduced-GMP maturation profile in whole bone marrow and LSK-mixed chimeras, since chemokine availability might be locally reduced in, for example, a DARC KO haematopoietic island.

Repetition of this experiment with modifications, such a FACS sorting LSK cells and mixing immediately with competitor cells, and using higher LSK cell numbers per irradiated mouse, may help clarify findings.

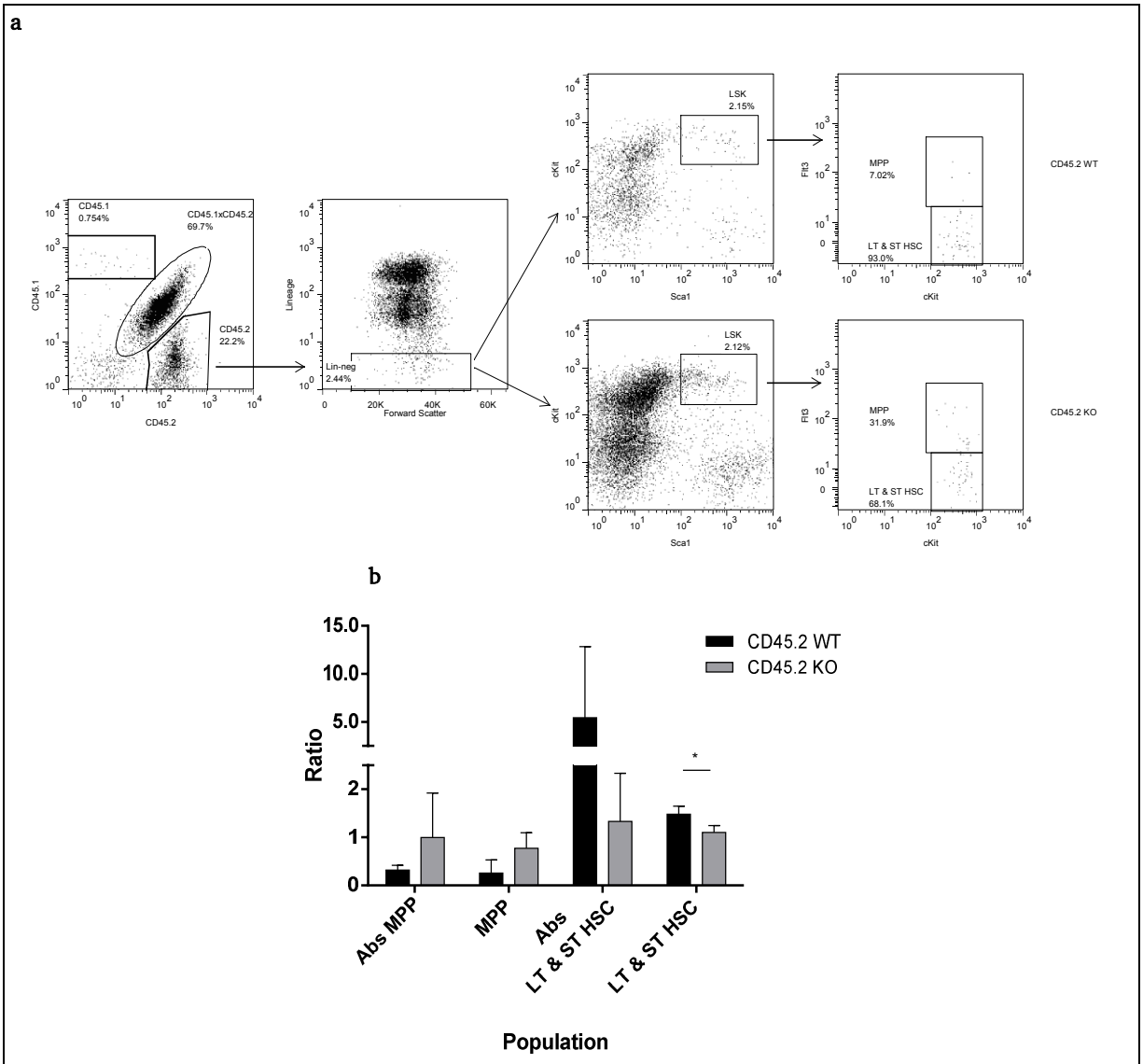

Figure 7.7 Bone marrow LSK sub-populations of LSK selected chimeras, representative gating (a), at 16 weeks following transplantation of 500 LSK cells, either CD45.2 WT or CD45.2 DARC KO mixed with 10^6 CD45.1xCD45.2 competitor into lethally irradiated CD45.1 hosts. Live cells were gated for CD45 expression, and then haematopoietic lineage-negativity. There after subgates examining LSK compartment. b) CD45.1xCD45.2+ cells were assigned a ratio of 1 within each mouse, and the proportion of CD45.2 cells (WT or KO) were computed. Shown are the relative contributions of CD45.2 WT or KO to CD45.1xCD45.2 competitors. Data from two animals from the WT-WT group was excluded as CD45.2 chimerism was <5% and hence HSPC data is not considered reliable owing to low cell numbers. n=3-5 per group.

References

Addison, CL, Belperio, JA, Burdick, MD*, et al.* 2004. Overexpression of the duffy antigen receptor for chemokines (DARC) by NSCLC tumor cells results in increased tumor necrosis. *BMC Cancer,* 4**,** 28.

Adolfsson, J, Borge, OJ, Bryder, D*, et al.* 2001. Upregulation of Flt3 expression within the bone marrow Lin(-)Sca1(+)c-kit(+) stem cell compartment is accompanied by loss of self-renewal capacity. *Immunity,* 15**,** 659-69.

Adolfsson, J, Mansson, R, Buza-Vidas, N*, et al.* 2005. Identification of Flt3+ lympho-myeloid stem cells lacking erythro-megakaryocytic potential a revised road map for adult blood lineage commitment. *Cell,* 121**,** 295-306.

Afenyi-Annan, A, Kail, M, Combs, MR*, et al.* 2008. Lack of Duffy antigen expression is associated with organ damage in patients with sickle cell disease. *Transfusion,* 48**,** 917-24.

Akashi, K, Traver, D, Miyamoto, T*, et al.* 2000. A clonogenic common myeloid progenitor that gives rise to all myeloid lineages. *Nature,* 404**,** 193-7.

Albrey, JA, Vincent, EE, Hutchinson, J*, et al.* 1971. A new antibody, anti-Fy3, in the Duffy blood group system. *Vox Sang,* 20**,** 29-35.

Anderson, KL, Smith, KA, Perkin, H*, et al.* 1999. PU.1 and the granulocyte- and macrophage colony-stimulating factor receptors play distinct roles in late-stage myeloid cell differentiation. *Blood,* 94**,** 2310-8.

Aplenc, R, Alonzo, TA, Gerbing, RB*, et al.* 2006. Ethnicity and survival in childhood acute myeloid leukemia: a report from the Children's Oncology Group. *Blood,* 108**,** 74-80.

Arai, F, Hirao, A, Ohmura, M*, et al.* 2004. Tie2/angiopoietin-1 signaling regulates hematopoietic stem cell quiescence in the bone marrow niche. *Cell,* 118**,** 149-61.

Arnaout, MA 1990. Structure and function of the leukocyte adhesion molecules CD11/CD18. *Blood,* 75**,** 1037-50.

Artinyan, A, Mailey, B, Sanchez-Luege, N*, et al.* 2010. Race, ethnicity, and socioeconomic status influence the survival of patients with hepatocellular carcinoma in the United States. *Cancer,* 116**,** 1367-77.

Auffray, C, Sieweke, MH & Geissmann, F 2009. Blood monocytes: development, heterogeneity, and relationship with dendritic cells. *Annu Rev Immunol,* 27**,** 669-92.

Avigdor, A, Goichberg, P, Shivtiel, S*, et al.* 2004. CD44 and hyaluronic acid cooperate with SDF-1 in the trafficking of human CD34+ stem/progenitor cells to bone marrow. *Blood,* 103**,** 2981-9.

Baba, T, Naka, K, Morishita, S*, et al.* 2013. MIP-1alpha/CCL3-mediated maintenance of leukemia-initiating cells in the initiation process of chronic myeloid leukemia. *J Exp Med,* 210**,** 2661-73.

Bach, PB, Schrag, D, Brawley, OW*, et al.* 2002. Survival of blacks and whites after a cancer diagnosis. *JAMA,* 287**,** 2106-13.

Bachelerie, F, Ben-Baruch, A, Burkhardt, AM*, et al.* 2014. International Union of Pharmacology. LXXXIX. Update on the extended family of chemokine receptors and introducing a new nomenclature for atypical chemokine receptors. *Pharmacol Rev,* 66**,** 1-79.

Bailly, E & Reed, SI 1999. Functional characterization of rpn3 uncovers a distinct 19S proteasomal subunit requirement for ubiquitin-dependent proteolysis of cell cycle regulatory proteins in budding yeast. *Mol Cell Biol,* 19**,** 6872-90.

Bain, BJ 1996. Ethnic and sex differences in the total and differential white cell count and platelet count. *J Clin Pathol,* 49**,** 664-6.

Bain, BJ 1999. *Interactive haematology imagebank [electronic resource] : with self assessment,* Oxford, Blackwell Science.

Bain, BJ, Clark, DMMD & Wilkins, B 2010. *Bone marrow pathology,* Chichester, Wiley-Blackwell.

Balabanian, K, Lagane, B, Infantino, S*, et al.* 2005. The chemokine SDF-1/CXCL12 binds to and signals through the orphan receptor RDC1 in T lymphocytes. *J Biol Chem,* 280**,** 35760-6.

Bandyopadhyay, S, Zhan, R, Chaudhuri, A*, et al.* 2006. Interaction of KAI1 on tumor cells with DARC on vascular endothelium leads to metastasis suppression. *Nat Med,* 12**,** 933-8.

Barnato, AE, Alexander, SL, Linde-Zwirble, WT*, et al.* 2008. Racial Variation in the Incidence, Care, and Outcomes of Severe Sepsis: Analysis of Population, Patient, and Hospital Characteristics. *Am. J. Respir. Crit. Care Med.,* 177**,** 279-284.

Barreda, DR, Hanington, PC & Belosevic, M 2004. Regulation of myeloid development and function by colony stimulating factors. *Dev Comp Immunol,* 28**,** 509-54.

Beck, Z, Brown, BK, Wieczorek, L*, et al.* 2009. Human erythrocytes selectively bind and enrich infectious HIV-1 virions. *PloS ONE,* 4**,** e8297.

Becker, AJ, Mc, CE & Till, JE 1963. Cytological demonstration of the clonal nature of spleen colonies derived from transplanted mouse marrow cells. *Nature,* 197**,** 452-4.

Behzad, O, Lee, CL, Gavin, J*, et al.* 1973. A new anti-erythrocyte antibody in the Duffy system: anti-Fy4. *Vox Sang,* 24**,** 337-42.

Bessis, M 1973. *Living blood cells and their ultrastructure,* Berlin, Springer.

Bessos, H & Seghatchian, J 2005. Red cell storage lesion: The potential impact of storage-induced CD47 decline on immunomodulation and the survival of leucofiltered red cells. *Transfusion and Apheresis Science,* 32**,** 227-232.

Bhatia, S 2011. Disparities in cancer outcomes: lessons learned from children with cancer. *Pediatr Blood Cancer,* 56**,** 994-1002.

Bierman, HR, Kelly, KH, Cordes, FL*, et al.* 1952. The release of leukocytes and platelets from the pulmonary circulation by epinephrine. *Blood,* 7**,** 683-92.

Blanchet, X, Langer, M, Weber, C*, et al.* 2012. Touch of chemokines. *Front Immunol,* 3**,** 175.

Bolstad, BM, Irizarry, RA, Astrand, M*, et al.* 2003. A comparison of normalization methods for high density oligonucleotide array data based on variance and bias. *Bioinformatics,* 19**,** 185-93.

Borregaard, N & Cowland, JB 1997. Granules of the human neutrophilic polymorphonuclear leukocyte. *Blood,* 89**,** 3503-21.

Boyd, MF & Stratman-Thomas, WK 1933. Studies on benign tertian malaria. 4. On the refractoriness of negroes to inoculation with Plasmodium vivax. . *Am J Hyg,* 18**,** 485-489.

Bozza, F, Salluh, J, Japiassu, A*, et al.* 2007. Cytokine profiles as markers of disease severity in sepsis: a multiplex analysis. *Critical Care,* 11**,** R49.

Brandt, E, Muller-Alouf, H, Desreumaux, P*, et al.* 1998. Circulating growth-regulator oncogene alpha contributes to neutrophil priming and interleukin-8-directed mucosal recruitment into chronic lesions of patients with Crohn's disease. *Eur Cytokine Netw,* 9**,** 647-53.

Bratton, DL, Fadok, VA, Richter, DA*, et al.* 1997. Appearance of phosphatidylserine on apoptotic cells requires calcium-mediated nonspecific flip-flop and is enhanced by loss of the aminophospholipid translocase. *J Biol Chem,* 272**,** 26159-65.

Brinkmann, V, Reichard, U, Goosmann, C*, et al.* 2004. Neutrophil extracellular traps kill bacteria. *Science,* 303**,** 1532-5.

Broun, GO, Herbig, FK & Hamilton, JR 1966. Leukopenia in Negroes. *New England Journal of Medicine,* 275**,** 1410-1413.

Broxmeyer, HE, Cooper, S, Hangoc, G*, et al.* 1999a. Dominant myelopoietic effector functions mediated by chemokine receptor CCR1. *J Exp Med,* 189**,** 1987-92.

Broxmeyer, HE, Cooper, S, Hangoc, G*, et al.* 2005a. Stromal cell-derived factor-1/CXCL12 selectively counteracts inhibitory effects of myelosuppressive chemokines on hematopoietic progenitor cell proliferation in vitro. *Stem Cells Dev,* 14**,** 199-203.

Broxmeyer, HE, Hangoc, G, Cooper, S*, et al.* 2007. AMD3100 and CD26 modulate mobilization, engraftment, and survival of hematopoietic stem and progenitor cells mediated by the SDF-1/CXCL12-CXCR4 axis. *Ann N Y Acad Sci,* 1106**,** 1-19.

Broxmeyer, HE & Kim, CH 1999. Regulation of hematopoiesis in a sea of chemokine family members with a plethora of redundant activities. *Exp Hematol,* 27**,** 1113-23.

Broxmeyer, HE, Kim, CH, Cooper, SH*, et al.* 1999b. Effects of CC, CXC, C, and CX3C chemokines on proliferation of myeloid progenitor cells, and insights into SDF-1-induced chemotaxis of progenitors. *Ann N Y Acad Sci,* 872**,** 142-62; discussion 163.

Broxmeyer, HE, Orazi, A, Hague, NL*, et al.* 1998. Myeloid progenitor cell proliferation and mobilization effects of BB10010, a genetically engineered variant of human macrophage inflammatory protein-1alpha, in a phase I clinical trial in patients with relapsed/refractory breast cancer. *Blood Cells Mol Dis,* 24**,** 14-30.

Broxmeyer, HE, Orschell, CM, Clapp, DW*, et al.* 2005b. Rapid mobilization of murine and human hematopoietic stem and progenitor cells with AMD3100, a CXCR4 antagonist. *J Exp Med,* 201**,** 1307-18.

Bruhl, H, Vielhauer, V, Weiss, M*, et al.* 2005. Expression of DARC, CXCR3 and CCR5 in giant cell arteritis. *Rheumatology (Oxford),* 44**,** 309-13.

Buchanan, DI, Sinclair, M, Sanger, R*, et al.* 1976. An Alberta Cree Indian with a rare Duffy antibody, anti-Fy 3. *Vox Sang,* 30**,** 114-21.

Burdon, PC, Martin, C & Rankin, SM 2008. Migration across the sinusoidal endothelium regulates neutrophil mobilization in response to ELR + CXC chemokines. *Br J Haematol,* 142**,** 100-8.

Cacalano, G, Lee, J, Kikly, K*, et al.* 1994. Neutrophil and B cell expansion in mice that lack the murine IL-8 receptor homolog. *Science,* 265**,** 682-4.

Carter, CC, Mcnamara, LA, Onafuwa-Nuga, A*, et al.* 2011. HIV-1 utilizes the CXCR4 chemokine receptor to infect multipotent hematopoietic stem and progenitor cells. *Cell Host Microbe,* 9**,** 223-34.

Cartwright, RA & Staines, A 1992. Acute leukaemias. *Baillieres Clin Haematol,* 5**,** 1-26.

Cavasini, CE, De Mattos, LC, Couto, AA*, et al.* 2007a. Duffy blood group gene polymorphisms among malaria vivax patients in four areas of the Brazilian Amazon region. *Malar J,* 6**,** 167.

Cavasini, CE, Mattos, LC, Couto, AA*, et al.* 2007b. Plasmodium vivax infection among Duffy antigen-negative individuals from the Brazilian Amazon region: an exception? *Trans R Soc Trop Med Hyg,* 101**,** 1042-4.

Chakera, A, Seeber, RM, John, AE*, et al.* 2008. The duffy antigen/receptor for chemokines exists in an oligomeric form in living cells and functionally antagonizes CCR5 signaling through hetero-oligomerization. *Mol Pharmacol,* 73**,** 1362-70.

Chan-Shu, SA 1980. The second example of anti-Duffy5. *Transfusion,* 20**,** 358-60.

Chaudhuri, A, Nielsen, S, Elkjaer, ML*, et al.* 1997. Detection of Duffy antigen in the plasma membranes and caveolae of vascular endothelial and epithelial cells of nonerythroid organs. *Blood,* 89**,** 701-12.

Chaudhuri, A, Polyakova, J, Zbrzezna, V*, et al.* 1995. The coding sequence of the Duffy blood group gene in humans and simians: restriction fragment length polymorphism, antibody and malarial parasite specificities, and expression in nonerythroid tissues in Duffy-negative individuals. *Blood,* 85**,** 615-621.

Chaudhuri, A, Polyakova, J, Zbrzezna, V*, et al.* 1993. Cloning of glycoprotein D cDNA, which encodes the major subunit of the Duffy blood group system and the receptor for the Plasmodium vivax malaria parasite. *Proc Natl Acad Sci U S A,* 90**,** 10793-7.

Chaudhuri, A, Yuen, G, Fang, F*, et al.* 2004. Development of Duffy transgenic mouse: in vivo expression of human Duffy gene with -33T-->C promoter mutation in non-erythroid tissues. *Br J Haematol,* 127**,** 356-9.

Chaudhuri, A, Zbrzezna, V, Polyakova, J*, et al.* 1994. Expression of the Duffy antigen in K562 cells. Evidence that it is the human erythrocyte chemokine receptor. *J Biol Chem,* 269**,** 7835-8.

Chen, L, Zhang, ZH & Sendo, F 2000. Neutrophils play a critical role in the pathogenesis of experimental cerebral malaria. *Clinical & Experimental Immunology,* 120**,** 125-133.

Cheshier, SH, Morrison, SJ, Liao, X*, et al.* 1999. In vivo proliferation and cell cycle kinetics of long-term self-renewing hematopoietic stem cells. *Proc Natl Acad Sci U S A,* 96**,** 3120-5.

Chi, AW, Chavez, A, Xu, L*, et al.* 2011. Identification of Flt3(+)CD150(-) myeloid progenitors in adult mouse bone marrow that harbor T lymphoid developmental potential. *Blood,* 118**,** 2723-32.

Chown, B, Lewis, M & Kaita, H 1965. The Duffy Blood Group System in Caucasians: Evidence for a New Allele. *Am J Hum Genet,* 17**,** 384-9.

Christensen, JL & Weissman, IL 2001. Flk-2 is a marker in hematopoietic stem cell differentiation: a simple method to isolate long-term stem cells. *Proc Natl Acad Sci U S A,* 98**,** 14541-6.

Christopher, MJ & Link, DC 2008. Granulocyte colony-stimulating factor induces osteoblast apoptosis and inhibits osteoblast differentiation. *J Bone Miner Res,* 23**,** 1765-74.

Christopher, MJ, Rao, M, Liu, F*, et al.* 2011. Expression of the G-CSF receptor in monocytic cells is sufficient to mediate hematopoietic progenitor mobilization by G-CSF in mice. *J Exp Med,* 208**,** 251-60.

Christopherson, KW, 2nd, Cooper, S & Broxmeyer, HE 2003. Cell surface peptidase CD26/DPPIV mediates G-CSF mobilization of mouse progenitor cells. *Blood,* 101**,** 4680-6.

Cline, MJ, Le Fevre, C & Golde, DW 1977. Organ interactions in the regulation of hematopoiesis: in vitro interactions of bone, thymus, and spleen with bone marrow stem cells in normal, Sl/Sld and W/Wv mice. *J Cell Physiol,* 90**,** 105-15.

Colledge, KI, Pezzulich, M & Marsh, WL 1973. Anti-Fy5, and antibody disclosing a probable association between the Rhesus and Duffy blood group genes. *Vox Sang,* 24**,** 193-9.

Creutzig, U, Zimmermann, M, Reinhardt, D*, et al.* 2004. Early deaths and treatment-related mortality in children undergoing therapy for acute myeloid leukemia: analysis of the multicenter clinical trials AML-BFM 93 and AML-BFM 98. *J Clin Oncol,* 22**,** 4384-93.

Crosslin, DR, Mcdavid, A, Weston, N*, et al.* 2012. Genetic variants associated with the white blood cell count in 13,923 subjects in the eMERGE Network. *Hum Genet,* 131**,** 639-52.

Culleton, RL, Mita, T, Ndounga, M*, et al.* 2008. Failure to detect Plasmodium vivax in West and Central Africa by PCR species typing. *Malar J,* 7**,** 174.

Cutbush, M & Mollison, PL 1950. The Duffy blood group system. *Heredity,* 4**,** 383-9.

Cutbush, M, Mollison, PL & Parkin, DM 1950. A new human blood group. *Nature,* 165**,** 188-190.

Czerwinski, M, Kern, J, Grodecka, M*, et al.* 2007. Mutational analysis of the N-glycosylation sites of Duffy antigen/receptor for chemokines. *Biochem Biophys Res Commun,* 356**,** 816-21.

Dahl, R, Iyer, SR, Owens, KS*, et al.* 2007. The transcriptional repressor GFI-1 antagonizes PU.1 activity through protein-protein interaction. *J Biol Chem,* 282**,** 6473-83.

Dancey, JT, Deubelbeiss, KA, Harker, LA*, et al.* 1976. Neutrophil kinetics in man. *J Clin Invest,* 58**,** 705-15.

Daniels, G 2002. Human blood groups. 2nd ed. Malden, MA: Blackwell Science.

Darbonne, WC, Rice, GC, Mohler, MA*, et al.* 1991. Red blood cells are a sink for interleukin 8, a leukocyte chemotaxin. *J Clin Invest,* 88**,** 1362-9.

Dawson, TC, Lentsch, AB, Wang, Z*, et al.* 2000. Exaggerated response to endotoxin in mice lacking the Duffy antigen/receptor for chemokines (DARC). *Blood,* 96**,** 1681-4.

De Koning, JP, Soede-Bobok, AA, Schelen, AM*, et al.* 1998. Proliferation signaling and activation of Shc, p21Ras, and Myc via tyrosine 764 of human granulocyte colony-stimulating factor receptor. *Blood,* 91**,** 1924-33.

De Wynter, EA, Durig, J, Cross, MA*, et al.* 1998. Differential response of CD34+ cells isolated from cord blood and bone marrow to MIP-1 alpha and the expression of MIP-1 alpha receptors on these immature cells. *Stem Cells,* 16**,** 349-56.

De Wynter, EA, Heyworth, CM, Mukaida, N*, et al.* 2001. CCR1 chemokine receptor expression isolates erythroid from granulocyte-macrophage progenitors. *J Leukoc Biol,* 70**,** 455-60.

Dean, PN, Dolbeare, F, Gratzner, H*, et al.* 1984. Cell-cycle analysis using a monoclonal antibody to BrdUrd. *Cell Tissue Kinet,* 17**,** 427-36.

Dekoter, RP, Walsh, JC & Singh, H 1998. PU.1 regulates both cytokine-dependent proliferation and differentiation of granulocyte/macrophage progenitors. *EMBO J,* 17**,** 4456-68.

Del Hoyo, GM, Martin, P, Vargas, HH*, et al.* 2002. Characterization of a common precursor population for dendritic cells. *Nature,* 415**,** 1043-7.

Dempsey, PW, Vaidya, SA & Cheng, G 2003. The art of war: Innate and adaptive immune responses. *Cell Mol Life Sci,* 60**,** 2604-21.

Denic, S, Showqi, S, Klein, C*, et al.* 2009. Prevalence, phenotype and inheritance of benign neutropenia in Arabs. *BMC Blood Disord,* 9**,** 3.

Desantis, C, Naishadham, D & Jemal, A 2013. Cancer statistics for African Americans, 2013. *CA Cancer J Clin,* 63**,** 151-66.

Deshmukh, HS, Liu, Y, Menkiti, OR*, et al.* 2014. The microbiota regulates neutrophil homeostasis and host resistance to Escherichia coli K1 sepsis in neonatal mice. *Nat Med,* 20**,** 524-30.

Devi, S, Wang, Y, Chew, WK*, et al.* 2013. Neutrophil mobilization via plerixafor-mediated CXCR4 inhibition arises from lung demargination and blockade of neutrophil homing to the bone marrow. *J Exp Med,* 210**,** 2321-36.

Di Carlo, E, Forni, G, Lollini, P*, et al.* 2001. The intriguing role of polymorphonuclear neutrophils in antitumor reactions. *Blood,* 97**,** 339-45.

Ding, L & Morrison, SJ 2013. Haematopoietic stem cells and early lymphoid progenitors occupy distinct bone marrow niches. *Nature,* 495**,** 231-5.

Doerschuk, CM, Markos, J, Coxson, HO*, et al.* 1994. Quantitation of neutrophil migration in acute bacterial pneumonia in rabbits. *J Appl Physiol (1985),* 77**,** 2593-9.

Dogusan, Z, Montecino-Rodriguez, E & Dorshkind, K 2004. Macrophages and stromal cells phagocytose apoptotic bone marrow-derived B lineage cells. *J Immunol,* 172**,** 4717-23.

Dombrovskiy, VY, Martin, AA, Sunderram, J*, et al.* 2007. Occurrence and outcomes of sepsis: influence of race. *Crit Care Med,* 35**,** 763-8.

Domen, J, Cheshier, SH & Weissman, IL 2000. The role of apoptosis in the regulation of hematopoietic stem cells: Overexpression of Bcl-2 increases both their number and repopulation potential. *J Exp Med,* 191**,** 253-64.

Donahue Rp, BW, Renwick Jh, Mckusick Va. 1968. Probable assignment of the Duffy blood group locus to chromosome 1 in man. *Proc Natl Acad Sci U S A,* 61**,** 949-955.

Dong, F, Hoefsloot, LH, Schelen, AM*, et al.* 1994. Identification of a nonsense mutation in the granulocyte-colony-stimulating factor receptor in severe congenital neutropenia. *Proc Natl Acad Sci U S A,* 91**,** 4480-4.

Doulatov, S, Notta, F, Laurenti, E*, et al.* 2012. Hematopoiesis: a human perspective. *Cell Stem Cell,* 10**,** 120-36.

Doycheva, D, Shih, G, Chen, H*, et al.* 2013. Granulocyte-colony stimulating factor in combination with stem cell factor confers greater neuroprotection after hypoxic-ischemic brain damage in the neonatal rats than a solitary treatment. *Transl Stroke Res,* 4**,** 171-178.

Drasar, ER, Menzel, S, Fulford, T*, et al.* 2013. The effect of Duffy antigen receptor for chemokines on severity in sickle cell disease. *Haematologica,* 98**,** e87-9.

Du, J, Luan, J, Liu, H*, et al.* 2002. Potential role for Duffy antigen chemokine-binding protein in angiogenesis and maintenance of homeostasis in response to stress. *J Leukoc Biol,* 71**,** 141-53.

Dunstan, RA 1986. Status of major red cell blood group antigens on neutrophils, lymphocytes and monocytes. *Br J Haematol,* 62**,** 301-9.

Durand, C & Dzierzak, E 2005. Embryonic beginnings of adult hematopoietic stem cells. *Haematologica,* 90**,** 100-8.

Durpes, MC, Hardy-Dessources, MD, El Nemer, W*, et al.* 2011. Activation state of alpha4beta1 integrin on sickle red blood cells is linked to the duffy antigen receptor for chemokines (DARC) expression. *J Biol Chem,* 286**,** 3057-64.

Dzierzak, E & Philipsen, S 2013. Erythropoiesis: development and differentiation. *Cold Spring Harb Perspect Med,* 3**,** a011601.

Eash, KJ, Greenbaum, AM, Gopalan, PK*, et al.* 2010. CXCR2 and CXCR4 antagonistically regulate neutrophil trafficking from murine bone marrow. *J Clin Invest,* 120**,** 2423-31.

Eash, KJ, Means, JM, White, DW*, et al.* 2009. CXCR4 is a key regulator of neutrophil release from the bone marrow under basal and stress granulopoiesis conditions. *Blood,* 113**,** 4711-9.

Ehninger, A & Trumpp, A 2011. The bone marrow stem cell niche grows up: mesenchymal stem cells and macrophages move in. *J Exp Med,* 208**,** 421-8.

Elson, JK, Beebe-Dimmer, JL, Morgenstern, H*, et al.* 2011. The Duffy Antigen/Receptor for Chemokines (DARC) and prostate-cancer risk among Jamaican men. *J Immigr Minor Health,* 13**,** 36-41.

Emanuele, E, Falcone, C, D'angelo, A*, et al.* 2006. Association of plasma eotaxin levels with the presence and extent of angiographic coronary artery disease. *Atherosclerosis,* 186**,** 140-5.

Ergen, AV, Boles, NC & Goodell, MA 2012. Rantes/Ccl5 influences hematopoietic stem cell subtypes and causes myeloid skewing. *Blood,* 119**,** 2500-9.

Esper, AM, Moss, M, Lewis, CA*, et al.* 2006a. The role of infection and comorbidity: Factors that influence disparities in sepsis. *Crit Care Med,* 34**,** 2576-82.

Esper, AM, Moss, M, Lewis, CA*, et al.* 2006b. The role of infection and comorbidity: Factors that influence disparities in sepsis. *Critical Care Medicine,* 34**,** 2576-2582 10.1097/01.CCM.0000239114.50519.0E.

Fan, X, Patera, AC, Pong-Kennedy, A*, et al.* 2007. Murine CXCR1 is a functional receptor for GCP-2/CXCL6 and interleukin-8/CXCL8. *J Biol Chem,* 282**,** 11658-66.

Fiedler, K & Brunner, C 2012. The role of transcription factors in the guidance of granulopoiesis. *Am J Blood Res,* 2**,** 57-65.

Fleming, HE, Janzen, V, Lo Celso, C*, et al.* 2008. Wnt signaling in the niche enforces hematopoietic stem cell quiescence and is necessary to preserve self-renewal in vivo. *Cell Stem Cell,* 2**,** 274-83.

Forbes, WH, Johnson, RE & Consolazio, F 1941. Leukopenia in Negro Workmen. *The American Journal of the Medical Sciences,* 201**,** 407-412.

Forlow, SB, Schurr, JR, Kolls, JK*, et al.* 2001. Increased granulopoiesis through interleukin-17 and granulocyte colony-stimulating factor in leukocyte adhesion molecule-deficient mice. *Blood,* 98**,** 3309-14.

Forsberg, EC, Serwold, T, Kogan, S*, et al.* 2006. New evidence supporting megakaryocyte-erythrocyte potential of flk2/flt3+ multipotent hematopoietic progenitors. *Cell,* 126**,** 415-26.

Frenette, PS, Mayadas, TN, Rayburn, H*, et al.* 1996. Susceptibility to infection and altered hematopoiesis in mice deficient in both P- and E-selectins. *Cell,* 84**,** 563-74.

Fukuda, S, Bian, H, King, AG*, et al.* 2007. The chemokine GRObeta mobilizes early hematopoietic stem cells characterized by enhanced homing and engraftment. *Blood,* 110**,** 860-9.

Fukuma, N, Akimitsu, N, Hamamoto, H*, et al.* 2003. A role of the Duffy antigen for the maintenance of plasma chemokine concentrations. *Biochem Biophys Res Commun,* 303**,** 137-9.

Fulkerson, PC, Fischetti, CA, Mcbride, ML*, et al.* 2006. A central regulatory role for eosinophils and the eotaxin/CCR3 axis in chronic experimental allergic airway inflammation. *Proc Natl Acad Sci U S A,* 103**,** 16418-23.

Fulzele, K, Krause, DS, Panaroni, C*, et al.* 2013. Myelopoiesis is regulated by osteocytes through Gsalpha-dependent signaling. *Blood,* 121**,** 930-9.

Gardner, L, Patterson, AM, Ashton, BA*, et al.* 2004. The human Duffy antigen binds selected inflammatory but not homeostatic chemokines. *Biochemical and Biophysical Research Communications,* 321**,** 306-312.

Gardner, L, Wilson, C, Patterson, AM*, et al.* 2006. Temporal expression pattern of Duffy antigen in rheumatoid arthritis: up-regulation in early disease. *Arthritis Rheum,* 54**,** 2022-6.

Geleff, S, Draganovici, D, Jaksch, P*, et al.* 2010. The role of chemokine receptors in acute lung allograft rejection. *Eur Respir J,* 35**,** 167-75.

Gilliland, DG & Griffin, JD 2002. The roles of FLT3 in hematopoiesis and leukemia. *Blood,* 100**,** 1532-42.

Goardon, N, Marchi, E, Atzberger, A*, et al.* 2011. Coexistence of LMPP-like and GMP-like leukemia stem cells in acute myeloid leukemia. *Cancer Cell,* 19**,** 138-52.

Goguet-Surmenian, E, Richard-Fiardo, P, Guillemot, E*, et al.* 2013. CXCR7-mediated progression of osteosarcoma in the lungs. *Br J Cancer,* 109**,** 1579-85.

Golan, K, Vagima, Y, Ludin, A*, et al.* 2012. S1P promotes murine progenitor cell egress and mobilization via S1P1-mediated ROS signaling and SDF-1 release. *Blood,* 119**,** 2478-88.

Goldman, DC, Bailey, AS, Pfaffle, DL*, et al.* 2009. BMP4 regulates the hematopoietic stem cell niche. *Blood,* 114**,** 4393-401.

Gong, Y, Fan, Y & Hoover-Plow, J 2011. Plasminogen regulates stromal cell-derived factor-1/CXCR4-mediated hematopoietic stem cell mobilization by activation of matrix metalloproteinase-9. *Arterioscler Thromb Vasc Biol,* 31**,** 2035-43.

Goodrick, M, Hadley, A & Poole, G 1997. Haemolytic disease of the fetus and newborn due to anti-Fy(a) and the potential clinical value of Duffy genotyping in pregnancies at risk. *Transfusion,* 7**,** 301-304.

Gotea, V & Ovcharenko, I 2008. DiRE: identifying distant regulatory elements of co-expressed genes. *Nucleic Acids Res,* 36**,** W133-9.

Graham, GJ, Wright, EG, Hewick, R*, et al.* 1990. Identification and characterization of an inhibitor of haemopoietic stem cell proliferation. *Nature,* 344**,** 442-4.

Green, SP, Chuntharapai, A & Curnutte, JT 1996. Interleukin-8 (IL-8), melanoma growth-stimulatory activity, and neutrophil-activating peptide selectively mediate priming of the neutrophil NADPH oxidase through the type A or type B IL-8 receptor. *J Biol Chem,* 271**,** 25400-5.

Greenbaum, A, Hsu, YM, Day, RB*, et al.* 2013. CXCL12 in early mesenchymal progenitors is required for haematopoietic stem-cell maintenance. *Nature,* 495**,** 227-30.

Greenbaum, AM & Link, DC 2011. Mechanisms of G-CSF-mediated hematopoietic stem and progenitor mobilization. *Leukemia,* 25**,** 211-7.

Greer, JP & Wintrobe, MM 2004. *Wintrobe's clinical hematology,* Philadelphia ; London, Lippincott Williams & Wilkins.

Guerra, CA, Howes, RE, Patil, AP*, et al.* 2010. The international limits and population at risk of Plasmodium vivax transmission in 2009. *PLoS Negl Trop Dis.,* 4**,** e774.

Hacker, G 2000. The morphology of apoptosis. *Cell Tissue Res,* 301**,** 5-17.

Haddy, TB, Rana, SR & Castro, O 1999. Benign ethnic neutropenia: What is a normal absolute neutrophil count? *Journal of Laboratory and Clinical Medicine,* 133**,** 15-22.

Hadley, TJ, Erkmen, Z, Kaufman, BM*, et al.* 1986. Factors influencing invasion of erythrocytes by Plasmodium falciparum parasites: the effects of an N-acetyl glucosamine neoglycoprotein and an anti-glycophorin A antibody. *Am J Trop Med Hyg,* 35**,** 898-905.

Hardman, JT & Beck, ML 1981. Hemagglutination in capillaries: correlation with blood group specificity and IgG subclass. *Transfusion,* 21**,** 343-6.

Harris, MI 1990. Noninsulin-dependent diabetes mellitus in black and white Americans. *Diabetes Metab Rev,* 6**,** 71-90.

Hartmann, TN, Grabovsky, V, Pasvolsky, R*, et al.* 2008. A crosstalk between intracellular CXCR7 and CXCR4 involved in rapid CXCL12-triggered integrin activation but not in chemokine-triggered motility of human T lymphocytes and CD34+ cells. *J Leukoc Biol,* 84**,** 1130-40.

Hasan, S, Dinh, K, Lombardo, F*, et al.* 2004. Doxorubicin cardiotoxicity in African Americans. *J Natl Med Assoc,* 96**,** 196-9.

Hattori, K, Heissig, B, Tashiro, K*, et al.* 2001. Plasma elevation of stromal cell-derived factor-1 induces mobilization of mature and immature hematopoietic progenitor and stem cells. *Blood,* 97**,** 3354-60.

Hauser, CJ, Fekete, Z, Goodman, ER*, et al.* 1999. CXCR2 stimulation primes CXCR1 [Ca2+]i responses to IL-8 in human neutrophils. *Shock,* 12**,** 428-37.

He, JR, Shen, GP, Ren, ZF*, et al.* 2012. Pretreatment levels of peripheral neutrophils and lymphocytes as independent prognostic factors in patients with nasopharyngeal carcinoma. *Head Neck,* 34**,** 1769-76.

He, W, Neil, S, Kulkarni, H*, et al.* 2008. Duffy antigen receptor for chemokines mediates trans-infection of HIV-1 from red blood cells to target cells and affects HIV-AIDS susceptibility. *Cell Host Microbe,* 4**,** 52-62.

Heissig, B, Hattori, K, Dias, S*, et al.* 2002. Recruitment of stem and progenitor cells from the bone marrow niche requires MMP-9 mediated release of kit-ligand. *Cell,* 109**,** 625-37.

Hengartner, MO 2000. The biochemistry of apoptosis. *Nature,* 407**,** 770-6.

Hernandez, PA, Gorlin, RJ, Lukens, JN*, et al.* 2003. Mutations in the chemokine receptor gene CXCR4 are associated with WHIM syndrome, a combined immunodeficiency disease. *Nat Genet,* 34**,** 70-4.

Hershman, D, Weinberg, M, Rosner, Z*, et al.* 2003. Ethnic neutropenia and treatment delay in African American women undergoing chemotherapy for early-stage breast cancer. *J Natl Cancer Inst,* 95**,** 1545-8.

Hirai, H, Zhang, P, Dayaram, T*, et al.* 2006. C/EBPbeta is required for 'emergency' granulopoiesis. *Nat Immunol,* 7**,** 732-9.

Hirose, J, Kouro, T, Igarashi, H*, et al.* 2002. A developing picture of lymphopoiesis in bone marrow. *Immunol Rev,* 189**,** 28-40.

Hock, H, Hamblen, MJ, Rooke, HM*, et al.* 2004. Gfi-1 restricts proliferation and preserves functional integrity of haematopoietic stem cells. *Nature,* 431**,** 1002-7.

Hock, H, Hamblen, MJ, Rooke, HM*, et al.* 2003. Intrinsic requirement for zinc finger transcription factor Gfi-1 in neutrophil differentiation. *Immunity,* 18**,** 109-20.

Hoggatt, J, Singh, P, Sampath, J*, et al.* 2009. Prostaglandin E2 enhances hematopoietic stem cell homing, survival, and proliferation. *Blood,* 113**,** 5444-55.

Hohaus, S, Petrovick, MS, Voso, MT*, et al.* 1995. PU.1 (Spi-1) and C/EBP alpha regulate expression of the granulocyte-macrophage colony-stimulating factor receptor alpha gene. *Mol Cell Biol,* 15**,** 5830-45.

Horne, KC, Li, X, Jacobson, LP*, et al.* 2009. Duffy antigen polymorphisms do not alter progression of HIV in African Americans in the MACS cohort. *Cell Host Microbe,* 5**,** 415-7; author reply 418-9.

Horton, LW, Yu, Y, Zaja-Milatovic, S*, et al.* 2007. Opposing roles of murine duffy antigen receptor for chemokine and murine CXC chemokine receptor-2 receptors in murine melanoma tumor growth. *Cancer Res,* 67**,** 9791-9.

Horuk, R, Chitnis, CE, Darbonne, WC*, et al.* 1993a. A receptor for the malarial parasite Plasmodium vivax: the erythrocyte chemokine receptor. *Science,* 261**,** 1182-4.

Horuk, R, Colby, TJ, Darbonne, WC*, et al.* 1993b. The human erythrocyte inflammatory peptide (chemokine) receptor. Biochemical characterization, solubilization, and development of a binding assay for the soluble receptor. *Biochemistry,* 32**,** 5733-8.

Horuk, R, Martin, AW, Wang, Z*, et al.* 1997. Expression of chemokine receptors by subsets of neurons in the central nervous system. *J Immunol,* 158**,** 2882-90.

Horuk, R, Wang, ZX, Peiper, SC*, et al.* 1994. Identification and characterization of a promiscuous chemokine-binding protein in a human erythroleukemic cell line. *J Biol Chem,* 269**,** 17730-3.

Horvitz, HR 1999. Genetic control of programmed cell death in the nematode Caenorhabditis elegans. *Cancer Res,* 59**,** 1701s-1706s.

Howes, RE, Patil, AP, Piel, FB*, et al.* 2011. The global distribution of the Duffy blood group. *Nat Commun. ,* 266**,** 1-10.

Hsieh, MM, Everhart, JE, Byrd-Holt, DD*, et al.* 2007. Prevalence of neutropenia in the U.S. population: age, sex, smoking status, and ethnic differences. *Ann Intern Med,* 146**,** 486-92.

Hsieh, MM, Tisdale, JF, Rodgers, GP*, et al.* 2010. Neutrophil count in African Americans: lowering the target cutoff to initiate or resume chemotherapy? *J Clin Oncol,* 28**,** 1633-7.

Hsing, AW & Devesa, SS 2001. Trends and patterns of prostate cancer: what do they suggest? *Epidemiol Rev,* 23**,** 3-13.

Hughes, LH, Rossi, KQ, Krugh, DW*, et al.* 2007. Management of pregnancies complicated by anti-Fy(a) alloimmunization. *Transfusion,* 47**,** 1858-61.

Hunt, SC, Chen, W, Gardner, JP*, et al.* 2008. Leukocyte telomeres are longer in African Americans than in whites: the National Heart, Lung, and Blood Institute Family Heart Study and the Bogalusa Heart Study. *Aging Cell,* 7**,** 451-8.

Igney, FH & Krammer, PH 2002. Death and anti-death: tumour resistance to apoptosis. *Nat Rev Cancer,* 2**,** 277-88.

Ikin, EW, Mourant, AE, Pettenkofer, HJ*, et al.* 1951. Discovery of the expected haemagglutinin, anti-Fyb. *Nature,* 168**,** 1077-8.

Inman, CF, Rees, LE, Barker, E*, et al.* 2005. Validation of computer-assisted, pixel-based analysis of multiple-colour immunofluorescence histology. *J Immunol Methods,* 302**,** 156-67.

Ito, CY, Li, CY, Bernstein, A*, et al.* 2003. Hematopoietic stem cell and progenitor defects in Sca-1/Ly-6A-null mice. *Blood,* 101**,** 517-23.

Iwama, A, Zhang, P, Darlington, GJ*, et al.* 1998. Use of RDA analysis of knockout mice to identify myeloid genes regulated in vivo by PU.1 and C/EBPalpha. *Nucleic Acids Res,* 26**,** 3034-43.

Iwamoto, S, Li, J, Omi, T*, et al.* 1996. Identification of a novel exon and spliced form of Duffy mRNA that is the predominant transcript in both erythroid and postcapillary venule endothelium. *Blood,* 87**,** 378-385.

Iwamoto, S, Omi, T, Kajii, E*, et al.* 1995. Genomic organization of the glycoprotein D gene: Duffy blood group Fya/Fyb alloantigen system is associated with a polymorphism at the 44-amino acid residue. *Blood,* 85**,** 622-6.

Iwasaki, H, Somoza, C, Shigematsu, H*, et al.* 2005. Distinctive and indispensable roles of PU.1 in maintenance of hematopoietic stem cells and their differentiation. *Blood,* 106**,** 1590-600.

Jacobsen, K, Kravitz, J, Kincade, PW*, et al.* 1996. Adhesion receptors on bone marrow stromal cells: in vivo expression of vascular cell adhesion molecule-1 by reticular cells and sinusoidal endothelium in normal and gamma-irradiated mice. *Blood,* 87**,** 73-82.

Jagels, MA, Chambers, JD, Arfors, KE*, et al.* 1995. C5a- and tumor necrosis factor-alpha-induced leukocytosis occurs independently of beta 2 integrins and L-selectin: differential effects on neutrophil adhesion molecule expression in vivo. *Blood,* 85**,** 2900-9.

Janeway, CA 2001. *Immunobiology : the immune system in health and disease*.

Janeway, CA, Jr. & Medzhitov, R 2002. Innate immune recognition. *Annu Rev Immunol,* 20**,** 197-216.

Jilma-Stohlawetz, P, Homoncik, M, Drucker, C*, et al.* 2001. Fy phenotype and gender determine plasma levels of monocyte chemotactic protein. *Transfusion,* 41**,** 378-81.

Jin, H, Zhang, G, Liu, X*, et al.* 2013. Blood neutrophil-lymphocyte ratio predicts survival for stages III-IV gastric cancer treated with neoadjuvant chemotherapy. *World J Surg Oncol,* 11**,** 112.

Julg, B, Reddy, S, Van Der Stok, M*, et al.* 2009. Lack of Duffy antigen receptor for chemokines: no influence on HIV disease progression in an African treatment-naive population. *Cell Host Microbe,* 5**,** 413-5; author reply 418-9.

Kadan-Lottick, NS, Ness, KK, Bhatia, S*, et al.* 2003. Survival variability by race and ethnicity in childhood acute lymphoblastic leukemia. *JAMA,* 290**,** 2008-14.

Kangelaris, KN, Sapru, A, Calfee, CS*, et al.* 2012. The association between a Darc gene polymorphism and clinical outcomes in African American patients with acute lung injury. *Chest,* 141**,** 1160-9.

Kansas, GS 1996. Selectins and their ligands: current concepts and controversies. *Blood,* 88**,** 3259-87.

Kao, SC, Pavlakis, N, Harvie, R*, et al.* 2010. High blood neutrophil-to-lymphocyte ratio is an indicator of poor prognosis in malignant mesothelioma patients undergoing systemic therapy. *Clin Cancer Res,* 16**,** 5805-13.

Karapetyan, AV, Klyachkin, YM, Selim, S*, et al.* 2013. Bioactive lipids and cationic antimicrobial peptides as new potential regulators for trafficking of bone marrow-derived stem cells in patients with acute myocardial infarction. *Stem Cells Dev,* 22**,** 1645-56.

Karayalcin, G, Rosner, F & Sawitsky, A 1972. Pseudo-neutropenia in American Negroes. *Lancet,* 1**,** 387.

Kasehagen, LJ, Mueller, I, Kiniboro, B*, et al.* 2007. Reduced Plasmodium vivax erythrocyte infection in PNG Duffy-negative heterozygotes. *PLoS One,* 2**,** e336.

Kashiwazaki, M, Tanaka, T, Kanda, H*, et al.* 2003. A high endothelial venule-expressing promiscuous chemokine receptor DARC can bind inflammatory, but not lymphoid, chemokines and is dispensable for lymphocyte homing under physiological conditions. *Int Immunol,* 15**,** 1219-27.

Katayama, Y, Battista, M, Kao, WM*, et al.* 2006. Signals from the sympathetic nervous system regulate hematopoietic stem cell egress from bone marrow. *Cell,* 124**,** 407-21.

Keegan, TH, John, EM, Fish, KM*, et al.* 2010. Breast cancer incidence patterns among California Hispanic women: differences by nativity and residence in an enclave. *Cancer Epidemiol Biomarkers Prev,* 19**,** 1208-18.

Kikushige, Y, Yoshimoto, G, Miyamoto, T*, et al.* 2008. Human Flt3 is expressed at the hematopoietic stem cell and the granulocyte/macrophage progenitor stages to maintain cell survival. *J Immunol,* 180**,** 7358-67.

King, CL, Adams, JH, Xianli, J*, et al.* 2011. Fy(a)/Fy(b) antigen polymorphism in human erythrocyte Duffy antigen affects susceptibility to Plasmodium vivax malaria. *Proc Natl Acad Sci U S A,* 108**,** 20113-8.

Klein, HG & Anstee, DJ 2005. *Mollison's blood transfusion in clinical medicine,* Malden, Mass. ; Oxford, Blackwell Pub.

Koay, DC & Sartorelli, AC 1999. Functional differentiation signals mediated by distinct regions of the cytoplasmic domain of the granulocyte colony-stimulating factor receptor. *Blood,* 93**,** 3774-84.

Kobayashi, I, Kawano, S, Tsuji, S*, et al.* 1998. Flow cytometric analysis of cell proliferation kinetics during duodenal ulcer healing. *J Gastroenterol Hepatol,* 13**,** 376-82.

Kocher, M, Siegel, ME, Edberg, JC*, et al.* 1997. Cross-linking of Fc gamma receptor IIa and Fc gamma receptor IIIb induces different proadhesive phenotypes on human neutrophils. *J Immunol,* 159**,** 3940-8.

Kohler, A, De Filippo, K, Hasenberg, M*, et al.* 2011. G-CSF-mediated thrombopoietin release triggers neutrophil motility and mobilization from bone marrow via induction of Cxcr2 ligands. *Blood,* 117**,** 4349-57.

Kondo, M, Weissman, IL & Akashi, K 1997. Identification of clonogenic common lymphoid progenitors in mouse bone marrow. *Cell,* 91**,** 661-72.

Koopman, G, Reutelingsperger, CP, Kuijten, GA*, et al.* 1994. Annexin V for flow cytometric detection of phosphatidylserine expression on B cells undergoing apoptosis. *Blood,* 84**,** 1415-20.

Kosanke, J 1983. Production of anti-Fya in Black Fy(a-b-) individuals. *Red Cell Free Press,* 8**,** 2.

Kosinski Ks, ML, White L. 1984. Three examples of anti-Fy3 produced in Negroes. *Rev Fr Transfus Immunohematol.,* 27**,** 619-624.

Kourtis, AP, Hudgens, MG, Kayira, D*, et al.* 2012. Neutrophil count in African mothers and newborns and HIV transmission risk. *N Engl J Med,* 367**,** 2260-2.

Kroepfl, JM, Pekovits, K, Stelzer, I*, et al.* 2012. Exercise increases the frequency of circulating hematopoietic progenitor cells, but reduces hematopoietic colony-forming capacity. *Stem Cells Dev,* 21**,** 2915-25.

Kulkarni, H, Marconi, VC, He, W*, et al.* 2009. The Duffy-null state is associated with a survival advantage in leukopenic HIV-infected persons of African ancestry. *Blood,* 114**,** 2783-2792.

Kusunoki, T, Tsuruta, S, Higashi, H*, et al.* 1994. Involvement of CD11b/CD18 in enhanced neutrophil adhesion by Fc gamma receptor stimulation. *J Leukoc Biol,* 55**,** 735-42.

Kyewski, B & Klein, L 2006. A central role for central tolerance. *Annu Rev Immunol,* 24**,** 571-606.

Lachgar, A, Jaureguiberry, G, Le Buenac, H*, et al.* 1998. Binding of HIV-1 to RBCs involves the Duffy antigen receptors for chemokines (DARC). *Biomed Pharmacother,* 52**,** 436-9.

Lacombe, F, Belloc, F, Bernard, P*, et al.* 1988. Evaluation of four methods of DNA distribution data analysis based on bromodeoxyuridine/DNA bivariate data. *Cytometry,* 9**,** 245-53.

Ladhani, S, Lowe, B, Cole, AO*, et al.* 2002. Changes in white blood cells and platelets in children with falciparum malaria: relationship to disease outcome. *Br J Haematol,* 119**,** 839-47.

Lai, AY & Kondo, M 2006. Asymmetrical lymphoid and myeloid lineage commitment in multipotent hematopoietic progenitors. *J Exp Med,* 203**,** 1867-73.

Lai, AY, Lin, SM & Kondo, M 2005. Heterogeneity of Flt3-expressing multipotent progenitors in mouse bone marrow. *J Immunol,* 175**,** 5016-23.

Laiosa, CV, Stadtfeld, M & Graf, T 2006. Determinants of lymphoid-myeloid lineage diversification. *Annu Rev Immunol,* 24**,** 705-38.

Lapidot, T & Petit, I 2002. Current understanding of stem cell mobilization: the roles of chemokines, proteolytic enzymes, adhesion molecules, cytokines, and stromal cells. *Exp Hematol,* 30**,** 973-81.

Lard, LR, Mul, FP, De Haas, M*, et al.* 1999. Neutrophil activation in sickle cell disease. *J Leukoc Biol,* 66**,** 411-5.

Laterveer, L, Lindley, IJ, Hamilton, MS*, et al.* 1995. Interleukin-8 induces rapid mobilization of hematopoietic stem cells with radioprotective capacity and long-term myelolymphoid repopulating ability. *Blood,* 85**,** 2269-75.

Le Pennec, PY, Rouger, P, Klein, MT*, et al.* 1987. Study of anti-Fya in five black Fy(a-b-) patients. *Vox Sang,* 52**,** 246-9.

Le Van Kim, C, Tournamille, C, Kroviarski, Y*, et al.* 1997. The 1.35-kb and 7.5-kb Duffy mRNA isoforms are differently regulated in various regions of brain, differ by the length of their 5' untranslated sequence, but encode the same polypeptide. *Blood,* 90**,** 2851-3.

Lee, G, Lo, A, Short, SA*, et al.* 2006a. Targeted gene deletion demonstrates that the cell adhesion molecule ICAM-4 is critical for erythroblastic island formation. *Blood,* 108**,** 2064-71.

Lee, JS, Frevert, CW, Thorning, DR*, et al.* 2003a. Enhanced expression of Duffy antigen in the lungs during suppurative pneumonia. *J Histochem Cytochem,* 51**,** 159-66.

Lee, JS, Frevert, CW, Wurfel, MM*, et al.* 2003b. Duffy Antigen Facilitates Movement of Chemokine Across the Endothelium In Vitro and Promotes Neutrophil Transmigration In Vitro and In Vivo. *The Journal of Immunology,* 170**,** 5244-5251.

Lee, JS, Wurfel, MM, Matute-Bello, G*, et al.* 2006b. The Duffy antigen modifies systemic and local tissue chemokine responses following lipopolysaccharide stimulation. *J Immunol,* 177**,** 8086-94.

Lekstrom-Himes, J & Xanthopoulos, KG 1998. Biological role of the CCAAT/enhancer-binding protein family of transcription factors. *J Biol Chem,* 273**,** 28545-8.

Levesque, JP, Hendy, J, Takamatsu, Y*, et al.* 2003a. Disruption of the CXCR4/CXCL12 chemotactic interaction during hematopoietic stem cell mobilization induced by GCSF or cyclophosphamide. *J Clin Invest,* 111**,** 187-96.

Levesque, JP, Hendy, J, Winkler, IG*, et al.* 2003b. Granulocyte colony-stimulating factor induces the release in the bone marrow of proteases that cleave c-KIT receptor (CD117) from the surface of hematopoietic progenitor cells. *Exp Hematol,* 31**,** 109-17.

Levesque, JP, Liu, F, Simmons, PJ*, et al.* 2004. Characterization of hematopoietic progenitor mobilization in protease-deficient mice. *Blood,* 104**,** 65-72.

Levesque, JP, Takamatsu, Y, Nilsson, SK*, et al.* 2001. Vascular cell adhesion molecule-1 (CD106) is cleaved by neutrophil proteases in the bone marrow following hematopoietic progenitor cell mobilization by granulocyte colony-stimulating factor. *Blood,* 98**,** 1289-97.

Lewis, M, Kaita, H & Chown, B 1957. The blood groups of a Japanese population. *Am J Hum Genet,* 9**,** 274-83.

Lewis, M, Kaita, H & Chown, B 1972. The Duffy blood group system in Caucasians. A further population sample. *Vox Sang,* 23**,** 523-7.

Ley, K 2003. The role of selectins in inflammation and disease. *Trends Mol Med,* 9**,** 263-8.

Ley, K, Laudanna, C, Cybulsky, MI*, et al.* 2007. Getting to the site of inflammation: the leukocyte adhesion cascade updated. *Nat Rev Immunol,* 7**,** 678-89.

Lieschke, GJ & Burgess, AW 1992. Granulocyte colony-stimulating factor and granulocyte-macrophage colony-stimulating factor (1). *N Engl J Med,* 327**,** 28-35.

Lieschke, GJ, Grail, D, Hodgson, G*, et al.* 1994. Mice lacking granulocyte colony-stimulating factor have chronic neutropenia, granulocyte and macrophage progenitor cell deficiency, and impaired neutrophil mobilization. *Blood,* 84**,** 1737-46.

Liu, F, Poursine-Laurent, J & Link, DC 2000. Expression of the G-CSF receptor on hematopoietic progenitor cells is not required for their mobilization by G-CSF. *Blood,* 95**,** 3025-31.

Liu, F, Poursine-Laurent, J, Wu, HY*, et al.* 1997. Interleukin-6 and the granulocyte colony-stimulating factor receptor are major independent regulators of granulopoiesis in vivo but are not required for lineage commitment or terminal differentiation. *Blood,* 90**,** 2583-90.

Liu, F, Wu, HY, Wesselschmidt, R*, et al.* 1996. Impaired production and increased apoptosis of neutrophils in granulocyte colony-stimulating factor receptor-deficient mice. *Immunity,* 5**,** 491-501.

Liu, XH, Hadley, TJ, Xu, L*, et al.* 1999. Up-regulation of Duffy antigen receptor expression in children with renal disease. *Kidney Int,* 55**,** 1491-500.

Lloyd-Jones, D, Adams, R, Carnethon, M*, et al.* 2009. Heart disease and stroke statistics--2009 update: a report from the American Heart Association Statistics Committee and Stroke Statistics Subcommittee. *Circulation,* 119**,** 480-6.

Lord, BI 1995. MIP-1 alpha increases the self-renewal capacity of the hemopoietic spleen-colony-forming cells following hydroxyurea treatment in vivo. *Growth Factors,* 12**,** 145-9.

Lord, BI, Woolford, LB, Wood, LM*, et al.* 1995. Mobilization of early hematopoietic progenitor cells with BB-10010: a genetically engineered variant of human macrophage inflammatory protein-1 alpha. *Blood,* 85**,** 3412-5.

Lucas, D, Scheiermann, C, Chow, A*, et al.* 2013. Chemotherapy-induced bone marrow nerve injury impairs hematopoietic regeneration. *Nat Med,* 19**,** 695-703.

Ludlow, LE, Purton, LE, Klarmann, K*, et al.* 2008. The role of p202 in regulating hematopoietic cell proliferation and differentiation. *J Interferon Cytokine Res,* 28**,** 5-11.

Luker, KE, Steele, JM, Mihalko, LA*, et al.* 2010. Constitutive and chemokine-dependent internalization and recycling of CXCR7 in breast cancer cells to degrade chemokine ligands. *Oncogene,* 29**,** 4599-610.

Luo, H, Chaudhuri, A, Johnson, KR*, et al.* 1997. Cloning, characterization, and mapping of a murine promiscuous chemokine receptor gene: homolog of the human Duffy gene. *Genome Res,* 7**,** 932-41.

Luo, H, Chaudhuri, A, Zbrzezna, V*, et al.* 2000. Deletion of the murine Duffy gene (Dfy) reveals that the Duffy receptor is functionally redundant. *Mol Cell Biol,* 20**,** 3097-101.

Luster, AD, Alon, R & Von Andrian, UH 2005. Immune cell migration in inflammation: present and future therapeutic targets. *Nat Immunol,* 6**,** 1182-90.

Ma, H, Gong, H, Chen, Z*, et al.* 2012. Association of Stat3 with HSF1 plays a critical role in G-CSF-induced cardio-protection against ischemia/reperfusion injury. *J Mol Cell Cardiol,* 52**,** 1282-90.

Ma, Q, Jones, D & Springer, TA 1999. The chemokine receptor CXCR4 is required for the retention of B lineage and granulocytic precursors within the bone marrow microenvironment. *Immunity,* 10**,** 463-71.

Mackarehtschian, K, Hardin, JD, Moore, KA*, et al.* 1995. Targeted disruption of the flk2/flt3 gene leads to deficiencies in primitive hematopoietic progenitors. *Immunity,* 3**,** 147-61.

Malinge, S, Thiollier, C, Chlon, TM*, et al.* 2013. Ikaros inhibits megakaryopoiesis through functional interaction with GATA-1 and NOTCH signaling. *Blood,* 121**,** 2440-51.

Mancini, SJ, Mantei, N, Dumortier, A*, et al.* 2005. Jagged1-dependent Notch signaling is dispensable for hematopoietic stem cell self-renewal and differentiation. *Blood,* 105**,** 2340-2.

Mangalmurti, NS, Xiong, Z, Hulver, M*, et al.* 2009. Loss of red cell chemokine scavenging promotes transfusion-related lung inflammation. *Blood,* 113**,** 1158-66.

Mantovani, A 1999. The chemokine system: redundancy for robust outputs. *Immunol Today,* 20**,** 254-7.

Manwani, D & Bieker, JJ 2008. The erythroblastic island. *Curr Top Dev Biol,* 82**,** 23-53.

Manz, MG, Traver, D, Miyamoto, T*, et al.* 2001. Dendritic cell potentials of early lymphoid and myeloid progenitors. *Blood,* 97**,** 3333-41.

Martin, C, Burdon, PC, Bridger, G*, et al.* 2003. Chemokines acting via CXCR2 and CXCR4 control the release of neutrophils from the bone marrow and their return following senescence. *Immunity,* 19**,** 583-93.

Martineau, AR, Newton, SM, Wilkinson, KA*, et al.* 2007. Neutrophil-mediated innate immune resistance to mycobacteria. *J Clin Invest,* 117**,** 1988-94.

Martinez, FO, Sica, A, Mantovani, A*, et al.* 2008. Macrophage activation and polarization. *Front Biosci,* 13**,** 453-61.

Mason, BA, Lessin, L & Schechter, GP 1979. Marrow granulocyte reserves in black Americans. Hydrocortisone-induced granulocytosis in the "benign" neutropenia of the black. *Am J Med,* 67**,** 201-5.

Masopust, D & Schenkel, JM 2013. The integration of T cell migration, differentiation and function. *Nat Rev Immunol,* 13**,** 309-20.

Masouredis, SP, Sudora, E, Mahan, L*, et al.* 1980. Quantitative immunoferritin microscopy of Fya, Fyb, Jka, U, and Dib antigen site numbers on human red cells. *Blood,* 56**,** 969-77.

Massberg, S, Schaerli, P, Knezevic-Maramica, I*, et al.* 2007. Immunosurveillance by hematopoietic progenitor cells trafficking through blood, lymph, and peripheral tissues. *Cell,* 131**,** 994-1008.

Mayr, FB, Spiel, AO, Leitner, JM*, et al.* 2008. Duffy antigen modifies the chemokine response in human endotoxemia. *Crit Care Med,* 36**,** 159-65.

Mayr, FB, Spiel, AO, Leitner, JM*, et al.* 2007. Ethnic differences in plasma levels of interleukin-8 (IL-8) and granulocyte colony stimulating factor (G-CSF). *Transl Res,* 149**,** 10-4.

Mayr, FB, Yende, S, Linde-Zwirble, WT*, et al.* 2010. Infection rate and acute organ dysfunction risk as explanations for racial differences in severe sepsis. *JAMA,* 303**,** 2495-503.

Maze, R, Sherry, B, Kwon, BS*, et al.* 1992. Myelosuppressive effects in vivo of purified recombinant murine macrophage inflammatory protein-1 alpha. *J Immunol,* 149**,** 1004-9.

Mazzone, A & Ricevuti, G 1995. Leukocyte CD11/CD18 integrins: biological and clinical relevance. *Haematologica,* 80**,** 161-75.

Mcdermott, DH, Liu, Q, Ulrick, J*, et al.* 2011. The CXCR4 antagonist plerixafor corrects panleukopenia in patients with WHIM syndrome. *Blood,* 118**,** 4957-62.

Mckercher, SR, Torbett, BE, Anderson, KL*, et al.* 1996. Targeted disruption of the PU.1 gene results in multiple hematopoietic abnormalities. *EMBO J,* 15**,** 5647-58.

Mcleod, HL, Lin, JS, Scott, EP*, et al.* 1994. Thiopurine methyltransferase activity in American white subjects and black subjects. *Clin Pharmacol Ther,* 55**,** 15-20.

Mcmorran, BJ, Wieczorski, L, Drysdale, KE*, et al.* 2012. Platelet factor 4 and Duffy antigen required for platelet killing of Plasmodium falciparum. *Science,* 338**,** 1348-51.

Mead, AJ, Kharazi, S, Atkinson, D*, et al.* 2013. FLT3-ITDs instruct a myeloid differentiation and transformation bias in lymphomyeloid multipotent progenitors. *Cell Rep,* 3**,** 1766-76.

Meffre, E, Casellas, R & Nussenzweig, MC 2000. Antibody regulation of B cell development. *Nat Immunol,* 1**,** 379-85.

Mei, J, Liu, Y, Dai, N*, et al.* 2010. CXCL5 regulates chemokine scavenging and pulmonary host defense to bacterial infection. *Immunity,* 33**,** 106-17.

Menard, D, Barnadas, C, Bouchier, C*, et al.* 2010. Plasmodium vivax clinical malaria is commonly observed in Duffy-negative Malagasy people. *Proc Natl Acad Sci U S A,* 107**,** 5967-71.

Mendes, C, Dias, F, Figueiredo, J*, et al.* 2011. Duffy negative antigen is no longer a barrier to Plasmodium vivax--molecular evidences from the African West Coast (Angola and Equatorial Guinea). *PLoS Negl Trop Dis,* 5**,** e1192.

Mendez-Ferrer, S, Lucas, D, Battista, M*, et al.* 2008. Haematopoietic stem cell release is regulated by circadian oscillations. *Nature,* 452**,** 442-7.

Mendez-Ferrer, S, Michurina, TV, Ferraro, F*, et al.* 2010. Mesenchymal and haematopoietic stem cells form a unique bone marrow niche. *Nature,* 466**,** 829-34.

Mendis, K, Sina, BJ, Marchesini, P*, et al.* 2001. The neglected burden of Plasmodium vivax malaria. *Am J Trop Med Hyg,* 64**,** 97-106.

Meyerson, M & Harlow, E 1994. Identification of G1 kinase activity for cdk6, a novel cyclin D partner. *Mol Cell Biol,* 14**,** 2077-86.

Michael, M, Goldstein, D, Clarke, SJ*, et al.* 2006. Prognostic factors predictive of response and survival to a modified FOLFOX regimen: importance of an increased neutrophil count. *Clin Colorectal Cancer,* 6**,** 297-304.

Miller, LH, Mason, SJ, Clyde, DF*, et al.* 1976. The resistance factor to Plasmodium vivax in blacks. The Duffy-blood-group genotype, FyFy. *N Engl J Med,* 295**,** 302-4.

Miller, LH, Mason, SJ, Dvorak, JA*, et al.* 1975. Erythrocyte receptors for (Plasmodium knowlesi) malaria: Duffy blood group determinants. *Science,* 189**,** 561-3.

Mintz, U & Sachs, L 1973. Normal granulocyte colony-forming cells in the bone marrow of Yemenite Jews with genetic neutropenia. *Blood,* 41**,** 745-51.

Molineux, G, Mccrea, C, Yan, XQ*, et al.* 1997. Flt-3 ligand synergizes with granulocyte colony-stimulating factor to increase neutrophil numbers and to mobilize peripheral blood stem cells with long-term repopulating potential. *Blood,* 89**,** 3998-4004.

Molineux, G, Migdalska, A, Szmitkowski, M*, et al.* 1991. The effects on hematopoiesis of recombinant stem cell factor (ligand for c-kit) administered in vivo to mice either alone or in combination with granulocyte colony-stimulating factor. *Blood,* 78**,** 961-6.

Morrison, SJ & Weissman, IL 1994. The long-term repopulating subset of hematopoietic stem cells is deterministic and isolatable by phenotype. *Immunity,* 1**,** 661-73.

Morton, JA 1962. Some Observations on the Action of Blood-Group Antibodies on Red Cells Treated with Proteolytic Enzymes. *Br J Haematol,* 8**,** 134-148.

Mourant, AE, Kopec, AC & Domaniewska-Sobczak, K 1976. *The distribution of the human blood groups, and other polymorphisms,* London, Oxford University Press.

Mullighan, CG, Marshall, SE, Fanning, GC*, et al.* 1998. Rapid haplotyping of mutations in the Duffy gene using the polymerase chain reaction and sequence-specific primers. *Tissue Antigens,* 51**,** 195-9.

Nakajima, H & Ihle, JN 2001. Granulocyte colony-stimulating factor regulates myeloid differentiation through CCAAT/enhancer-binding protein epsilon. *Blood,* 98**,** 897-905.

Nalls, MA, Wilson, JG, Patterson, NJ*, et al.* 2008. Admixture mapping of white cell count: genetic locus responsible for lower white blood cell count in the Health ABC and Jackson Heart studies. *Am J Hum Genet,* 82**,** 81-7.

Naumann, U, Cameroni, E, Pruenster, M*, et al.* 2010. CXCR7 functions as a scavenger for CXCL12 and CXCL11. *PLoS One,* 5**,** e9175.

Nebor, D, Durpes, MC, Mougenel, D*, et al.* 2010. Association between Duffy antigen receptor for chemokines expression and levels of inflammation markers in sickle cell anemia patients. *Clin Immunol,* 136**,** 116-22.

Neote, K, Darbonne, W, Ogez, J*, et al.* 1993. Identification of a promiscuous inflammatory peptide receptor on the surface of red blood cells. *J Biol Chem,* 268**,** 12247-9.

Neote, K, Mak, JY, Kolakowski, LF, Jr.*, et al.* 1994. Functional and biochemical analysis of the cloned Duffy antigen: identity with the red blood cell chemokine receptor. *Blood,* 84**,** 44-52.

Neusser, MA, Kraus, AK, Regele, H*, et al.* 2010. The chemokine receptor CXCR7 is expressed on lymphatic endothelial cells during renal allograft rejection. *Kidney Int,* 77**,** 801-8.

Nguyen-Jackson, H, Panopoulos, AD, Zhang, H*, et al.* 2010. STAT3 controls the neutrophil migratory response to CXCR2 ligands by direct activation of G-CSF-induced CXCR2 expression and via modulation of CXCR2 signal transduction. *Blood,* 115**,** 3354-63.

Nibbs, RJ & Graham, GJ 2013. Immune regulation by atypical chemokine receptors. *Nat Rev Immunol,* 13**,** 815-29.

Nichols, ME, Rubinstein, P, Barnwell, J*, et al.* 1987. A new human Duffy blood group specificity defined by a murine monoclonal antibody. Immunogenetics and association with susceptibility to Plasmodium vivax. *J Exp Med,* 166**,** 776-85.

Nie, Y, Han, YC & Zou, YR 2008. CXCR4 is required for the quiescence of primitive hematopoietic cells. *J Exp Med,* 205**,** 777-83.

Nimmerjahn, F & Ravetch, JV 2008. Fcgamma receptors as regulators of immune responses. *Nat Rev Immunol,* 8**,** 34-47.

Nishijima, I, Watanabe, S, Nakahata, T*, et al.* 1997. Human granulocyte-macrophage colony-stimulating factor (hGM-CSF)-dependent in vitro and in vivo proliferation and differentiation of all hematopoietic progenitor cells in hGM-CSF receptor transgenic mice. *J Allergy Clin Immunol,* 100**,** S79-86.

Nitsche, A, Junghahn, I, Thulke, S*, et al.* 2003. Interleukin-3 promotes proliferation and differentiation of human hematopoietic stem cells but reduces their repopulation potential in NOD/SCID mice. *Stem Cells,* 21**,** 236-44.

Nogueira, BV, Palomino, Z, Porto, ML*, et al.* 2012. Granulocyte colony stimulating factor prevents kidney infarction and attenuates renovascular hypertension. *Cell Physiol Biochem,* 29**,** 143-52.

Novitzky-Basso, I & Rot, A 2012. Duffy antigen receptor for chemokines and its involvement in patterning and control of inflammatory chemokines. *Front Immunol,* 3**,** 266.

O'sullivan, RJ & Karlseder, J 2010. Telomeres: protecting chromosomes against genome instability. *Nat Rev Mol Cell Biol,* 11**,** 171-81.

O'leary, PA 1927. Treatment of neurosyphilis by malaria: Report on the three years' observation of the first one hundred patients treated. . *J Am Med Assoc,* 89.

Oakes, J, Taylor, D, Johnson, C*, et al.* 1978. Fy3 antigenicity of blood of newborns. *Transfusion,* 18**,** 127-8.

Oberdorfer, CE, Kahn, B, Moore, V*, et al.* 1974. A second example of anti-Fy3 in the Duffy blood group system. *Transfusion,* 14**,** 608-11.

Ogawa, M 1993. Differentiation and proliferation of hematopoietic stem cells. *Blood,* 81**,** 2844-53.

Olsson, ML, Smythe, JS, Hansson, C*, et al.* 1998. The Fy(x) phenotype is associated with a missense mutation in the Fy(b) allele predicting Arg89Cys in the Duffy glycoprotein. *Br J Haematol,* 103**,** 1184-91.

Opferman, JT 2007. Life and death during hematopoietic differentiation. *Curr Opin Immunol,* 19**,** 497-502.

Oreskovic, RT, Dumaswala, UJ & Greenwalt, TJ 1992. Expression of blood group antigens on red cell microvesicles. *Transfusion,* 32**,** 848-9.

Orkin, SH 2000. Diversification of haematopoietic stem cells to specific lineages. *Nat Rev Genet,* 1**,** 57-64.

Orkin, SH & Zon, LI 2008. Hematopoiesis: an evolving paradigm for stem cell biology. *Cell,* 132**,** 631-44.

Papayannopoulou, T, Craddock, C, Nakamoto, B*, et al.* 1995. The VLA4/VCAM-1 adhesion pathway defines contrasting mechanisms of lodgement of transplanted murine hemopoietic progenitors between bone marrow and spleen. *Proc Natl Acad Sci U S A,* 92**,** 9647-51.

Papayannopoulou, T, Nakamoto, B, Andrews, RG*, et al.* 1997. In vivo effects of Flt3/Flk2 ligand on mobilization of hematopoietic progenitors in primates and potent synergistic enhancement with granulocyte colony-stimulating factor. *Blood,* 90**,** 620-9.

Papayannopoulou, T, Priestley, GV & Nakamoto, B 1998. Anti-VLA4/VCAM-1-induced mobilization requires cooperative signaling through the kit/mkit ligand pathway. *Blood,* 91**,** 2231-9.

Pastorek, JG, Guillory, BA & Veith, RW 1996. Infection After Gynecologic Surgery: Implications of Racial Leukopenia in Black Women. *Medscape Womens Health,* 1**,** 3.

Patterson, AM, Siddall, H, Chamberlain, G*, et al.* 2002. Expression of the duffy antigen/receptor for chemokines (DARC) by the inflamed synovial endothelium. *J Pathol,* 197**,** 108-16.

Peiper, SC, Wang, ZX, Neote, K*, et al.* 1995. The Duffy antigen/receptor for chemokines (DARC) is expressed in endothelial cells of Duffy negative individuals who lack the erythrocyte receptor. *J Exp Med,* 181**,** 1311-7.

Peled, A, Gonzalo, JA, Lloyd, C*, et al.* 1998. The chemotactic cytokine eotaxin acts as a granulocyte-macrophage colony-stimulating factor during lung inflammation. *Blood,* 91**,** 1909-16.

Pelus, LM & Fukuda, S 2006. Peripheral blood stem cell mobilization: the CXCR2 ligand GRObeta rapidly mobilizes hematopoietic stem cells with enhanced engraftment properties. *Exp Hematol,* 34**,** 1010-20.

Perry, C & Soreq, H 2002. Transcriptional regulation of erythropoiesis. Fine tuning of combinatorial multi-domain elements. *Eur J Biochem,* 269**,** 3607-18.

Person, RE, Li, FQ, Duan, Z*, et al.* 2003. Mutations in proto-oncogene GFI1 cause human neutropenia and target ELA2. *Nat Genet,* 34**,** 308-12.

Petit, I, Szyper-Kravitz, M, Nagler, A, *et al.* 2002. G-CSF induces stem cell mobilization by decreasing bone marrow SDF-1 and up-regulating CXCR4. *Nat Immunol,* 3**,** 687-94.

Phillips-Howard, PA, Radalowicz, A, Mitchell, J, *et al.* 1990. Risk of malaria in British residents returning from malarious areas. *BMJ,* 300**,** 499-503.

Phillips, D, Rezvani, K & Bain, BJ 2000. Exercise induced mobilisation of the marginated granulocyte pool in the investigation of ethnic neutropenia. *J Clin Pathol,* 53**,** 481-3.

Philpott, NJ, Prue, RL, Marsh, JC, *et al.* 1997. G-CSF-mobilized CD34 peripheral blood stem cells are significantly less apoptotic than unstimulated peripheral blood CD34 cells: role of G-CSF as survival factor. *Br J Haematol,* 97**,** 146-52.

Pillay, J, Den Braber, I, Vrisekoop, N, *et al.* 2010. In vivo labeling with 2H2O reveals a human neutrophil lifespan of 5.4 days. *Blood,* 116**,** 625-7.

Platzer, E, Welte, K, Gabrilove, JL, *et al.* 1985. Biological activities of a human pluripotent hemopoietic colony stimulating factor on normal and leukemic cells. *J Exp Med,* 162**,** 1788-801.

Ponomaryov, T, Peled, A, Petit, I, *et al.* 2000. Induction of the chemokine stromal-derived factor-1 following DNA damage improves human stem cell function. *J Clin Invest,* 106**,** 1331-9.

Pruenster, M, Mudde, L, Bombosi, P, *et al.* 2009. The Duffy antigen receptor for chemokines transports chemokines and supports their promigratory activity. *Nat Immunol,* 10**,** 101-8.

Pruenster, M & Rot, A 2006. Throwing light on DARC. *Biochem Soc Trans,* 34**,** 1005-8.

Pui, CH, Pei, D, Pappo, AS, *et al.* 2012. Treatment outcomes in black and white children with cancer: results from the SEER database and St Jude Children's Research Hospital, 1992 through 2007. *J Clin Oncol,* 30**,** 2005-12.

Race, RR, Sanger, R & Lehane, D 1953. Quantitative aspects of the blood group Fya. *Ann Eugen,* 17**,** 255-66.

Radtke, F, Macdonald, HR & Tacchini-Cottier, F 2013. Regulation of innate and adaptive immunity by Notch. *Nat Rev Immunol,* 13**,** 427-37.

Ramirez, P, Rettig, MP, Uy, GL, *et al.* 2009. BIO5192, a small molecule inhibitor of VLA-4, mobilizes hematopoietic stem and progenitor cells. *Blood,* 114**,** 1340-3.

Ramji, DP & Foka, P 2002. CCAAT/enhancer-binding proteins: structure, function and regulation. *Biochem J,* 365**,** 561-75.

Ramsuran, V, Kulkarni, H, He, W, *et al.* 2011. Duffy-Null-Associated Low Neutrophil Counts Influence HIV-1 Susceptibility in High-Risk South African Black Women. *Clinical Infectious Diseases,* 52**,** 1248-1256.

Rana, SR, Castro, OL & Haddy, TB 1985. Leukocyte counts in 7,739 healthy black persons: effects of age and sex. *Ann Clin Lab Sci,* 15**,** 51-4.

Ratajczak, J, Reca, R, Kucia, M, *et al.* 2004. Mobilization studies in mice deficient in either C3 or C3a receptor (C3aR) reveal a novel role for complement in retention of hematopoietic stem/progenitor cells in bone marrow. *Blood,* 103**,** 2071-8.

Reddy, VA, Iwama, A, Iotzova, G, *et al.* 2002. Granulocyte inducer C/EBPalpha inactivates the myeloid master regulator PU.1: possible role in lineage commitment decisions. *Blood,* 100**,** 483-90.

Rehman, MQ, Beal, D, Liang, Y*, et al.* 2013. B cells secrete eotaxin-1 in human inflammatory bowel disease. *Inflamm Bowel Dis,* 19**,** 922-33.

Reich, D, Nalls, MA, Kao, WH*, et al.* 2009. Reduced neutrophil count in people of African descent is due to a regulatory variant in the Duffy antigen receptor for chemokines gene. *PLoS Genet,* 5**,** e1000360.

Reid, ME & Lomas-Francis, C 2004. *The Blood Group Antigen Facts Book,* New York, Elsevier Academic Press.

Reid, S, Ritchie, A, Boring, L*, et al.* 1999. Enhanced myeloid progenitor cell cycling and apoptosis in mice lacking the chemokine receptor, CCR2. *Blood,* 93**,** 1524-33.

Reiner, AP, Lettre, G, Nalls, MA*, et al.* 2011. Genome-wide association study of white blood cell count in 16,388 African Americans: the continental origins and genetic epidemiology network (COGENT). *PLoS Genet,* 7**,** e1002108.

Reutershan, J, Harry, B, Chang, D*, et al.* 2009. DARC on RBC limits lung injury by balancing compartmental distribution of CXC chemokines. *Eur J Immunol,* 39**,** 1597-607.

Rezvani, K, Flanagan, AM, Sarma, U*, et al.* 2001. Investigation of ethnic neutropenia by assessment of bone marrow colony-forming cells. *Acta Haematol,* 105**,** 32-7.

Rippey, JJ 1967. Leucopenia in West Indians and Africans. *The Lancet,* 290**,** 44-44.

Robbins, AS, Pavluck, AL, Fedewa, SA*, et al.* 2009. Insurance status, comorbidity level, and survival among colorectal cancer patients age 18 to 64 years in the National Cancer Data Base from 2003 to 2005. *J Clin Oncol,* 27**,** 3627-33.

Robinson, SD, Frenette, PS, Rayburn, H*, et al.* 1999. Multiple, targeted deficiencies in selectins reveal a predominant role for P-selectin in leukocyte recruitment. *Proc Natl Acad Sci U S A,* 96**,** 11452-7.

Robinson, SN, Pisarev, VM, Chavez, JM*, et al.* 2003. Use of matrix metalloproteinase (MMP)-9 knockout mice demonstrates that MMP-9 activity is not absolutely required for G-CSF or Flt-3 ligand-induced hematopoietic progenitor cell mobilization or engraftment. *Stem Cells,* 21**,** 417-27.

Rodrigues, NP, Boyd, AS, Fugazza, C*, et al.* 2008. GATA-2 regulates granulocyte-macrophage progenitor cell function. *Blood,* 112**,** 4862-73.

Rosenthal, KS & Tan, MJ 2011. *Rapid review microbiology and immunology,* Philadelphia, PA, Mosby/Elsevier.

Ross, EA, Freeman, S, Zhao, Y*, et al.* 2008. A novel role for PECAM-1 (CD31) in regulating haematopoietic progenitor cell compartmentalization between the peripheral blood and bone marrow. *PloS ONE,* 3**,** e2338.

Ryan, JR, Stoute, JA, Amon, J*, et al.* 2006. Evidence for transmission of Plasmodium vivax among a duffy antigen negative population in Western Kenya. *Am J Trop Med Hyg,* 75**,** 575-81.

Sadeghi, N, Badalato, GM, Hruby, G*, et al.* 2012. Does absolute neutrophil count predict high tumor grade in African-American men with prostate cancer? *Prostate,* 72**,** 386-91.

Sadowitz, PD & Oski, FA 1983. Differences in polymorphonuclear cell counts between healthy white and black infants: response to meningitis. *Pediatrics,* 72**,** 405-7.

Sanchez-Martin, L, Estecha, A, Samaniego, R*, et al.* 2011. The chemokine CXCL12 regulates monocyte-macrophage differentiation and RUNX3 expression. *Blood,* 117**,** 88-97.

Sanchez, X, Suetomi, K, Cousins-Hodges, B, *et al.* 1998. CXC chemokines suppress proliferation of myeloid progenitor cells by activation of the CXC chemokine receptor 2. *J Immunol,* 160**,** 906-10.

Sarkar, CA & Lauffenburger, DA 2003. Cell-level pharmacokinetic model of granulocyte colony-stimulating factor: implications for ligand lifetime and potency in vivo. *Mol Pharmacol,* 63**,** 147-58.

Scandura, JM, Boccuni, P, Massague, J, *et al.* 2004. Transforming growth factor beta-induced cell cycle arrest of human hematopoietic cells requires p57KIP2 up-regulation. *Proc Natl Acad Sci U S A,* 101**,** 15231-6.

Schmidt, H, Suciu, S, Punt, CJ, *et al.* 2007. Pretreatment levels of peripheral neutrophils and leukocytes as independent predictors of overall survival in patients with American Joint Committee on Cancer Stage IV Melanoma: results of the EORTC 18951 Biochemotherapy Trial. *J Clin Oncol,* 25**,** 1562-9.

Schnabel, R, Baumert, J, Barbalic, M, *et al.* 2010. Duffy antigen receptor for chemokines (Darc) polymorphism regulates circulating concentrations of monocyte chemoattractant protein-1 and other inflammatory mediators. *Blood,* 115**,** 5289-99.

Schnog, JB, Keli, SO, Pieters, RA, *et al.* 2000. Duffy phenotype does not influence the clinical severity of sickle cell disease. *Clin Immunol,* 96**,** 264-8.

Schuettpelz, LG, Borgerding, JN, Christopher, MJ, *et al.* 2014. G-CSF regulates hematopoietic stem cell activity, in part, through activation of Toll-like receptor signaling. *Leukemia.*

Schulz, C, Gomez Perdiguero, E, Chorro, L, *et al.* 2012. A lineage of myeloid cells independent of Myb and hematopoietic stem cells. *Science,* 336**,** 86-90.

Schymeinsky, J, Mocsai, A & Walzog, B 2007. Neutrophil activation via beta2 integrins (CD11/CD18): molecular mechanisms and clinical implications. *Thromb Haemost,* 98**,** 262-73.

Seer 2012. Surveillance, Epidemiology, and End Results (SEER) Program (www.seer.cancer.gov) SEER*Stat Database: Mortality - All COD, Aggregated With State, Total U.S. (1969-2009) <Katrina/Rita Population Adjustment>, National Cancer Institute, DCCPS, Surveillance Research Program, Surveillance Systems Branch, released April 2012. Underlying mortality data provided by NCHS (www.cdc.gov/nchs).

Segerer, S, Regele, H, Mac, KM, *et al.* 2000. The Duffy antigen receptor for chemokines is up-regulated during acute renal transplant rejection and crescentic glomerulonephritis. *Kidney Int,* 58**,** 1546-56.

Semerad, CL, Christopher, MJ, Liu, F, *et al.* 2005. G-CSF potently inhibits osteoblast activity and CXCL12 mRNA expression in the bone marrow. *Blood,* 106**,** 3020-7.

Semerad, CL, Liu, F, Gregory, AD, *et al.* 2002. G-CSF is an essential regulator of neutrophil trafficking from the bone marrow to the blood. *Immunity,* 17**,** 413-23.

Serwold, T, Ehrlich, LI & Weissman, IL 2009. Reductive isolation from bone marrow and blood implicates common lymphoid progenitors as the major source of thymopoiesis. *Blood,* 113**,** 807-15.

Seymour, JF, Lieschke, GJ, Grail, D*, et al.* 1997. Mice lacking both granulocyte colony-stimulating factor (CSF) and granulocyte-macrophage CSF have impaired reproductive capacity, perturbed neonatal granulopoiesis, lung disease, amyloidosis, and reduced long-term survival. *Blood,* 90**,** 3037-49.

Sharpe, AH & Freeman, GJ 2002. The B7-CD28 superfamily. *Nat Rev Immunol,* 2**,** 116-26.

Shaz, BH, Stowell, SR & Hillyer, CD 2011. Transfusion-related acute lung injury: from bedside to bench and back. *Blood,* 117**,** 1463-1471.

Shen, H, Schuster, R, Stringer, KF*, et al.* 2006. The Duffy antigen/receptor for chemokines (DARC) regulates prostate tumor growth. *FASEB J,* 20**,** 59-64.

Shimizu, Y, Ao, H, Soemantri, A*, et al.* 2000. Sero- and molecular typing of Duffy blood group in Southeast Asians and Oceanians. *Hum Biol,* 72**,** 511-8.

Shirvaikar, N, Marquez-Curtis, LA, Shaw, AR*, et al.* 2010. MT1-MMP association with membrane lipid rafts facilitates G-CSF--induced hematopoietic stem/progenitor cell mobilization. *Exp Hematol,* 38**,** 823-35.

Shoenfeld, Y, Alkan, ML, Asaly, A*, et al.* 1988. Benign familial leukopenia and neutropenia in different ethnic groups. *Eur J Haematol,* 41**,** 273-7.

Shoenfeld, Y, Ben-Tal, O, Berliner, S*, et al.* 1985. The outcome of bacterial infection in subjects with benign familial leukopenia (BFL). *Biomed Pharmacother,* 39**,** 23-6.

Shoenfeld, Y, Modan, M, Berliner, S*, et al.* 1982. The mechanism of benign hereditary neutropenia. *Arch Intern Med,* 142**,** 797-9.

Shojaei, F, Wu, X, Zhong, C*, et al.* 2007. Bv8 regulates myeloid-cell-dependent tumour angiogenesis. *Nature,* 450**,** 825-31.

Shulman, Z, Cohen, SJ, Roediger, B*, et al.* 2012. Transendothelial migration of lymphocytes mediated by intraendothelial vesicle stores rather than by extracellular chemokine depots. *Nat Immunol,* 13**,** 67-76.

Siemerink, EJ, Van Der Aa, MA, Siesling, S*, et al.* 2011. Survival of non-Western first generations immigrants with stomach cancer in North East Netherlands. *Br J Cancer,* 104**,** 1193-5.

Sierro, F, Biben, C, Martinez-Munoz, L*, et al.* 2007. Disrupted cardiac development but normal hematopoiesis in mice deficient in the second CXCL12/SDF-1 receptor, CXCR7. *Proc Natl Acad Sci U S A,* 104**,** 14759-64.

Silver, JD, Ritchie, ME & Smyth, GK 2009. Microarray background correction: maximum likelihood estimation for the normal-exponential convolution. *Biostatistics,* 10**,** 352-63.

Siminovitch, L, Mcculloch, EA & Till, JE 1963. The Distribution of Colony-Forming Cells among Spleen Colonies. *J Cell Physiol,* 62**,** 327-36.

Simon, HU 2001. Regulation of eosinophil and neutrophil apoptosis--similarities and differences. *Immunol Rev,* 179**,** 156-62.

Smith, K, Wray, L, Klein-Cabral, M*, et al.* 2005. Ethnic disparities in adjuvant chemotherapy for breast cancer are not caused by excess toxicity in black patients. *Clin Breast Cancer,* 6**,** 260-6; discussion 267-9.

Smith, LT, Hohaus, S, Gonzalez, DA*, et al.* 1996. PU.1 (Spi-1) and C/EBP alpha regulate the granulocyte colony-stimulating factor receptor promoter in myeloid cells. *Blood,* 88**,** 1234-47.

Smyth, GK 2004. Linear models and empirical bayes methods for assessing differential expression in microarray experiments. *Stat Appl Genet Mol Biol,* 3**,** Article3.

Socolovsky, M, Nam, H, Fleming, MD*, et al.* 2001. Ineffective erythropoiesis in Stat5a(-/-)5b(-/-) mice due to decreased survival of early erythroblasts. *Blood,* 98**,** 3261-73.

Soni, S, Bala, S, Gwynn, B*, et al.* 2006. Absence of erythroblast macrophage protein (Emp) leads to failure of erythroblast nuclear extrusion. *J Biol Chem,* 281**,** 20181-9.

Spooner, CJ, Cheng, JX, Pujadas, E*, et al.* 2009. A recurrent network involving the transcription factors PU.1 and Gfi1 orchestrates innate and adaptive immune cell fates. *Immunity,* 31**,** 576-86.

Stark, MA, Huo, Y, Burcin, TL*, et al.* 2005. Phagocytosis of apoptotic neutrophils regulates granulopoiesis via IL-23 and IL-17. *Immunity,* 22**,** 285-94.

Steinl, C, Essl, M, Schreiber, TD*, et al.* 2013. Release of matrix metalloproteinase-8 during physiological trafficking and induced mobilization of human hematopoietic stem cells. *Stem Cells Dev,* 22**,** 1307-18.

Stirewalt, DL & Radich, JP 2003. The role of FLT3 in haematopoietic malignancies. *Nat Rev Cancer,* 3**,** 650-65.

Sugiyama, T, Kohara, H, Noda, M*, et al.* 2006. Maintenance of the hematopoietic stem cell pool by CXCL12-CXCR4 chemokine signaling in bone marrow stromal cell niches. *Immunity,* 25**,** 977-88.

Suratt, BT, Eisner, MD, Calfee, CS*, et al.* 2009. Plasma granulocyte colony-stimulating factor levels correlate with clinical outcomes in patients with acute lung injury. *Crit Care Med,* 37**,** 1322-8.

Suratt, BT, Young, SK, Lieber, J*, et al.* 2001. Neutrophil maturation and activation determine anatomic site of clearance from circulation. *Am J Physiol Lung Cell Mol Physiol,* 281**,** L913-21.

Szabo, MC, Soo, KS, Zlotnik, A*, et al.* 1995. Chemokine class differences in binding to the Duffy antigen-erythrocyte chemokine receptor. *J Biol Chem,* 270**,** 25348-51.

Szymanski, IO, Huff, SR & Delsignore, R 1982. An autoanalyzer test to determine immunoglobulin class and IgG subclass of blood group antibodies. *Transfusion,* 22**,** 90-5.

Takano, H, Ema, H, Sudo, K*, et al.* 2004. Asymmetric division and lineage commitment at the level of hematopoietic stem cells: inference from differentiation in daughter cell and granddaughter cell pairs. *J Exp Med,* 199**,** 295-302.

Tazzyman, S, Lewis, CE & Murdoch, C 2009. Neutrophils: key mediators of tumour angiogenesis. *Int J Exp Pathol,* 90**,** 222-31.

Teramukai, S, Kitano, T, Kishida, Y*, et al.* 2009. Pretreatment neutrophil count as an independent prognostic factor in advanced non-small-cell lung cancer: an analysis of Japan Multinational Trial Organisation LC00-03. *Eur J Cancer,* 45**,** 1950-8.

Theilgaard-Monch, K, Jacobsen, LC, Borup, R*, et al.* 2005. The transcriptional program of terminal granulocytic differentiation. *Blood,* 105**,** 1785-96.

Thoren, LA, Liuba, K, Bryder, D*, et al.* 2008. Kit regulates maintenance of quiescent hematopoietic stem cells. *J Immunol,* 180**,** 2045-53.

Tian, SS, Lamb, P, Seidel, HM*, et al.* 1994. Rapid activation of the STAT3 transcription factor by granulocyte colony-stimulating factor. *Blood,* 84**,** 1760-4.

Till, JE & Mcculloch, EA 1961. A direct measurement of the radiation sensitivity of normal mouse bone marrow cells. *Radiat Res,* 14**,** 213-22.

Tipping, AJ, Pina, C, Castor, A*, et al.* 2009. High GATA-2 expression inhibits human hematopoietic stem and progenitor cell function by effects on cell cycle. *Blood,* 113**,** 2661-72.

Tjwa, M, Janssens, S & Carmeliet, P 2008. Plasmin therapy enhances mobilization of HPCs after G-CSF. *Blood,* 112**,** 4048-50.

Tjwa, M, Sidenius, N, Moura, R*, et al.* 2009. Membrane-anchored uPAR regulates the proliferation, marrow pool size, engraftment, and mobilization of mouse hematopoietic stem/progenitor cells. *J Clin Invest,* 119**,** 1008-18.

To, LB, Haylock, DN, Kimber, RJ*, et al.* 1984. High levels of circulating haemopoietic stem cells in very early remission from acute non-lymphoblastic leukaemia and their collection and cryopreservation. *Br J Haematol,* 58**,** 399-410.

Torossian, F, Anginot, A, Chabanon, A*, et al.* 2014. CXCR7 participates in CXCL12-induced CD34+ cell cycling through beta-arrestin-dependent Akt activation. *Blood,* 123**,** 191-202.

Tournamille, C, Colin, Y, Cartron, JP*, et al.* 1995. Disruption of a GATA motif in the Duffy gene promoter abolishes erythroid gene expression in Duffy-negative individuals. *Nat Genet,* 10**,** 224-8.

Tournamille, C, Filipe, A, Badaut, C*, et al.* 2005. Fine mapping of the Duffy antigen binding site for the Plasmodium vivax Duffy-binding protein. *Mol Biochem Parasitol,* 144**,** 100-3.

Tournamille, C, Filipe, A, Wasniowska, K*, et al.* 2003. Structure-function analysis of the extracellular domains of the Duffy antigen/receptor for chemokines: characterization of antibody and chemokine binding sites. *Br J Haematol,* 122**,** 1014-23.

Tournamille, C, Le Van Kim, C, Gane, P*, et al.* 1997. Close association of the first and fourth extracellular domains of the Duffy antigen/receptor for chemokines by a disulfide bond is required for ligand binding. *J Biol Chem,* 272**,** 16274-80.

Tournamille, C, Le Van Kim, C, Gane, P*, et al.* 1998. Arg89Cys substitution results in very low membrane expression of the Duffy antigen/receptor for chemokines in Fy(x) individuals. *Blood,* 92**,** 2147-56.

Traver, D, Akashi, K, Manz, M*, et al.* 2000. Development of CD8alpha-positive dendritic cells from a common myeloid progenitor. *Science,* 290**,** 2152-4.

Tsai, FY, Keller, G, Kuo, FC*, et al.* 1994. An early haematopoietic defect in mice lacking the transcription factor GATA-2. *Nature,* 371**,** 221-6.

Tsan, MF 2011. Heat shock proteins and high mobility group box 1 protein lack cytokine function. *J Leukoc Biol,* 89**,** 847-53.

Ulvmar, MH, Hub, E & Rot, A 2011. Atypical chemokine receptors. *Exp Cell Res,* 317**,** 556-68.

Ulvmar, MH, Werth, K, Braun, A*, et al.* 2014. The atypical chemokine receptor CCRL1 shapes functional CCL21 gradients in lymph nodes. *Nat Immunol*.

Ulyanova, T, Scott, LM, Priestley, GV*, et al.* 2005. VCAM-1 expression in adult hematopoietic and nonhematopoietic cells is controlled by tissue-inductive signals and reflects their developmental origin. *Blood,* 106**,** 86-94.

Velzing-Aarts, FV, Muskiet, FA, Van Der Dijs, FP*, et al.* 2002a. High serum interleukin-8 levels in afro-caribbean women with pre-eclampsia. Relations with tumor necrosis factor-alpha, duffy negative phenotype and von Willebrand factor. *Am J Reprod Immunol,* 48**,** 319-22.

Velzing-Aarts, FV, Van Der Dijs, FP, Muskiet, FA*, et al.* 2002b. The association of pre-eclampsia with the Duffy negative phenotype in women of West African descent. *BJOG,* 109**,** 453-5.

Vengelen-Tyler, V 1983. Letter to the editor. *Red Cell Free Press,* 8**,** 1.

Vengelen-Tyler, V 1985. Anti-Fya preceding anti-Fy3 or -Fy5: a study of five cases (abstract). *Transfusion,* 25**,** 1.

Vergara, C, Tsai, YJ, Grant, AV*, et al.* 2008. Gene encoding Duffy antigen/receptor for chemokines is associated with asthma and IgE in three populations. *Am J Respir Crit Care Med,* 178**,** 1017-22.

Vermeulen, M, Le Pesteur, F, Gagnerault, MC*, et al.* 1998. Role of adhesion molecules in the homing and mobilization of murine hematopoietic stem and progenitor cells. *Blood,* 92**,** 894-900.

Vielhauer, V, Allam, R, Lindenmeyer, MT*, et al.* 2009. Efficient renal recruitment of macrophages and T cells in mice lacking the duffy antigen/receptor for chemokines. *Am J Pathol,* 175**,** 119-31.

Villeda, SA, Luo, J, Mosher, KI*, et al.* 2011. The ageing systemic milieu negatively regulates neurogenesis and cognitive function. *Nature,* 477**,** 90-4.

Vivier, E, Raulet, DH, Moretta, A*, et al.* 2011. Innate or adaptive immunity? The example of natural killer cells. *Science,* 331**,** 44-9.

Voruganti, VS, Laston, S, Haack, K*, et al.* 2012. Genome-wide association replicates the association of Duffy antigen receptor for chemokines (DARC) polymorphisms with serum monocyte chemoattractant protein-1 (MCP-1) levels in Hispanic children. *Cytokine,* 60**,** 634-8.

Walker, WS, Singer, JA, Morrison, M*, et al.* 1984. Preferential phagocytosis of in vivo aged murine red blood cells by a macrophage-like cell line. *Br J Haematol,* 58**,** 259-66.

Walley, NM, Julg, B, Dickson, SP*, et al.* 2009. The Duffy antigen receptor for chemokines null promoter variant does not influence HIV-1 acquisition or disease progression. *Cell Host Microbe,* 5**,** 408-10; author reply 418-9.

Wang, J, Ou, ZL, Hou, YF*, et al.* 2006. Enhanced expression of Duffy antigen receptor for chemokines by breast cancer cells attenuates growth and metastasis potential. *Oncogene,* 25**,** 7201-11.

Wang, L, Shah, PK, Wang, W*, et al.* 2013. Tenascin-C deficiency in apo E-/- mouse increases eotaxin levels: implications for atherosclerosis. *Atherosclerosis,* 227**,** 267-74.

Wang, W, Wang, X, Ward, AC*, et al.* 2001. C/EBPalpha and G-CSF receptor signals cooperate to induce the myeloperoxidase and neutrophil elastase genes. *Leukemia,* 15**,** 779-86.

Ward, AC, Loeb, DM, Soede-Bobok, AA*, et al.* 2000. Regulation of granulopoiesis by transcription factors and cytokine signals. *Leukemia,* 14**,** 973-90.

Welte, K, Bonilla, MA, Gillio, AP*, et al.* 1987. Recombinant human granulocyte colony-stimulating factor. Effects on hematopoiesis in normal and cyclophosphamide-treated primates. *J Exp Med,* 165**,** 941-8.

Wengner, AM, Pitchford, SC, Furze, RC*, et al.* 2008. The coordinated action of G-CSF and ELR + CXC chemokines in neutrophil mobilization during acute inflammation. *Blood,* 111**,** 42-9.

Wick, N, Haluza, D, Gurnhofer, E*, et al.* 2008. Lymphatic precollectors contain a novel, specialized subpopulation of podoplanin low, CCL27-expressing lymphatic endothelial cells. *Am J Pathol,* 173**,** 1202-9.

Williams, D, Johnson, CL & Marsh, WL 1981. Duffy antigen changes on red blood cells stored at low temperature. *Transfusion,* 21**,** 357-359.

Williams, SC, Cantwell, CA & Johnson, PF 1991. A family of C/EBP-related proteins capable of forming covalently linked leucine zipper dimers in vitro. *Genes Dev,* 5**,** 1553-67.

Winkler, CA, An, P, Johnson, R*, et al.* 2009. Expression of Duffy antigen receptor for chemokines (DARC) has no effect on HIV-1 acquisition or progression to AIDS in African Americans. *Cell Host Microbe,* 5**,** 411-3; author reply 418-9.

Winkler, IG, Bendall, LJ, Forristal, CE*, et al.* 2013. B-lymphopoiesis is stopped by mobilizing doses of G-CSF and is rescued by overexpression of the anti-apoptotic protein Bcl2. *Haematologica,* 98**,** 325-33.

Winkler, IG & Levesque, JP 2006. Mechanisms of hematopoietic stem cell mobilization: when innate immunity assails the cells that make blood and bone. *Exp Hematol,* 34**,** 996-1009.

Wishart, TM, Macdonald, SH, Chen, PE*, et al.* 2007. Design of a novel quantitative PCR (QPCR)-based protocol for genotyping mice carrying the neuroprotective Wallerian degeneration slow (Wlds) gene. *Mol Neurodegener,* 2**,** 21.

Woldearegai, TG, Kremsner, PG, Kun, JF*, et al.* 2013. Plasmodium vivax malaria in Duffy-negative individuals from Ethiopia. *Trans R Soc Trop Med Hyg,* 107**,** 328-31.

Wong, HR, Cvijanovich, N, Wheeler, DS*, et al.* 2008. Interleukin-8 as a Stratification Tool for Interventional Trials Involving Pediatric Septic Shock. *Am. J. Respir. Crit. Care Med.,* 178**,** 276-282.

Woodward, WA, Huang, EH, Mcneese, MD*, et al.* 2006. African-American race is associated with a poorer overall survival rate for breast cancer patients treated with mastectomy and doxorubicin-based chemotherapy. *Cancer,* 107**,** 2662-8.

Woolley, IJ, Hotmire, KA, Sramkoski, RM*, et al.* 2000. Differential expression of the duffy antigen receptor for chemokines according to RBC age and FY genotype. *Transfusion,* 40**,** 949-53.

Wright, DE, Bowman, EP, Wagers, AJ*, et al.* 2002. Hematopoietic stem cells are uniquely selective in their migratory response to chemokines. *J Exp Med,* 195**,** 1145-54.

Wurtz, N, Mint Lekweiry, K, Bogreau, H*, et al.* 2011. Vivax malaria in Mauritania includes infection of a Duffy-negative individual. *Malar J,* 10**,** 336.

Wysoczynski, M, Reca, R, Ratajczak, J*, et al.* 2005. Incorporation of CXCR4 into membrane lipid rafts primes homing-related responses of hematopoietic stem/progenitor cells to an SDF-1 gradient. *Blood,* 105**,** 40-8.

Xiong, Z, Cavaretta, J, Qu, L*, et al.* 2010. Red blood cell microparticles show altered inflammatory chemokine binding and release ligand upon interaction with platelets. *Transfusion*.

Yamanaka, R, Barlow, C, Lekstrom-Himes, J*, et al.* 1997. Impaired granulopoiesis, myelodysplasia, and early lethality in CCAAT/enhancer binding protein epsilon-deficient mice. *Proc Natl Acad Sci U S A,* 94**,** 13187-92.

Yan, B, Wei, JJ, Yuan, Y*, et al.* 2013. IL-6 cooperates with G-CSF to induce protumor function of neutrophils in bone marrow by enhancing STAT3 activation. *J Immunol,* 190**,** 5882-93.

Youn, BS, Mantel, C & Broxmeyer, HE 2000. Chemokines, chemokine receptors and hematopoiesis. *Immunol Rev,* 177**,** 150-74.

Zabel, BA, Wang, Y, Lewen, S*, et al.* 2009. Elucidation of CXCR7-mediated signaling events and inhibition of CXCR4-mediated tumor cell transendothelial migration by CXCR7 ligands. *J Immunol,* 183**,** 3204-11.

Zarbock, A, Bishop, J, Muller, H*, et al.* 2010. Chemokine homeostasis vs. chemokine presentation during severe acute lung injury: the other side of the Duffy antigen receptor for chemokines. *Am J Physiol Lung Cell Mol Physiol,* 298**,** L462-71.

Zarbock, A, Ley, K, Mcever, RP*, et al.* 2011. Leukocyte ligands for endothelial selectins: specialized glycoconjugates that mediate rolling and signaling under flow. *Blood,* 118**,** 6743-51.

Zarbock, A, Schmolke, M, Bockhorn, SG*, et al.* 2007. The Duffy antigen receptor for chemokines in acute renal failure: A facilitator of renal chemokine presentation. *Crit Care Med,* 35**,** 2156-63.

Zhang, CC & Lodish, HF 2008. Cytokines regulating hematopoietic stem cell function. *Curr Opin Hematol,* 15**,** 307-11.

Zhang, DE, Zhang, P, Wang, ND*, et al.* 1997. Absence of granulocyte colony-stimulating factor signaling and neutrophil development in CCAAT enhancer binding protein alpha-deficient mice. *Proc Natl Acad Sci U S A,* 94**,** 569-74.

Zhang, P, Iwasaki-Arai, J, Iwasaki, H*, et al.* 2004. Enhancement of hematopoietic stem cell repopulating capacity and self-renewal in the absence of the transcription factor C/EBP alpha. *Immunity,* 21**,** 853-63.

Zhu, J & Emerson, SG 2002. Hematopoietic cytokines, transcription factors and lineage commitment. *Oncogene,* 21**,** 3295-313.

Zimmerman, PA, Woolley, I, Masinde, GL*, et al.* 1999. Emergence of FY*A(null) in a Plasmodium vivax-endemic region of Papua New Guinea. *Proc Natl Acad Sci U S A,* 96**,** 13973-7.

Zlotnik, A & Yoshie, O 2012. The chemokine superfamily revisited. *Immunity,* 36**,** 705-16.

Zohar, Y, Wildbaum, G, Novak, R*, et al.* 2014. CXCL11-dependent induction of FOXP3-negative regulatory T cells suppresses autoimmune encephalomyelitis. *J Clin Invest,* 124**,** 2009-22.